Unravelling the functional dynamics between the human gut microbiome and intestinal inflammatory responses

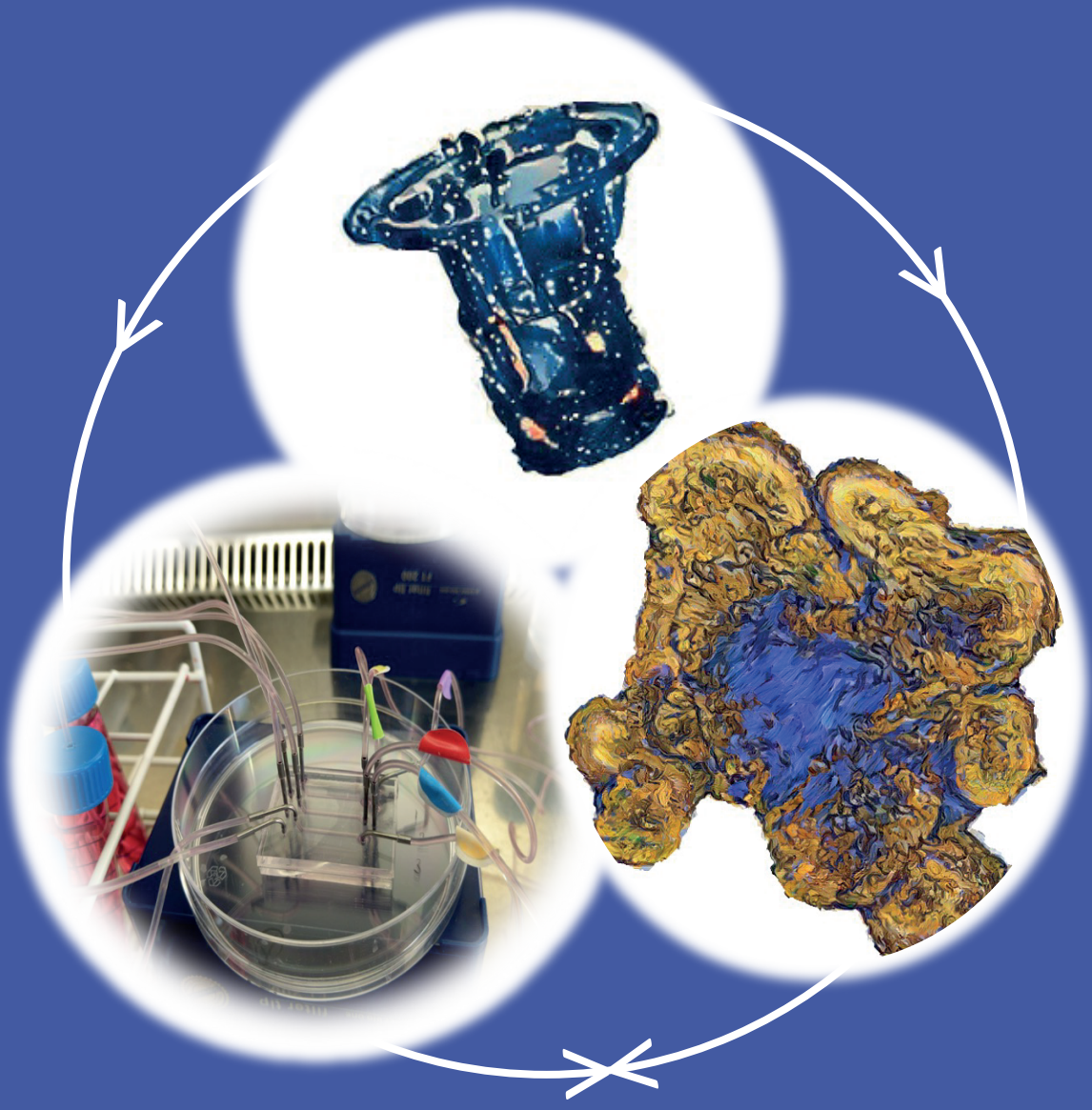

Menno Grouls

Propositions

1. *In vitro* methods using induced pluripotent stem cells provide an adequate model to study intestinal innate immunity. (this thesis)

2. Studying the effect of short chain fatty acids on the human intestinal epithelium *in vitro* requires a battery of tests. (this thesis)

3. Originality in research is a bonus, not a requirement.

4. Artificial intelligence facilitates systematic reviews.

5. Some setbacks are best left ignored.

6. The media propagates societal polarization.

Propositions belonging to the thesis, entitled

Unravelling the functional dynamics between the human gut microbiome and intestinal inflammatory responses

Menno Grouls
Wageningen, 9 May 2023

Unravelling the functional dynamics between the human gut microbiome and intestinal inflammatory responses

Menno Grouls

Thesis Committee

Promotors

Dr Hans Bouwmeester
Associate professor, Toxicology
Wageningen University & Research

Prof. Dr Ivonne M.C.M. Rietjens
Professor of Toxicology
Wageningen University & Research

Co-promotor

Dr Meike van der Zande
Scientist, Team Toxicology
Wageningen University & Research

Other Members

Prof. Dr Mangala Srinivas, Wageningen University & Research
Dr Raymond H.H. Pieters, Utrecht University
Dr Anja Wilmes, Vrije Universiteit Amsterdam
Dr Roel P.F. Schins, Leibniz-Institut für Umweltmedizinische Forschung, Germany

This research was conducted under the auspices of VLAG Graduate School (Biobased, Biomolecular, Chemical, Food, and Nutrition sciences)

Unravelling the functional dynamics between the human gut microbiome and intestinal inflammatory responses

Menno Grouls

Thesis

submitted in fulfilment of the requirements for the degree of doctor
at Wageningen University
by the authority of the Rector Magnificus,
Prof. Dr A.P.J. Mol,
in the presence of the
Thesis Committee appointed by the Academic Board
to be defended in public
on Tuesday 9 May 2023
at 4 p.m. in the Omnia Auditorium.

Menno Grouls

Unravelling the functional dynamics between the human gut microbiome and intestinal inflammatory responses, 182 pages.

PhD thesis, Wageningen University, Wageningen, the Netherlands (2023)
With references, with summary in English

ISBN: 978-94-6447-572-2
DOI: https://doi.org/10.18174/586019

Table of contents

Chapter 1

General Introduction

To understand why it is important to know so much about the intestine for a toxicologist it is important to understand toxicology. This starts with Paracelsus' statement; *"All things are poisons, and nothing is without poison, the dosage alone makes it so a thing is not a poison"*. All compounds can have an effect on the body, and within toxicology one looks at these effects and determines at which dose levels compounds start being detrimental. To do this, we not only need to understand how a compound interacts with the human body, but also how it enters and is distributed, metabolized and excreted from the body. In other words, we need to understand both the compound and the organs that are important for its kinetics and effects. With a focus on oral exposure, the intestine and more specifically the intestinal epithelium plays a key role in toxicology.

1.1 The digestive tract

The average Dutch person consumes about 3.1 kg of food per day [1], out of which the human body has to extract proteins, sugars, vitamins and much more. This happens in a stepwise process in our gastrointestinal tract that spans nine meters from our mouth to our anus [2]. The food digestion starts in the mouth where food is chewed to reduce its size and thereby increasing its surface area optimizing the food digestion. At the same time saliva is added which contains enzymes that start breaking down starch and lipids in the food [3, 4]. After swallowing, the food, or as it is often called, the bolus, experiences peristalsis for the first time. Peristalsis is a wave-like movement of muscles that pushes the bolus through the esophagus into the stomach. Peristalsis is present throughout the gastrointestinal (GI) tract and keeps the bolus moving, albeit at different rates in different parts of the GI tract. The bolus remains for several hours in the stomach, which has a very low pH (between 1-3) that causes a denaturation of proteins. In addition, the stomach contains enzymes that break down peptides and lipids. A mucus layer that lines the stomach wall protects the stomach itself from its acidic environment [5]. Over time, the stomach content is pushed towards the sphincter, a sort of one-way valve, and into the intestine.

The intestine is divided in two major parts, the small and large intestine. The small intestine is specialized in the absorption of nutrients. In the small intestine the strong acidity of the stomach is neutralized by the production and secretion of bicarbonate into the lumen, as the low pH would otherwise harm the intestine. To facilitate the absorption of nutrients, the breakdown or digestion of the bolus is continued by the introduction of even more enzymes. The enzymes that are present in the small intestine are produced by the small intestine itself and by the pancreas, which subsequently secretes them into the intestinal lumen [6]. Together, they break down sugars, peptides and lipids into building blocks that are small enough to be absorbed by the small intestinal epithelium into our body. Once absorbed, they are used by our body as energy or building blocks for its own proteins. However not everything can be broken down in the small intestine, and what's left over ends up in the large intestine.

A traditional description of the large intestine would be that it is the part where waste is stored until defecation. However, it is now known that also in the large intestine further breakdown of the bolus and absorption takes place. In the large intestine the digestion of food is not done by our own cells or enzymes secreted by them, but by the gut microbiome that is present in the large intestine. The microbiome consists of bacteria that use the remnants of the original food bolus as a source of food while the breakdown products they excrete can be used by other bacteria or absorbed by the large intestine via the

portal vein and the liver into the systemic circulation [7]. Overall, the digestive tract is an optimized organ designed to get as much as possible out of the food that is ingested.

1.2 The small intestine

The main function of the small intestine is absorption of nutrients, and knowledge on its structural features is important to fully understand its functioning. The small intestinal tissue consists of four layers each with their own role (figure 1.). Starting at the side of the tissue that is in contact with the rest of the body, there is a layer of cells (called the serous membrane or serosa) that excretes fluid to lubricate the intestinal tissue to reduce friction of the muscles present in the second layer, the muscularis (a layer of muscles that creates peristalsis) with the body. The third layer, is called the submucosa and contains connective tissue that connects the muscles to the fourth and last layer, the mucosa, that is closest to the digested food. The mucosa is subdivided into a layer of muscle, a layer of connective tissue (the lamina propria) that contains the lymph and blood vessels, and the epithelium. The epithelium is a layer of cells on the inside of the small intestine which secretes mucous that lines the intestinal tissue and forms the barrier between the digested food and the intestinal tissue. The main focus within this thesis is on the layer of cells that lines the small intestine, also called the intestinal epithelium. The three dimensional structure of the intestinal epithelium consists of crypts, that are tucked into the mucosa, and villi finger like structures that protrude from the mucosa to increase the surface area of the epithelium. At the bottom of the crypt intestinal epithelial stem cells are found, stem cells that can only differentiate into the cell types that form the intestinal epithelium. As these stem cells divide to create more cells one of two newly generated cells stays in the bottom of the crypt and remains as a stem cell while the other starts migrating towards the villi and differentiates into one of the other intestinal epithelial cell types.

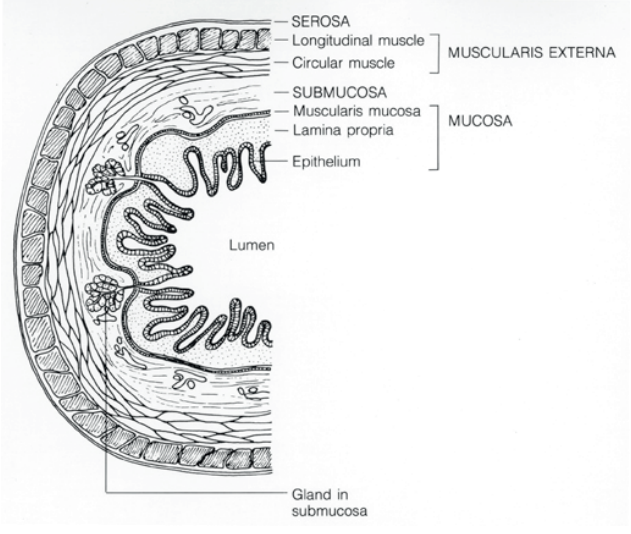

Figure 1. *Anatomy of the intestinal wall showing the four main layers, the serosa, muscularis externa, submucosa and mucosa and their subdivisions. Reproduced from the national cancer instutute* [8].

In the crypts and on the villi different cell types are found (figure 2.). Interspersed with the stem cells in the crypts one mostly finds Paneth cells, this is the only cell type that stays within the crypt (with the stem cells) while all other cell types slowly migrate upwards towards the villi. Paneth cells are the main source of antimicrobial peptide production that are secreted into the lumen, the inside of the intestine. These antimicrobial peptides form a defense against bacterial infection of the body, by disrupting the membrane of bacteria, leading to lysis of the bacteria [9]. The other cells in the epithelium that move from the crypt towards the villi keep moving upwards and are shed from the top of the villi into the lumen once they are too old. The most abundant epithelial cell type is the enterocyte, which is specialized in the absorption of nutrients. They express transporters that are important for transcellular transport (transport through the cells) and produce proteins involved in metabolism of xenobiotics that can be present in the food including toxic compounds. On their luminal surface enterocytes display microvilli, also called the brush border, which are even smaller finger like structures that increase the intestinal surface area even further [10]. Enterocytes are one of the most important cell types to be considered within toxicological studies, as they are responsible for the absorption of compounds from the intestinal lumen into the body. How much of a compound is absorbed and ends up in the body is a key aspect for the potential effect of that compound. The second most abundant cell type in the intestinal epithelium is the goblet cell. Goblet cells are specialized in producing and secreting mucus which lines the epithelium and forms a barrier between the cells and the content of the small intestine. This barrier protects the intestinal cells from direct contact with the bolus and acts as a barrier for certain compounds reducing their exposure to the enterocytes and hence reducing their transport [11, 12].

Finally, there are three much less abundant intestinal cell types. These include enteroendocrine cells, Microfold or M cells and tuft cells. The enteroendocrine cells secrete gastrointestinal hormones that serve as signals for both local and body wide communication [13, 14]. Microfold or M cells sample antigens, consisting of anything foreign to the body, and transport them to the lymphoid tissue where immune cells interact with these antigens and induce required responses [15]. Lastly there are tuft cells, that also sample what happens in the epithelium and signal to the immune system, but other than M cells they are associated with parasitic infections [16]. Between all the different cell types tight junctions are formed which form a seal between the cells to avoid unwanted paracellular transport (transport in between the cells).

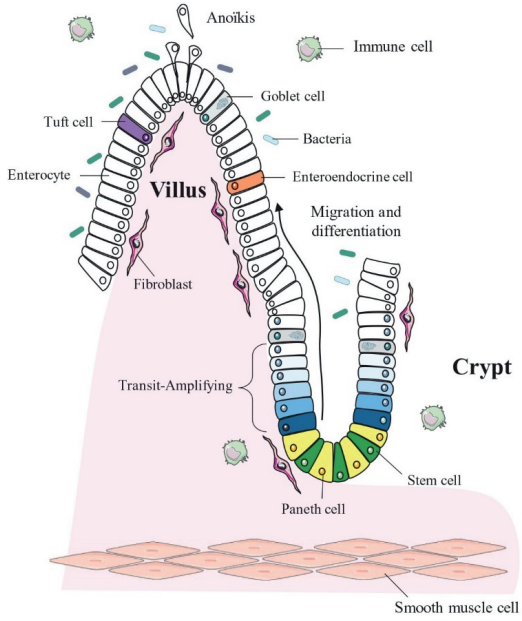

Figure 2. *The small intestinal epithelium showing the crypts, villi and most cell types. The crypts contain proliferative cells which divide, the newly formed cells move up while differentiating. Adapted from Creff et al.* [17] *under CC BY-NC 4.0* [18].

1.3 The large intestine

The overall tissue structure of the large intestine is comparable to that of the small intestine, with the same four cell layers. However, there are some variations in the epithelium due to the difference in function compared to the small intestine. Because there is less absorption the villi are shorter as there is less need to increase the surface area. There are also two changes in the cell composition, firstly enterocytes are replaced by colonocytes. Though their function stays similar, absorption, the expression of transporters is different as colonocytes absorb different compounds [19]. Secondly, there are no Paneth cells in the large intestine. At the same time the goblet cells excrete more mucus in the large intestine forming a thicker layer to better protect the epithelium. This thicker layer of mucus is needed because the content of the large intestine has lost a lot of its smaller components and water is extracted, so that the resulting faeces requires more force for its transport along the intestine requiring increased lubrication and protection of the large intestinal epithelium by mucus. Traditionally the large intestine was only seen as an organ for storage before excretion of the content as faeces. However, over time the importance of the large intestine has become more apparent, with more absorption and metabolism taking place than originally thought. Most of this is attributed to the large intestinal microbiota, that is estimated to consist of a total of 10^{12} bacteria [20]. These bacteria reside in the lumen but many also live in the mucus layer, being a secondary reason for the increase in mucus in the large intestine. The bacteria live on the food that cannot be digested and excrete breakdown products that the human body or other microbiota can use. One example is the breakdown of dietary fibers into short chain fatty acids, which are both a source

of energy for intestinal cells and signaling molecules [21]. The microbiota can differ greatly between individuals and its disruption is associated with many diseases.

1.4 The intestinal immune system

The immune system in the human body protects it from infections by bacteria, viruses and parasites. A properly functioning immune system is important for human health, and it can be disrupted by compounds that can reduce our defense against infection or cause unwanted inflammation. The study of the potentially adverse interactions between compounds and the immune system is called immunotoxicology and requires a good understanding of how the immune system functions. There are two major parts to the immune system, the innate immune system and the adaptive immune system.

The innate immune system is provided by intestinal epithelial cells, and many other cells in our body. The innate immune system acts as a first line of defense against anything non-self. The innate immune system includes physical and biochemical barriers, and also immune cells designed for host defense responses [22]. Several cell types are involved in the innate immune system and some also provide critical signals to initiate adaptive immune responses. Cells involved in the innate immune system express receptors that respond to soluble components. Focusing on the intestine, the soluble components are often microbiota related. The soluble components contain so called molecular patterns which can be recognized by pattern recognition receptors (PRRs) present on intestinal epithelial cells [23]. The molecular patterns can be subdivided in damage-associated molecular patterns (DAMPs) and pathogen-associated molecular patterns (PAMPs). DAMPs relate to damaged cells and (sub)cellular fragments. DAMPS are also sometime referred to as alarmins [24]. PAMPs are parts of the functional systems of the respective microorganisms, and hence their structure is conserved as mutations likely result in diminished microorganism functioning [25, 26]. As a result these PAMPs are an optimal target for the innate immune system. In the intestinal epithelium the activation of the innate immune system leads to production of antimicrobial peptides by the Paneth cells but also causes the secretion of chemokines or cytokines that activate inflammatory pathways including the recruitment of immune cells. Compounds containing either PAMPs or DAMPs are often used in vaccines to initiate the innate immune response to improve the efficacy of the vaccination, as such they are often referred to as adjuvants [27].

The two key features of the adaptive immune system are specificity and memory. Specificity means that the adaptive immune system responds to specific infectious agents. Memory means that the adaptive immune system is capable of remembering the pathogen, and can more efficiently protect the host from subsequent infections by the same agent. The adaptive immune system has two branches, the humoral and the cell mediated immunity. The humoral immunity depends on the production of antigen-specific antibodies by B cells and coordinated interaction with other immune cells. The first step in this process is the binding of an antigen to the antigen receptor of the naïve B cells (and dendritic cells, collectively called antibody producing cells), which happens via soluble antigens that end up in the lymph or via antigen presenting cells. This leads to differentiation of naïve B cells into memory B cells and plasma cells that are able to generate antibodies that specifically recognize the presented antigen, this is called the antibody

response. These antibodies are excreted into the bloodstream where they will bind to the same antigens present near the infection and the antigen-antibody complexes thus formed either inactivate the microorganism or virus and/or mark them for destruction by other parts of the immune system. After the infection is cured the body still contains the memory B cells that upon the same exposure or infection can immediately activate the adaptive immune system [28, 29]. T cells on the other hand contain a receptor that recognizes a random pattern, after removing those T cells (in the thymus) that recognize the own body these are released into the bloodstream. Antigen presenting cells process an engulfed antigen and then present it on their surface on either MHC complex I or II. The T cells then recognize the combination of the MHC complex and the antigen, MHC II is limited to professional antigen presenting cells while MHC I is present on every nucleated cell. Because an antigen presenting cell is needed the second branch of the adaptive immune system is called the cell-mediated immunity. Antigen presenting cells present the antigen to different (sub)types of T cells. Depending on the T cell type this results either in a T cell memory or in T cells that can kill other antigen-infected cells [22, 30, 31].

In general, the innate immune response can be initiated by intestinal epithelial cells (and immune cells that reside in the intestinal epithelium) when exposed to anything non-self that contains a conserved molecular pattern while the adaptive immune system is dependent on the presence of (specific) immune cells. In this thesis the focus was on the intestinal epithelial and vascular endothelial cells, which implies that the studied responses are part of the innate immune system. The research in this thesis focused on the early steps in the innate immune response. As mentioned earlier, PRRs have a key role in the first steps of activating the innate immune response, Toll like receptors (TLRs) are a specific subset of PRRs. In the context of toxicology the relationship between an exposure and the eventual outcome, in this case inflammation, is often described in an Adverse Outcome Pathway (AOP). In an AOP a biological process is presented by defining a Molecular Initiating Event (MIE) that starts the process and is followed by a number of Key Events (KE) that represent important steps in the pathway that leads to the adverse outcome [32–34]. The binding of an adjuvant to the PRR represents the MIE considered in the thesis, and the responses studied can be considered as KEs related to immune effects [35]. More specifically, in the thesis the in vitro models selected were investigated for their potential to reflect the cytokine production upon PRR activation and thus to reflect the initial KE in an AOP following the MIE of TLR receptor activation.

The used exposures in this thesis are focused on adjuvants generated by pathogens containing PAMPs. For intestinal epithelial cells the presence of adjuvants containing PAMPs is an indication of an active infection leading to induction of an immune response. This immune response comes at the cost of energy, destroyed cells and stress for surrounding cells. Herein lies the challenge in the intestine in that the large intestine contains 10^{12} bacteria [20] all presenting adjuvants with a smaller number of bacteria and related adjuvants also being present in the small intestine. However, these bacteria are most of the time in a state of mutualism or commensalism with the host, so they do not harm and, in some cases, actually benefit the intestinal tissue [23]. So, there is a large number of adjuvants in the intestine that could initiate an immune response in the absence of an actual infection. This activation of the immune response by the

intestinal bacteria is partially prevented by the mucus that the goblet cells excrete. This layer of mucus not only is a food source for some microbes but also forms a barrier that prevents the bacteria from reaching the intestinal epithelial cells [11]. All these described elements together contributes to keeping a proper balance between pro- and anti-inflammatory signals [24].

1.5 Intestinal models used in toxicology

1.5.1 Animal models

The intestinal uptake (and subsequent systemic effects) of compounds were and still are mostly studied using animal tests, in which an animal is exposed orally to the compound and the blood plasma concentration is determined to reflect uptake. These *in vivo* experiments are generally performed in rodents (e.g. rats and mice), but also non-rodents (e.g. pigs, primates, dogs) or even humans might be used. Rodents are most frequently used due to their relatively low costs and the large database of available knowledge on these animal models. Other experimental animal species are chosen depending on the specific research question, due to the differences between the physiological, anatomical and microbiological characteristics of each animal model and the potential to translate this to the human body. Clearly, animal studies are not only used to study the intestinal uptake of compounds, but also to learn more about the potential toxicity of a compound. In the end all data derived from both toxicokinetic (absorption, distribution, metabolism and excretion) and toxicodynamic (mechanism of action) studies are taken into account when translating data to human health based guidance values. This translation is done by using an interspecies safety factor to extrapolate results obtained from animal models towards humans [36], and an intraspecies safety factor, which accounts for the variation within the human population [37].

Given the drawbacks of *in vivo* animal studies, such as that animals may not adequately reflect the human situation and that animal experiments are increasingly considered unethical, the development of so-called alternative testing strategies also called new approach methodologies (NAMs) has gained increased attention. The first step moving away from using experimental animals to study the intestinal uptake of compounds was taken by using *ex vivo* models, where material was taken from sacrificed experimental animals and kept in optimal conditions *in vitro*. If this is done using spare animals from other experiments this can help reduce animal use, but if animals are bred and sacrificed for these experiments the same ethical problems remain. An example of an *ex vivo* model is the Ussing chamber, in which a piece of intestinal tissue separates two chambers filled with fluid which allows for the measurement of transport [38]. However, *ex vivo* tissue models have a limited timeframe in which they can be used before the tissue start deteriorating and are still dependent on animal material. At the same time they bring the advantage of offering the complete cellular complexity of the organ, while not affecting the welfare of the animals used. Over time there has been a switch to *in vitro* models, not only because of ethical considerations but also because they can be based on human cells avoiding intraspecies differences.

1.5.2 *In vitro* models for studies on intestinal functions

In 1959 Russel and Burch wrote “The Principles of humane experimental technique” in which they introduced the 3Rs (Replacement, Reduction and Refinement) principle [39]. Starting with the ultimate

goal, replacement aiming at changing to methods that do not use animals. If replacement is not possible reduction aims at improving methods to get to similar levels of information and confidence with the use of less animals. Lastly refinement, aiming at improving animal experiment practices to minimize the pain and stress experienced by laboratory animals. Over time the emphasis on replacement has increased, through the trajectory "Transitie Proefdiervrije Innovatie" (TPI), the Netherlands wants to realize its ambition to be a frontrunner in the field of animal-free alternatives [40, 41]. Within the cosmetic sector, animal testing has already been banned completely, and the safety of novel compounds to be used in cosmetic products may not be studied using animals [42].

To achieve the replacement or at least reduction of animal experiments a large investment in developing and characterizing *in vitro* models is needed. In these models cells are grown on glass or plastic to allow for their exposure to compounds. The major advantage of these *in vitro* models is that they allow for the use of cells that originate from humans. As work described in this thesis focuses on human intestinal *in vitro* models, the introduction of *in vitro* models is limited to intestinal *in vitro* models. Most intestinal models were originally developed to be used as models for absorption. To achieve this cells are often grown in cell culture inserts, called Transwells, which are a sort of cup with a porous membrane on the bottom side. They are placed in a well with medium, after which cells are grown on the membrane. The cells form a barrier between the inside of the Transwell and the well it is placed in which allows for the measurement of transport over the cell layers. There are many options for cells that can be used and developments in the technology used to grow them (Table 1). While originally developed for absorption studies, intestinal *in vitro* models can also be used to study other intestinal functions such as interactions with the microbiota and intestinal inflammatory responses. Table 1 presents an overview of the different cell types and *in vitro* models that can be used to study intestinal functions and the models are described in more detail in the following sections.

Table 1 intestinal models used in Toxicological studies.

		Cell type(s)	Origin	Characteristics
Cell line				
Caco-2		Enterocyte	Human colon adenocarcinoma	Well characterized Small intestinal markers Need to be differentiated (21 days)
HT29-p		Enterocyte*		Undifferentiated, expression does change over time Microvilli
HT29-MTX		Goblet cell		Mucus production Already differentiated
T84		Colonocyte	Human colonic carcinoma (lung metastasis)	Colon markers Need to be differentiated (14-21 days)
Co-culture models				
Combined growth on apical side of the membrane e.g. Caco-2/HT29-MTX		Combination of intestinal cells mentioned above		Combined functions of respective cell lines Variation final ratio cells
Separated growth on apical and basolateral side of the membrane i.e. Caco-2/HMVEC-d		Intestinal cells with other cells i.e. blood vessel, immune relevant cells		Interaction of intestinal cells and cells from other organ(s) Varying growth medium
Stem cell based				
Adult stem cells	3D	Enterocyte Paneth cell M cell Tuft cell Stem cell	Patient/donor material from the intestine	Growth/differentiation over 7 days* Spheric form with the apical/lumen side on interior of organoid
	2D			Growth/differentiation over 10 days* Cell layers with an easy accessible apical side
Induced pluripotent stem cells	3D	Enterocyte Paneth cell Goblet cell Enteroendocrine cell Mesenchymal cell Stem cell	Patient/donor material (e.g. skin, blood, urine etc.)	Growth/differentiation over 42 days Spheric form with the apical/lumen side on interior iPSC cells commercially available
	2D			Growth/differentiation over 24 days iPSC cells commercially available Cell layers with an easy Apical side accessible apical side
Primary cell based				
Primary human small intestinal epithelial		Enterocyte, Paneth Cell M Cell, Tuft cell Stem cells	Patient/donor material	Ready to use tissue, no further differentiation needed Easy to use Expensive

2D = 2-Dimensional, 3D = 3-Dimensional. *depending on protocol used during growth

1.5.3 Primary cells

There are a number of options when choosing cells to be incorporated into an *in vitro* model. Primary cells are taken directly from living intestinal tissue. Afterwards these cells are grown in a specialized medium in which they can propagate. The advantage of these cells is that they represent completely differentiated cells that are close to the corresponding cells in healthy human individuals. However, they can only be maintained for a limited time before they start behaving differently because of changes in gene expression, cell functioning and cell morphology [43–45]. Another disadvantage can be the, sometimes large, inter-donor variability. While it has been attempted to use primary enterocytes in *in vitro* models this was not successful for a long time. More recently commercial models have been established like EpiIntestinal, which is a primary human small intestinal epithelial (PHSIE) cell model [46]. The model claims the presence of enterocytes, Paneth cells, M cells, tuft cells and intestinal stem cells with 3D villi structures, obtained from a single donor and grown on Transwells. The disadvantage of such primary cell models is that they are delivered directly from the supplier and cannot be sub-cultured in the lab, so for each experiment a new batch has to be ordered which comes with high costs and dependence on outside sources. Also, one can expect inter-donor so batch-to-batch variability. A more successful type of primary cell types that also can be incorporated into intestinal *in vitro* models are human microvascular endothelial cells (HMVEC) isolated from the skin or dermis (HMVEC-d). As said, this model contains cells from both blood and lymphatic vessels and can be co-cultured with intestinal epithelial cells. HMVEC-d cells can be sub-cultured for about 10 to 12 times before they are no longer considered reliable as a model for endothelial cells [47, 48].

1.5.4 Cell lines

Cell lines are immortalized cells that can be grown for a longer period of time, so they do not have to be replaced as often as primary cells. They also have less stringent requirements for the growth medium, since they do not require growth factors and can survive on simple sugars. As such these cell models are far cheaper to work with, with higher reproducibility. Most cell lines are derived from cancers in which cells grow uncontrollably. This requires mutations in many cellular pathways such as cell signaling, programmed cell death and energy household [49]. Their mutated characteristics also allow them to continuously multiply where they would normally die. The most well-known intestinal cell line is the Caco-2 cell line, which was derived from a human colorectal adenocarcinoma [50]. Even though these cells originate from the large intestine they were found to spontaneously differentiate into cells that exhibit small intestine enterocyte signatures, especially when grown on Transwells. The cells express some of the transporters found in the small intestine and form tight junctions between the cells though these are less permeable than what is observed in the *in vivo* situation [50]. They also form microvilli, leading to a similar increase in surface area as found in the human intestine [51–53]. As such the Caco-2 cells can be used as a model for transport in the human intestine when grown on Transwells. Many compounds have been found to transport similarly in this *in vitro* Caco-2 Transwell model to what is observed in the *in vivo* situation and as such it has been extensively used in toxicological research [50, 54].

Other frequently used intestinal cell lines are the HT29 cell line, which was similarly derived from a human colorectal adenocarcinoma but, in contrast to what is observed for the Caco-2 cells, the physiology of

HT29 cells largely depends on the growth protocol that is used. The parental cell line, or HT29-p, can still form many cell types with some protocols allowing for the formation of enterocyte like cells. HT29 cells were found to produce mucus if grown in the presence of methotrexate, though the exact composition of the produced mucus differs from that produced by the goblet cells *in vivo* [55]. The mucus producing HT29 cells were established as a subclone called HT29-MTX and are often used as a model for goblet cells. The mucus forms a barrier that is similarly found in the human intestine and can have an effect on transport. To this end the HT29-MTX cells are often grown in a co-culture together with Caco-2, providing a model that represents the two most prominent cell types found in the small intestinal epithelium. There are also many other intestinal cell lines that may each fulfill their own role. One example is the T84 cell line that provides cells that mimic colonocytes. This broad range of cell lines allows for the selection of specific cell lines depending on the research question studied (see table 1). It is also of interest to note that combined growth of cells from different intestinal cell lines on the apical side of the Transwell may lead to variations in the final ratio of cells due to varying growth rates [56], though this can be avoided using higher (or lower) seeding densities of the individual cells. Growing cells on the basolateral side of the Transwell, either on the membrane or in the medium, allows for the addition of a different cell type such as immune cells or blood vessel cells such as HMVEC-d to the intestinal Transwell model. This allows for expansion of the model to include the interaction between the different cells type themselves or upon stimulation with xenobiotics and or bacteria.

1.5.5 Stem cell based models

The third type of cell models available for *in vitro* studies on intestinal function are stem cell based models. Stem cells have nowadays been observed in most if not all tissues in our body and have the ability to differentiate into multiple different cell types. Undifferentiated they can proliferate for a longer period compared to differentiated cells, even when cultured outside the body. In toxicology the presence of multiple cell types and lack of mutations associated with cell lines means that the model better mimics certain aspects of the *in vivo* organ. The first example of exploiting intestinal stem cells was the establishment of 3D organoids derived from stem cells obtained from the intestine of mice in 2009 [57]. Since then the same has been done with stem cells obtained from human intestinal tissue that was left over after surgery [58].

Stem cells obtained from the organ itself are called adult stem cells, they are derived from maturate organs and can only differentiate into the cell types associated with that organ. The other type of stem cells are called induced pluripotent stem cells (iPSC), these can be derived from any cell type in the body and are de-differentiated towards stem cells that have the potential to differentiate into any cell type including the cell types present in the intestine. The differentiation of iPSC into intestinal cells is often done in multiple steps, to properly direct the differentiation [59–61]. As they first need to be differentiated into intestinal stem cells followed by differentiation into the various intestinal cells more time is needed to perform experiments than when using adult stem cells. Therefore, models based on adult stem cells only require a culture time of approximately seven or ten days, depending on whether they are grown as 3D organoid or as a cell layer, compared to approximately 42 and 24 days for iPSC based models. Also, the medium composition differs between the two types of stem cells, but media for both type of stem cells contain a selection of growth factors that can change over time to allow for gradual

differentiation. The advantage of (both) stem cell based models is that they can be derived from patient material, and are thus interesting in the field of personalized medicine and as disease models in toxicology. At the same time this allows for comparison of donor variability, giving insight into the interspecies differences. Stem cell derived intestinal models also contain most of the cell types found in the human intestine, the exact composition depending on stem cell source and culturing protocol used. Adult stem cell based organoids have been reported to differentiate better than iPSC derived organoids [17, 62]. The adult stem cells do require permission of patients and access to a hospital for material, the iPSC cells are commercially available and only require such permissions when material is needed from a specific patient. The same iPSCs once bought can also be used to generate other organ types, reducing donors and connections needed since each organ often comes from a different surgeon when obtaining patient material. A disadvantage of 3D (organoid) models is that exposure to compounds at the luminal side is technically challenging, which is especially problematic for transport studies. There is also an accumulation of cell debris on the luminal side, which can limit the time the organoids can be maintained before they need to be sub-cultured. A solution to this is growing stem cell derived cells on a Transwell coated with the extracellular matrix enabling the formation of a cell layer, and in this way forming a barrier similar to the Transwell models with Caco-2 cells [63]. These intestinal epithelial cell (IEC) layers can then be exposed in the same way as Caco-2 cell based models. At present, there is a large ongoing development in the methods for and application of these stem cell based models.

1.5.6 Dynamic culturing of *in vitro* models

Next to the potential use of different cell types in *in vitro* models, the way cells are grown can also be varied. As mentioned, intestinal cell models are frequently created on Transwell membranes. A recent and rapidly developing field is the use of microfluidic technology for growth of intestinal models to make so-called gut-on-a-chip devices. Depending on the chip design, these models generally include a flow of medium through two chambers that are separated by a porous membrane or barrier on which the intestinal cells are attached and grow. This allows for both a constant refreshing of the medium and for the cells to experience shear stress due to the medium flow. As described before, in the human intestine there is constant peristalsis that slowly pushes the bolus through the GI-tract. This means that the cells experience multiple forces, with the force induced by the bolus motion in the lumen being shear stress. Initial experiments with gut-on-a-chip devices showed that this shear stress caused cells to differentiate differently from cells grown on Transwells under static conditions [64, 65].

There are a number of designs currently in use for (micro)fluidic systems. The most basic design adjusts existing Transwells to include flow while maintaining the large cell culture area and volume, and relative ease of use. More advanced designs are made of parallel channels often made by pouring a plastic like PDMS into a mould to form the different parts of the chip [65, 66]. These chips allow for more directed flow over the cells enabling generation of higher shear stresses, but they often have a smaller cell culture area. The number of channels can differ per design with some designs introducing extra channels, for instance to allow incorporation of a separate microbiome compartment. The introduction of the microbiota in the system is one of the advantages of the presence of flow. In traditional static models bacteria tend to quickly overgrow the cells, whereas the introduced flow in gut-on-a-chip devices can remove excess bacteria. This allows for the study on the interaction between a living microbiome and the

intestinal cells [67, 68]. Given that the gut microbiota prefer to operate under anaerobic conditions multiple designs have been developed which include anaerobic compartments [68, 69]. The ability to include the microbiota is an added advantage of these microfluidic models while transport and effect studies are also still possible [70, 71].

Despite many advantages, these gut-on-a-chip models also come with their own disadvantages. Academic laboratories are often utilizing their own design and methodology, whereas in companies more often commercial devices are being used. There are some commercially available systems but these come with a high cost and require a highly-skilled and trained technicians technician and are generally low throughput [72]. There is currently a push to introduce a standardized design for these chips which would make comparison between studies easier [73]. At the same time this would pave the way for robust benchmarking of the system to change it into a well-defined model that can help replace animal studies.

1.6 Important compounds used in this thesis

In this thesis intestinal cell models have been exposed to several compounds that are known to interact with the intestinal epithelium. Compounds were selected to have a relation with the intestinal microbiome and/or the local intestinal immune system. The following sections provide some background information on the model compounds included in the studies, and the endpoints measured to study their effects in the selected *in vitro* models.

1.6.1 TLR agonists

As previously introduced this thesis focusses on the innate immune response initiated by compounds containing PAMPS. Specifically compounds containing PAMPs that activate the innate immune system via the Toll-like receptors (TLRs) which are a subset of the PRRs. Therefore, instead of using the more general term adjuvants or TLR ligand which only focusses on binding to the receptor, throughout this thesis compounds studied are called TLR agonists since we focus on compounds that activate the receptor. TLR agonists were selected because of their role in the interaction between the microbiota and the (host) intestinal epithelium, specifically because of the important role of TLR agonists as mediators of inflammatory pathways. TLR agonists are an important indicator for the human body of the presence of bacteria and serve to initiate the innate immune response. The large number of bacteria in the intestine means that there is a large presence of TLR agonists so it is important for an intestinal model to be able to recapitulate this interaction.

Similarly to how PAMPs are conserved between microorganisms TLRs are also conserved between many organisms, fulfilling the role of pattern recognition. There are ten functional TLRs in humans. To bind TLR agonists they form pairs with either the same TLR or one of the other TLRs [74, 75]. After binding the TLR agonists they activate the innate immune system, mostly via the myeloid differentiation primary response protein 88 (MyD88) dependent pathway [76]. Lipopeptides represent an important type of bacterial TLR agonists, being cell wall components found in both gram-positive and gram-negative bacteria. Pam3CSK4 is a synthetic triacetylated lipopeptide that is bound by a combination of TLR1 and TLR2 [77], and was tested in cell line-, stem cell- and primary cell based models in chapter 2 and 3 of this thesis. The second

TLR agonist used in the thesis was double stranded RNA (dsRNA), which is a hallmark for a group of viruses that use dsRNA as their genome. Most RNA such as that present in humans is single stranded, so all dsRNA is non-self and an indication of viral infection. Instead of a naturally occurring dsRNA a synthetic dsRNA Poly(I:C) was used which, like all dsRNA, is bound by TLR3 [78]. Poly(I:C) was tested in cell line and stem cell based models in chapter 2 and 3 respectively. The third TLR agonist used were lipopolysaccharides (LPS), large molecules that are present in the outer membrane of gram-negative bacteria that bind to TLR4 [79, 80]. LPS are important for the integrity of the outer membrane and most gram-negative bacteria without them are not viable [81]. LPS was tested in cell line, stem cell and primary cell based models in chapter 2 and 3. The fourth TLR agonist used was flagellin, which is part of the bacterial flagellum. The flagellum extrudes from the exterior of cells and is important for motility of bacteria, though some bacteria have incorporated it in a sensory organ [82]. Due to the importance of motility, flagellin is present in many bacteria and is thus recognized by the innate immune system, in this case via TLR5. Flagellin was tested in cell line, stem cell and primary cell based models in chapter 2 and 3. The last TLR agonist used in this thesis was single stranded RNA (ssRNA), which is similar to human RNA. The difference is that viral ssRNA, such as the ssRNA40 that was used, contains GU-rich sequences which are bound by TLR8 [83]. ssRNA40 was tested in cell line and stem cell based models in chapter 2 and 3 respectively.

1.6.2 Cytokines

Cytokines are signaling molecules involved in TLR mediated responses. As stated above, when TLR agonists bind to the TLRs they may activate the MyD88 pathway. Depending on the TLR, the TLR agonist and its position compared to the cell the exact response can differ but, there are always signaling molecules involved in the TLR response. These signaling molecules mostly are cytokines. The site of exposure of cells (apical or basolateral: i.e. the lumen side or the body side of an intestinal cell) to the TLR agonist is important because some TLRs are expressed more on one side or the other or inside the cell [84]. There are many different cytokines in the human body with each having its own role. It is important to understand that most of these cytokines have many effects, and those mentioned are often only the most important or well-known ones. In both chapter 2 and 3 of this thesis the production of the cytokines was measured to assess the capability of the tested TLR agonists to initiate an immune response in the different *in vitro* intestinal models. This was done to see if the models can be used to model this aspect of the interaction with the microbial TLR agonists. Excretion of Interleukin-8 (IL-8) by cell line, stem cell and primary cell models in response to a selection of TLR agonists was measured in both chapter 2 and 3. There are many different receptors that can bind IL-8 leading to different effects but its most common role is as a cytokine that attracts leukocytes, mostly neutrophils. These neutrophils then phagocytize infected cells, so the production, location and concentration of IL-8 is important to attract the neutrophiles to the correct cells [85, 86]. In chapter 3 the production of the chemokine (C-C) ligand 20 (CCL20) upon exposure of stem cell and primary cell based models to a selection of TLR agonists was measured. Similar to IL-8, CCL20 attracts leukocytes but, in this case, mostly lymphocytes such as natural killer cells that can distinguish infected from non-infected cells [87]. The third cytokine studied in the stem cell and primary cell based model of chapter 3 of this thesis is C-X-C motif chemokine ligand 10 (CXCL10), which similarly to CCL20 activates lymphocytes [88]. The last cytokine reported on in chapter 3 is interleukin-6, which moves to the liver and stimulates acute phase responses, stimulates antibody

production and can promote differentiation of some cell types [89, 90]. All four cytokines are considered pro-inflammatory cytokines and can cause further activation of the immune system, so their production in the cell lines, stem cell or primary cell based models upon exposure to Pam3CSK4, Poly(I:C), LPS, flagellin or ssRNA reflects an immune pathway activation.

1.6.3 Short chain fatty acids

While activation of the immune system mostly represents a negative interaction with the microbiota it is also known for its positive interactions. This happens via other signaling molecules and a model aiming to combine the intestinal epithelium and microbiota should also be able to recapitulate these interactions. One group of such signaling molecules are short chain fatty acids (SCFA). As already mentioned above SCFAs are produced by the microbiome upon the metabolism of dietary fibers. SCFAs are defined by having six or fewer carbon atoms. In chapter 4 three different SCFAs are exposed, acetate (2 carbon atoms), propionate (3 carbon atoms) and butyrate (4 carbon atoms), which are the three most common SCFAs [21, 91]. These compounds have many different effects in the human body, with the most basic one being a source of energy for many cell types. Furthermore, they have been shown to affect immune related signaling pathways, influence the barrier function of the intestinal epithelium, adjust proliferation and differentiation of intestinal epithelial cells and induce histone modification [92, 93]. A proper balance of SCFAs is important because a disbalance has been associated with diseases such as Inflammatory Bowel Disease (IBD) [94], Alzheimer's disease [95] and Parkinson's disease [96, 97]. Early studies on the effect of SCFAs using cell lines showed the induction of cell death which turned out to be specific to cancer cells like Caco-2 cells. It was found that due to mutations these cells can no longer use butyrate as a source of energy which causes intracellular accumulation and ultimately apoptosis [98–100]. More advanced models such as adult stem cell derived organoids were used to give improved insights in the actual effect of these SCFAs in the human intestine as they support the study of more benign effects such as changes in expression and production of selected differentiation markers and on barrier function [101].

1.7 Aim and outline of the thesis

There are currently large developments in improving intestinal models both in terms of the cell used and in terms of technology of devices to grow cells in. These developments include the definition of alternatives to both the traditional Caco-2 cells and to the Transwell model system. The advances create opportunities for exciting new studies. The aim of the research in this thesis was to explore the use, advantages and disadvantages of intestinal models available to study interactions of intestinal cells with the microbiota and to fill in some of the gaps in available knowledge needed for future studies in this direction.

In **chapter 2** the ability of cell lines to induce an immune response via TLR interactions after exposure to a selection of TLR agonists was assessed. This was used to see if these models can be used to study the interaction of the microbiota with the innate immune system of the intestinal epithelium. To this end Caco-2 and HT29-p monocultures, Caco-2/HT29-MTX co-cultures and Caco-2/HT29-MTX/HMVEC-d co-cultures were exposed to Pam3CSK4, Poly(I:C), LPS, flagellin and ssRNA. IL-8, a pro-inflammatory cytokine, was measured to assess the response of the cells. Since the cell lines showed limited responses to the agonists, in **chapter 3** the ability of two more advanced models, iPSC derived organoids and PHSIE, to

induce an immune response via TLR interactions after exposure to a selection of TLR agonists was assessed. To this end iPSC derived organoids and PHSIE were exposed to Pam3CSK4, Poly(I:C), LPS, flagellin and ssRNA. The induced production of multiple cytokines was measured, including CCL20, CXCL10, IL-6 and IL-8. In **chapter 4** the focus switched to interactions of the microbiota and intestinal epithelium via signaling molecules, in this case SCFAs produced by the microbiota via the metabolism of dietary fibers. To this end iPSC derived intestinal epithelial cell layers were exposed to three SCFAs, butyrate, propionate and acetate and RNA-sequencing was performed to characterize the response of all processes on a gene expression level. In **chapter 5** existing gene expression data sets of intestinal models that can be used for transport studies were extracted from literature and checked for the effects of selected *in vitro* experimental variables on gene expression. This was done to see how these variables influence the intestinal models and their reproducibility and to check certain claims made in relation to these variables, all in order to define how use of the intestinal models can be improved in the future. Lastly, in **chapter 6** a general discussion is presented on the results obtained along with future perspectives.

References

1. RIVM. Voedsel-consumptie in Nederland. 2016.
2. Hounnou G, Destrieux C, Desmé J, Bertrand P, Velut S. Anatomical study of the length of the human intestine. Surg Radiol Anat. 2002;24:290–4.
3. Mandel ID. The Functions of Saliva. J Dent Res. 1987;66:623–7.
4. Humphrey SP, Williamson RT. A review of saliva: Normal composition, flow, and function. J Prosthet Dent. 2001;85:162–9.
5. Allen A, Flemström G. Gastroduodenal mucus bicarbonate barrier: Protection against acid and pepsin. Am J Physiol - Cell Physiol. 2005;288 1 57-1.
6. Whitcomb DC, Lowe ME. Human pancreatic digestive enzymes. Digestive diseases and sciences. 2007;52:1–17.
7. Turnbaugh PJ, Ley RE, Mahowald MA, Magrini V, Mardis ER, Gordon JI. An obesity-associated gut microbiome with increased capacity for energy harvest. Nat 2006 4447122. 2006;444:1027–31.
8. Mucosa: Image Details - NCI Visuals Online. https://visualsonline.cancer.gov/details.cfm?imageid=1781. Accessed 14 Jan 2023.
9. Clevers HC, Bevins CL. Paneth Cells: Maestros of the Small Intestinal Crypts. https://doi-org.ezproxy.library.wur.nl/101146/annurev-physiol-030212-183744. 2013;75:289–311.
10. Snoeck V, Goddeeris B, Cox E. The role of enterocytes in the intestinal barrier function and antigen uptake. Microbes Infect. 2005;7:997–1004.
11. McCauley HA, Guasch G. Three cheers for the goblet cell: maintaining homeostasis in mucosal epithelia. Trends Mol Med. 2015;21:492–503.
12. Birchenough GMH, Johansson MEV, Gustafsson JK, Bergström JH, Hansson GC. New developments in goblet cell mucus secretion and function. Mucosal Immunol 2015 84. 2015;8:712–9.
13. Gribble FM, Reimann F. Function and mechanisms of enteroendocrine cells and gut hormones in metabolism. Nat Rev Endocrinol 2019 154. 2019;15:226–37.
14. Gunawardene AR, Corfe BM, Staton CA. Classification and functions of enteroendocrine cells of the lower gastrointestinal tract. Int J Exp Pathol. 2011;92:219–31.
15. Kraehenbuhl JP, Neutra MR. Epithelial M Cells: Differentiation and Function. https://doi-org.ezproxy.library.wur.nl/101146/annurev.cellbio161301. 2003;16:301–32.
16. Gerbe F, Sidot E, Smyth DJ, Ohmoto M, Matsumoto I, Dardalhon V, et al. Intestinal epithelial tuft cells initiate type 2 mucosal immunity to helminth parasites. Nat 2016 5297585. 2016;529:226–30.

17. Creff J, Malaquin L, Besson A. In vitro models of intestinal epithelium: Toward bioengineered systems. J Tissue Eng. 2021;12.
18. Creative Commons — Attribution-NonCommercial 4.0 International — CC BY-NC 4.0. https://creativecommons.org/licenses/by-nc/4.0/. Accessed 15 Jan 2023.
19. Devriese S, Van den Bossche L, Van Welden S, Holvoet T, Pinheiro I, Hindryckx P, et al. T84 monolayers are superior to Caco-2 as a model system of colonocytes. Histochem Cell Biol 2017 1481. 2017;148:85–93.
20. Sender R, Fuchs S, Milo R. Revised Estimates for the Number of Human and Bacteria Cells in the Body. PLoS Biol. 2016;14.
21. Koh A, De Vadder F, Kovatcheva-Datchary P, Bäckhed F. From Dietary Fiber to Host Physiology: Short-Chain Fatty Acids as Key Bacterial Metabolites. Cell. 2016;165:1332–45.
22. Klaassen C, Casarett LJ, Doull J. Casarett & Doull's Toxicology: The Basic Science of Poisons, Eighth Edition. McGraw-Hill Education; 2013.
23. Takeuchi O, Akira S. Pattern Recognition Receptors and Inflammation. Cell. 2010;140:805–20.
24. Bianchi ME. DAMPs, PAMPs and alarmins: all we need to know about danger. J Leukoc Biol. 2007;81:1–5.
25. Kawai T, Akira S. The role of pattern-recognition receptors in innate immunity: update on Toll-like receptors. Nat Immunol 2010 115. 2010;11:373–84.
26. Janeway CA, Medzhitov R. Innate immune recognition. Annu Rev Immunol. 2002;20:197–216.
27. Pulendran B, S. Arunachalam P, O'Hagan DT. Emerging concepts in the science of vaccine adjuvants. Nat Rev Drug Discov 2021 206. 2021;20:454–75.
28. Akkaya M, Kwak K, Pierce SK. B cell memory: building two walls of protection against pathogens. Nat Rev Immunol. 2020;20:229–38.
29. Cyster JG, Allen CDC. B Cell Responses: Cell Interaction Dynamics and Decisions. Cell. 2019;177:524–40.
30. Alberts B, Johnson A, Lewis J, Walter P, Raff M, Roberts K. Molecular Biology of the Cell 4th Edition: International Student Edition. Routledge; 2002.
31. Annunziato F, Romagnani C, Romagnani S. The 3 major types of innate and adaptive cell-mediated effector immunity. J Allergy Clin Immunol. 2015;135:626–35.
32. Lozano-Ojalvo D, Benedé S, Antunes CM, Bavaro SL, Bouchaud G, Costa A, et al. Applying the adverse outcome pathway (AOP) for food sensitization to support in vitro testing strategies. Trends Food Sci Technol. 2019;85:307–19.
33. Ankley GT, Bennett RS, Erickson RJ, Hoff DJ, Hornung MW, Johnson RD, et al. Adverse outcome pathways: A conceptual framework to support ecotoxicology research and risk assessment. Environ Toxicol Chem. 2010;29:730–41.
34. OECD. Handbook supplement to the Guidance Document for developing and assessing Adverse Outcome Pathways. 2018. https://doi.org/https://doi.org/https://doi.org/10.1787/5jlv1m9d1g32-en.
35. Selvaraj S, Oh JH, Borlak J. An adverse outcome pathway for immune-mediated and allergic hepatitis: a case study with the NSAID diclofenac. Arch Toxicol. 2020;94:2733.
36. Center for Drug Evaluation and Research. Guidance for Industry: Estimating the Maximum Safe Starting Dose in Initial Clinical Trials for Therapeutics in Adult Healthy Volunteers. 2005.
37. Mak IWY, Evaniew N, Ghert M. Lost in translation: animal models and clinical trials in cancer treatment. Am J Transl Res. 2014;6:114.
38. Clarke LL. A guide to Ussing chamber studies of mouse intestine. Am J Physiol Gastrointest Liver Physiol. 2009;296.
39. Russell WMS, Burch RL. The principles of humane experimental technique. 1959.
40. Staghouwer H. Kamerbrief commissiedebat dierproeven en transitie proefdiervrije innovatie. 2022.
41. Animal Free Innovation TPI. https://www.animalfreeinnovationtpi.nl/. Accessed 18 Jan 2023.

42. EUR-LEX. Regulation (EC) No 1223/2009 of the European Parliament and of the Council of 30 November 2009 on cosmetic products (recast) (Text with EEA relevance). 2009.
43. Jaffe EA, Nachman RL, Becker CG, Minick CR. Culture of human endothelial cells derived from umbilical veins. Identification by morphologic and immunologic criteria. J Clin Invest. 1973;52:2745–56.
44. Bachetti T, Morbidelli L. Endothelial cells in culture: A model for studying vascular functions. Pharmacol Res. 2000;42:9–19.
45. Bouïs D, Hospers GAP, Meijer C, Molema G, Mulder NH. Endothelium in vitro: A review of human vascular endothelial cell lines for blood vessel-related research. Angiogenesis. 2001;4:91–102.
46. Ayehunie S, Stevens Z, Landry T, Klausner M, Hayden P, Letasiova S. Novel 3-D human small intestinal tissue model to assess drug permeation, inflammation, and wound healing. Toxicol Lett. 2014;229:S144.
47. Maschmeyer I, Hasenberg T, Jaenicke A, Lindner M, Lorenz AK, Zech J, et al. Chip-based human liver–intestine and liver–skin co-cultures – A first step toward systemic repeated dose substance testing in vitro. Eur J Pharm Biopharm. 2015;95:77–87.
48. Schimek K, Busek M, Brincker S, Groth B, Hoffmann S, Lauster R, et al. Integrating biological vasculature into a multi-organ-chip microsystem. Lab Chip. 2013;13:3588–98.
49. Maqsood MI, Matin MM, Bahrami AR, Ghasroldasht MM. Immortality of cell lines: challenges and advantages of establishment. Cell Biol Int. 2013;37:1038–45.
50. Artursson P, Palm K, Luthman K. Caco-2 monolayers in experimental and theoretical predictions of drug transport. Adv Drug Deliv Rev. 2001;46:27–43.
51. Pinto M, Robine-Leon S, Appay MD, Kedinger M, Triadou N, Dussaulx E, et al. Enterocyte-like differentiation and polarization of the human colon carcinoma cell line Caco-2 in culture. BiolCell. 1983;47:323–30.
52. Hidalgo IJ, Raub TJ, Borchardt RT. Characterization of the human colon carcinoma cell line (Caco-2) as a model system for intestinal epithelial permeability. Gastroenterology. 1989;96:736–49.
53. Wilson G, Hassan IF, Dix CJ, Williamson I, Shah R, Mackay M, et al. Transport and permeability properties of human Caco-2 cells: An in vitro model of the intestinal epithelial cell barrier. J Control Release. 1990;11:25–40.
54. Hubatsch I, Ragnarsson EGE, Artursson P. Determination of drug permeability and prediction of drug absorption in Caco-2 monolayers. Nat Protoc. 2007;2:2111–9.
55. Martínez-Maqueda D, Miralles B, Recio I. HT29 cell line. In: The Impact of Food Bioactives on Health: In Vitro and Ex Vivo Models. Springer International Publishing; 2015. p. 113–24.
56. Briske-Anderson MJ, Finley JW, Newman SM. The Influence of Culture Time and Passage Number on the Morphological and Physiological Development of Caco-2 Cells. Proc Soc Exp Biol Med. 1997;214:248–57.
57. Sato T, Vries RG, Snippert HJ, Van De Wetering M, Barker N, Stange DE, et al. Single Lgr5 stem cells build crypt-villus structures in vitro without a mesenchymal niche. Nat 2009 4597244. 2009;459:262–5.
58. Sato T, Stange DE, Ferrante M, Vries RGJ, van Es JH, van den Brink S, et al. Long-term Expansion of Epithelial Organoids From Human Colon, Adenoma, Adenocarcinoma, and Barrett's Epithelium. Gastroenterology. 2011;141:1762–72.
59. Mccracken KW, Howell JC, Wells JM, Spence JR, Org; KM, Org; JH, et al. Generating human intestinal tissue from pluripotent stem cells in vitro. Nat Protoc. 2011;6:1920–8.
60. Tamminen K, Balboa D, Toivonen S, Pakarinen MP, Wiener Z, Alitalo K, et al. Intestinal Commitment and Maturation of Human Pluripotent Stem Cells Is Independent of Exogenous FGF4 and R-spondin1. PLoS One. 2015;10:e0134551–e0134551.
61. Watson CL, Mahe MM, Múnera J, Howell JC, Sundaram N, Poling HM, et al. An in vivo model of human small intestine using pluripotent stem cells. Nat Med. 2014;20:1310–4.
62. Jung KB, Lee H, Son YS, Lee MO, Kim YD, Oh SJ, et al. Interleukin-2 induces the in vitro maturation of

human pluripotent stem cell-derived intestinal organoids. Nat Commun 2018 91. 2018;9:1–13.
63. Kabeya T, Mima S, Imakura Y, Miyashita T, Ogura I, Yamada T, et al. Pharmacokinetic functions of human induced pluripotent stem cell-derived small intestinal epithelial cells. Drug Metab Pharmacokinet. 2020;35:374–82.
64. Fois CAM, Schindeler A, Valtchev P, Dehghani F. Dynamic flow and shear stress as key parameters for intestinal cells morphology and polarization in an organ-on-a-chip model. Biomed Microdevices. 2021;23:1–12.
65. Kim HJ, Ingber DE. Gut-on-a-Chip microenvironment induces human intestinal cells to undergo villus differentiation. Integr Biol. 2013;5:1130.
66. Shim KY, Lee D, Han J, Nguyen NT, Park S, Sung JH. Microfluidic gut-on-a-chip with three-dimensional villi structure. Biomed Microdevices. 2017;19:1–10.
67. Kim HJ, Li H, Collins JJ, Ingber DE. Contributions of microbiome and mechanical deformation to intestinal bacterial overgrowth and inflammation in a human gut-on-a-chip. Proc Natl Acad Sci U S A. 2016;113:E7–15.
68. Shah P, Fritz J V., Glaab E, Desai MS, Greenhalgh K, Frachet A, et al. A microfluidics-based in vitro model of the gastrointestinal human-microbe interface. Nat Commun. 2016;7:1–15.
69. Jalili-Firoozinezhad S, Gazzaniga FS, Calamari EL, Camacho DM, Fadel CW, Bein A, et al. A complex human gut microbiome cultured in an anaerobic intestine-on-a-chip. Nat Biomed Eng 2019 37. 2019;3:520–31.
70. Kulthong K, Duivenvoorde L, Mizera BZ, Rijkers D, Dam G Ten, Oegema G, et al. Implementation of a dynamic intestinal gut-on-a-chip barrier model for transport studies of lipophilic dioxin congeners. RSC Adv. 2018;8:32440–53.
71. Kulthong K, Duivenvoorde L, Sun H, Confederat S, Wu J, Spenkelink B, et al. Microfluidic chip for culturing intestinal epithelial cell layers: Characterization and comparison of drug transport between dynamic and static models. Toxicol Vitr. 2020;65:104815.
72. Ma C, Peng Y, Li H, Chen W. Organ-on-a-Chip: A New Paradigm for Drug Development. Trends Pharmacol Sci. 2021;42:119–33.
73. Vollertsen AR, Vivas A, van Meer B, van den Berg A, Odijk M, van der Meer AD. Facilitating implementation of organs-on-chips by open platform technology. Biomicrofluidics. 2021;15:1ENG.
74. Price AE, Shamardani K, Lugo KA, Deguine J, Roberts AW, Lee BL, et al. A Map of Toll-like Receptor Expression in the Intestinal Epithelium Reveals Distinct Spatial, Cell Type-Specific, and Temporal Patterns. Immunity. 2018;49:560-575.e6.
75. Ozinsky A, Underhill DM, Fontenot JD, Hajjar AM, Smith KD, Wilson CB, et al. The repertoire for pattern recognition of pathogens by the innate immune system is defined by cooperation between Toll-like receptors. Proc Natl Acad Sci U S A. 2000;97:13766–71.
76. Takeda K, Akira S. TLR signaling pathways. Semin Immunol. 2004;16:3–9.
77. Weng M, Walker WA, Sanderson IR. Butyrate regulates the expression of pathogen-triggered IL-8 in intestinal epithelia. Pediatr Res. 2007;62:542–6.
78. Fortier ME, Kent S, Ashdown H, Poole S, Boksa P, Luheshi GN. The viral mimic, polyinosinic:polycytidylic acid, induces fever in rats via an interleukin-1-dependent mechanism. Am J Physiol - Regul Integr Comp Physiol. 2004;287 4 56-4.
79. Faure E, Equils O, Sieling PA, Thomas L, Zhang FX, Kirschning CJ, et al. Bacterial lipopolysaccharide activates NF-κB through toll-like receptor 4 (TLR-4) in cultured human dermal endothelial cells. Differential expression of TLR-4 and TLR-2 in endothelial cells. J Biol Chem. 2000;275:11058–63.
80. Triantafilou M, Triantafilou K. Lipopolysaccharide recognition: CD14, TLRs and the LPS-activation cluster. Trends in Immunology. 2002;23:301–4.
81. Caroff M, Karibian D. Structure of bacterial lipopolysaccharides. Carbohydr Res. 2003;338:2431–47.
82. Haiko J, Westerlund-Wikström B. The role of the bacterial flagellum in adhesion and virulence.

Biology. 2013;2:1242–67.
83. Triantafilou K, Vakakis E, Orthopoulos G, Ahmed MAE, Schumann C, Lepper PM, et al. TLR8 and TLR7 are involved in the host's immune response to human parechovirus 1. Eur J Immunol. 2005;35:2416–23.
84. Abreu MT. Toll-like receptor signalling in the intestinal epithelium: how bacterial recognition shapes intestinal function. Nat Rev Immunol 2010 102. 2010;10:131–44.
85. Mitsuyama K, Toyonaga A, Sasaki E, Watanabe K, Tateishi H, Nishiyama T, et al. IL-8 as an important chemoattractant for neutrophils in ulcerative colitis and Crohn's disease. Clin Exp Immunol. 1994;96:432–6.
86. Kucharzik T, Hudson JT, Lügering A, Abbas JA, Bettini M, Lake JG, et al. Acute induction of human IL-8 production by intestinal epithelium triggers neutrophil infiltration without mucosal injury. Gut. 2005. https://doi.org/10.1136/gut.2004.061168.
87. Schutyser E, Struyf S, Van Damme J. The CC chemokine CCL20 and its receptor CCR6. Cytokine Growth Factor Rev. 2003;14:409–26.
88. Lee EY, Lee ZH, Song YW. CXCL10 and autoimmune diseases. Autoimmun Rev. 2009;8:379–83.
89. Kimura A, Kishimoto T. IL-6: Regulator of Treg/Th17 balance. Eur J Immunol. 2010;40:1830–5.
90. Castell J V., Gómez-Lechón MJ, David M, Andus T, Geiger T, Trullenque R, et al. Interleukin-6 is the major regulator of acute phase protein synthesis in adult human hepatocytes. FEBS Lett. 1989;242:237–9.
91. Cummings JH, Pomare EW, Branch HWJ, Naylor CPE, MacFarlane GT. Short chain fatty acids in human large intestine, portal, hepatic and venous blood. Gut. 1987;28:1221–7.
92. Hamer HM, Jonkers D, Venema K, Vanhoutvin S, Troost FJ, Brummer RJ. Review article: the role of butyrate on colonic function. Aliment Pharmacol Ther. 2008;27:104–19.
93. van der Hee B, Wells JM. Microbial Regulation of Host Physiology by Short-chain Fatty Acids. Trends Microbiol. 2021;29:700–12.
94. Venegas DP, De La Fuente MK, Landskron G, González MJ, Quera R, Dijkstra G, et al. Short chain fatty acids (SCFAs)mediated gut epithelial and immune regulation and its relevance for inflammatory bowel diseases. Front Immunol. 2019;10 MAR:277.
95. Chen H, Meng L, Shen L. Multiple roles of short-chain fatty acids in Alzheimer disease. Nutrition. 2022;93.
96. Li W, Wu X, Hu X, Wang T, Liang S, Duan Y, et al. Structural changes of gut microbiota in Parkinson's disease and its correlation with clinical features. Sci China Life Sci 2017 6011. 2017;60:1223–33.
97. Sun MF, Zhu YL, Zhou ZL, Jia XB, Xu Y Da, Yang Q, et al. Neuroprotective effects of fecal microbiota transplantation on MPTP-induced Parkinson's disease mice: Gut microbiota, glial reaction and TLR4/TNF-α signaling pathway. Brain Behav Immun. 2018;70:48–60.
98. Lupton JR. Microbial Degradation Products Influence Colon Cancer Risk: the Butyrate Controversy. J Nutr. 2004;134:479–82.
99. Ryu SH, Kaiko GE, Stappenbeck TS. Cellular differentiation: Potential insight into butyrate paradox? Mol Cell Oncol. 2018;5:1212685.
100. Salvi PS, Cowles RA. Butyrate and the Intestinal Epithelium: Modulation of Proliferation and Inflammation in Homeostasis and Disease. Cells 2021, Vol 10, Page 1775. 2021;10:1775.
101. Pearce SC, Weber GJ, Van Sambeek DM, Soares JW, Racicot K, Breault DT. Intestinal enteroids recapitulate the effects of short-chain fatty acids on the intestinal epithelium. PLoS One. 2020;15:e0230231.

Chapter 2

Responses of increasingly complex intestinal epithelium in vitro models to bacterial Toll-like receptor agonists

Based on: Grouls M, van der Zande M, de Haan L, Bouwmeester H. Responses of increasingly complex intestinal epithelium in vitro models to bacterial toll-like receptor agonists. Toxicol In Vitro. 2022 Mar;79:105280. doi: 10.1016/j.tiv.2021.105280. Epub 2021 Nov 27. PMID: 34843883.

Menno Grouls[1], Meike van der Zande[2], Laura de Haan[1], Hans Bouwmeester[1]

[1] Division of Toxicology, Wageningen University and Research, Wageningen, The Netherlands;
[2] Wageningen Food Safety Research, Wageningen University and Research, Wageningen, The Netherlands

Highlights:

- Flagellin increased IL-8 apical secretion in all tested in vitro intestinal models
- IL-8 secretion was lower basolaterally than apically except in HT29-p cells
- Poly (I:C) increased IL-8 secretion in HT29-p cells only
- Di-culture model of Caco-2/ HT29-MTX has no additional value to study immunomodulation

Abstract

The intestine fulfills roles in the uptake of nutrients and water regulation and acts as a gatekeeper for the intestinal microbiome. For the latter, the intestinal gut barrier system is able to respond to a broad range of bacterial adjuvants, generally through Toll-like receptor (TLR) signaling pathways. To test the capacity of various *in vitro* intestinal models, we studied IL-8 secretion, as a marker of pro-inflammatory response through the TLR pathway, in a Caco-2 monoculture, Caco-2/HT29-MTX di-culture, Caco-2/HT29-MTX/HMVEC-d tri-culture and in a HT29-p monoculture in response to exposure to various TLR agonists. Twenty-one-day-old differentiated cells in Transwells were exposed to Pam3CSK4 (TLR1/2), lipopolysaccharide (TLR4), single-stranded RNA (TLR7/8), Poly(I:C) (TLR3) and flagellin (TLR5) for 24 hours. In all systems IL-8 secretion was increased in response to flagellin exposure, with HT29-p cells also responding to Poly(I:C) exposure. All other agonists did not induce an IL-8 response in the tested *in vitro* models, indicating that the specific TLRs are either not present or not functional in these models. This highlights the need for careful selection of *in vitro* models when studying intestinal immune responses and the need for improved *in vitro* models that better recapitulate intestinal immune responses.

Keywords: Intestine, complex *in vitro* models, Toll-like receptors, Toll-like receptor pathways, IL-8

2.1 Introduction

The intestine fulfills many roles such as digestion of food, nutrient uptake, water regulation and it acts as a gatekeeper for the intestinal microbiome [1]. Specifically, the intestinal epithelium fulfills many of these roles and contains different cell types supporting these different functions of the intestine. *In vitro* systems that can emulate these different functions of the intestinal epithelium are important for the acute toxicological assessment of chemicals. Current intestinal epithelium *in vitro* systems heavily rely on immortalized cell lines like Caco-2. Although Caco-2 cells originate from a large intestinal source, in culture they differentiate into cells with a functionality resembling that of small intestinal enterocytes. Monolayers of differentiated Caco-2 cells are commonly used as a model to assess the potential transport of compounds from the intestine into the systemic blood circulation. This Caco-2 cell-layer model has shown a high predictability towards intestinal transport *in vivo* for certain compounds [2]. In addition, this model has also been used to study direct effects of chemicals on the intestinal epithelium and to study interactions between the epithelium and bacteria residing in the human intestine [3, 4].

Interactions between commensal bacteria and the intestinal epithelium influence many aspects of the intestinal functionality, including immune responses, metabolism of exogenous substances and barrier integrity [5]. Interactions of commensal bacteria and pathogenic bacteria with the intestinal epithelium can activate immune responses. Toll-like receptors (TLRs), expressed on intestinal epithelial cells, play a crucial role in the recognition of the different bacteria. TLRs can be activated by pathogen associated molecular patterns (PAMPs), which are structurally conserved molecular components located intracellularly and on the surface of bacteria [6]. Different TLRs recognize specific PAMPs and the various cell types in the human intestinal epithelium display different TLR expression patterns, so not every intestinal epithelial cell type has the same TLRs [7]. Binding of a bacterial TLR agonist to a specific TLR activates an innate immune response. Intracellularly, the TLR signal transduction initiates the myeloid differentiation primary response protein 88 (MyD88) pathway, which leads to the production of pro-inflammatory cytokines such as IL-8 [8]. The recruitment of neutrophils from the blood and lymphatic system caused by the IL-8 secretion initiates the next steps in the intestinal innate immune response. [9–11].

The TLR1/2 heterodimer recognizes, amongst others, bacterial triacyl lipopeptides, TLR3 recognizes dsRNA, TLR4 recognizes lipopolysaccharides (LPS), TLR5 is well-known for recognizing flagellin, and lastly TLR7 and 8 both recognize ssRNA. The most commonly used *in vitro* intestinal epithelial model, Caco-2 cells, is an obvious choice to develop an intestinal model combining the intestinal barrier with the microbiome. Current knowledge however, indicates the presence of TLR3 and TLR5, but absence of TLR2 and TLR4 in Caco-2 cells [12]. The presence of the other TLRs in Caco-2 cells is largely unknown. Absence of TLRs leads to an inability to respond to microbial TLR agonists like LPS. Therefore, to obtain the full range of TLR agonist responsiveness co-culturing of Caco-2 cells with other intestinal cell-types needs to be explored.

HT29-parental (HT29-p) cells were isolated from a colorectal adenocarcinoma and were shown to behave differently depending on the culture method. In glucose containing medium they mostly form a multilayer of undifferentiated intestinal cells. Exposure of the HT29-p cells to methotrexate results in cells with an

increased mucus production (the so-called HT29-MTX cells). Therefore these cells, are considered an *in vitro* model for goblet cells [13]. Mucus is an important intestinal barrier and energy source for intestinal bacteria and is thus an important feature to enable coculture of intestinal epithelial cells with a microbiome in future experiments [14, 15].

Lastly, vascular endothelial cells have an important function in the intestinal mucosa[16, 17], not so much in terms of barrier properties, but mainly for signaling and communication between epithelial cells. HMVEC-d cells are human dermal microvascular cells isolated from small vessels within the skin and are commonly used as an endothelial cell model[18, 19]. Models combining microvascular cells and Caco-2 cells have previously been used to study interactions between the cells and the microbiome[20, 21]. They have been shown to express most TLRs except for TLR7, 8 and 10 [22]. It has been shown that TLR agonists, like LPS, can be transported through the intestinal epithelium, so endothelial cells can also play a role in the intestinal immune responses [23]. There are multiple studies that show that different intestinal epithelial cells and HMVEC-d cells that show different immune responses and TLR expression patterns compared to Caco-2 cells [24, 25]. Combining all these different cells into one model may potentially result in a model that is able to respond to a larger variety of bacterial TLR agonists [26].

We aim to create an *in vitro* gut barrier system that is able to respond to a broad range of bacterial TLR agonists. To do this, we expand on the traditional Caco-2 monolayer cultured in Transwells by the addition of different cell types and we evaluated the contribution of the different cells on the immuno-responsiveness of the model by exposure to a panel of TLR agonists. As an immune response readout we measured the production of IL-8 [8]. The selected agonists and their targets were Pam3CSK4 (TLR1/2), poly(I:C) (TLR3), lipopolysaccharide (TLR2/4), flagellin (TLR5) and single-stranded RNA (TLR7/8).

2.2 Materials and methods

2.2.1 Cell lines

The human intestinal epithelial Caco-2 (ATCC HTB-37) cell line was used from passage 5 to 30 and HT29-p (ATCC HTB38) cells, used from passage 5 to 30, were obtained from ATCC (United Kingdom). The mucus secreting HT29-MTX-E12 (ECACC 12040401) cell line (further referred to as HT29-MTX) was used from passage 5 to 30 and was obtained from the HPA culture collections (Sigma-Aldrich, Germany). The human dermal microvascular cell line HMVEC-d used until passage 10 was obtained from Lonza (Bazel Switzerland). Caco-2, HT29-MTX and HT29-p were cultured in Dulbecco's modified Eagle's medium + GlutaMAX (DMEM+GlutaMAX, Life technologies, Belgium) with 10% FCS (Sigma-Aldrich, The Netherlands), 1% non-essential amino acids (Invitrogen, Breda, The Netherlands) and 1% penicillin/streptomycin (Invitrogen, The Netherlands), further referred to as complete medium. HMVEC-d was grown in Microvascular Endothelial Basal Medium (Sigma-Aldrich, The Netherlands) with Microvascular Endothelial Cell Growth Supplements (Sigma-Aldrich, The Netherlands). The cells were grown in 75 cm^2 flasks (Greiner, The Netherlands) at 37°C 5% CO_2 in an incubator and passaged by trypsinization at 70-90% confluence.

2.2.2 TLR agonists

TLR1/2 agonist Pam3CSK4, TLR3 agonist Poly(I:C) high molecular weight, TLR2 and 4 agonist standard LPS from *E. coli* O111:B4, TLR5 agonist flagellin from *S. typhimurium* Ultrapure and TLR8 agonist ssRNA40/LyoVec were obtained from InvivoGen (France).

2.2.3 Transwell culture

Cells were grown in 12-well Transwell permeable supports, with an 0.4 µm polycarbonate membrane of Corning costar (VWR, the Netherlands). These were coated with a Collagen-1 solution from human fibroblasts (Sigma-Aldrich, The Netherlands) at 10 µg/cm^2 by dissolving the Collagen-1 in 0.25 acetic acid and incubating the solution at 37°C for at least three hours in the Transwell inserts before removing the liquid. All Transwells were seeded apically at 4x10^4 cells per insert. For the di-culture of Caco-2/HT29-MTX cells were seeded at a 3:1 ratio. Cells were maintained in complete medium for 21 days which is required for the differentiation of Caco-2 cells [27], the medium was replaced three times per week.

For the tri-culture model, HMVEC-d cells were seeded on the basolateral side of the Transwells on day 0 before seeding the epithelial cells on the apical side. To do this, the Transwell inserts were inverted and placed on the lid of a 6-well plate placing sterile caps of Eppendorf tubes on the corners to avoid contact between the lid and the drops [28]. HMVEC-d cells were seeded at 2x10^4 cells per Transwell by pipetting a droplet onto the inverted inserts. After putting the lid on top of the caps 3M micropore tape was used to cover the gap between the lid and the plate. The plates were placed in an incubator at 37°C and 5% CO_2 for 2 hours to allow the cells to attach to the membrane. The Transwells inserts were then inverted back to their original configuration and placed in a 12 wells-plate with HMVEC-d medium in each well. Following, the Caco-2 and HT29-MTX cells were seeded at 4x10^4 cells per insert at a 3:1 ratio. Cells were maintained for three weeks with complete medium apically and HMVEC-d medium basolaterally, medium on both sides was replaced three times per week.

TEER was measured three times per week using a Millicell ERS-2 (Merck Millipore, USA) after refreshing the medium. Washing is needed to remove old medium that might have a changed pH and contain breakdown products that can affect the TEER measurements. The Transwells were allowed to rest for at least three hours between changing the medium and the TEER measurement, as also recommended by [27]. We also checked paracellular fluorescein translocation after 21 days to further assess the monolayer integrity. Fluorescein was diluted in HBSS without Phenol red at 10 µM and 500 µL was added to the apical compartment. After one hour 150 µL was taken from both compartments. Fluorescence was measured using a spectramax spectrophotometer (Molecular Devices, USA) at 494/512 nm.

2.2.4 Transwell exposure

After 21 days of growth and differentiation of the cells, the Transwells were exposed to the TLR agonists for 24 hours (Table 1). The final concentrations, LPS (20 µg/mL), Pam3CSK4 (300 ng/mL), Poly(I:C) (20 µg/mL), flagellin (100 ng/mL) or ssRNA (5 µg/mL), were achieved by dissolving stock solutions in complete medium and afterwards added to the apical compartment[7, 29–31]. These concentrations are regarded as non-cytotoxic because they are lower than used in previous studies (see table 2). Reported cytotoxicity following exposure to LPS for instance was in the mg/ml concentration range [32]. Complete medium

without agonists was added to the basolateral compartment. The Transwells were then either processed for confocal microscopy or cells were collected for protein content determination. All experiments were done in technical and biological triplicates.

Table 2. Agonists and their associated TLRs.

Compound	Concentrations used	TLR
Pam3CSK4	300 ng/mL	1/2
Poly(I:C)	20 µg/mL	3
LPS	20 µg/mL	4
Flagellin	100 ng/mL	5
ssRNA	5 µg/mL	7 + 8

2.2.5 IL-8 measurement

The IL-8 concentration in the apical and basolateral medium was measured separately using an ELISA (Enzo life sciences, Belgium) according to the manufacturers protocol. Medium was collected directly after exposure and stored at -80 °C before analysis. The concentration was calculated using a 4-parameter logistic curve. The results are presented as amount secreted (pg) and thus corrected for the different volumes in the apical and basolateral compartments of the Transwells. Statistical significance was analyzed using a one-way ANOVA to compare the effects of the exposures to their relative controls.

2.2.6 Confocal microscopy

The Transwells were fixated with 4% formaldehyde in PBS for 10 minutes followed by three wash steps with PBS, permeabilization with 0.25% Triton x-100 and blocking with 1% acetylated-BSA in PBS. Samples were first incubated with ZO-1/TJP1 Antibody Rabbit (polyclonal) - Alexa Fluor 594 (Invitrogen, The Netherlands) at 10 µg/mL for 1 hour to stain the tight junctions followed by three washing steps with PBS. Then with Phalloidin Alexa Fluor 488 diluted 1:50 (Life technologies, Belgium) at 6 units/well for 30 minutes to stain the actin followed by three washing steps with PBS and finally with DRAQ5 (Abcam, United Kingdom) at 10 µM for 30 minutes to stain the nuclei. The membranes were then cut from the Transwell inserts using a scalpel and tweezers, the mono- and di-cultures were placed on a microscope slide while the tri-culture was placed on a coverslip. SecureSeal Imaging Spacers (Sigma-Aldrich, The Netherlands) were used to avoid crushing of the cells, ProLong Diamond Antifade mountant (life technologies, Belgium) was added to reduce fading. The slides were analyzed using a Leica TCS SP8 laser scanning microscope using an Apochromatic 63x/1.20 water immersion objective with a white light laser and 440 pulsed laser. EX488/EM525 (Phalloidin) EX594/EM617 (ZO-1) and EX594/EM725 (DRAQ5) with pinhole 122.7 µM.

2.3 Results

2.3.1 Barrier integrity

To assess monolayer integrity TEER was measured on the same days as the medium was refreshed. During cell differentiation the TEER steadily increased over time, in some cases a slight decline was seen during the last few days. Between day 18 and 20 the final TEER measurement was performed to determine whether the Transwells could be used. Of the studied cell models, the final TEER measurement showed the highest TEER values for the Caco-2 cell-layers, i.e. >500 $\Omega \cdot cm^2$ (data not shown). The TEER values were lowest for the HT29-p cells, i.e. <100 $\Omega \cdot cm^2$, and TEER values of the Caco-2/HT29-MTX and Caco-2/HT29-MTX/HMVEC-d di-and tri-culture were >400 $\Omega \cdot cm^2$ (data not shown).

For all models, except HT29-p, only Transwells with a TEER value >300 were used in the experiments (in accordance with [27]). For the HT29-p Transwells the lack of TEER has to be taken into account as it indicates that there is no proper barrier so the direction of the response cannot be assessed.

Besides TEER measurements, also fluorescein translocation experiments (Fig. 1) were performed to evaluate the barrier integrity. Fluorescein translocation was measured on day 21, before the exposure. The Caco-2 monoculture showed an average of 3.3% translocation. The Caco-2/HT29-MTX di-culture and the Caco-2/HT29-MTX/HMVEC-d tri-culture showed an average of 2.2% and 3.8% translocation, respectively, and did not significantly differ from the Caco-2 monoculture. However, at 11.9%, the HT29-p monoculture showed a significantly higher translocation than the Caco-2 cells, again indicating improper barrier function in this model.

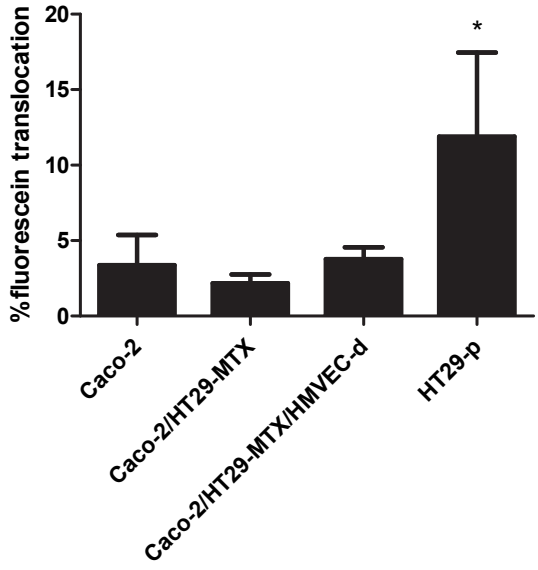

Figure 3. *Percentage of fluorescein translocation from the apical to basolateral side in the different cell systems after one hour of incubation with 10 µM fluorescein. * Statistical significance compared to the Caco-2 monoculture (p <0.05%).*

2.3.2 Cellular morphology

We assessed the cellular morphology of the different models using confocal microscopy. Representative images are shown in Fig. 2. The cells on the apical side of the membrane in the Caco-2 monolayer (Fig. 2A) and in the Caco-2/HT29-MTX di-culture (Fig. 2B) strongly expressed the zonula occludens 1 (ZO-1) protein, also known as tight junction protein 1, between the cells. In all three models confluent cell-layers were observed and no overlapping cells could be noted. For the HT29-p model (Fig. 2D and E) we observed overlapping cells indicating that these cells formed a multilayer.

Lastly, the HMVEC-d cells, grown on the basolateral side of the membranes in the tri-culture model, are shown in Fig. 2C. HMVEC-d cells displayed a pronounced actin skeleton and had a wider flattened morphology compared with the intestinal cells. As can be observed from Fig. 2C there were gaps in the cell coverage of the basolateral side of the membrane, indicating that the HMVEC-d cells did not form a confluent monolayer.

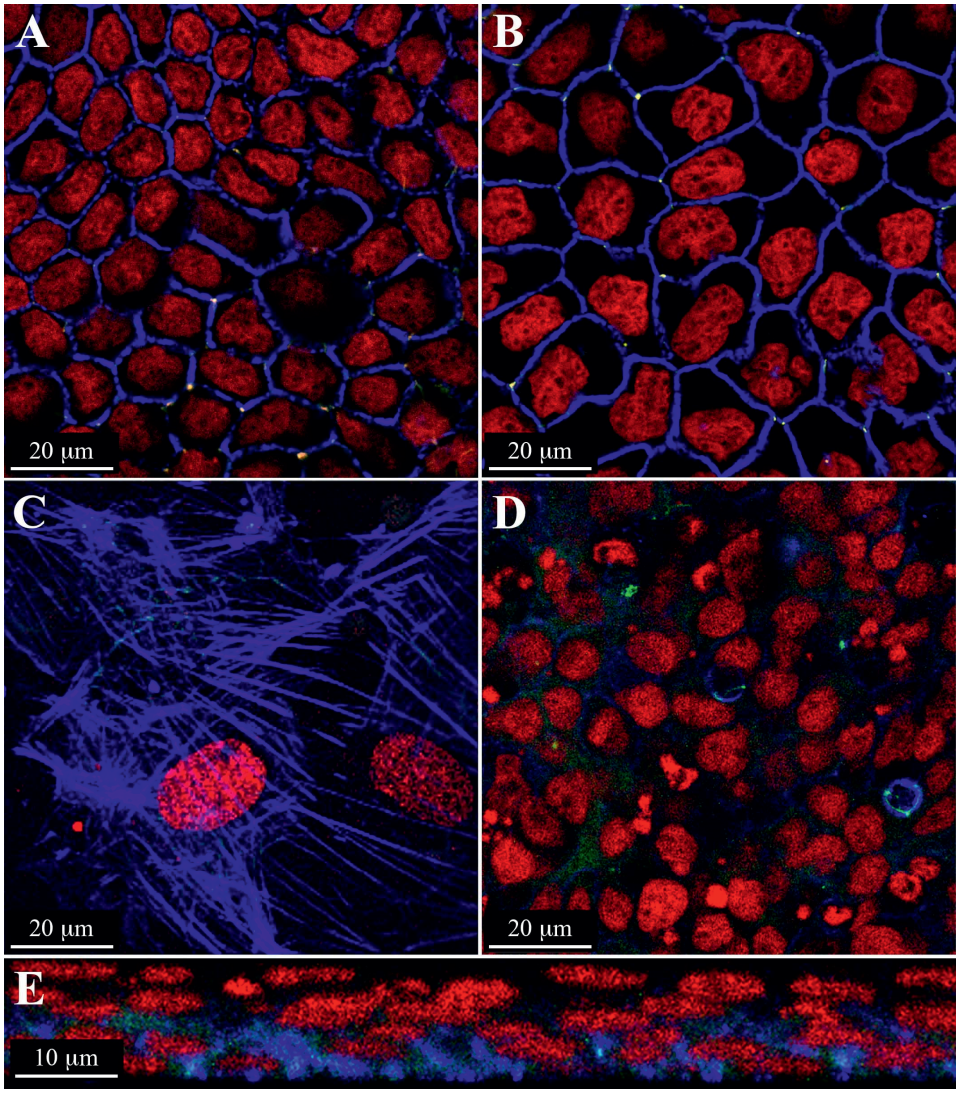

***Figure 2**. Confocal images of a horizontal cross-section of the Caco-2 monoculture (A), the Caco-2/HT29-MTX di-culture (B) on the apical side, and of the HMVEC-d cells in the Caco-2/HT29-MTX/HMVEC-d tri-culture on the basolateral side (C). Confocal image of a horizontal cross-section on the apical side (D) and a vertical cross-section (E) of the HT29-p monoculture. Used stainings were for actin (blue C, D and E), DNA (red) and ZO-1 (green, due to the co-localization of action and Zo-1 the green color is only visible at the crossings of cells (see arrowheads in A and B). Image A and B separated per staining and all images of the apical side of Caco-2/HT29-MTX/HMVEC-d tri-culture are shown in suppl. Fig. S2.*

2.3.3 IL-8 measurement

We aim to create an *in vitro* gut barrier system that is able to respond to a broad range of bacterial TLR agonists, and therefore used models with increasing cellular complexity. We firstly determined the baseline secretion of IL-8 of each cell model (mono-, di- and tri- cultures) without the addition of TLR agonists (Fig. 3). Monocultures of Caco-2 cells produced a low amount of IL-8, with values often at or below the limit of detection at 7.8 pg. No differences were observed between apical and basolateral secretion of IL-8. The di-culture model, obtained by the addition of HT29-MTX cells to the model resulted in an increased IL-8 secretion of 38 pg apically and 98 pg basolaterally. The basal IL-8 secretion was further enhanced, and significantly different from the Caco-2 model, by combining Caco-2 with HT29-MTX cells on the apical side of the membrane and growing HMVEC-d cells on the basolateral side of the membrane. In this tri-culture model the amount of IL-8 released was 189 pg IL-8 apically and 336 pg basolaterally. The highest basal overall IL-8 production, and significantly different from the Caco-2 model, was observed in the HT29-p cells, which produced an average of 260 pg apically and 321 pg basolaterally (suppl. Fig. S1).

In the next step we exposed our four *in vitro* models, i.e. the Caco-2 monoculture (Fig. 3), the Caco-2/HT29-MTX di-culture (Fig. 4), the Caco-2/HT29-MTX/HMVEC-d tri-culture (Fig. 5) and the HT29-p monoculture (Fig. 6), to five TLR agonists interacting with the TLR1/2 heterodimer, TLR3, 4, 5, 7 or TLR8 (see Table 1). In the Caco-2 monoculture, following exposure to the TLR agonist flagellin, we observed a significant increase in the apical IL-8 concentration ($p<0.01$) (Fig. 3). No significant responses were observed following exposure to LPS, poly(I:C), Pam3CSK4 and ssRNA. The IL-8 concentrations on the basolateral side were lower as compared to the apical concentrations, but exposure to flagellin also significantly increased the IL-8 concentration basolaterally ($p<0.05$).

A significant increase in apical secretion of IL-8 was also observed in the Caco-2/HT29-MTX di-culture following exposure to flagellin (Fig. 4; $p<0.001$), while exposure to LPS, Pam3CSK4, poly(I:C) and ssRNA did not induce an IL-8 response. On the basolateral side none of the compounds induced an increase in IL-8 secretion.

In the Caco-2/HT29-MTX/HMVEC-d tri-culture (Fig. 4) we observed a significant increase in apical IL-8 secretion after exposure to flagellin ($p<0.001$), with no IL-8 response following exposure to LPS, poly(I:C), Pam3CSK4 and ssRNA. On the basolateral side none of the agonists induced an increase in IL-8 concentration in the medium.

In the HT29-p monoculture (Fig. 5) we observed a significant IL-8 increase both apically and basolaterally following exposure to Poly(I:C) and flagellin ($p<0.01$). No increase in IL-8 secretion was seen following the other exposures.

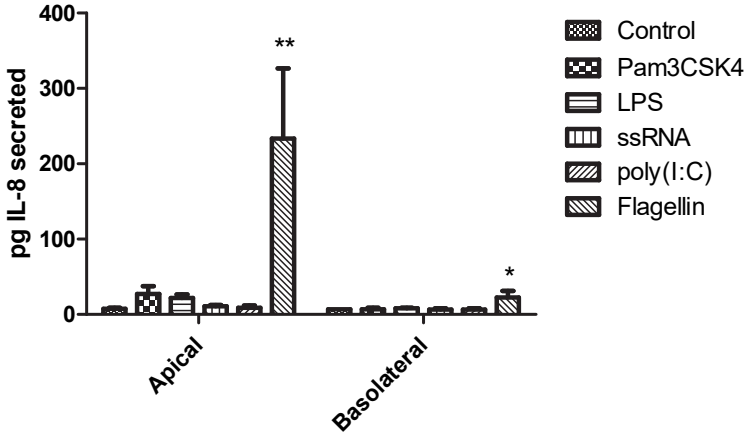

Figure 3. IL-8 secretion by the Caco-2 monoculture into the apical or basolateral medium after 24 hours of exposure to Pam3CSK4 (300 ng/mL), LPS (20 µg/mL), ssRNA (5 µg/mL), poly(I:C) (20 µg/mL), or flagellin (100 ng/mL). Significant differences versus the control (no exposure) samples are indicated with *=p<0.05 and **=p<0.01

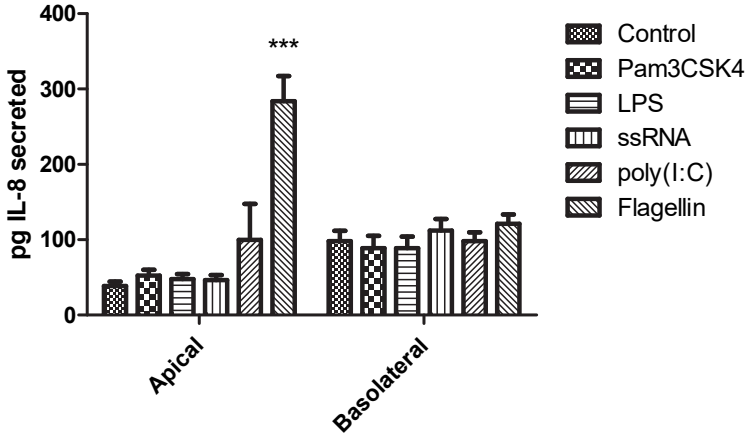

Figure 4. IL-8 secretion by the Caco-2/HT29-MTX di-culture into the apical or basolateral medium after 24 hours of exposure to Pam3CSK4 (300 ng/mL), LPS (20 µg/mL), ssRNA (5 µg/mL), poly(I:C) (20 µg/mL) or flagellin (100 ng/mL). Significant differences versus the control (no exposure) samples are indicated with *** = p<0.001

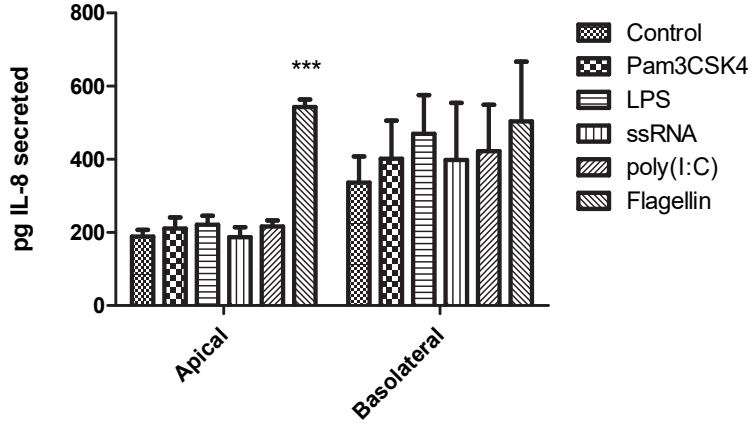

Figure 5. IL-8 secretion by the Caco-2/HT29-MTX/HMVEC-d tri-culture into the apical or basolateral medium after 24 hours of exposure to Pam3CSK4 (300 ng/mL), LPS (20 µg/mL), ssRNA (5 µg/mL), poly(I:C) (20 µg/mL) or flagellin (100 ng/mL). Significant differences versus the control (no exposure) samples are indicated with *** = p<0.001

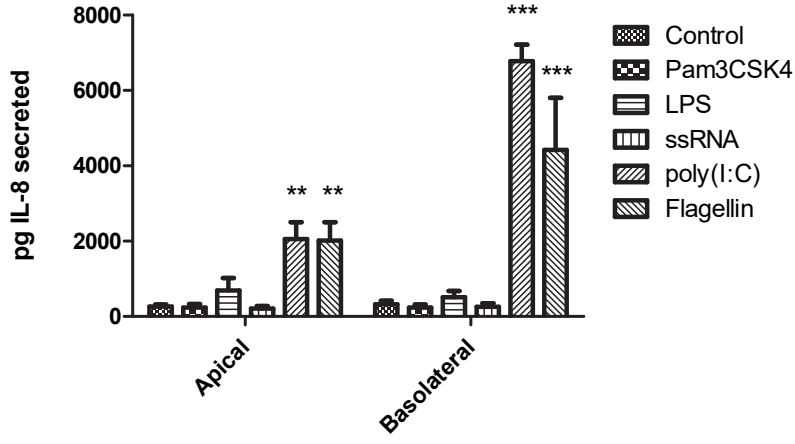

Figure 6. IL-8 secretion by the HT29-p monoculture into the apical or basolateral medium after 24 hours of to Pam3CSK4 (300 ng/mL), LPS (20 µg/mL), ssRNA (5 µg/mL), poly(I:C) (20 µg/mL) or flagellin (100 ng/mL). Significant differences versus the control (no exposure) samples are indicated with **=p<0.01 and *** = p<0.001.

2.3.4 Literature review of present of TLR receptors and IL-8 secretion by intestinal cells in vitro

IL-8 responses of the individual cell types used in this study to TLR agonists have been reported before. No studies using co-culture models were identified by us. However, there are large differences in study design and reported effects. Therefore, these studies have been analyzed and summarized in table 2. From this overview it becomes clear that the direction (i.e. apical or basolateral) of IL-8 secretion has only been studied to a limited extent. The IL-8 responses of Caco-2 cells exposed to LPS are variable, where some studies report IL-8 secretion after LPS exposure while others do not observe this, even when comparable LPS concentrations were used (see Table 2). Pam2CSK4 exposure of Caco-2 cells consistently resulted in an IL-8 secretion at high exposure concentrations (see Table 2). Only very few studies investigated the IL-8 responses of Caco-2 cells to poly(I:C) and ssPolyU.

HT29-MTX cells can respond with IL-8 secretion to LPS exposure as observed in some, but not all, studies (see Table 2), while flagellin triggers the excretion of IL-8 in all studies. No studies were found that exposed HT29-MTX cells to our other TLR agonists.

HT29-p cells have previously been exposed to LPS and in all studies IL-8 secretion was observed (see Table 2), which was the same for flagellin. Pam3CSK4 exposure did not result in IL-8 secretion by HT29-p cells, while only one study showed IL-8 secretion by HT29-p cells following exposure to both poly(I:C) and ssPolyU (see Table 2).

The gene expression of TLRs in the Caco-2, HT29-p and HMVEC-d cells has been studied extensively before. The overview of the literature data is summarized in Table 3. For Caco-2 cells the TLR expression has been studied most extensively. In the case of TLR 1, 3, 5 and 7, the available studies unanimously reported the gene expression of these TLRs. For TLR 2, 4 and 8, the results were contradictory. The latter is likely due to the different read-outs and methods that were used in the expression studies. Most studies used gene expression (qPCR on pooled cells) as a read-out, but some studies (e.g. Uehara et al. (2007) and Bocker et al. (2003)) used protein expression (flow cytometry or western blotting) as an additional read-out. Read-out on a protein level showed that 9.6% of the cells expressed TLR 2 and 7.7% of the Caco-2 cells expressed TLR4, but no expression of TLR2 and 4 in Caco-2 cells was shown using western blotting as a read-out by Bocker et al. (2003). In HT29-p there is largely a consensus in the literature on the presence of all the TLRs, only for TLR2 some ambiguity is present on the expression of this TLR (See table 2), which is again likely due to a different read-out. No expression of TLR2 in HT29-p cells was shown on a protein level (i.e. western blotting) by Bocker et al. (2003), whereas the expression of TLR2 was positive on a gene expression level ([25, 33]). For HT29-MTX cells there is very limited data on TLR expression, but it is expected that the TLR expression will not differ from that observed in the parental HT29-p cell line. All 8 TLRs genes are expressed in HMVEC-d cells (Fitzner et al. 2008). For TLR 1-5 expression was present in resting cells and in cells that were activated by exposure to proinflammatory cytokines. Activated cells showed a relatively higher expression of TLR 2 and 4 than observed in the resting cells. For TLR 7 and 8 there was no expression under resting conditions, but both TLRs were expressed in activated cells (Fitzner et al. 2008).

Table 2. Summary of IL-8 responses of Caco-2 HT29-MTX, HT29-p cells from previous studies.

Cells used	Exposure	Concentration (ng/mL)	Exposure time (hour)	TLR target	Barrier Integrity	IL-8 response /base level (pg/mL)	Direction of secretion	Comment	Reference
Caco-2	Flagellin	100	3	TLR5	N.T.	191 ± 28.7 / None	N.T.	Oxidative stress response induced by H_2O_2 increases the IL-8 excretion	[30]
Caco-2	Flagellin	500.000	16	TLR5	TEER, no effect	160 / None	Not reported	Secretion of CCL20 was also increased. C. difficile toxin B increased the IL-8 response to flagellin likely by disrupting the tight junctions.	[34]
Caco-2	Flagellin	1000	2 and 24	TLR5	N.T.	330/100 +110 / 100	N.T.	Brucella (flagellated) did not induce an IL-8 response. Response was given as an increase over basal excretion.	[35]
Caco-2	LPS	100.000	24	TLR4	N.T.	70 / 25	N.T.	Glutamine decreased the LPS induced IL-8 production. IL-6, TNF-α and IL-10 were below the LOD in all cases.	[36]
Caco-2	LPS	100	16	TLR4	N.T.	N.O. / 100 ±70	N.T.	An IL-8 response in Caco-2 was observed for IL-1β, but not for IFN-γ, TNF-α and LPS.	[37]
Caco-2	LPS	1-10.000	24	TLR4	N.T.	N.O. / N.R.	N.T.	The cells showed no TLR4 or 2 mRNA and protein expression.	[12]
Caco-2	LPS	100	12	TLR4	N.T.	N.O. / 250	N.T.	IL-1β and TNF-α induced an IL-8 response.	[38]
Caco-2	LPS	20.000	24	TLR4	TEER, decreased	120 / 80	Not checked	IL-8 response was attenuated by chitosan nanoparticles. The same trend was seen for the TNF-α, MIF and MCP-1 levels after exposure. Expression of TLR4 was observed (qPCR) in Caco-2 cells.	[29]
Caco-2	Pam2CSK4	100	24	TLR2	TEER, effect not checked	140 / 10	Not checked	Lipoteichoic acid inhibited the response to Pam2CSK4. There was no IL-8 mRNA response to LPS and Poly(I:C).	[39]

Caco-2	Pam2CSK4	10.000	24	TLR2/6	TEER, no effect	30 apical 3 basolateral / none	Secretion mostly apical	Apical exposure resulted in higher responses than basolateral exposure. Used the Caco-2 BBE strain.	[40]
Caco-2	Pam3CSK4	50.000	1-24	TLR1/2	Not checked	1200 / <50	Not checked	Response to Pam3CSK4 was time dependent between 1-24 hours. Butyrate attenuated the IL-8 response via A20, which blocks the NF-κβ pathway.	[41]
Caco-2	Pam3CSK4	20.000	24	TLR1/2	TEER, no effect	7 apical 3 basolateral / none	Secretion mostly apical	Apical exposure resulted in higher responses than basolateral exposure. Used the Caco-2 BBE strain.	[40]
Caco-2	Pam3CSK4	Not reported	24	TLR1/2	N.T.	+70 / 100	N.T.	Response was noted as increase over basal excretion.	[35]
Caco-2	Poly(I:C)	10.000	24	TLR3	N.T.	N.O. / none	N.T.	8.1% of cells expressed TLR 3 protein. They showed that there was no clear link between TLR expression and immune response.	[25]
Caco-2	ssPolyU	1000	24	TLR8	N.T.	N.O. / none	N.T.	They showed that there was no clear link between TLR expression and immune response.	[25]
HT29-MTX	LPS	1-10.000	24	TLR4	N.T.	No / 175	N.T.	The cells showed no TLR4 or 2 mRNA expression.	[12]
HT29-MTX	LPS	1-100	12-48	TLR4	N.T.	2800 at highest conc / 300	N.T.	Concentration dependent response. The response could be measured between 12 and 48 hours after stimulation with a peak at 24 hours. LPS also stimulated mucin production.	[42]
HT29-p	Flagellin	500.000	5	TLR5	TEER, effect not checked	±700 / ±220	Not reported	Also showed an increase in CCL20. C. difficile toxin B increased the IL-8 response to flagellin likely by disrupting the tight junctions.	[34]

HT29-p	Flagellin	1000	24	TLR5	N.T.	±13.000 / <100	N.T.	Brucella (flagellated) did not induce an IL-8 response.	[35]
HT29-p	LPS	100	16	TLR4	N.T.	±10000 / 1400±100	N.T.	Concentration dependent IL-8 response starting at 0.1-100 ng/mL. TNF-α, IFN-γ and IL-1β exposure also induced an IL-8 response.	[37]
HT29-p	LPS	1-10.000	24	TLR4	N.T.	1200 at highest conc / 100	N.T.	Exposure to butyrate reduced TLR4 mRNA expression and IL-8 excretion in response to LPS. The cells only showed TLR4 expression, not TLR2.	[12]
HT29-p	LPS	100	12	TLR4	N.T.	4500 / 600	N.T.	IL-1β and TNF-α also induced an IL-8 response. Differentiation of HT29-P using butyrate reduced the IL-8 response and the increase in TLR-4 expression.	[38]
HT29-p	Pam3CSK4	Not reported	6	TLR1/2	N.T.	No / <4000	N.T.	TNF-α induced an IL-8 response, IFN-γ did not. Lipoteichoic acid attenuated the response.	[33]
HT29-p	Pam3CSK4	Not reported	24	TLR1/2	N.T.	No / N.R.	N.T.	Brucella (flagellated) did not induce an IL-8 response.	[35]
HT29-p	Poly(I:C)	10.000	24	TLR3	N.T.	±2800 / <200	N.T.	19.3% of cells expressed TLR 3 protein. They showed that there was no clear link between TLR expression and immune response.	[25]
HT29-p	ssPolyU	1000	24	TLR8	N.T.	±3600 / <200	N.T.	They showed that there was no clear link between TLR expression and immune response.	[25]

Legend: N.O. = Not observed, N.R. = Not reported, N.T. = No Transwell used

Table 3. Summary of TLR gene expression data from literature in Caco-2, HT29-MTX, HT29-p and HMVEC-d cells.

Cell type	TLR	Gene expression	Reference
Caco-2	1	+	[43]
	2	+	[12, 43]
	3	+	[43, 44]
	4	+/-	[25, 29, 43] /[12]
	5	+	[45]
	7	+	[44, 46]
	8	+/-	[47] / [48]
HT29-MTX	1	N.A.	
	2	-	[12]
	3	N.A.	
	4	-	[12]
	5	N.A.	
	7	N.A.	
	8	N.A.	
HT29-p	1	+	[43, 49, 50]
	2	+/-	[25, 33]/ [12]
	3	+	[43, 49, 50]
	4	+	[12, 25, 38, 43]
	5	+	[49, 50]
	7	+	[49, 50]
	8	+	[49, 50]
HMVEC-d	1-8	+	[22]

Legend: N.A. no information available, + TLR expression confirmed, - TLR expression not confirmed; +/- ambiguous results

2.4 Discussion

We aimed to evaluate the potential of *in vitro* intestinal models with increasing cellular complexity to study immunomodulation induced by exogenous factors by measuring their IL-8 responses to a broad range of bacterial TLR agonists. For this, we compared monocultures and combined cultures of different epithelial cell lines, i.e. Caco-2 and HT29-p cells, a di-culture of Caco-2 and HT29-MTX cells, and a tri-culture of Caco-2 and HT29-MTX cells with the microvascular cell line HMVEC-d, and evaluated their responses to five TLR agonists, Pam3CSK4, LPS, ssRNA, poly(I:C) and flagellin. These agonists represent model compounds for important TLRs that respond to infection in the human intestine. As no co-culture models studies are available where the following TLR agonist exposure are reported we compare our observations to results obtained from mono-culture models.

A striking difference between all the cell models evaluated in this study is their secretion of IL-8 without immunological stimulation. Caco-2 cells show a relatively low baseline IL-8 secretion while the HT29-p cells and the co- and tri-culture models with HT29-MTX and HMVEC-d cells show a higher baseline secretion. All cell models have been cultured for 21 days, we and others have previously shown that after 21 days of culturing the intestinal cells are fully differentiated as indicated by the activity of alkaline phosphatase [51]. Co-culturing of Caco-2 with HT29-MTX results in the secretion of a mucus layer on top of the cells [52]. Mucus is a porous gel-like material with pore sizes reported around 200 nm (for porcine and mouse mucus) [53] and will therefore not act as a size exclusion barrier for the studied agonists. The binding affinity of mucin for bacterial cell wall components like LPS are also reported to be low [42, 54], so taken together mucus will most likely not pose a barrier to the compounds used in this study.

A review of the literature, as presented in Table 2, showed the same general trend, for Caco-2 the baseline IL-8 expression ranged between 10-250 pg, for HT29-MTX cells it ranged between 175-300 pg and for HT29-p it ranged between 100-1400 pg, while the baseline IL-8 secretion by HMVEC-d cells has not been reported. Most studies were not performed in a Transwell system, so no information is available on the direction of IL-8 secretion (i.e. apical or basolateral). Besides the difference in intrinsic cell line properties the variety in culture methods makes it difficult to pinpoint a specific factor that contributes to this variation in IL-8 secretion The expression of the TLRs in the individual cell lines has been studied before, as presented in Table 3, showing general consensus on the presence or absence of specific TLR expression in Caco-2 and HT29-p cells. Only for HT29-MTX cells has the TLR expression been limitedly studied. In this study, we focused on the functionality of the models, and thus we studied both the apical and basolateral secretion of IL-8. When the IL-8 secretion was increased following TLR agonist exposure, the direction of the IL-8 secretion was in most cases bilateral. This can be understood from a functional point of view. IL-8 functions as a chemoattractant for neutrophils [55], therefore secretion from both sides of the intestinal barrier is needed to guide the neutrophils from the bloodstream to the site of the infection. An extreme situation of this can be seen in ulcerative colitis patients as they show high levels of IL-8 leading to migration of neutrophils to the mucosa on the apical side [56, 57]. A similar response can be expected in case of a bacterial infection. The intestinal microbiome represents a complex system with complex and extensive interactions with the intestinal epithelium. These interactions can be mediated via a range of signaling molecules and bacterial metabolites and other bacterial products [58, 59]. In our study we look at the very first step of interaction between bacteria and the intestinal epithelium via the immune system focusing on the stimulation of IL-8 by well characterized TLR agonists.

Flagellin is a part of the bacterial flagellum, which plays a role in the motility, adhesion and invasion of cells by (certain) bacteria [60]. In literature, concentration ranges between 100 – 500,000 ng/mL were used for *in vitro* testing, we used a concentration of 100 ng/mL, as flagellin is known to be a potent immune activator which acts via TLR5 [61, 62]. Even though we exposed our cells to a relatively low concentration of flagellin the detected response was as high or higher than that reported in literature for monocultures of Caco-2 and HT29-p cells (Table 2, [30, 34]). No human *in vivo* data are available. The only *in vivo* data that are available are derived from a rodent study. Exposure to flagellin in mice resulted in system-wide immune activation, in this study flagellin was administered via injection in the bloodstream [63, 64].

Poly(I:C) is a synthetic double stranded RNA used to simulate viral infection [65] and is recognized by TLR3. We observed a significant IL-8 response against Poly(I:C) in the HT29-p culture, but there was no response in the other cell systems. This corroborates with the results described in literature for Caco-2 and HT29-p cells, as Poly(I:C) exposure to HT29-P or Caco-2 cells induced a response in HT29-p cells only. The cause of this difference is unknown as both cell types were shown to express TLR3 protein where Caco-2 and HT29-p cells expressed TLR3 on 19.3% and 8.1% of the total number of cells, respectively [25]. The exposure of the di-culture of Caco-2 and HT29-MTX cells to Poly(I:C) did not induce an IL-8 response, which indicates that the HT29-MTX cells differ from their parental cell line in their response to Poly(I:C).

Lipopolysaccharides are part of the outer membrane of gram-negative bacteria and are recognized by TLR4 [66, 67]. In our studies we did not observe a response to LPS in Caco-2 cells, which is in accordance with most of the existing literature. Reports of responses by Caco-2 cells to LPS vary, some sources report an increase in IL-8 excretion [36, 37], while most sources report a lack of responses attributed to low TLR4 expression [12, 38]. Our di-culture model with HT29-MTX cells also did not show a response to LPS. In the literature, the reported responses of HT29-MTX cells against LPS are variable, likely because various strains of the cell line have been used [12, 42]. We did not observe an IL-8 response in HT29-p cells following the LPS exposure, while such a response has been reported before [38]. Lastly, the inclusion of HMVEC-d cells in our model also did not change the response of the model to LPS. This lack of response can be due a low basolateral LPS concentration upon apical administration of the agonist as monocultures of HMVEC-d have been reported to respond to LPS stimulation by secretion of IL-8 [68] and have been shown to express TLR4 mRNA [66].

Pam3CSK4 is a TLR1/2 agonist that has been reported to induce an IL-8 response in Caco-2 cells [41], while this response has not been reported for HT29-p cells [33]. In our results none of the cell lines responded to stimulation with Pam3CSK4. In the previously reported studies far higher Pam3CSK4 concentrations were used, which may explain the difference in results. However, the working concentration of the compound, as recommended by the producer, was between 0.1 – 10 ng/mL. In order for cells to respond to Pam3CSK4 they need to express both TLR1 and TLR2 [69]. Reports on the expression of TLR1/2 in intestinal cell lines are ambiguous. Some report expression of both TLR1 and 2 in Caco-2 cells [43], while others report very low expression of TLR1 in Caco-2 cells [24]. For HT29-p cells the presence of both TLR1 and 2 was reported [24, 70]. The observed absence of an IL-8 response in our cell models could be due to the absence of TLR1 and/or 2.

ssRNA is recognized by both TLR7 and TLR8. TLR8 is considered the most important of the two in humans, it is normally present in intracellular compartments like the endosomes [71], so activation of the immune response requires endocytosis. Therefore, the ssRNA used for exposure was combined

with LyoVec to facilitate its uptake into the cells. The ssRNA40 we used did not elicit a response in any of the models. Very little is reported on the immune responses of intestinal epithelial cells to ssRNA. It has been reported that ssPolyU, a synthetic ssRNA, stimulates IL-8 excretion in HT29-p cells but not in Caco-2 cells [25]. The concentration of ssPolyU used by Uehara et al. (2017) was five times lower than the one we used for ssRNA to elicit this response, so potentially a synthetic variant like ssPolyU is more potent. In a comparison between IBD and healthy patients immunofluorescence microscopy and immune-EM showed the presence of TLR8 on the luminal epithelial membrane in both groups, which is in contrast to the expected intracellular localization of the receptor that is generally described in literature. They also show that TLR8 mediates IL-8 secretion [72]. Therefore, the lack of an IL-8 response in our system could indicate the absence of a functional TLR8 in the cells used in this study.

We set out to study which cell model could best be used for future studies focusing on immunomodulation in the human gut. Firstly, we conclude that a di-culture model of Caco-2 and HT29-MTX does not deliver an additional value for this purpose, as both the Caco-2 mono- and di-cultures showed similar responses. The HT29-p monoculture even showed an advantage by additionally responding to Poly(I:C), but does not grow a monolayer. Overall, the monocultures will make interpretation of results easier due to the differences in basal excretion of IL-8 between the cell lines. The addition of the human microvascular cell line HMVEC-d also did not result in a different response pattern but did induce the baseline IL-8 concentrations as well as the IL-8 concentration after exposure to flagellin, thus HMVEC-d cells participate in propagating the immune response, and therefore add to the physiological relevance of the model. Secondly, we conclude that epithelial cell lines cannot capture all the immunomodulatory responses seen in human gut epithelial cells *in vivo*. While the use of cell lines have important practical advantages in the laboratory in terms of reproducibility in comparison with the use of primary cells or stem cell-derived models, exploration of these models needs to be considered in the future. TLR1 through 9, with the exception of TLR10, has for instance been shown to be expressed in freshly isolated intestinal epithelium [73]. Therefore a careful selection of the *in vitro* model remains needed in future studies and should be based on the research question.

Acknowledgements

The authors acknowledge the constructive comments on this work provided by Ivonne M. C. M. Rietjens. For this work MG was supported by a grant funded by the Dutch Research Council, a Building Blocks of Life project (No. 737.016.003). Work on this project by MvdZ was supported by the Dutch Ministry of Agriculture, Nature and Food Quality (Grant: KB-37-002-020).

References

1. Silverthorn DU, Johnson BR, Ober WC, Ober CE, Silverthorn AC. Human physiology : an integrated approach. 2016.
2. Artursson P, Palm K, Luthman K. Caco-2 monolayers in experimental and theoretical predictions of drug transport. Adv Drug Deliv Rev. 2001;46:27–43.
3. Tang AS, Chikhale PJ, Shah PK, Borchardt RT. Utilization of a Human Intestinal Epithelial Cell Culture System (Caco-2) for Evaluating Cytoprotective Agents. Pharm Res An Off J Am Assoc Pharm Sci. 1993;10:1620–6.
4. Sadabad MS, Von Martels JZH, Khan MT, Blokzijl T, Paglia G, Dijkstra G, et al. A simple coculture system shows mutualism between anaerobic faecalibacteria and epithelial Caco-2 cells. Sci Rep. 2015;5.
5. Peterson LW, Artis D. Intestinal epithelial cells: Regulators of barrier function and immune homeostasis. Nature Reviews Immunology. 2014;14:141–53.

6. Abreu MT. Toll-like receptor signalling in the intestinal epithelium: how bacterial recognition shapes intestinal function. Nat Rev Immunol 2010 102. 2010;10:131–44.
7. Price AE, Shamardani K, Lugo KA, Deguine J, Roberts AW, Lee BL, et al. A Map of Toll-like Receptor Expression in the Intestinal Epithelium Reveals Distinct Spatial, Cell Type-Specific, and Temporal Patterns. Immunity. 2018;49:560-575.e6.
8. Takeda K, Akira S. TLR signaling pathways. Semin Immunol. 2004;16:3–9.
9. Säemann MD, Böhmig GA, Österreicher CH, Burtscher H, Parolini O, Diakos C, et al. Anti-inflammatory effects of sodium butyrate on human monocytes: potent inhibition of IL-12 and up-regulation of IL-10 production. FASEB J. 2000;14:2380–2.
10. Rakoff-Nahoum S, Paglino J, Eslami-Varzaneh F, Edberg S, Medzhitov R. Recognition of commensal microflora by toll-like receptors is required for intestinal homeostasis. Cell. 2004;118:229–41.
11. Newberry RD, Lorenz RG. Organizing a mucosal defense. Immunol Rev. 2005;206:6–21.
12. Böcker U, Yezerskyy O, Feick P, Manigold T, Panja A, Kalina U, et al. Responsiveness of intestinal epithelial cell lines to lipopolysaccharide is correlated with Toll-like receptor 4 but not Toll-like receptor 2 or CD14 expression. Int J Colorectal Dis. 2003;18:25–32.
13. Martínez-Maqueda D, Miralles B, Recio I. HT29 cell line. In: The Impact of Food Bioactives on Health: In Vitro and Ex Vivo Models. Springer International Publishing; 2015. p. 113–24.
14. Ottman N, Geerlings SY, Aalvink S, de Vos WM, Belzer C. Action and function of Akkermansia muciniphila in microbiome ecology, health and disease. Best Pract Res Clin Gastroenterol. 2017;31:637–42.
15. McGuckin MA, Lindén SK, Sutton P, Florin TH. Mucin dynamics and enteric pathogens. Nat Rev Microbiol. 2011;9:265–78.
16. Tarnawski A, Ahluwalia A, Jones M. The mechanisms of gastric mucosal injury: focus on microvascular endothelium as a key target. Curr Med Chem. 2012;19:4–15.
17. Ferrari D, Cimino F, Fratantonio D, Molonia MS, Bashllari R, Busà R, et al. Cyanidin-3-O-Glucoside Modulates the in Vitro Inflammatory Crosstalk between Intestinal Epithelial and Endothelial Cells. Mediators Inflamm. 2017;2017.
18. Maschmeyer I, Hasenberg T, Jaenicke A, Lindner M, Lorenz AK, Zech J, et al. Chip-based human liver–intestine and liver–skin co-cultures – A first step toward systemic repeated dose substance testing in vitro. Eur J Pharm Biopharm. 2015;95:77–87.
19. Schimek K, Busek M, Brincker S, Groth B, Hoffmann S, Lauster R, et al. Integrating biological vasculature into a multi-organ-chip microsystem. Lab Chip. 2013;13:3588–98.
20. Kim HJ, Li H, Collins JJ, Ingber DE. Contributions of microbiome and mechanical deformation to intestinal bacterial overgrowth and inflammation in a human gut-on-a-chip. Proc Natl Acad Sci U S A. 2016;113:E7–15.
21. Shin W, Hinojosa CD, Ingber DE, Kim HJ. Human Intestinal Morphogenesis Controlled by Transepithelial Morphogen Gradient and Flow-Dependent Physical Cues in a Microengineered Gut-on-a-Chip. iScience. 2019;15:391–406.
22. Fitzner N, Clauberg S, Essmann F, Liebmann J, Kolb-Bachofen V. Human skin endothelial cells can express all 10 TLR genes and respond to respective ligands. Clin Vaccine Immunol. 2008;15:138–46.
23. Akiba Y, Maruta K, Takajo T, Narimatsu K, Said H, Kato I, et al. Lipopolysaccharides transport during fat absorption in rodent small intestine. Am J Physiol - Gastrointest Liver Physiol. 2020;318:G1070–87.
24. Melmed G, Thomas LS, Lee N, Tesfay SY, Lukasek K, Michelsen KS, et al. Human Intestinal Epithelial Cells Are Broadly Unresponsive to Toll-Like Receptor 2-Dependent Bacterial Ligands: Implications for Host-Microbial Interactions in the Gut. J Immunol. 2003;170:1406–15.
25. Uehara A, Fujimoto Y, Fukase K, Takada H. Various human epithelial cells express functional Toll-like receptors, NOD1 and NOD2 to produce anti-microbial peptides, but not proinflammatory cytokines. Mol Immunol. 2007;44:3100–11.
26. Angrisano T, Pero R, Peluso S, Keller S, Sacchetti S, Bruni CB, et al. LPS-induced IL-8 activation in human intestinal epithelial cells is accompanied by specific histone H3 acetylation and methylation

changes. BMC Microbiol. 2010;10:1–8.
27. Hubatsch I, Ragnarsson EGE, Artursson P. Determination of drug permeability and prediction of drug absorption in Caco-2 monolayers. Nat Protoc. 2007;2:2111–9.
28. Kamelia L, Louisse J, de Haan L, Rietjens IMCM, Boogaard PJ. Prenatal developmental toxicity testing of petroleum substances: Application of the mouse embryonic stem cell test (EST) to compare in vitro potencies with potencies observed in vivo. Toxicol Vitr. 2017;44:303–12.
29. Tu J, Xu Y, Xu J, Ling Y, Cai Y. Chitosan nanoparticles reduce LPS-induced inflammatory reaction via inhibition of NF-κB pathway in Caco-2 cells. Int J Biol Macromol. 2016;86:848–56.
30. Ivison SM, Wang C, Himmel ME, Sheridan J, Delano J, Mayer ML, et al. Oxidative stress enhances IL-8 and inhibits CCL20 production from intestinal epithelial cells in response to bacterial flagellin. Am J Physiol - Gastrointest Liver Physiol. 2010;299:G733–41.
31. Ashtekar AR, Zhang P, Katz J, Deivanayagam CCS, Rallabhandi P, Vogel SN, et al. TLR4-mediated activation of dendritic cells by the heat shock protein DnaK from Francisella tularensis . J Leukoc Biol. 2008;84:1434–46.
32. Guo S, Al-Sadi R, Said HM, Ma TY. Lipopolysaccharide Causes an Increase in Intestinal Tight Junction Permeability in Vitro and in Vivo by Inducing Enterocyte Membrane Expression and Localization of TLR-4 and CD14. Am J Pathol. 2013;182:375–87.
33. Kim H, Jung BJ, Jung JH, Kim JY, Chung SK, Chung DK. Lactobacillus plantarum Lipoteichoic Acid Alleviates TNF-α-Induced Inflammation in the HT-29 Intestinal Epithelial Cell Line. Mol Cells. 2012;33:479–86.
34. Yoshino Y, Kitazawa T, Ikeda M, Tatsuno K, Yanagimoto S, Okugawa S, et al. Clostridium difficile flagellin stimulates toll-like receptor 5, and toxin B promotes flagellin-induced chemokine production via TLR5. Life Sci. 2013;92:211–7.
35. Ferrero MC, Fossati CA, Rumbo M, Baldi PC. Brucella invasion of human intestinal epithelial cells elicits a weak proinflammatory response but a significant CCL20 secretion. FEMS Immunol Med Microbiol. 2012;66:45–57.
36. Huang Y, Li N, Liboni K, Neu J. Glutamine decreases lipopolysaccharide-induced IL-8 production in Caco-2 cells through a non-NF-κB p50 mechanism. Cytokine. 2003;22:77–83.
37. Schuerer-Maly CC, Eckmann L, Kagnoff MF, Falco MT, Maly FE. Colonic epithelial cell lines as a source of interleukin-8: stimulation by inflammatory cytokines and bacterial lipopolysaccharide. Immunology. 1994;81:85–91.
38. Sang KL, Tae IK, Yun KK, Chang HC, Kyung MY, Chae B, et al. Cellular differentiation-induced attenuation of LPS response in HT-29 cells is related to the down-regulation of TLR4 expression. Biochem Biophys Res Commun. 2005;337:457–63.
39. Noh SY, Kang SS, Yun CH, Han SH. Lipoteichoic acid from Lactobacillus plantarum inhibits Pam2CSK4-induced IL-8 production in human intestinal epithelial cells. Mol Immunol. 2015;64:183–9.
40. Rossi O, Karczewski J, Stolte EH, Brummer RJM, Van Nieuwenhoven MA, Meijerink M, et al. Vectorial secretion of interleukin-8 mediates autocrine signalling in intestinal epithelial cells via apically located CXCR1. BMC Res Notes. 2013;6:1–10.
41. Weng M, Walker WA, Sanderson IR. Butyrate regulates the expression of pathogen-triggered IL-8 in intestinal epithelia. Pediatr Res. 2007;62:542–6.
42. Smirnova MG, Guo L, Birchall JP, Pearson JP. LPS up-regulates mucin and cytokine mRNA expression and stimulates mucin and cytokine secretion in goblet cells. Cell Immunol. 2003;221:42–9.
43. Furrie E, Macfarlane S, Thomson G, Macfarlane GT. Toll-like receptors-2, -3 and -4 expression patterns on human colon and their regulation by mucosal-associated bacteria. Immunology. 2005;115:565–74.
44. Salaris C, Scarpa M, Elli M, Bertolini A, Guglielmetti S, Pregliasco F, et al. Lacticaseibacillus paracasei DG enhances the lactoferrin anti-SARS-CoV-2 response in Caco-2 cells. https://doi-org.ezproxy.library.wur.nl/101080/1949097620211961970. 2021;13:1961970.
45. Devriese S, Van den Bossche L, Van Welden S, Holvoet T, Pinheiro I, Hindryckx P, et al. T84 monolayers are superior to Caco-2 as a model system of colonocytes. Histochem Cell Biol 2017 1481. 2017;148:85–93.

46. Yi JY, Jung YJ, Choi SS, Hwang J, Chung E. Autophagy-mediated anti-tumoral activity of imiquimod in Caco-2 cells. Biochem Biophys Res Commun. 2009;386:455–8.
47. Cammarota M, De Rosa M, Stellavato A, Lamberti M, Marzaioli I, Giuliano M. In vitro evaluation of Lactobacillus plantarum DSMZ 12028 as a probiotic: Emphasis on innate immunity. Int J Food Microbiol. 2009;135:90–8.
48. Toki S, Kagaya S, Shinohara M, Wakiguchi H, Matsumoto T, Takahata Y, et al. Lactobacillus rhamnosus GG and Lactobacillus casei Suppress Escherichia coli-Induced Chemokine Expression in Intestinal Epithelial Cells. Int Arch Allergy Immunol. 2009;148:45–58.
49. Tian Z, Yang L, Li P, Xiao Y, Peng J, Wang X, et al. The inflammation regulation effects of Enterococcus faecium HDRsEf1 on human enterocyte-like HT-29 cells. http://dx.doi.org.ezproxy.library.wur.nl/101080/1976835420161160955. 2016;20:70–6.
50. Graves CL, Harden SW, LaPato M, Nelson M, Amador B, Sorenson H, et al. A method for high purity intestinal epithelial cell culture from adult human and murine tissues for the investigation of innate immune function. J Immunol Methods. 2014;414:20–31.
51. Kulthong K, Duivenvoorde L, Sun H, Confederat S, Wu J, Spenkelink B, et al. Microfluidic chip for culturing intestinal epithelial cell layers: Characterization and comparison of drug transport between dynamic and static models. Toxicol Vitr. 2020;65:104815.
52. Walczak AP, Kramer E, Hendriksen PJM, Tromp P, Helsper JPFG, Zande M van der, et al. Translocation of differently sized and charged polystyrene nanoparticles in in vitro intestinal cell models of increasing complexity. http://dx.doi.org.ezproxy.library.wur.nl/103109/174353902014944599. 2015;9:453–61.
53. Bajka BH, Rigby NM, Cross KL, Macierzanka A, Mackie AR. The influence of small intestinal mucus structure on particle transport ex vivo. Colloids Surfaces B Biointerfaces. 2015;135:73–80.
54. Kim YS, Ho SB. Intestinal Goblet Cells and Mucins in Health and Disease: Recent Insights and Progress. Curr Gastroenterol Rep. 2010;12:319.
55. Miller MD, Krangel MS. Biology and biochemistry of the chemokines - a family of chemotactic and inflammatory cytokines. Crit Rev Immunol. 1992;12:17–46.
56. Mitsuyama K, Toyonaga A, Sasaki E, Watanabe K, Tateishi H, Nishiyama T, et al. IL-8 as an important chemoattractant for neutrophils in ulcerative colitis and Crohn's disease. Clin Exp Immunol. 1994;96:432–6.
57. Mahida YR, Ceska M, Effenberger F, Kurlak L, Lindley I, Hawkey CJ. Enhanced synthesis of neutrophil-activating peptide-I/interleukin-8 in active ulcerative colitis. Clin Sci. 1992;82:273–5.
58. Kau AL, Ahern PP, Griffin NW, Goodman AL, Gordon JI. Human nutrition, the gut microbiome and the immune system. Nat 2011 4747351. 2011;474:327–36.
59. Thaiss CA, Zmora N, Levy M, Elinav E. The microbiome and innate immunity. Nat 2016 5357610. 2016;535:65–74.
60. Haiko J, Westerlund-Wikström B. The role of the bacterial flagellum in adhesion and virulence. Biology. 2013;2:1242–67.
61. Murthy KGK, Deb A, Goonesekera S, Szabó C, Salzman AL. Identification of Conserved Domains in Salmonella muenchen Flagellin That Are Essential for Its Ability to Activate TLR5 and to Induce an Inflammatory Response in Vitro. J Biol Chem. 2004;279:5667–75.
62. Gewirtz AT, Navas TA, Lyons S, Godowski PJ, Madara JL. Cutting Edge: Bacterial Flagellin Activates Basolaterally Expressed TLR5 to Induce Epithelial Proinflammatory Gene Expression. J Immunol. 2001;167:1882–5.
63. Rolli J, Loukili N, Levrand S, Rosenblatt-Velin N, Rignault-Clerc S, Waeber B, et al. Bacterial flagellin elicits widespread innate immune defense mechanisms, apoptotic signaling, and a sepsis-like systemic inflammatory response in mice. Crit Care. 2010;14:R160.
64. Strindelius L, Filler M, Sjöholm I. Mucosal immunization with purified flagellin from Salmonella induces systemic and mucosal immune responses in C3H/HeJ mice. Vaccine. 2004;22:3797–808.
65. Fortier ME, Kent S, Ashdown H, Poole S, Boksa P, Luheshi GN. The viral mimic, polyinosinic:polycytidylic acid, induces fever in rats via an interleukin-1-dependent mechanism. Am J Physiol - Regul Integr Comp Physiol. 2004;287 4 56-4.

66. Faure E, Equils O, Sieling PA, Thomas L, Zhang FX, Kirschning CJ, et al. Bacterial lipopolysaccharide activates NF-κB through toll-like receptor 4 (TLR-4) in cultured human dermal endothelial cells. Differential expression of TLR-4 and TLR-2 in endothelial cells. J Biol Chem. 2000;275:11058–63.
67. Triantafilou M, Triantafilou K. Lipopolysaccharide recognition: CD14, TLRs and the LPS-activation cluster. Trends in Immunology. 2002;23:301–4.
68. Arlian LG, Elder BL, Morgan MS. House Dust Mite Extracts Activate Cultured Human Dermal Endothelial Cells to Express Adhesion Molecules and Secrete Cytokines. J Med Entomol. 2009;46:595–604.
69. Ozinsky A, Underhill DM, Fontenot JD, Hajjar AM, Smith KD, Wilson CB, et al. The repertoire for pattern recognition of pathogens by the innate immune system is defined by cooperation between Toll-like receptors. Proc Natl Acad Sci U S A. 2000;97:13766–71.
70. Saegusa S, Totsuka M, Kaminogawa S, Hosoi T. *Candida albicans* and *Saccharomyces cerevisiae* induce interleukin-8 production from intestinal epithelial-like Caco-2 cells in the presence of butyric acid. FEMS Immunol Med Microbiol. 2004;41:227–35.
71. Triantafilou K, Vakakis E, Orthopoulos G, Ahmed MAE, Schumann C, Lepper PM, et al. TLR8 and TLR7 are involved in the host's immune response to human parechovirus 1. Eur J Immunol. 2005;35:2416–23.
72. Steenholdt C, Andresen L, Pedersen G, Hansen A, Brynskov J. Expression and function of toll-like receptor 8 and Tollip in colonic epithelial cells from patients with inflammatory bowel disease. Scand J Gastroenterol. 2009;44:195–204.
73. Otte JM, Cario E, Podolsky DK. Mechanisms of Cross Hyporesponsiveness to Toll-Like Receptor Bacterial Ligands in Intestinal Epithelial Cells. Gastroenterology. 2004;126:1054–70.

Supplementary files

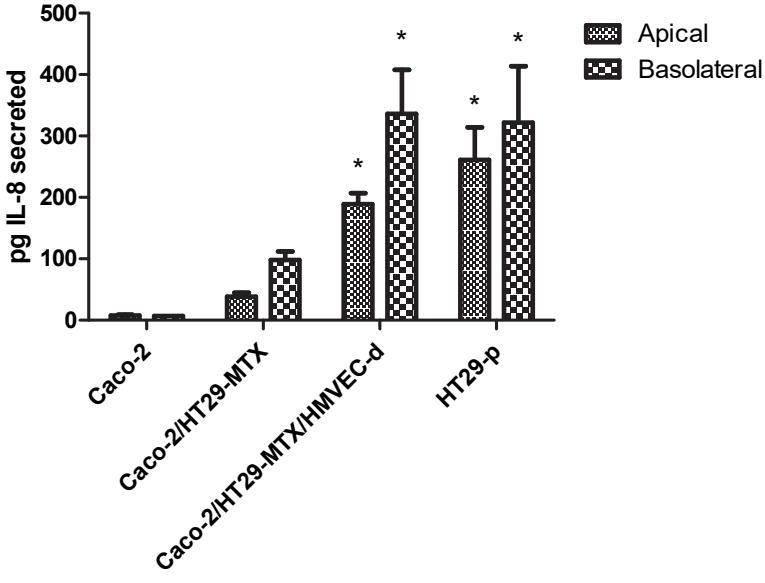

Supplementary Figure 1. Baseline IL-8 secretion of the Caco-2 monoculture, Caco-2/HT29-MTX di- and Caco-2/HT29-MTX/HMVEC-d tri-culture into the apical or basolateral medium. *Statistical significance ($p<0.05$) compared to the Caco-2 culture on the respective side.

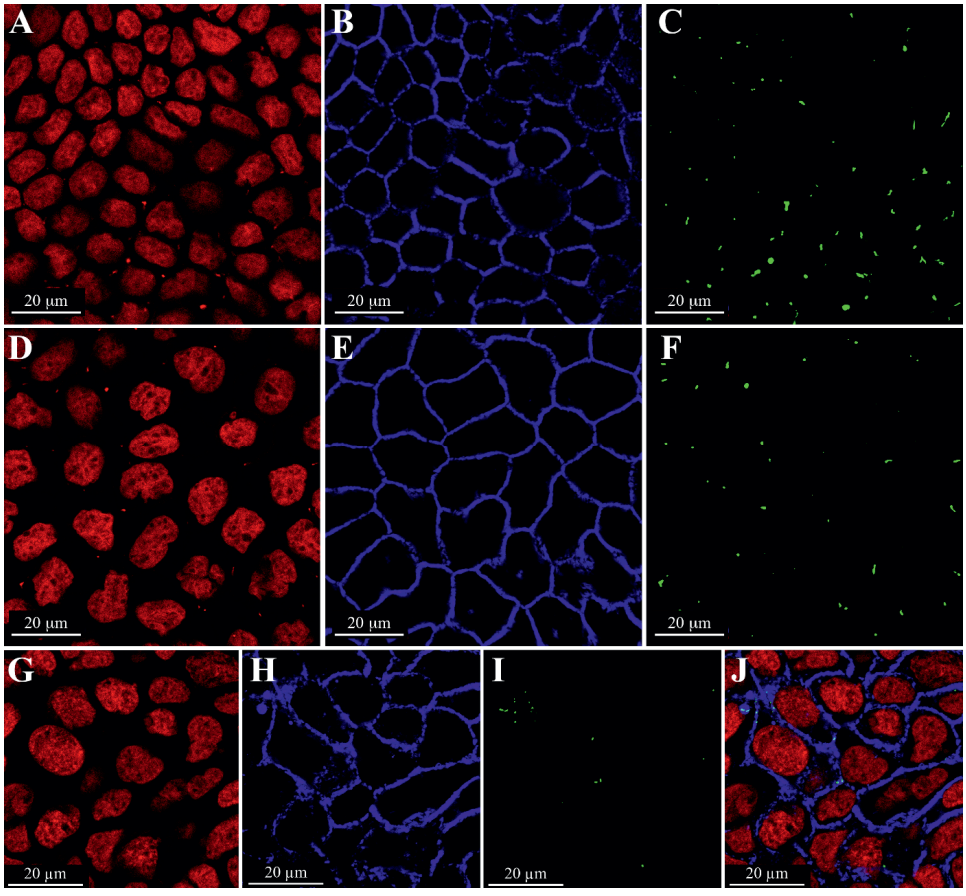

Supplementary Figure 2. Confocal images of a horizontal cross-section of the Caco-2 monoculture (A, B, C) and the Caco-2/HT29-MTX di-culture (D, E, F) and the apical side of the Caco-2/HT29-MTX/HMVEC-d tri-culture (G-J). Used stainings were for DNA (red, A, D, G, J), actin (blue, B, E, H, J), and ZO-1 (green, C, F, I, J).

Chapter 3

Toll-like receptor gene expression and responsiveness to specific agonists in human induced pluripotent stem cell-derived intestinal organoids and primary human small intestinal epithelial cells

Menno Grouls[1], Aafke Janssen[2], Meike van der Zande[2], Laura de Haan[1], Hans Bouwmeester[1]

[1] Division of Toxicology, Wageningen University, Wageningen University & Research
[2] Wageningen Food Safety Research, Wageningen University & Research

Abstract

The human intestine fulfils many roles such as digestion of food, nutrient uptake and water balance regulation. In addition, the intestinal epithelium is an important protective barrier and plays a critical role in immune responses. Toll-like receptors (TLRs) that are expressed on and in intestinal epithelial cells, recognize and respond to various stimuli, including those present on intestinal bacteria. We studied the immunomodulatory capacity of two advanced intestinal models, human induced pluripotent stem cell (iPSC) derived intestinal organoids and primary human small intestinal epithelial (PHSIE) cells, that aim to mimic the complex human intestinal epithelium. Both models were exposed for 24 hours to the bacterial related TLR agonists Pam3CSK4 (TLR1/2), lipopolysaccharide (TLR4) and flagellin (TLR5), while the iPSC derived organoids were additionally exposed to the viral related agonists single-stranded RNA (TLR7/8) and Poly(I:C) (TLR3). We measured changes in TLR gene expression and cytokine excretion after exposure in both cell models. Firstly, the baselevel TLR gene expression in the PHSIE cell model was lower than that of the iPSC derived organoids. Secondly, upon stimulation with the TLR agonists, the iPSC derived organoids excreted four cytokines while the PHSIE cell model only excreted IL-8. We also showed that effects on TLR gene expression are an important response to TLR agonists. In conclusion, the iPSC derived organoids were able to respond to a range of bacterial and viral TLR agonists, while the PHSIE cell model, like previously studied cell line based models, only displayed a limited ability to respond to the bacterial TLR agonists. Therefore, it is concluded that the iPSC derived organoids are a promising model to further study intestinal immune responses.

Keywords: Intestine; Advanced *in vitro* models, iPSC, organoids, primary cells, Toll-like Receptors

3.1 Introduction

The human intestine fulfils many important roles such as digestion of food, nutrient uptake and water balance regulation [1]. Selecting an *in vitro* intestinal model that emulates one or all of these functions is important for the toxicological assessment of chemicals with minimal (or no) reliance on animal derived data [2]. The last decades great progress has been made in the development of advanced *in-vitro* systems that allow for such an animal data free toxicological assessment [3]. A powerful approach is the use of cells that more closely mimic the complex cellular biology of the human intestinal epithelium. One approach is to use intestinal cells obtained from healthy (adult) donors that are expanded into monolayers. This results in a model that contains enterocytes, Paneth cells, M cells, tuft cells and stem cells that form villi-crypt structures [4]. Another approach is using induced pluripotent stem cells to generate intestinal organoids containing enterocytes, stem cells, goblet cells, Paneth cells, enteroendocrine cells and mesenchymal cells [5–8]. Also, this model mimics the crypt-villi microarchitecture as seen in the intestinal tissue *in vivo*. Both models are promising *in-vitro* models to assess the consequences of chemical and microbiological exposure.

Many aspects such as metabolism of xenobiotics, barrier function and transport of chemicals have already been assessed in such systems [9–11]. However, also interactions between pathogens or metabolites thereof and the intestinal epithelium influence many aspects of the intestinal functionality and therefore need to be assessed. Toll-like receptors (TLRs) that are expressed by intestinal epithelial cells, play a crucial role in the recognition of different pathogens and in the subsequent epithelial responses following the initial interactions [12]. Pathogen associated molecular patterns (PAMPs) are structurally conserved molecular components of bacteria which can be recognized by TLRs. Each TLR recognizes a specific set of PAMPs and the expression of TLRs differs per cell type and compartment of the human intestine [13]. In somewhat more detail, the TLR1/2 heterodimer recognizes, amongst others, bacterial triacyl lipopeptides, TLR3 recognizes dsRNA, TLR4 recognizes lipopolysaccharides (LPS), TLR5 is well-known for recognizing flagellin, and lastly TLR7 and 8 both recognize ssRNA [14]. Binding of an agonist, a compound containing a PAMP, to TLRs induces an innate immune response via the myeloid differentiation primary response protein 88 (MyD88) pathway. This leads to multiple effects in the epithelial cell such as changes in expression of TLRs in the cells and the excretion of cytokines that regulate further activation of immune cells present in the intestinal mucosal layers that are involved in innate immune responses [12, 15].

The general suggestion from human studies using biopsies taken from different parts of the intestine and stem cell-based intestinal models is that 8 types of TLRs are expressed in the human intestine, while there is some ambiguity on the level of expression of the different TLRs [16–24]. Previously we studied the expression of TLRs in cell-lines and we studied the IL-8 excretion following TLR agonist stimulation in cell models of increasing complexity based on cell-lines [25]. We concluded that cell lines only show a limited response to TLR agonists with only flagellin and poly(I:C) inducing IL-8 excretion in one or more of the cell lines used.

In the present study we aimed to investigate the capability of advanced *in vitro* models to express a range of TLRs and to respond to a broad range of TLR agonists to evaluate how well they emulate the *in vivo* intestinal responses. Therefore we studied the gene expression of TLRs and the cytokine excretion profile,

at baseline level and following TLR agonist induction, in a human induced pluripotent stem cell (iPSC) derived intestinal epithelial model [10] and a primary human small intestinal epithelial (PHSIE) cell model [4]. We evaluated the immuno-responsiveness of both models following exposure to a panel of TLRs (i.e. Pam3CSK4 (TLR1/2), poly(I:C) (TLR3), lipopolysaccharide (LPS) (TLR2/4), flagellin (TLR5) and single-stranded RNA (TLR7/8) as used before (Grouls et al., 2021). As an immune response readout we measured an array of cytokines, CCL20, IL-8, CXCL10, TNF-α, IL-10 and IL-12p40, IL-6 and the gene expression of TLRs 1, 2, 3, 4, 5, 7, 8 and 9 (qPCR).

3.2 Materials & Methods

3.2.1 EpiIntestinal culture

The PHSIE cell model (MatTek Life Sciences, Bratislava, Slovak Republic) consists of enterocytes, Paneth cells, M cells, tuft cells and intestinal stem cells cultured in permeable cell culture inserts [4]. Cell culture inserts (inner diameter of 8.8 mm) were placed in 12-well plates and cells were maintained in 100 µl maintenance medium (MatTek Life Sciences) in the apical compartment and 5 ml maintenance medium in the basolateral compartment upon arrival. After 24 hours of recovery all medium was removed and 50 µL of exposure medium containing LPS, PAM3CSK4 or flagellin (only bacterial TLR agonists were used for this model) at the concentrations described in Table 1 was added to the apical side, 5 mL maintenance medium was added to the basolateral side.

3.2.2 hiPSC culture

The hiPSC cell line (CS83iCTR-33n1) was provided by the Cedars-Sinai Medical Center's David and Janet Polak Foundation Stem Cell Core Laboratory. These cells have been generated through episomal reprogramming of fibroblasts of a 31-year-old healthy female. The cell line has been fully characterized and no karyotype abnormalities have been found [26]. hiPSCs were cultured on growth factor-reduced matrigel-coated (Corning) cell culture plates in mTeSR1 medium (Stem Cell Technologies, Vancouver, Canada) and were passaged using gentle cell dissociation reagent (Stem Cell Technologies).

3.2.3 hiPSC differentiation into intestinal organoids

For differentiation, hiPSCs were dissociated into single cells using accutase (Stem Cell Technologies) and cultured on human embryonic stem cell qualified matrigel-coated 24-well plates in mTeSR1 supplemented with 10 µM Y-27632 (Stem Cell Technologies) for 1 day. hiPSCs were subsequently differentiated into definitive endoderm (DE) by incubation in RPMI1640 medium containing 1% non-essential amino acids (Gibco, Waltham, USA), 100 ng/ml Activin A (Cell Guidance Systems, Cambridge, UK) with increasing concentrations of fetal bovine serum (0%, 0.2% and 2% on day 1, 2 and 3, respectively). 15 ng/ml BMP4 (R&D Systems, Minneapolis, USA) was also added during the first day of definitive endoderm formation. After three days hindgut endoderm formation was induced by changing the medium to RPMI1640 medium containing 1% non-essential amino acids (Gibco), 2% fetal bovine serum, 500 ng/ml FGF4 (R&D Systems) and 3 µM Chiron99021 (Stemgent, Cambridge, USA). After 4 days, free-floating spheroids were collected and embedded into domes of Matrigel (Corning, Corning, USA). Spheroids were cultured in Advanced DMEM/F-12 containing 1 × B27 (Gibco), 1 × N2 (Gibco), 15 mM HEPES (Gibco), 1%

penicillin/streptomycin (Gibco), 2 mM l-glutamine (Gibco), 50 ng/ml EGF (R&D Systems), 100 ng/ml Noggin (R&D Systems) and 500 ng/ml RSpondin-1 (R&D Systems). Medium was refreshed every 2–3 days and iPSC derived organoids were passaged every 10–14 days. Organoids used for experiments were grown in Matrigel for 28 days prior to exposure. To promote intestinal differentiation, 0.5 µM A-83-01 (Sigma, Saint Louis, USA), 20 µM PD98059 (Stem Cell Technologies), 5 mM 5-aza-2'-deoxycytidine (Sigma), and 5 µM DAPT (Sigma) were added to the medium after day 28 for a period of 7 days. After 35 days cells were exposed to the TLR agonists LPS, Pam3CSK4, flagellin, Poly(I:C) or ssRNA on the apical side at the concentrations in Table 1.

Table 1. Selected agonists their concentration used in the experiments and the associated TLRs.

Compound	Concentrations used	TLR
Pam3CSK4	300 ng/mL	1/2
Poly(I:C)	20 µg/mL	3
LPS	20 µg/mL	4
Flagellin	100 ng/mL	5
ssRNA	**3.2.4 µg/mL**	**7 + 8**

3.2.4 Cytokine measurement

In the PHSIE cell model medium was harvested at the basolateral side, in the iPSC model medium was harvested from the wells. For both models medium was harvested after 24 hours of exposure and stored at -80°C until cytokine measurement. The concentrations of macrophage inflammatory protein-3 (CCL-20/MIP3A), IFN-Gamma-Inducible Protein 10 (IP-10/CXCL10), Interleukin-8 (IL-8/CXCL8), Interleukin-6 (IL-6), Interleukin-10 (IL-10), Interleukin-1-beta (IL-1β), Interleukin-12p40 (IL-12p40) and Tumor Necrosis Factor alpha (TNF-α) were quantified using two human multiplex assay (Thermo Fischer, Waltham, MA, USA) on a Luminex FlexMap 3D (Merck Millipore, Burlington, MA, USA) according to manufacturer's protocol. Statistical significance was analyzed using a one-way ANOVA with a Dunnett's post-test to compare the effects of the exposures to their relative controls when comparing within models, when comparing the controls of the two models a t-test was used.

3.2.5 RNA isolation and qPCR

Following collection of the medium the cells were washed with 100 µL $DMEM^{+}$. After that, 350 µL RA1 lysis buffer (Macherey-Nagel, Duren, Germany) was added and incubated for 5 min. The entire volume of RA1 solution was collected as cell lysate and kept on ice until extraction. Total RNA was extracted from these samples using the NucleoSpin RNA isolation kit (Macherey-Nagel) according to manufacturer's instructions. Quality of the RNA was checked using a NanoDrop One (ratio absorbance at 260/280 > 1.8) (ThermoFisher, Wilmington, Delaware, USA). Then 300 ng of RNA was reverse transcribed to cDNA using the QuantiTect Reverse Transcription Kit (Qiagen, Venlo, The Netherlands). Expression of RPL27 (housekeeping gene) and genes coding for TLR1, TLR2, TLR 3, TLR4, TLR5, TLR7, TLR8 and TLR9 were quantified by RT-qPCR using the Rotor-Gene SYBR® Green Kit (Qiagen) and the Rotor-Gene 6000 cycler

(Qiagen) following the manufacturer's protocol. Primers were ordered at eurogentec (Seraing, Belgium) using the sequences in Table 2. Statistical significance was analyzed using a one-way ANOVA with a Dunnett's post-test to compare the effects of the exposures to their relative controls.

Table 2. qPCR primer sequences used for measurements of the housekeeping gene (hRPL27) and the TLRs.

Primer	Direction	Sequence
hRPL27_f	Forward	ATCGCCAAGAGATCAAAGATAA
hRPL27_r	Reverse	TCTGAAGACATCCTTATTGACG
hTLR1_f	Forward	TTCAAACGTGAAGCTACAGGG
hTLR1_r	Reverse	CCGAACACATCGCTGACAACT
hTLR2_f	Forward	ATCCTCCAATCAGGCTTCTCT
hTLR2_r	Reverse	GGACAGGTCAAGGCTTTTTACA
hTLR3_f	Forward	CAAACACAAGCATTCGGAATCTG
hTLR3_r	Reverse	AAGGAATCGTTACCAACCACATT
hTLR4_f	Forward	AGTTGATCTACCAAGCCTTGAGT
hTLR4_r	Reverse	GCTGGTTGTCCCAAAATCACTTT
hTLR5_f	Forward	CCGGGTTTGGCTTCCATAACA
hTLR5_r	Reverse	TGTGAAAGATCCAGGTGTCTCA
hTLR7_f	Forward	CACATACCAGACATCTCCCCA
hTLR7_r	Reverse	CCCAGTGGAATAGGTACACAGTT
hTLR8_f	Forward	ATGTTCCTTCAGTCGTCAATGC
hTLR8_r	Reverse	TTGCTGCACTCTGCAATAACT
hTLR9_f	Forward	AATCCCTCATATCCCTGTCCC
hTLR9_r	Reverse	GTTGCCGTCCATGAATAGGAAG

3.2.6 Analysis

The relative fold gene expression of the samples was calculated using the Delta-Delta Ct method ($2^{-\Delta\Delta Ct}$ method), in which each sample is corrected using the average of the three controls. This was also done for each control sample separately to show the deviation in the controls, as correction with the average ΔCt of the controls is done before conversion to $2^{-\Delta\Delta Ct}$ the average of the resulting values is not necessarily equal to one for the controls. For the baselevel gene expression of TLR2, 3, 4, 5, 7, 8 and 9 the relative gene expression was calculated relative to the gene expression of TLR1 of each model.

In addition the relative gene expression of each TLR in the iPSC model was calculated relative to the gene expression of the same TLR in the PHSIE model. Following the exposure to the agonists, the relative gene expression of the TLRs was compared to the control. For the cytokine excretion baselevel excretion of each cytokine was compared between the controls of the iPSC and PHSIE model. Following exposure to agonists the cytokine excretion was compared to the controls of their respective model.

3.3 Results

3.3.1 Baselevel gene expression of TLRs in both models

The cytokine excretion by the cells following exposure to the TLR agonists is dependent on the presence of TLRs. Therefore, we first studied the baselevel gene expression of TLR genes in the two cell models. In the control samples of the iPSC derived organoids the highest relative gene expression levels were observed for TLR3 and TLR9 being 29.1-fold and 49.5 fold higher than the TLR1 gene expression. Gene expression of TLR2 was also higher than that of TLR1 with a 5.8 fold difference in the relative expression level. For TLR4, TLR7 and TLR8 a relatively low gene expression was observed in the iPSC derived organoids, with a fold difference of 0.2, 0.04 and 0.01 respectively versus TLR1 (Fig. 1). In the iPSC derived organoids TLR5 was expressed at a level not significantly different from that of TRL1. In the control samples of the PHSIE cell model TLR 2, TLR3, and especially TLR9 were expressed at relatively higher levels than TLR1 with a fold difference relative to the expression of TLR1 of 22.2, 14.3, and 72.1 respectively. Low relative gene expression was observed for TLR 4, TLR7 and TLR8 with a fold difference of 0.001, 0.02 and 0.03 respectively versus TLR1 expression in the PHSIE cell model (Fig. 2). Also, in the PHSIE model TLR5 was expressed at a level not significantly different from that of TRL1.

When comparing the two models using the expression of the corresponding TLR in the PHSIE cells as the reference (Fig. 3) the iPSC derived organoids had a significantly higher relative gene expression of TLR1, TLR4 and TLR5 compared to their expression in the PHSIE model. In qualitative terms the TLR patterns in both cell models showed comparable trends with in both models TLR2, TLR3 and especially TLR9 being expressed at a higher level than TLR1, and TLR4, TLR7 and TLR8 being expressed to a relatively lower extent than TR1, while TLR5 was expressed at a similar level as TLR1.

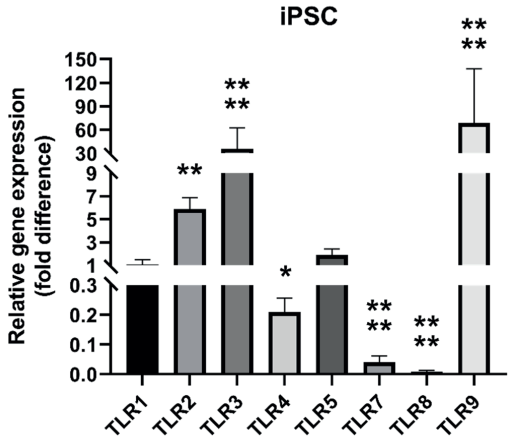

Figure 4. *Gene expression of TLRs in the iPSC derived organoids relative to the expression of TLR1. Significant differences* versus *TLR1 expression are indicated with * =* p *< 0.05, ** = p < 0.01 and **** = p < 0.0001.*

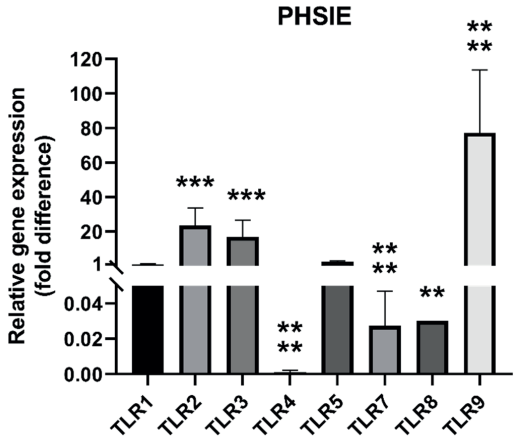

Figure 5. *Gene expression of in the PHSIE cell model TLRs relative to the expression of TLR1. Significant differences* versus *TLR1 expression are indicated with ** = p < 0.01, *** =* p *< 0.001 and **** = p < 0.0001.*

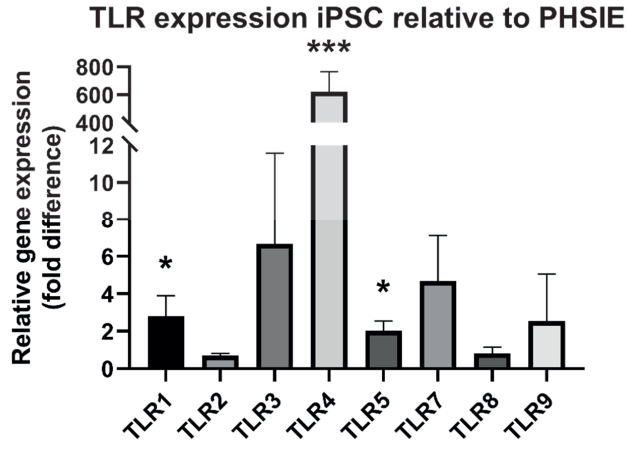

Figure 6. *Relative gene expression of TLRs in the iPSC model when compared to the corresponding TLR in PHSIE cell model. Significant differences are expressed with * = p < 0.05 and *** = p < 0.001.*

3.3.2 Gene expression of TLRs in both models after exposure to TLR agonists

Next, we studied the gene expression of the TLRs following exposure to the selected TLR agonists by measuring relative gene expression compared to the average expression of the same TLR in the control to investigate whether agonist exposure would affect the basal levels of TLR expression, since that could potentially influence the agonist response to be quantified in subsequent experiments. The results obtained are presented in Fig. 4 and 5 for the iPSC derived organoids and PHSIE cell model respectively.

The changes in the iPSC derived organoids were limited to some moderate changes in expression levels compared to the levels in untreated control cells (Fig. 4), with the only significant effects being a 3.38 fold induction of TLR2 by the TLR1/2 agonist Pam3CSK4, a 3.13, 3.31 and 3.28 fold induction of TLR4, TLR5 and TLR7 by the TLR3 agonist Poly(I:C), a 2.63, 2.33 and 2.33 fold reduction of respectively TLR2, TLR4 and TLR7 by the TLR4 agonist LPS, and a 2.28 fold induction of TLR4 by the TLR5 agonist flagellin. In the iPSC derived organoids especially expression levels of TLR9 showed high variability. Overall, the increases in expression levels were moderate, and not pointing at a systematic induction of the TLR receptor expression levels by the respective corresponding agonists, except for the TLR4 induction by LPS and the TLR2 induction by Pam3CSK4. The three bacterial TLR agonists tested in the PHSIE cell model, PAM3CSK4, LPS and flagellin, did not modify the TLR expression levels as compared to the untreated controls, except for the level of TLR9 that was significantly induced by the TLR1/2 agonist Pam3CSK4. A high interexperimental variability in TLR9 was observed also in the PHSIE cell model following exposure to the other two bacterial TLR agonists, hampering detection of significant changes (Fig. 5).

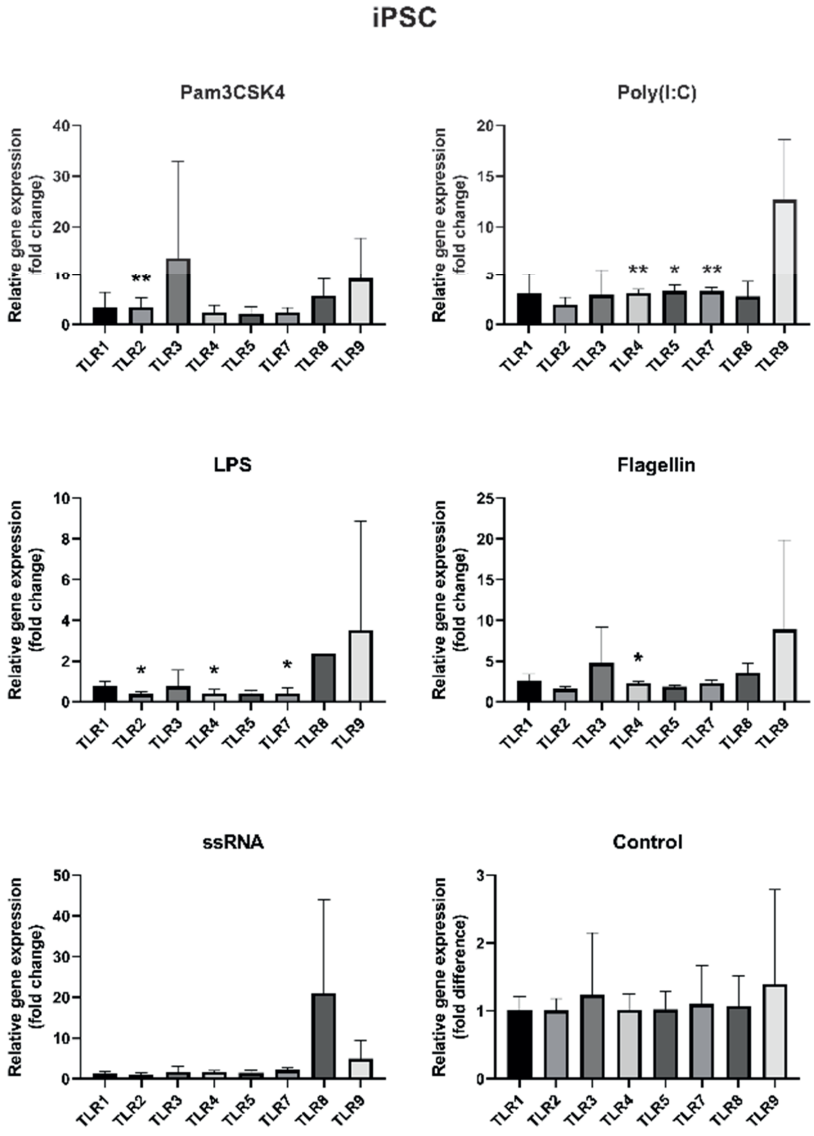

Figure 7. *Relative gene expression of TLRs by the iPSC derived organoids after 24 h of exposure to Pam3CSK4 (300 ng/mL), LPS (20 µg/mL), ssRNA (5 µg/mL), poly(I:C) (20 µg/mL), or flagellin (100 ng/mL) relative to the average expression in the control of the same TLR. For the control gene expression is calculated per sample and corrected by the average before conversion to* $2^{-\Delta\Delta Ct}$*, as correction with the average ΔCt of the controls is done before conversion to 2–ΔΔCt, the average of the resulting values is not necessarily equal to one (see materials and methods). Significant differences* versus *control expression are indicated with * =* p *< 0.05 and **= p < 0.01.*

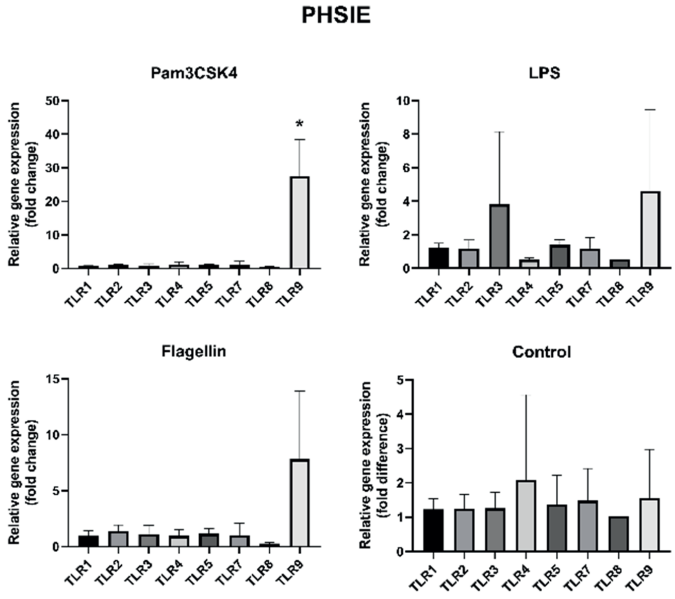

Figure 8. *Relative gene expression of TLRs by the PHSIE cell model after 24 h of exposure to Pam3CSK4 (300 ng/mL), LPS (20 µg/mL), ssRNA (5 µg/mL), poly(I:C) (20 µg/mL), or flagellin (100 ng/mL) relative to the average expression of the control of the same TLR. For the control gene expression is calculated per sample and corrected by the average before conversion to* $2^{-\Delta\Delta Ct}$*, as correction with the average ΔCt of the controls is done before conversion to 2–ΔΔCt, the average of the resulting values is not necessarily equal to one (see materials and methods) Significant differences* versus *control expression are indicated with * =* $p < 0.05$.

3.3.3 Excretion of cytokines after exposure to selected TLR agonists

Following characterizing of the two cell models with respect to the TLR expression levels and the effect of TLR agonists on these expression levels, the effect of the selected TLR agonists on the excretion of a series of cytokines was quantified. This was done to characterize whether the model systems provide a suitable model to mimic an *in vitro* gut barrier system that is able to respond to a broad range of TLR agonists and that has a cytokine excretion pattern comparable to the *in vivo* situation. To this end we determined the excretion in the cell models of seven cytokines being the macrophage inflammatory protein-3 (CCL-20/MIP3A), IFN-Gamma-Inducible Protein 10 (IP-10/CXCL10), Interleukin-8 (IL-8/CXCL8), Interleukin-6 (IL-6), Interleukin-10 (IL-10), Interleukin-1-beta (IL-1β), Interleukin-12p40 (IL-12p40) and Tumor Necrosis Factor alpha (TNF-α) both under control conditions and following TLR agonist exposure. In both cell models no excretion of IL-12p40, TNF-α and IL-10 was detected in the control exposure (< LOD; LOD = 1.81 pg/mL, 8.54 pg/mL and 2.44 pg/mL respectively) nor upon exposure to the panel of TLR agonists

(data not shown). Four cytokines (i.e. CCL20, CXCL10, IL-6 and IL-8) were excreted by one or both of the cell models following exposure to some of the TLR agonists. We converted all concentrations to pg excreted in 24 h to correct for the difference in volume between the two systems. Fig. 6 presents the cytokine excretions as detected under control conditions. It can be observed that four cytokines (i.e. CCL20, CXCL10, IL-6 and IL-8) were excreted by the iPSC derived organoids while in the PHSIE model only IL-8 was detectable. Fig. 7 and 8 present the responses of the two cell models with respect to cytokine excretion upon 24 h exposure to the selected TLR agonists.

In the iPSC derived organoids several TLR agonists induced cytokine excretion. This included: i) a 2.67-fold increased ($p < 0.05$) excretion of IL-6 following exposure to ssRNA, ii) a 1.65-fold increase ($p < 0.05$) and a 1.91 fold increase ($p<0.05$) for excretion of respectively CXCL10 and IL-8 after 24 h exposure to the TLR5 agonist flagellin, while iii) exposure to Poly(I:C) resulted in a significant 4.62-fold decrease ($p < 0.05$) in the excretion of IL-8 (Fig. 6).

In the PHSIE cell model again the three bacterial TLR agonists PAM3CSK4, LPS and flagellin, were tested. Upon exposure of the PHSIE cells to these bacterial TLR agonists no induction in excretion of cytokines was observed except for i) the excretion of IL-8 upon exposure to the TLR4 agonist LPS at a level that was 1.5-fold higher ($p<0.01$) than what was already observed in the control cells without TLR agonist exposure, ii) excretion of CXCL10 and IL-6, not observed in the control, but detected at 2.8 pg and 7.1 pg upon 24 h exposure to the TLR4 agonist LPS, iii) excretion of CXCL10, that was not detectable in the control, but observed at 66 pg upon 24 hour exposure to the TLR5 agonist flagellin, while iv) excretion of IL-8 was significantly reduced compared to the control and was no longer detectable upon 24 h exposure to flagellin (Fig. 7).

Comparison of the effects in the two cell models indicates that both models showed an increased excretion of CXCL10 upon exposure to flagellin, and in both models IL-8 excretion was affected by the exposure to some of the TLR agonists.

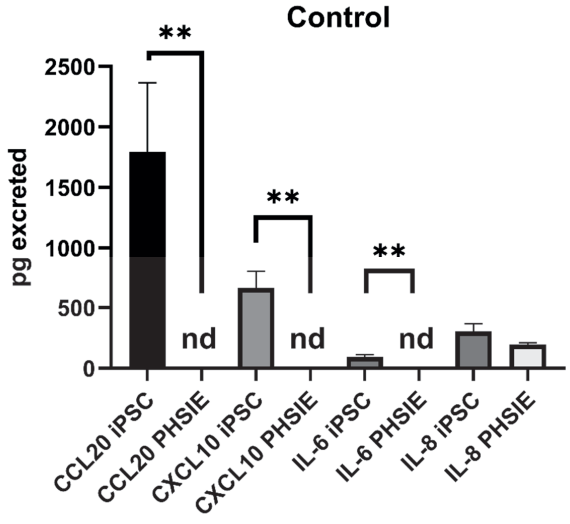

Figure 9. *Excretion of cytokines by the control iPSC derived organoids and PHSIE cell model into the medium after 24 h. Significant differences* between models *are indicated with ** = p < 0.01. nd = not detected.*

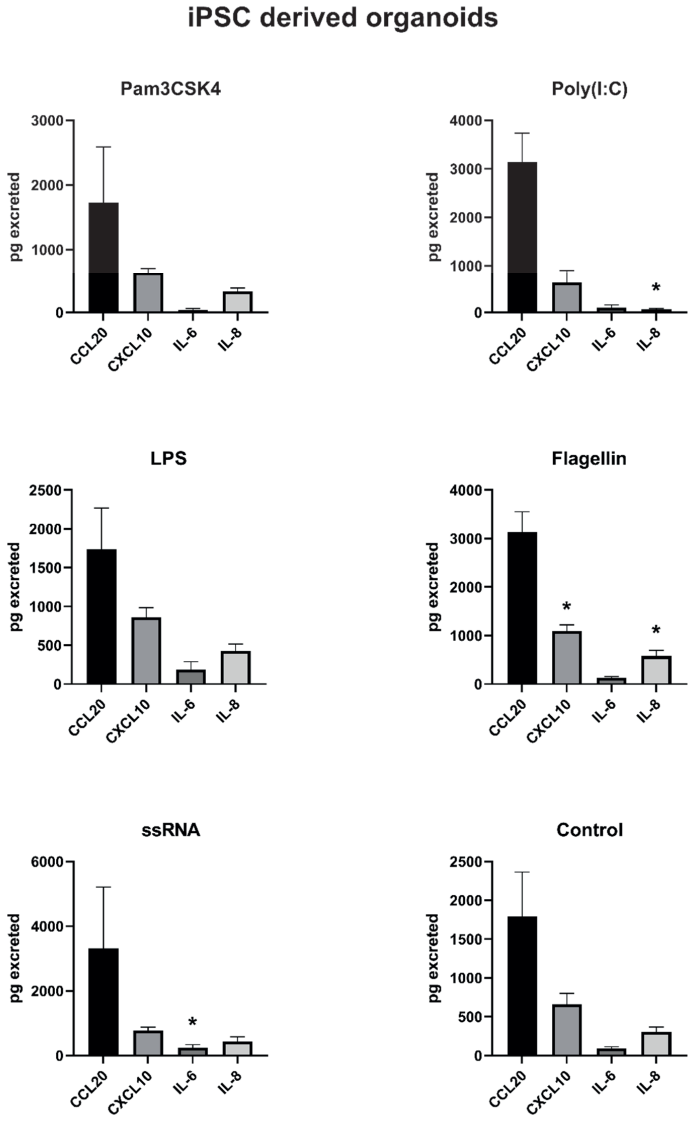

Figure 10. *Excretion of cytokines by the iPSC derived organoids into the medium after 24 h exposure to Pam3CSK4 (300 ng/mL), poly(I:C) (20 µg/mL), LPS (20 µg/mL), flagellin (100 ng/mL), or ssRNA (5 µg/mL). Significant differences* versus *control excretion are indicated with * =* $p < 0.05$.

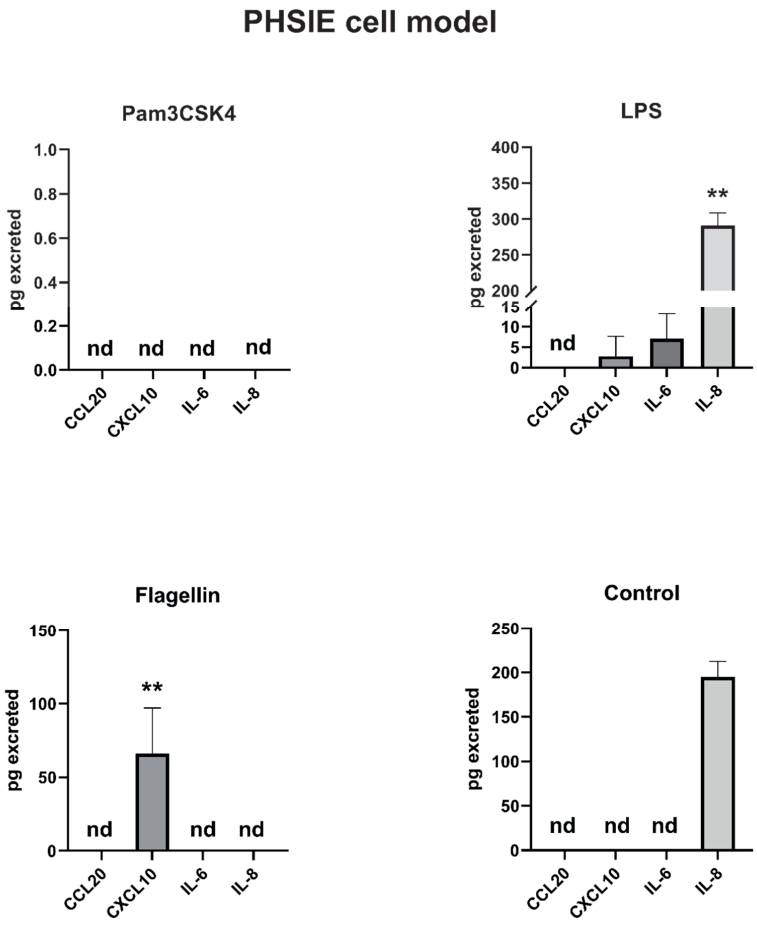

Figure 11. *Excretion of cytokines by the PHSIE cell model into the medium after 24 h exposure to Pam3CSK4 (300 ng/mL), poly(I:C) (20 µg/mL), LPS (20 µg/mL), flagellin (100 ng/mL), or ssRNA (5 µg/mL). Significant differences* versus *control excretion are indicated with **= p < 0.01.*

3.3.4 Literature review of presence of TLR receptors in human biopsies or organoids

To allow comparison of the expression levels of the TLRs in the two *in vitro* models, the presence and expression levels of TLRs in intestinal biopsies from humans and human iPSC or adult stem cell derived organoids as reported in the literature is summarized in Table 3. TLR gene expression data have been reported for fetal ileal epithelial, and adult colon biopsies. Gene expression of TLR1 in the colon biopsies was only reported in a single study [16]. For TLR2 several studies confirmed the expression in different intestinal epithelial segments and also in both iPSC and adult stem cell derived *in-vitro* models [16–22].

For TLR3 three studies reported expression in colonic biopsies and one in adult stem cell derived organoids from both the colon and small intestine [16, 17, 19, 21]. For TLR4 expression in different intestinal segments was reported in several studies, though two reported a relatively low expression [16–19, 21–23]. One study reported an absence of TLR4 expression in both fetal explants and biopsies from small bowel restrictions [20]. For TLR5 four studies reported expression in colonic biopsies, fetal colonic xenografts and adult stem cell derived organoids from both the colon and small intestine [16, 17, 22, 24]. For TLR7 expression was reported in two studies using colonic biopsies and iPSC derived organoids [16, 21]. For TLR8 and 9 expression was reported in one study using colon biopsies [16]. The TLR gene expression in the PHSIE cell model as used in this study has not been reported in the literature before.

Table 3 *Overview of the presence of TLR in human biopsies or organoids according to literature.*

TLR	Origin of cells	Intestinal segment	Expression	TLR expression detection method	Ref
1	Biopsies	Colon	+	RT-PCR	[16]
2	Biopsies	Colon	+	RT-PCR	[16]
	Biopsies	Colon	±	Immunohistochemistry	[17]
	Biopsies	Fetal ileal	+	RT-PCR + Western Blot	[18]
	Biopsies	Colon	+	Immunohistochemistry	[19]
	Biopsies	Fetal explants + adult small bowel resection	+	RT-PCR	[20]
	In vitro induced SC	General	+	qPCR	[21]
	In vitro adult SC	Colon + small intestine	+	rnaSEQ	[22]
3	Biopsies	Colon	+	RT-PCR	[16]
	Biopsies	Colon	+	Immunohistochemistry	[17]
	Biopsies	Colon	+	Immunohistochemistry	[19]
	In vitro induced SC	General	+	qPCR	[21]
4	Biopsies	Colon	+	RT-PCR	[16]
	Biopsies	Colon	±	Immunohistochemistry	[17]
	Biopsies	Fetal ileal	+	RT-PCR + Western Blot	[18]
	Biopsies	Colon	+	Immunohistochemistry	[19]
	Biopsies	Fetal explants + adult small bowel resection	-	RT-PCR	[20]
	Biopsies	Infant small intestine	+	qPCR + SDS-PAGE	[23]
	In vitro induced SC	General	+	qPCR	[21]
	In vitro adult SC	Colon	+	rnaSEQ	[22]
	In vitro adult SC	Small intestine	±	rnaSEQ	
5	Biopsies	Colon	+	RT-PCR	[16]
	Biopsies	Colon	+	Immunohistochemistry	[17]
	Biopsies	Colon	+	qPCR + Immunohistochemistry	[24]
	Xenograft	Fetal colon		Immunohistochemistry	
	In vitro adult SC	Colon + small intestine	+	rnaSEQ	[22]
7	Biopsies	Colon	±	RT-PCR	[16]
	In vitro induced SC	General	±	qPCR	[21]
8	Biopsies	Colon	+	RT-PCR	[16]
9	Biopsies	Colon	+	RT-PCR	[16]

SC = stem cell; TLR = Toll-Like Receptor; SEQ = Sequencing

3.4 Discussion

We aimed to identify an *in vitro* gut barrier system that is able to respond to a broad range of TLR agonists similar to the *in vivo* situation. For this, we characterized the basal and TLR agonist induced levels of the TLR receptors in iPSC derived organoids and a primary human small intestinal epithelial (PHSIE) cell model and subsequently challenged these model barrier systems to a panel of TLR-agonists measuring the effects on the excretion of a number of cytokines. We also collected available data on TLR gene expression in *ex vivo* and advanced intestinal *in vitro* models for comparison. We evaluated responses following exposure to bacterial agonists; flagellin, LPS and PAM3CSK4 in both models and in the iPSC derived organoids and

we additionally evaluated responses following exposure to viral mimicking agonists ssRNA and Poly(I:C). These agonists represent model compounds for important TLRs that respond to TLR agonist exposure in the human intestine.

We compared two systems that use a different approach to achieve the same goal, to create an intestinal model that closely mimics the *in vivo* gut. The difference in approaches used does create a number of uncertainties when comparing the two models. Characterization of both models has revealed the presence of different cell types with both models containing enterocytes, Paneth cells and stem cells but the PHSIE cell model also contains M cells and tuft cells while iPSC derived organoids also contain goblet cells, enteroendocrine cells and mesenchymal cells [4–8]. It has been reported that various cell types in the human intestinal epithelium display different TLR expression patterns [13], so this can influence the ability of the systems to respond to TLR agonist exposure. The PHSIE cell model forms a layer but due to the small apical volume cytokines could only be measured in the basolateral compartment. The iPSC derived organoids form spherical organoids with the internal compartment of the organoid representing the intestinal lumen. We measured the cytokines in the medium on the outside of the organoid which represents the basolateral side. The difference in structure also means that the number of cells in the two systems is not directly comparable, so besides the difference in cellular makeup also a potential difference in cell number, makes comparison of basal cytokine levels difficult. Measurement of total protein content could correct for the cell number but not for differences in cellular makeup. However, both models include extracellular matrices consisting of proteins that interfere with a total protein measurement. Total RNA content could be used as an indication for difference in cell number, which in our case is about four times higher in the PHSIE control samples compared to the iPSC derived organoid control samples (Table S1). This means the differences between the two systems might be even bigger than shown by the cytokine excretion levels. The qPCR expression levels can be compared more easily as this measures copy number in a specific amount of mRNA and thus is independent of cell number.

When looking at the TLR gene expression before the agonist exposure we observed that the TLR9 gene is significantly higher expressed than the TLR1 gene in both models. Similarly, TLR2, 3 and 5 gene expression levels were relatively high in both models. Comparatively, TLR 4, 7 gene expression was lower than TLR1 gene expression in both models. In the PHSIE cell model TLR8 could not be detected in two out of the three samples. Based on our review of literature we concluded that all TLRs can be expected to be expressed in all compartments of the human intestine, with only TLR4 being reported as absent in one study [20]. Except for the variable presence of a detectable level of TLR8 in the PHSIE cell model our results match with these literature data.

In spite of the overall qualitative similarities in the TLR patterns of both cell models there were substantial differences both in basal TLR expression levels, and in the effects of TLR agonist exposures on these levels. We observed a clear difference in TLR4 gene expression between both models with the iPSC derived organoids expressing the TLR4 gene 600 times higher compared to the PHSIE cell model, though expression of the TLR4 gene in both models is low compared to the gene expression of the other TLRs. We found one study in the literature that also studied TLR expression levels in iPSC derived organoids [21]. The authors detected five out of the eight TLRs that we analyzed, comparatively they report that TLR4 has the highest level of expression while TLR7 had the lowest and TLR 2, 3 and 9 were similar in expression.

So even though they used a similar model, iPSC derived organoids, they observed different relative expression levels. This can be partially attributed to donor variation of the iPSC cells but it is also of interest to note that the TLR expression in their lung organoids derived from the same iPSC cells is twenty times lower than that in their intestinal organoids indicating that the expression is also influenced by the differentiation protocol [21].

Exposure of the PHSIE cell model to the three bacterial TLR agonists generally did not result in significant increases in TLR gene expression, with the exception of TLR9, that was significantly induced by the TLR1/2 agonist Pam3CSK4, while showing high interexperimental variability hampering detection of significant changes in this TLR9 expression by the other two bacterial TLR agonists. Also the iPSC derived organoids showed limited, albeit some significant, changes in TLR expression levels upon exposure to some of the TLR agonists. This implies that the two in vitro model systems did not show a comparable response of their TLR expression levels upon exposure to the TLR agonists. In addition literature also reports effects, in both in vitro and ex vivo models, that are different from what was observed in our in vitro models. In literature for example, colon xenografts are reported to show a large increase in TLR5 gene expression after exposure to the TLR5 agonist flagellin [24]. For LPS, no effect on TLR gene expression was previously observed in intestinal biopsies while a decrease in TLR4 expression was reported in fetal ileal biopsies similar to our results in the PHSIE cell model [16, 18]. The results of the present study confirm that there is not a systematic induction of the TLR receptor expression level by the respective corresponding agonists, except for the TLR4 induction by LPS and the TLR2 induction by Pam3CSK4 in the iPSC derived organoids.

The production of the cytokines in the control samples also showed differences between the two *in vitro* models. While the PHSIE cell model under standard culture conditions only produced a detectable level of IL-8, the iPSC derived organoids produced four cytokines, CCL20, CXCL10, IL6 and IL8. Furthermore, we were unable to detect IL-12p40, TNF-α and IL-10 in the models, while these have been reported in other *in vitro* cell models [21, 27]. Upon exposure to the different TLR agonists further differences in cytokine production between the two models and between the two *in vitro* models and literature reported *in vitro* and *in vivo* data were noted.

Pam3CSK4 is a potent synthetic TLR1/2 agonist, this TLR1/2 dimer normally recognizes bacterial lipoproteins and lipopeptides [28]. The iPSC derived organoid exposure to Pam3CSK4 did not induce the excretion of any of the cytokines while it decreased the IL-6 excretion. The exposure to Pam3CSK4 in PHSIE cell model did not result in detectable levels of any of the cytokines in the medium, for IL-8 this implies a decreased excretion compared to the control. In adult stem cell derived organoids from all parts of the colon a low increase in IL-8 expression after exposure to Pam3CSK4 was observed which matched with the low gene expression of TLR2 in those colon parts compared to the organoids derived from the stomach [22]. Also in colonic adult stem cell derived organoids increased IL-6 expression after exposure to Pam3CSK4 using was observed [29]. So, our results show that the most important response to Pam3CSK4 might be a change in TLR gene expression and not cytokine production. Overall, neither model showed a significant response in cytokine excretion after exposure with Pam3CSK4.

Poly(I:C) is a synthetic double stranded RNA used to simulate viral infection [30] and is recognized by TLR3. In the present study only the iPSC derived organoids were exposed to viral TLR agonists. We observed a

decrease in IL-8 excretion after exposure to Poly(I:C) in iPSC derived organoids. This differs from literature where an increase in excretion of IL-6 and IL-8 after exposure to Poly(I:C) was reported for colonic adult stem cell derived organoids, with an accompanying increase in all other measured cytokines [21].

Lipopolysaccharides are part of the outer membrane of gram-negative bacteria and are recognized by TLR4 [31, 32]. Only the PHSIE model showed a significant response to LPS with an increased excretion of IL-8. This effect of LPS is not consistent with the results following MAPK activation in human biopsies [16] and the observed increased gene expression and excretion of IL-1β, IL-6, IL-8, MCP-1 and TNF-α but not IL-12p40 expression in adult stem cell derived intestinal organoids exposed to LPS [21]. The lack of significant response in the iPSC derived organoids exposed to LPS was also seen before following LPS exposure of adult stem cell derived organoids [22].

Flagellin is a part of the bacterial flagellum, which plays a role in the motility, adhesion and invasion of cells by (certain) bacteria [33]. Flagellin is known to be a potent immune activator which acts via TLR5 [34, 35]. In the iPSC derived organoids we observed an increase in CXCL10 and IL-8 excretion upon flagellin exposure. In the PHSIE cell model only the excretion of CXCL10 was significantly increased upon exposure to flagellin, while, similar to the unexposed control, the other three cytokines could not be detected in the medium. In the PHSIE cell model excretion of IL-8 was significantly reduced compared to the control situation. In literature human adult stem cell derived organoids displayed an increase in IL-8 gene expression after exposure to flagellin in jejunum and colon but not the duodenum and ileum derived organoids [22], pointing at a difference between the *in vivo* situation and the PHSIE cell model while the iPSC derived organoids adequately mimicked the results. All together the iPSC organoids appeared to reflect the multitude of effects of flagellin, which is considered a potent immunomodulatory agent [36], better than the PHSIE cell model.

ssRNA is recognized by both TLR7 and TLR8 in intracellular compartments like the endosomes [14] so activation requires endocytosis of the agonist. In our experiments we assured internalization of ssRNA by the addition of LyoVec during the exposure. The PHSIE cell model was only exposed to the bacterial agonists, so for this cell model no data are available for the viral TLR agonist ssRNA and poly(I:C). The iPSC derived organoids showed a significantly increased excretion of IL-6 upon exposure to ssRNA. Previously it was shown that exposure of colonic adult stem cell derived organoids to another TLR 7/8 agonist, R848, increased the IL-6 expression [29].

We set out to study which cell model could best be used for future studies focusing on immunomodulation in the human gut. Firstly, we conclude that TLR gene expression in the PHSIE cell model was lower than that of the iPSC derived organoids, with for example TLR8 gene expression only being detectable in one of the PHSIE cell model samples. Previous studies indicated that all TLRs are expressed in the human intestine or advanced intestinal models, so the iPSC derived organoids better emulate the *in vivo* intestinal situation. Secondly, cytokine production in the control samples of the PHSIE cell model was below detectable levels except for IL-8, and only CXCL10 and IL-8 showed a significant response to one TLR agonist tested. Comparatively, the iPSC derived organoids showed measurable levels of four cytokines in the control samples and a wider range of responses against the TLR agonists. Importantly the results show the importance of measuring more than one endpoint with none of the cytokines showing the same response to all agonists. Thirdly, we also observed differences in the level of gene expression between the

different TLRs after exposure to agonists. Measuring one singular TLR does not give the full overview of effects so measuring a wide array like performed here is the best approach. Lastly, effects on cytokines and TLRs can be opposite, as observed for Poly(I:C) where IL-8 excretion decreased but TLR expression increased, showing the importance of measuring both endpoints. Overall, the PHSIE cell model, like previously studied cell line based models [25], only displayed a limited ability to respond to the bacterial TLR agonists. While the iPSC derived organoids were able to respond to a range of bacterial and viral TLR agonists. Therefore, it is concluded that the iPSC derived organoids are a promising model to further study intestinal immune responses.

Acknowledgements

The authors acknowledge the constructive comments on this work provided by Ivonne M. C. M. Rietjens. For this work MG was supported by a grant funded by the Dutch Research Council, a Building Blocks of Life project (No. 737.016.003). Work on this project by AJ and MvdZ was supported by the Dutch Ministry of Agriculture, Nature and Food Quality (Grant: KB-37-002-020).

The author would like to thank Claudia Beaurivage (at that time employed by Galapagos, Leiden, The Netherlands) for the cytokine measurements performed on our samples.

References

1. Silverthorn DU, Johnson BR, Ober WC, Ober CE, Silverthorn AC. Human physiology : an integrated approach. 2016.
2. Russell WMS, Burch RL. The principles of humane experimental technique. 1959.
3. Costa J, Ahluwalia A. Advances and Current Challenges in Intestinal in vitro Model Engineering: A Digest. Front Bioeng Biotechnol. 2019;7 JUN:144.
4. Ayehunie S, Stevens Z, Landry T, Klausner M, Hayden P, Letasiova S. Novel 3-D human small intestinal tissue model to assess drug permeation, inflammation, and wound healing. Toxicol Lett. 2014;229:S144.
5. Tamminen K, Balboa D, Toivonen S, Pakarinen MP, Wiener Z, Alitalo K, et al. Intestinal Commitment and Maturation of Human Pluripotent Stem Cells Is Independent of Exogenous FGF4 and R-spondin1. PLoS One. 2015;10:e0134551–e0134551.
6. Mccracken KW, Howell JC, Wells JM, Spence JR, Org; KM, Org; JH, et al. Generating human intestinal tissue from pluripotent stem cells in vitro. Nat Protoc. 2011;6:1920–8.
7. Kabeya T, Mima S, Imakura Y, Miyashita T, Ogura I, Yamada T, et al. Pharmacokinetic functions of human induced pluripotent stem cell-derived small intestinal epithelial cells. Drug Metab Pharmacokinet. 2020;35:374–82.
8. Iwao T, Kodama N, Kondo Y, Kabeya T, Nakamura K, Horikawa T, et al. Generation of Enterocyte-Like Cells with Pharmacokinetic Functions from Human Induced Pluripotent Stem Cells Using Small-Molecule Compounds. Drug Metab Dispos. 2015;43:603–10.
9. Hill DR, Spence JR. Gastrointestinal Organoids: Understanding the Molecular Basis of the Host–Microbe Interface. Cell Mol Gastroenterol Hepatol. 2017;3:138.
10. Janssen AWF, Duivenvoorde LPM, Rijkers D, Nijssen R, Peijnenburg AACM, van der Zande M, et al. Cytochrome P450 expression, induction and activity in human induced pluripotent stem cell-derived intestinal organoids and comparison with primary human intestinal epithelial cells and Caco-2 cells. Arch

Toxicol. 2020;95:907–22.
11. Zachos NC, Kovbasnjuk O, Foulke-Abel J, In J, Blutt SE, De Jonge HR, et al. Human Enteroids/Colonoids and Intestinal Organoids Functionally Recapitulate Normal Intestinal Physiology and Pathophysiology *. J Biol Chem. 2016;291:3759–66.
12. Abreu MT. Toll-like receptor signalling in the intestinal epithelium: how bacterial recognition shapes intestinal function. Nat Rev Immunol 2010 102. 2010;10:131–44.
13. Price AE, Shamardani K, Lugo KA, Deguine J, Roberts AW, Lee BL, et al. A Map of Toll-like Receptor Expression in the Intestinal Epithelium Reveals Distinct Spatial, Cell Type-Specific, and Temporal Patterns. Immunity. 2018;49:560-575.e6.
14. Triantafilou K, Vakakis E, Orthopoulos G, Ahmed MAE, Schumann C, Lepper PM, et al. TLR8 and TLR7 are involved in the host's immune response to human parechovirus 1. Eur J Immunol. 2005;35:2416–23.
15. Takeda K, Akira S. TLR signaling pathways. Semin Immunol. 2004;16:3–9.
16. Otte JM, Cario E, Podolsky DK. Mechanisms of Cross Hyporesponsiveness to Toll-Like Receptor Bacterial Ligands in Intestinal Epithelial Cells. Gastroenterology. 2004;126:1054–70.
17. Cario E, Podolsky DK. Differential alteration in intestinal epithelial cell expression of Toll-like receptor 3 (TLR3) and TLR4 in inflammatory bowel disease. Infect Immun. 2000;68:7010–7.
18. Fusunyan RD, Nanthakumar NN, Baldeon ME, Walker WA. Evidence for an innate immune response in the immature human intestine: Toll-like receptors on fetal enterocytes. Pediatr Res. 2001;49 4 I:589–93.
19. Furrie E, Macfarlane S, Thomson G, Macfarlane GT. Toll-like receptors-2, -3 and -4 expression patterns on human colon and their regulation by mucosal-associated bacteria. Immunology. 2005;115:565–74.
20. Naik S, Kelly EJ, Meijer L, Pettersson S, Sanderson IR. Absence of Toll-like receptor 4 explains endotoxin hyporesponsiveness in human intestinal epithelium. J Pediatr Gastroenterol Nutr. 2001;32:449–53.
21. Jose SS, De Zuani M, Tidu F, Hortová Kohoutková M, Pazzagli L, Forte G, et al. Comparison of two human organoid models of lung and intestinal inflammation reveals Toll-like receptor signalling activation and monocyte recruitment. Clin Transl Immunol. 2020;9:e1131.
22. Kayisoglu O, Weiss F, Niklas C, Pierotti I, Pompaiah M, Wallaschek N, et al. Original research: Location-specific cell identity rather than exposure to GI microbiota defines many innate immune signalling cascades in the gut epithelium. Gut. 2021;70:687.
23. Leaphart CL, Cavallo J, Gribar SC, Cetin S, Li J, Branca MF, et al. A Critical Role for TLR4 in the Pathogenesis of Necrotizing Enterocolitis by Modulating Intestinal Injury and Repair. J Immunol. 2007;179:4808–20.
24. Miyamoto Y, Iimura M, Kaper JB, Torres AG, Kagnoff MF. Role of Shiga toxin versus H7 flagellin in enterohaemorrhagic Escherichia coli signalling of human colon epithelium in vivo. Cell Microbiol. 2006;8:869–79.
25. Grouls M, van der Zande M, de Haan L, Bouwmeester H. Responses of increasingly complex intestinal epithelium in vitro models to bacterial toll-like receptor agonists. Toxicol Vitr. 2022;79:105280.
26. Mattis VB, Tom C, Akimov S, Saeedian J, Østergaard ME, Southwell AL, et al. HD iPSC-derived neural progenitors accumulate in culture and are susceptible to BDNF withdrawal due to glutamate toxicity. Hum Mol Genet. 2015;24:3257–71.

27. Beaurivage C, Kanapeckaite A, Loomans C, Erdmann KS, Stallen J, Janssen RAJ. Development of a human primary gut-on-a-chip to model inflammatory processes. Sci Reports 2020 101. 2020;10:1–16.
28. Oliveira-Nascimento L, Massari P, Wetzler LM. The role of TLR2 ininfection and immunity. Front Immunol. 2012;3 APR:79.
29. Stanifer ML, Mukenhirn M, Muenchau S, Pervolaraki K, Kanaya T, Albrecht D, et al. Asymmetric distribution of TLR3 leads to a polarized immune response in human intestinal epithelial cells. Nat Microbiol 2019 51. 2019;5:181–91.
30. Fortier ME, Kent S, Ashdown H, Poole S, Boksa P, Luheshi GN. The viral mimic, polyinosinic:polycytidylic acid, induces fever in rats via an interleukin-1-dependent mechanism. Am J Physiol - Regul Integr Comp Physiol. 2004;287 4 56-4.
31. Faure E, Equils O, Sieling PA, Thomas L, Zhang FX, Kirschning CJ, et al. Bacterial lipopolysaccharide activates NF-κB through toll-like receptor 4 (TLR-4) in cultured human dermal endothelial cells. Differential expression of TLR-4 and TLR-2 in endothelial cells. J Biol Chem. 2000;275:11058–63.
32. Triantafilou M, Triantafilou K. Lipopolysaccharide recognition: CD14, TLRs and the LPS-activation cluster. Trends in Immunology. 2002;23:301–4.
33. Haiko J, Westerlund-Wikström B. The role of the bacterial flagellum in adhesion and virulence. Biology. 2013;2:1242–67.
34. Gewirtz AT, Navas TA, Lyons S, Godowski PJ, Madara JL. Cutting Edge: Bacterial Flagellin Activates Basolaterally Expressed TLR5 to Induce Epithelial Proinflammatory Gene Expression. J Immunol. 2001;167:1882–5.
35. Murthy KGK, Deb A, Goonesekera S, Szabó C, Salzman AL. Identification of Conserved Domains in Salmonella muenchen Flagellin That Are Essential for Its Ability to Activate TLR5 and to Induce an Inflammatory Response in Vitro. J Biol Chem. 2004;279:5667–75.
36. Hajam IA, Dar PA, Shahnawaz I, Jaume JC, Lee JH. Bacterial flagellin—a potent immunomodulatory agent. Exp Mol Med. 2017;49:e373–e373.

Supplementary files

Table S3 RNA concentration in control samples of the iPSC derived organoids and PHSIE model. Same elution volume was used in both models.

Control	ng/µl RNA iPSC derived organoids	ng/µl RNA PHSIE
1	201.2	547
2	111.7	637
3	131	643.5

Chapter 4

Differential gene expression in iPSC-derived human intestinal epithelial cell layers following exposure to two concentrations of butyrate, propionate and acetate

Based on: Grouls, M., Janssen, A.W.F., Duivenvoorde, L.P.M. et al. Differential gene expression in iPSCderived human intestinal epithelial cell layers following exposure to two concentrations of butyrate, propionate and acetate. Sci Rep 12, 13988 (2022). https://doi.org/10.1038/s41598-022-17296-8.

Menno Grouls[1], Aafke W.F. Janssen[2], Loes P.M. Duivenvoorde[2], Guido J.E.J. Hooiveld[3], Hans Bouwmeester[1], and Meike van der Zande[2]

[1] Division of Toxicology, Wageningen University, Wageningen University & Research, Postbus 8000, 6700 EA, Wageningen, The Netherlands
[2] Wageningen Food Safety Research, Wageningen University & Research, Wageningen, The Netherlands
[3] Division of Human Nutrition, Wageningen University, Wageningen University & Research, Wageningen, The Netherlands

Abstract

Intestinal epithelial cells and the intestinal microbiota are in a mutualistic relationship that is dependent on communication. This communication is multifaceted, but one aspect is communication through compounds produced by the microbiota such as the short-chain fatty acids (SCFAs) butyrate, propionate and acetate. Studying the effects of SCFAs and especially butyrate in intestinal epithelial cell lines like Caco-2 cells has been proven problematic. In contrast to the *in vivo* intestinal epithelium, Caco-2 cells do not use butyrate as an energy source, leading to a build-up of butyrate. Therefore, we used human induced pluripotent stem cell derived intestinal epithelial cells, grown as a cell layer, to study the effects of butyrate, propionate and acetate on whole genome gene expression in the cells. For this, cells were exposed to concentrations of 1 and 10 mM of the individual short-chain fatty acids for 24 hours. Unique gene expression profiles were observed for each of the SCFAs in a concentration-dependent manner. Evaluation on both an individual gene level and pathway level showed that butyrate induced the biggest effects followed by propionate and then acetate. Several known effects of SCFAs on intestinal cells were confirmed, such as effects on metabolism and immune responses. The changes in metabolic pathways in the intestinal epithelial cell layers in this study demonstrate that there is a switch in energy *homeostasis, this is likely associated with the use of* SCFAs as an energy source by the induced pluripotent stem cell derived intestinal epithelial cells similar to *in vivo* intestinal tissues where butyrate is an important energy source.

Keywords: SCFA, butyrate, propionate, acetate, intestine, intestinal epithelial cells, iPSC, RNA sequencing, Complex *in vitro* models

4.1 Introduction

The interactions between the host intestinal mucosa and the intestinal microbiota is a mutualistic relationship that is important for maintaining the host's health. The human intestine offers a niche for many bacteria to live in, and in turn these bacteria fulfil an important role in metabolism of drugs and food related chemicals, and synthesis of beneficial chemicals like vitamins [1]. Upon microbial fermentation of dietary fibers, the intestinal microbiota produces short chain fatty acids (SCFAs) which are fatty acids with fewer than six carbon atoms [2, 3]. The total concentration of SCFAs in the intestinal tract ranges from ~11-13 mM in the distal small intestine to 50-100 mM in the colon [3].

Butyrate, acetate and propionate are three of the most abundantly produced intestinal SCFAs. These SCFAs serve as a prominent energy source in various cell types, and have been shown to regulate immune responses in the gut by affecting immune related signaling pathways in epithelial cells [4, 5], which in turn affect immune cells residing in the lamina propria such as monocytes (i.e. reduction in migration) and macrophages (i.e. reduction of IL-12 excretion and induction of IL-10 excretion) [6, 7]. These SCFAs have also been shown to affect the barrier function of the intestinal epithelium by modulating tight junction formation [8] and by adjusting proliferation and differentiation of intestinal epithelial cells [9, 10]. Butyrate is the most studied SCFA, it maintains gastrointestinal health by serving as the main energy source for enterocytes, enhancing epithelial barrier integrity and by inhibiting inflammation [11].

A disbalance in intestinal SCFA levels has been associated with a dysbiosis in the intestinal microbiota and has been linked to a still increasing number of diseases such as Inflammatory Bowel Disease (IBD) [12], Alzheimer's disease [13] and Parkinson's disease [14, 15]. In IBD patients, the concentrations of SCFAs in the intestine are decreased due to a decrease in the number of butyrate producing bacteria that make up the microbiota [12, 16, 17]. The relation of SCFAs with Alzheimer's disease is multifactorial encompassing five aspects; epigenetic regulation, modulation of neuroinflammation, maintenance of the blood-brain barrier, regulation of brain metabolism and interference in amyloid protein formation with butyrate being the most impactful SCFA [13]. For Parkinson's disease it has been observed that changes in the makeup of the gut microbiota, in particular a decrease in SCFA producing fiber degrading bacterial strains, correlate with disease progression [14].

Several human intestinal cell models have been used to study the mode of action of SCFAs. Initially, well-characterized conventional cell-line based models like Caco-2 cells and their coculture variants (i.e. Caco-2 and HT29 cells) were exposed to SCFAs to study their effects [18, 19]. However, these are cancer cells and the effects of SCFAs on these cells cannot be easily extrapolated to human *in vivo* conditions as cancer cells do not use butyrate as their energy source. This leads to a build-up of butyrate and is referred to as the butyrate paradox [20–23]. Novel directions in research have been made possible after the hallmark success of culturing primary intestinal tissues and adult stem cell-based 3D human intestinal organoids (HIOs) *in vitro*. Subsequently, induced pluripotent stem cell (iPSC) based 3D HIOs were developed [24]. iPSCs can be differentiated into a large variety of cells in the human body by applying growth factors during their development. Using a protocol for differentiation into HIOs resulted in a microarchitecture and cell type composition similar to the human intestine. iPSC derived HIOs consist of enterocytes, goblet cells, mesenchymal and enteroendocrine cells [25–28]. Furthermore, iPSC derived HIOs have shown

improved cytochrome P450 and transporter expression in comparison with Caco-2 cells [29, 30]. More recently, iPSCs have been used to create 2D intestinal epithelial cell (IEC) layers that emulate the full cellular complexity of the 3D HIOs, but have an easily accessible apical and basolateral side in comparison with their 3D HIO variants which are closed spheres. This difference makes it easier to perform relevant experiments as compounds can be added to the apical side which represents the lumen, there is no build-up of cellular debris near the cells, cells are not encompassed in extracellular matrix providing free access and samples opportunities.

3D HIOs and 2D IEC layers have yet been used very limitedly to study the effect of SCFAs and predict potential responses *in vivo*. An early study in 2014 reported effects of SCFAs and products generated by two abundant microbiota species *Akkermansia muciniphila* and *Faecalibacterium prausnitzii* on adult stem cell derived mouse intestinal organoids. The authors showed that exposure induced cellular lipid metabolism, cell growth and cell survival pathways [31]. More recently, a limited gene expression study using qPCR analysis was performed on mouse and human adult stem cell based intestinal organoids and IEC layers, which were exposed to butyrate, propionate or acetate (at 1 and 10 mM for 24 hours). It was shown that propionate and butyrate affected cell differentiation and expression of selected genes [32].

In this study, we aimed to assess the effects of the SCFAs butyrate, propionate and acetate on human iPSC derived 2D IEC layers on a whole genome gene expression level. To this end, IEC layers were exposed to butyrate, propionate, and acetate at 1 and 10 mM for 24 h. To study the effects on a whole genome gene expression level, RNA was extracted after exposure and sequenced using next-generation sequencing. Data analysis was done at an individual gene level and at a pathway level using Gene Set Enrichment Analysis (GSEA). The present study provides novel insights into the effects of butyrate, acetate and propionate on whole genome gene expression profiles and their differences, and on the applicability of human iPSC derived IEC layers for SCFA research.

4.2 Materials and Methods

4.2.1 Human induced pluripotent stem cell culture

The human iPSC cell line (CS83iCTR-33n1) was provided by the Cedars-Sinai Medical Center's David and Janet Polak Foundation Stem Cell Core Laboratory. These cells were established through episomal reprogramming of fibroblasts of a 31-year-old healthy female. The cell line has been fully characterized and no karyotype abnormalities have been found. Undifferentiated human iPSCs were cultured in feeder free conditions using mTeSR1 medium (Stem Cell Technologies, Vancouver, Canada) on human embryonic stem cell qualified matrigel (Corning, New York, NY). For passage, iPSC colonies were dissociated using gentle cell dissociation reagent (Stem Cell Technologies).

4.2.2 Human induced pluripotent stem cell differentiation into intestinal epithelial cell layers

For differentiation, human iPSCs were dissociated into single cells using accutase (Stem Cell Technologies) and cultured on human embryonic stem cell qualified matrigel-coated 24-well plates in mTeSR1 supplemented with 10 µM Y-27632 (Stem Cell Technologies) for 1 day. Human iPSCs were subsequently differentiated into definitive endoderm (DE) by incubation in RPMI1640 medium containing 1% non-essential amino acids (Gibco) and 100 ng/ml Activin A (Cell Guidance Systems, Cambridge, UK), with

increasing concentrations of fetal bovine serum (0%, 0.2% and 2% on day 1, 2 and 3, respectively). 15 ng/ml BMP4 (R&D Systems, Minneapolis, MN) was also added during the first day of definitive endoderm formation. Differentiation into intestinal stem cells was subsequently induced by changing medium into DMEM/F12 containing 2% fetal bovine serum, 1% GlutaMAX (Gibco) and 250 ng/ml FGF2 (R&D Systems). After 4 days, cells were dissociated using Accutase and seeded onto polyester transwell inserts (0.4 µm, Corning) coated with Growth Factor Reduced matrigel. Cells were cultured for 7 days in intestinal differentiation medium (DMEM/F-12 containing 2% fetal bovine serum, 1% non-essential amino acids (Gibco), 1 × B27 (Gibco), 1 × N2 (Gibco), 1% penicillin/streptomycin (Gibco) and 2 mM L-glutamine (Gibco)) supplemented with 20 ng/ml EGF (R&D Systems) and 1 mM 8-Br-cAMP (Sigma). The ROCK inhibitor, y-27632 (final concentration 10 µM; Stem Cell Technologies), was added during the initial 24 hours after seeding to reduce cell death. The cells were subsequently cultured for 12 days in intestinal differentiation medium supplemented with 20 ng/ml EGF, 500 µM IBMX (Sigma), 5 µM 5-aza-2'-deoxycytidine (Sigma), 20 µM PD98059 (Stem Cell Technologies), and 0.5 µM A-83-01 (Sigma). Medium was refreshed every 2–3 days.

4.2.3 RNA isolation and sequencing

After the last day of differentiation cells were exposed to sodium-butyrate, sodium-propionate and sodium-acetate (Sigma-Aldrich, Steinheim, Germany) at 1 and 10mM in triplicate *(n=3)*. After the 24h incubation the cells were washed with 100µL DMEM^{+}. After that, 350µL RA1 lysis buffer was added and incubated for 5 min. The entire volume of RA1 solution was collected as cell lysate and total RNA. Total RNA from the iPSC derived IECs was extracted using the NucleoSpin RNA isolation kit (Macherey-Nagel, Duren, Germany) according to manufacturer's instructions. Quality of the RNA was checked using a NanoDrop One (ThermoFisher, Wilmington, Delaware, USA) and bioanalyzer (Agilent). Samples (n=3 per treatment) were sent to BGI (Hong Kong) for transcriptome sequencing using the DNBSEQ Technology Platform with 20M reads per sample. All the generated raw sequencing reads were filtered, by removing reads with adaptors, reads with more than 10% of unknown bases, and low quality reads. Clean reads were then obtained and stored as FASTQ format.

4.2.4 Raw data processing

The RNA-seq reads were used to quantify transcript abundances. To this end the tool *Salmon* [33] (version 1.3.0) was used to map the sequencing reads to the GRCh38.p13 human genome assembly-based transcriptome sequences as annotated by the GENCODE consortium (release 35) [34]. The obtained transcript abundance estimates and lengths were then imported in R using the package *tximport* (version 1.18.0) [35], scaled by average transcript length and library size, and summarized on the gene-level. Such scaling corrects for bias due to correlation across samples and transcript length and has been reported to improve the accuracy of differential gene expression analysis [35]. Differential gene expression was determined using the package *limma* (version 3.46.0) [36] using the obtained scaled gene-level counts. Briefly, before statistical analyses, counts for only protein-coding genes were retained, whereafter nonspecific filtering of the count table was performed to increase detection power [37], based on the requirement that a gene should have an expression level greater than 10 counts, that is, 0.5 count per million reads (cpm) mapped, for at least three libraries across all 21 samples. *These three libraries did not*

have to be within a single treatment group. Differences in library size were adjusted by the trimmed mean of M-values normalization method [38]. Counts were then transformed to log-cpm values and associated precision weights, and entered into the *limma* analysis pipeline [39]. GEO accession number: "GSE200309".

4.2.5 Data analysis at the individual gene level

Differentially expressed genes were identified by using generalized linear models that incorporate empirical Bayes methods to shrink the standard errors towards a common value, thereby improving testing power [36, 40]. Genes were defined as significantly changed when *FDR* < 0.05. Venn diagrams, showing the differentially expressed genes were made using *Venny* 2.1 [41]. The top 500 genes with the most variation were selected by using the interquartile range (IQR) as a measure, which is the difference between the 25th and 75th percentile. The coefficient of variation, which measures how much the values differ within a treatment, was set to 0.5 to select for differential gene expression that was related to the treatment instead of at random. Data was standardized by converting values to a z-score which sets the average to 0 and scales the other values from -2 to 2. A principle component analysis (PCA) was performed using the library *PCAtools* on the top 500 differentially expressed genes (see selection process of the genes below) [42]. Subsequently, all individual samples were hierarchically clustered based on of the top 500 differentially expressed genes and presented in a heatmap using *heatmapper* [43].

4.2.6 Characterization of cellular makeup of IEC layers

To characterize the cellular makeup of the IEC layers and to evaluate the effects of the SCFAs on differentiation of the IECs, gene expression data of cell type specific markers and differentiation markers was analyzed. For characterization of the cellular makeup, markers were obtained from studies using single cell surveys looking for cell type specific markers. In the two enterocyte sets the proximal set represents the duodenum and jejunum while the distal set represents the ileum [44]. The gene expression data of the individual control samples was pooled and gene expression was given in log2(cpm) values. For evaluation of the effects of the SCFAs on differentiation of the IECs, markers were selected from literature performing single-cell surveys on cells extracted from the intestine [44, 45] and *Kyoto Encyclopedia of Genes and Genomes (KEGG)* cell type signature sets. Log2(cpm) values of individual samples were averaged per exposure group and compared with the control group.

4.2.7 Data analysis at the biological pathway level

Changes in gene expression were related to biologically meaningful changes using gene set enrichment analysis (GSEA). It is well accepted that GSEA has multiple advantages over analyses performed on the level of individual genes [46–48]. GSEA evaluates gene expression on the level of gene sets that are based on prior biological knowledge, GSEA is unbiased, because no gene selection step (fold change and/or p-value cut-off) is used. A GSEA score is computed based on expression of all genes in the gene set and allows for the detection of affected biological processes that are due to only subtle changes in expression of individual genes. Gene sets were retrieved from the expert-curated KEGG database [48] (BRITE Functional Hierarchy level 1). Six level-1 KEGG categories were included in the analysis, metabolism, genetic information processing, environmental information processing, cellular processes, organismal

system and human diseases Moreover, only gene sets comprising more than 15 and fewer than 500 genes were taken into account. For each comparison, genes were ranked based on their t-value that was calculated by the moderated t-test. Statistical significance of GSEA results was determined using 10.000 permutations.

4.3 Results

4.3.1 Presence of different cell types in IEC layers

The cellular makeup of the IEC layers was characterized by evaluating the expression of known cell type specific gene markers in the control samples. This was done to determine the similarities in cellular makeup between the IEC layers and the *in vivo* gut. Table 1 summarizes the expression of these marker genes and indicated that enterocytes, goblet cells, Paneth cells, tuft cells, enteroendocrine cells, and stem cells were present in our IEC layers. In the total RNA pool, 13 out of 14 goblet cell markers were expressed, 13 out of 14 enterocyte (proximal) cell markers, 13 out of 14 enterocyte (distal) cell markers, 8 out of 14 Paneth cell markers, 12 out of 14 tuft cell markers, 8 out of 14 enteroendocrine cell markers and 11 out of 14 stem cell markers.

4.3.2 Differential gene expression

Gene expression profiles of IEC layers exposed to the three individual SCFAs at two concentrations were evaluated by a PCA. A PCA scatterplot representing the first two principle components based on the transcriptome profiles of the six exposure groups and the controls is shown in Fig. 1. PC1 and PC2 explain 54.71% and 5.64% of the total variation, respectively. The control samples and samples exposed to 1mM and 10mM acetate, and 1mM propionate clustered together, indicating little variation in gene expression between the groups. Based on the first component (PC1), samples exposed to 10 mM butyrate differed most from the control samples, as shown by the largest distance between the two groups. Also, samples exposed to 10 mM propionate and to a lesser extent samples exposed to 1 mM butyrate differed from the control samples and these groups were located between the control and butyrate 10 mM samples. Based on the second component (PC2), samples exposed to 10 mM propionate and 1mM butyrate differed most from the control samples.

4.3.3 Gene expression data analysis at the individual gene level

The original dataset consisted of 60,237 genes in 21 samples, after filtering for low count genes this was reduced to 19,654 genes. Of these genes, 3,534 were not protein coding resulting in a data set containing 16,120 genes. For comparison of exposure conditions a False Discovery Rate (FDR) cut-off value of <0.05 was used resulting in 1,636 down- and 1,665 upregulated genes for butyrate 1 mM, 5,093 down- and 5,103 upregulated genes for butyrate 10 mM, 15 down- and 28 upregulated genes for propionate 1 mM, 2,741 down- and 2,681 upregulated genes for propionate 10 mM, 2 down- and 11 upregulated genes for acetate 1 mM, and 24 down- and 18 upregulated genes for acetate 10 mM. At 1 mM there were no shared genes between all three compounds, at 10 mM there were 15 down- and 13 upregulated shared genes. Between butyrate and propionate there were 14 down- and 27- upregulated shared genes at 1 mM and 2,271 down- and 2,138 upregulated shared genes at 10 mM. Between butyrate and acetate there were 1

down- and 5- upregulated shared genes at 1 mM and 2 down- and 0 upregulated shared genes at 10 mM. Between acetate and propionate there was only 1 shared upregulated gene at 1 mM and 2 down- and 4 upregulated genes at 10 mM (Fig. 2). To obtain a visual overview of differential gene expression at the individual gene level all samples were hierarchically clustered based on the top 500 highest differentially expressed genes and presented in a heatmap (Fig.3).

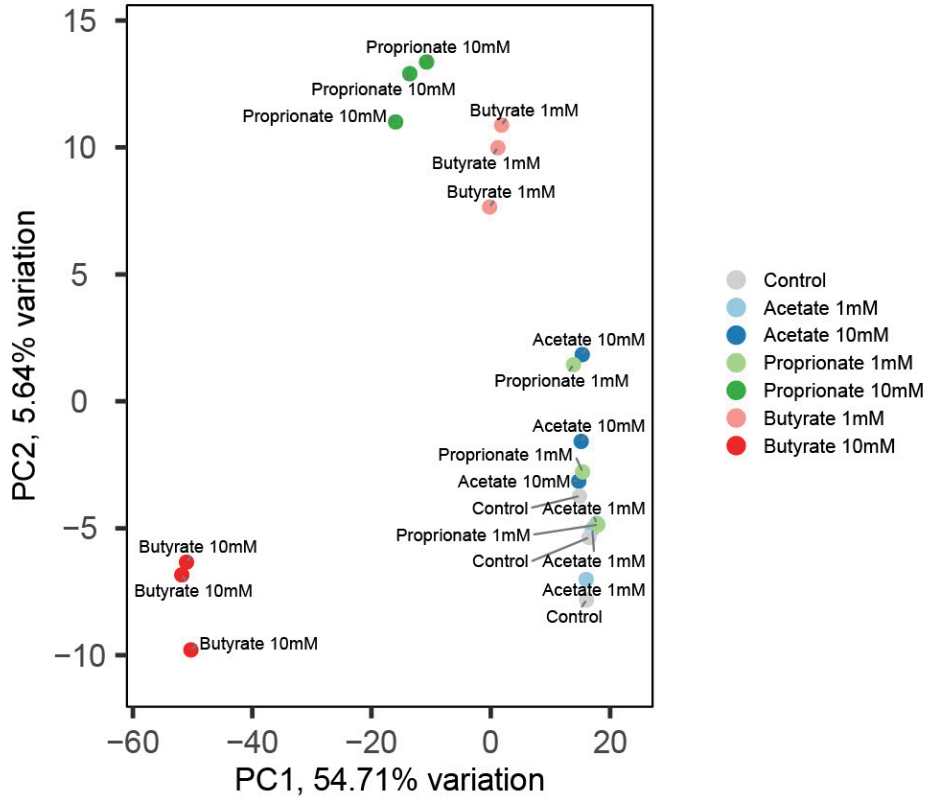

Figure 12. *PCA plot of induced pluripotent stem cell derived intestinal epithelial cell layers exposed to 1 or 10 mM butyrate, propionate, acetate or control for 24 hours.*

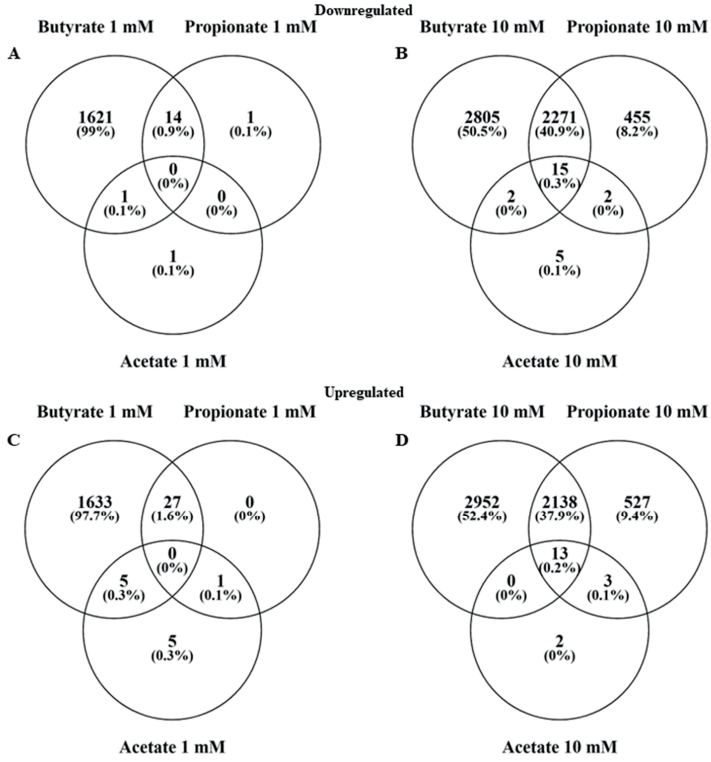

Figure 2. *Venn diagrams showing the differentially expressed genes (FDR<0.05) in induced pluripotent stem cell derived intestinal epithelial cell layers exposed to 1 or 10 mM butyrate, propionate or acetate for 24 hours versus the control.* ***A*** *downregulated genes in IEC layers exposed to 1 mM butyrate, propionate or acetate,* ***B*** *downregulated genes in IEC layers exposed to 10 mM butyrate, propionate or acetate,* ***C*** *upregulated genes in IEC layers exposed to 1 mM butyrate, propionate or acetate,* ***D*** *upregulated genes in IEC layers exposed to 10 mM butyrate, propionate or acetate.*

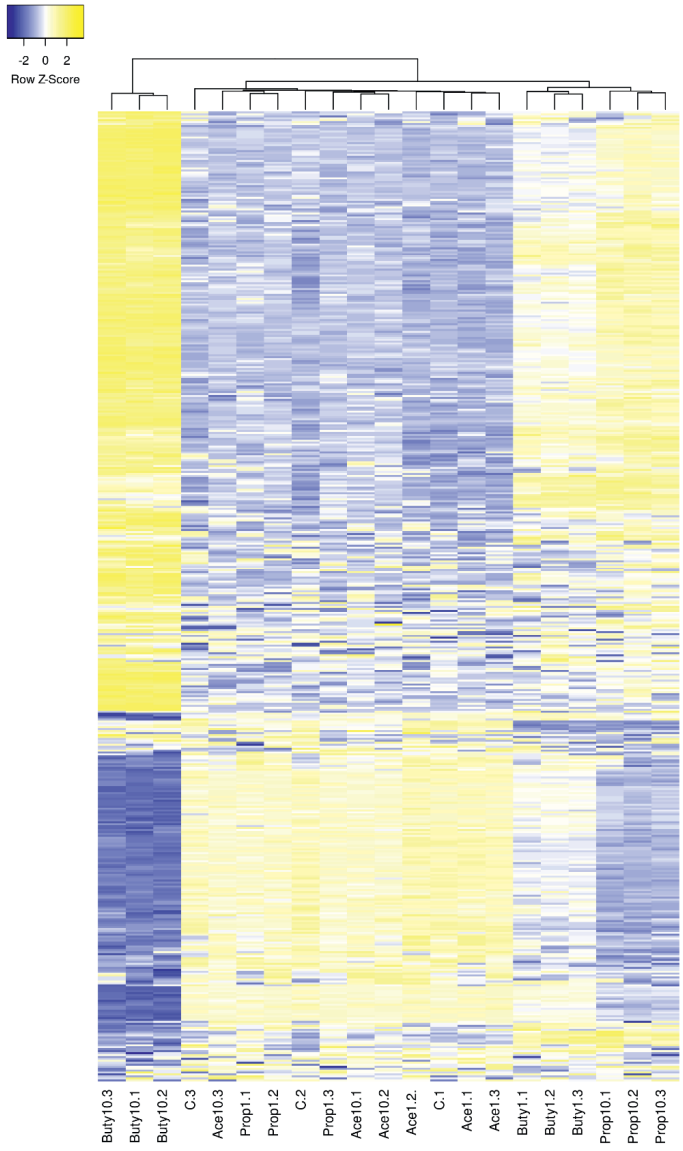

Figure 3. *Heatmap of the top 500 differentially expressed genes in induced pluripotent stem cell derived intestinal epithelial cell layers exposed to 1 or 10 mM butyrate (Buty), propionate (Prop) or acetate (Ace) and in the control samples (C) with 3 samples per condition. Blue indicates below average expression and yellow indicates above average expression. Made using heatmapper, http://www.heatmapper.ca* [43, 49].

4.3.4 SCFAs effects on IEC differentiation

To evaluate the effects of the SCFAs on differentiation of IECs, gene expression of specific differentiation and cell type markers was analyzed in all exposure groups versus the control group. Table 2 summarizes the expression of these marker genes. The stem cell marker *LGR5* was significantly reduced after acetate 1 and 10 mM, propionate 10 mM and butyrate 10 mM exposure. The enterocyte marker Alkaline Phosphatase intestinal (*ALPi*) was significantly increased after acetate 1 mM and butyrate 1 mM exposure, but reduced after butyrate 10 mM exposure. The goblet cell marker Mucin 2 (*MUC2*) was significantly increased after exposure of the cells to 1 mM acetate, but significantly reduced after propionate 10mM and butyrate 10mM exposure. The enteroendocrine marker chromogranin A (*CHGA*) was significantly increased after butyrate 10mM exposure. The Paneth cell marker lysozyme (*LYZ*) was significantly increased after acetate 1mM exposure, but significantly reduced after butyrate 10 mM exposure. The tight junction marker claudin-3 (CLDN3) was significantly increased after butyrate 1 mM exposure, but significantly reduced after butyrate 10 mM exposure. Another tight junction marker, occludin (*OCLN*), was also significantly reduced after butyrate 10 mM exposure. A third tight junction marker, zona-occludens 1 (*TJP1*), was significantly reduced after acetate 10 mM, propionate 1 mM and 10 mM and butyrate 1 mM and 10 mM exposure. Finally, the tuft cell marker Doublecortin Like Kinase 1 (*DCLK1*) was significantly increased after butyrate 10 mM exposure. In general, exposure to butyrate 10 mM had most pronounced effects on the selected differentiation markers.

Table 1. *Gene expression in log2 values (counts per million) of selected marker genes for specific intestinal cell types in induced pluripotent stem cell derived intestinal epithelial cell layer control samples.*

Goblet cell		Enterocyte(Proxi)		Enterocyte(Distal)		Paneth cell		Tuft cell		Enteroendocrine cell		Stem cell	
Gene	log2CPM	Gene	log2CPM	Gene	log2CPM	Gene	log2CPM	Gene	log2CPM	Gene	log2CPM	Gene	log2CPM
AGR2	9.372883	*GSTA1*	7.845325	*TMIGD1*	0.020751	*LYZ*	3.792942	*ALOX5AP*	-1.29392	*CHGB*	1.261364	*LGR5*	4.181984
FCGBP	3.077028	*RBP2*	0.9363	*FABP6*	-0.8252	*DEFA5*	N.D.	*LRMP*	0.686782	*GFRA3*	N.D.	*GKN3*	N.D.
TFF3	0.875449	*APOA4*	7.318537	*SLC51B*	3.095253	*DEFA6*	N.D.	*HCK*	-0.0652	*CCK*	-1.30207	*ASCL2*	N.D.
CLCA1	1.532495	*REG3A*	N.D.	*SLC51A*	4.084541	*PLA2G2A*	6.454531	*AVIL*	-0.1728	*VWA5B2*	2.903324	*OLFM4*	2.375712
ZG16	4.914768	*CREB3L3*	4.060139	*MEP1A*	7.241497	*CLCA1*	1.532495	*RGS13*	N.D.	*NEUROD1*	N.D.	*RGMB*	4.111343
TPSG1	N.D	*MS4A10*	-0.78756	*FAM151A*	4.987734	*ITLN2*	5.377578	*LTC4S*	N.D.	*FEV*	N.D.	*IGFBP4*	6.757845
MUC2	5.78067	*ACE*	4.224451	*NAALADL1*	N.D.	*REG3A*	N.D.	*TRPM5*	-1.77287	*APLP1*	N.D.	*JUN*	6.22456
GALNT12	3.832918	*ALDH1A1*	8.0723	*SLC34A2*	3.539111	*ITLN1*	2.759173	*DCLK1*	1.845717	*SCGN*	3.279521	*PDGFA*	5.522184
ATOH1	0.370397	*HSD17B6*	1.412997	*PLB1*	4.870576	*LCN2*	N.D.	*SPIB*	-0.05089	*NEUROG3*	N.D.	*SOAT1*	6.374078
REP15	-1.00208	*GSTM3*	5.817105	*NUDT4*	9.473245	*PRSS1*	3.487301	*FYB*	-2.51985	*RESP18*	N.D.	*TNFRSF19*	6.15123
S100A6	7.145416	*GDA*	6.55424	*DPEP1*	3.972728	*GUCA2A*	2.19674	*PTPN6*	3.854257	*BEX2*	3.833314	*CYP2E1*	N.D.
PDIA5	6.98822	*APOC3*	5.602248	*PMP22*	4.713771	*TFF3*	0.875449	*MATK*	-0.91463	*RPH3AL*	3.0133	*FSTL1*	10.71206
KLK1	-0.08483	*GPD1*	2.430314	*XPNPEP2*	3.040461	*SPINK4*	N.D.	*SNRNP25*	2.777507	*SCG5*	2.230468	*IFITM3*	5.416186
PLA2G10	1.095422	*FABP1*	6.376665	*MUC3*	5.097441	*RETNLB*	N.D.	*SH2D7*	-1.49594	*PCSK1*	1.591055	*PRELP*	-0.84328

N.D.: not detectable. Colors were scaled from low expression (yellow) to high expression (green). Data are expressed as averages of 3 samples.

Table 2. *Gene expression data of specific differentiation and cell type markers.*

	Acetate		Propionate		Butyrate	
Gene	1 mM	10 mM	1 mM	10 mM	1 mM	10 mM
LGR5	0.78	0.72	0.83	0.30	0.83	0.15
ALPi	1.38	0.999437	1.08	1.02	1.46	0.68
MUC2	1.46	1.08045	1.00	0.60	0.98	0.39
CHGA	1.26	0.839668	0.93	0.68	1.23	4.66
LYZ	1.24	1.133515	1.20	0.97	1.06	0.53
CLDN3	1.02	1.006666	1.15	1.12	1.40	0.36
OCLN	1.06	0.971462	1.09	1.04	1.02	0.36
TJP1	0.98	0.85	0.90	0.77	0.81	0.72
DCLK1	1.29	1.007723	0.99	0.93	0.78	1.97

Gene expression ratios in induced pluripotent stem cell derived intestinal epithelial cell layers exposed to 1 or 10 mM butyrate, propionate or acetate for 24 hours compared with the control. Each ratio is based on the average expression data of 3 samples. Blue cells are significantly downregulated and yellow cells are significantly upregulated (p<0.05). The markers represent stem cells (LGR5), enterocytes (Alkaline Phosphatase intestinal; ALPi), goblet cells (Mucin 2; Muc2), enteroendocrine cells (chromogranin A; CHGA), Paneth cells (Lysozyme; LYZ), tight junction proteins (Claudin-3; CLDN3, Occludin; OCLN and Zonule-occludens 1; TJP1), and tuft cells (Doublecortin Like Kinase 1; DLK1).

4.3.5 Gene set enrichment analysis of gene expression data from iPSC derived IECs exposed to 1 and 10 mM butyrate or 10 mM propionate.

GSEA was performed for an in-depth evaluation of the effects of exposure to SCFAs on a biological pathway level. Six KEGG categories were included in the analysis; metabolism, genetic information processing, environmental information processing, cellular processes, organismal system and human diseases (BRITE Functional Hierarchy level 1). Gene sets were ranked based on the Normalized Enrichment Score (NES) to select the most enriched pathways. Cut-off values $p<0.05$ and $FDR<0.25$ were applied to select statistically significant pathways based on standard GSEA practice. Propionate at 1 mM exposure resulted in a total of 56 upregulated gene sets and a total of 0 downregulated gene sets. Acetate exposure at both 1 mM and 10 mM, resulted in a total of 95 and 2 upregulated gene sets and a total of 13 and 98 downregulated gene sets, respectively. Due to these relatively low numbers of enriched pathways and because they grouped together with the controls in previous analyses, propionate at 1 mM and acetate at both concentrations were excluded from this analysis, leaving the exposure groups butyrate 1 mM and 10 mM, and propionate 10 mM. Exposure to butyrate 1 mM resulted in a total of 8 downregulated gene sets divided over the metabolism, genetic information processing, cellular processes and human diseases categories and 74 upregulated gene sets divided over the metabolism, environmental information processing, organismal systems, human diseases and general categories (Fig. 4A). Butyrate 10 mM exposure resulted in a total of 89 downregulated gene sets divided over all 6 categories (Metabolism, Genetic Information Processing, Environmental Information Processing, Cellular Processes, Organismal Systems and Human Diseases) and 18 upregulated gene sets divided over the metabolism, genetic information processing, organismal systems, and human diseases categories (Fig. 4A). Propionate 10 mM exposure resulted in a total of 16 downregulated gene sets divided over all 6 categories and 32 upregulated gene sets which were also divided over all 6 categories (Fig.4A). When comparing the three

exposure groups there were 7 shared upregulated gene sets and 2 shared downregulated gene sets for all three exposures. There were no additional shared gene sets between the butyrate 10 and 1 mM exposure groups. The butyrate 10 mM and propionate 10 mM exposure groups shared 3 upregulated and 8 downregulated gene sets, while the butyrate 1mM and propionate 10mM exposure groups shared 18 upregulated and 5 downregulated gene sets (Fig. 4B+C).

For further analysis on the pathway level, pathways related to the intestine were selected based on expert judgement. The top 10 of this selection, is given in Tables 3-5 for butyrate, propionate and acetate exposure induced pathways, respectively. Following butyrate 10 mM exposure the most upregulated gene set was DNA replication in the KEGG category Genetic Information Processing and the KEGG category subgroup Replication and repair (NES=2.43), the most downregulated gene set was the p53 signaling pathway in the KEGG category Human Diseases and the KEGG category subgroup Cell growth and death (NES=-1.99) (Table 3). Following butyrate 1 mM exposure the most upregulated gene set was chemical carcinogenesis in the KEGG category Human Diseases and KEGG category subgroup Cancer: overview (NES=2.26), the most downregulated gene set was the proteasome set in the KEGG category Genetic Information Processing and the KEGG category subgroup Folding, sorting and degradation (NES=-2.17) (Table 4). Following propionate 10 mM exposure the most upregulated gene set was circadian entrainment in the KEGG category Organismal Systems and KEGG category subgroup Environmental adaptation (NES=1.83), the most downregulated gene set was the p53 signaling pathway in the KEGG category Human Diseases and the KEGG category subgroup Cell growth and death (NES=-2.08) (Table 5).

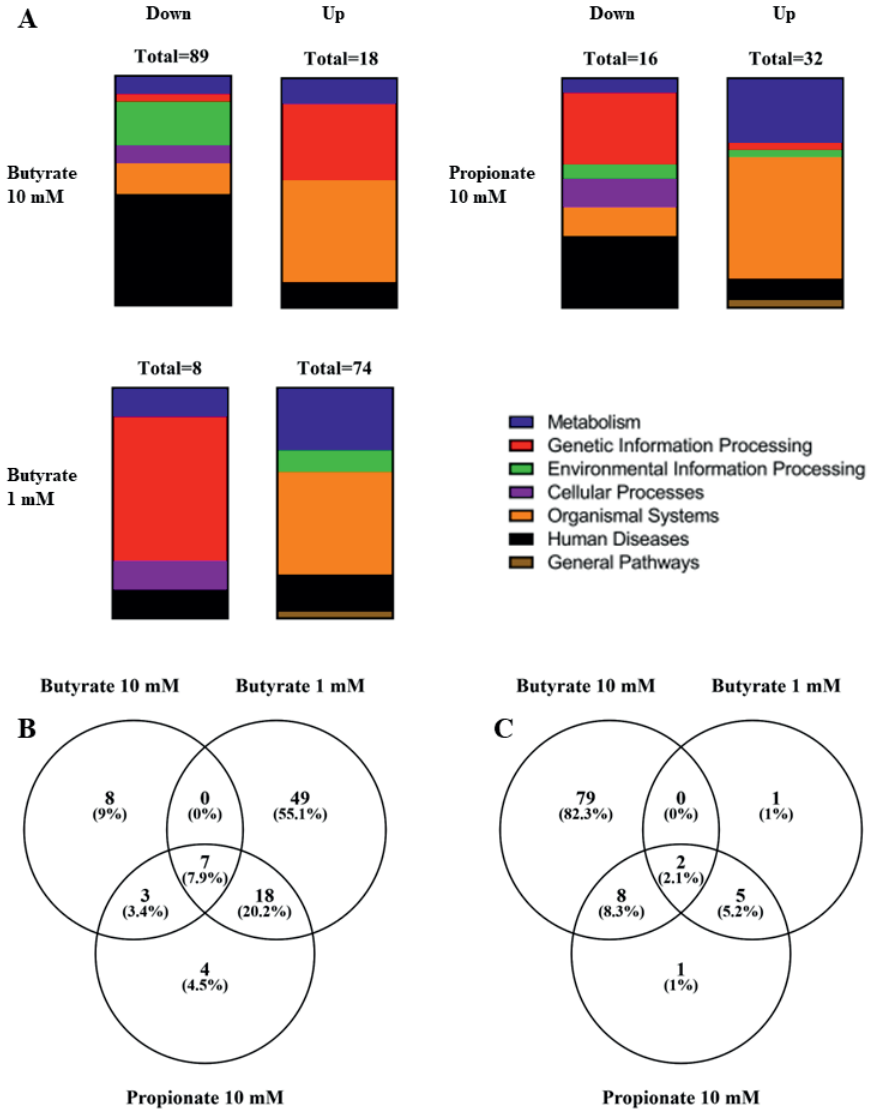

Figure 4. *Differentially regulated pathways (p<0.05, FDR<0.25) in induced pluripotent stem cell derived intestinal epithelial cell layers exposed to 1 or 10 mM butyrate or 10 mM Propionate for 24 hours.* ***A*** *vertical slice graphs showing the distribution of the up- or downregulated pathways over six KEGG categories.* ***B*** *Venn diagram showing the upregulated pathways, and* ***C*** *Venn diagram showing the downregulated pathways versus the control.*

Table 3. Top 10 most enriched (based on NES) up- and downregulated pathways related to the intestine in induced pluripotent stem cell derived intestinal epithelial cell layers exposed to 10 mM butyrate compared with the control.

KEGG pathway name	KEGG category	KEGG category subgroup	Genes	NES	p-value	FDR
Upregulated pathways*						
DNA replication	Genetic Information Processing	Replication and repair	36	2.43	0.000	0.000
Mismatch repair	Genetic Information Processing	Replication and repair	23	2.18	0.000	0.000
Fanconi anemia pathway	Genetic Information Processing	Replication and repair	54	2.15	0.000	0.000
Homologous recombination	Genetic Information Processing	Replication and repair	41	1.99	0.000	0.004
RNA polymerase	Genetic Information Processing	Transcription	29	1.72	0.007	0.058
Fatty acid biosynthesis	Metabolism	Lipid metabolism	16	1.59	0.027	0.142
Nucleotide excision repair	Genetic Information Processing	Replication and repair	46	1.59	0.012	0.128
Endocrine and other factor regulated calcium reabsorption	Organismal Systems	Excretory system	48	1.55	0.012	0.135
Alanine, aspartate and glutamate metabolism	Metabolism	Amino acid metabolism	35	1.48	0.035	0.150
Mineral absorption	Organismal Systems	Digestive system	56	1.47	0.022	0.143
Downregulated pathways*						
P53 signaling pathway	Cellular Processes	Cell growth and death	73	-1.99	0.000	0.010
Pathogenic Escherichia Coli infection	Human Diseases	Infectious disease: bacterial	179	-1.97	0.000	0.007
Steroid hormone biosynthesis	Metabolism	Lipid metabolism	49	-1.95	0.000	0.007
Shigellosis	Human Diseases	Infectious disease: bacterial	224	-1.91	0.000	0.010
ECM receptor interaction	Environmental Information Processing	Signaling molecules and interaction	78	-1.86	0.000	0.013
NF kappa B signaling pathway	Environmental Information Processing	Signal transduction	94	-1.83	0.000	0.020
Glutathione metabolism	Metabolism	Metabolism of other amino acids	46	-1.81	0.001	0.023
Hippo signaling pathway multiple species	Environmental Information Processing	Signal transduction	29	-1.80	0.003	0.019
Regulation of actin cytoskeleton	Cellular Processes	Cell motility	194	-1.74	0.000	0.030
JAK STAT signaling pathway	Environmental Information Processing	Signal transduction	110	-1.73	0.000	0.030

*References indicating their role or relationship to the intestine for the selected pathways are given in the supplementary files; Table S1

Table 4. Top 10 most enriched (based on NES) up- and downregulated pathways related to the intestine in induced pluripotent stem cell derived intestinal epithelial cell layers exposed to 1mM butyrate compared with the control.

KEGG pathway name	KEGG category	KEGG category subgroup	Genes	NES	p-value	FDR
Upregulated pathways*						
Chemical carcinogenesis	Human Diseases	Cancer: overview	65	2.26	0.000	0.000
Mineral absorption	Organismal Systems	Digestive system	56	2.26	0.000	0.000
Fat digestion and absorption	Organismal Systems	Digestive system	30	2.21	0.000	0.000
Tryptophan metabolism	Metabolism	Amino acid metabolism	36	2.02	0.000	0.003
Glycine serine and threonine metabolism	Metabolism	Amino acid metabolism	37	1.97	0.000	0.004
Circadian entrainment	Organismal Systems	Environmental adaptation	86	1.86	0.000	0.018
Metabolism of xenobiotics by cytochrome P450	Metabolism	Xenobiotics biodegradation and metabolism	57	1.86	0.001	0.015
Ubiquinone and other terpenoid quinone biosynthesis	Metabolism	Metabolism of cofactors and vitamins	11	1.86	0.001	0.014
PPAR signaling pathway	Organismal Systems	Endocrine system	69	1.85	0.000	0.014
Arachidonic acid metabolism	Metabolism	Lipid metabolism	47	1.81	0.002	0.017
Downregulated pathways*						
Proteasome	Genetic Information Processing	Folding, sorting and degradation	43	-2.17	0.000	0.001
P53 signaling pathway	Cellular Processes	Cell growth and death	73	-2.16	0.000	0.000
Spliceosome	Genetic Information Processing	Transcription	134	-1.99	0.000	0.004
Ribosome biogenesis in eukaryotes	Genetic Information Processing	Translation	73	-1.93	0.000	0.007
RNA transport	Genetic Information Processing	Translation	157	-1.91	0.000	0.007
Starch and sucrose metabolism	Metabolism	Carbohydrate metabolism	28	-1.68	0.010	0.073
MRNA surveillance pathway	Genetic Information Processing	Translation	90	-1.60	0.002	0.130

*References indicating their role or relationship to the intestine for the selected pathways are given in the supplementary files; Table S2

Table 5. Top 10 most enriched (based on NES) up- and downregulated pathways related to the intestine in induced pluripotent stem cell derived intestinal epithelial cell layers exposed to 10 mM propionate compared with the control.

KEGG pathway name	KEGG category	KEGG category subgroup	Genes	NES	p-value	FDR
Upregulated pathways*						
Circadian entrainment	Organismal Systems	Environmental adaptation	86	1.83	0.000	0.059
Thiamine metabolism	Metabolism	Metabolism of cofactors and vitamins	15	1.82	0.002	0.046
Mismatch repair	Genetic Information Processing	Replication and repair	23	1.77	0.005	0.058
Tryptophan metabolism	Metabolism	Amino acid metabolism	36	1.76	0.002	0.045
Fat digestion and absorption	Organismal Systems	Digestive system	30	1.74	0.003	0.046
Glycine serine and threonine metabolism	Metabolism	Amino acid metabolism	37	1.68	0.008	0.060
Aldosterone regulated sodium reabsorption	Organismal Systems	Excretory system	33	1.65	0.010	0.065
Endocrine and other factor regulated sodium reabsorption	Organismal Systems	Excretory system	48	1.64	0.008	0.073
Longevity regulating pathway	Organismal Systems	Aging	59	1.60	0.007	0.085
Mineral absorption	Organismal Systems	Digestive system	56	1.58	0.008	0.092
Downregulated pathways*						
P53 signaling pathway	Cellular Processes	Cell growth and death	73	-2.08	0.000	0.003
Proteasome	Genetic Information Processing	Folding, sorting and degradation	43	-2.00	0.000	0.006
NF kappa B signaling pathway	Environmental Information Processing	Signal transduction	94	-1.93	0.000	0.011
Spliceosome	Genetic Information Processing	Transcription	134	-1.86	0.000	0.021
Pathogenic Escherichia Coli infection	Human Diseases	Infectious disease: bacterial	179	-1.84	0.000	0.020
Ribosome biogenesis in eukaryotes	Genetic Information Processing	Translation	73	-1.82	0.000	0.024
RNA transport	Genetic Information Processing	Translation	157	-1.79	0.000	0.029
Shigellosis	Human Diseases	Infectious disease: bacterial	224	-1.75	0.000	0.035
Protein processing in endoplasmic reticulum	Genetic Information Processing	Folding, sorting and degradation	163	-1.66	0.001	0.085
Starch and sucrose metabolism	Metabolism	Carbohydrate metabolism	28	-1.59	0.021	0.133

*References indicating their role or relationship to the intestine for the selected pathways are given in the supplementary files; Table S3

4.4 Discussion

The aim of the current study was to investigate the effects of three short chain fatty acids on gene expression profiles of human induced pluripotent stem cell (iPSC) derived intestinal epithelial cell (IEC) layers by whole genome analysis. The IEC layers were exposed to acetate, propionate and butyrate at 1 and 10 mM for 24 hours. Analysis of RNA-sequencing data revealed differential gene expression of 16,120 unique protein coding genes when comparing the treatments to their controls, where exposure to butyrate resulted in the strongest responses, followed by propionate, while acetate only marginally affected the gene expression profile of the IEC layers.

Human iPSCs that are differentiated into IEC layers have previously been shown to differentiate into multiple cell types (i.e. enterocytes, goblet cells, Paneth cells, tuft cells, and enteroendocrine cells) that are commonly present in the human intestinal epithelium *in vivo* [50–53]. To confirm the presence of these cell types in our IEC model we evaluated the expression of a panel of cell specific marker genes. We selected 14 marker genes for each important intestinal cell type by searching literature and KEGG cell type signature sets [44, 45] (Table 1). Enterocytes are the most abundantly present cell type in the intestinal epithelium (*in vivo*), which were divided into proximal (i.e. duodenum/jejunum) and distal (i.e. ileum) enterocytes. Of the marker gene sets for both the proximal and distal enterocytes, 13 of the marker genes were expressed, indicating that the model is not specific for one of these two regions. The IEC layers clearly contained enterocytes with a small intestinal gene expression footprint, but due to a lack of markers specific for colonic cells we cannot confirm that the model only contains small intestinal cells. Similarly, expression of 13 markers for goblet cells was observed, indicating the presence of goblet cells in the IEC layers. For Paneth and enteroendocrine cells, expression of several of the marker genes was not detectable. Each of the cell types makes up for <5% of the total amount of cells in the intestinal epithelium *in vivo* [44, 54, 55]. Therefore, a low signal may be expected as pooled RNA from all IECs was analyzed. The expression of tuft cell markers in our IEC layer was the lowest, which again is likely due to a low abundance of the cells in the IEC layers. Literature reported a very low abundance of tuft cells in the human intestine and in adult mouse intestinal epithelium they only represented 0.4% of the total amount of cells [45, 56]. Lastly, we also observed expression of gene markers for stem cells, most importantly the well-known marker *LGR5*, which had high expression values indicating an abundance of stem cells as observed in mammalian crypts *in vivo* [57]. In summary, based on gene expression evaluation, the human iPSC derived IEC layers used in this study contained all important cell types found in the human intestine thus representing the cellular complexity as seen *in vivo*. However, based on the present data we were not able to identify whether the iPSC derived IECs are more resembling the small or large intestine.

The used exposure concentrations of butyrate, propionate and acetate (1 mM and 10 mM) were based on a recent study in adult stem cell derived IECs [32], and selected to represent human *in vivo* intestinal concentrations. Regional differences in SCFA concentrations in the human intestine have been reported. Total SCFA concentrations typically range from 50 to 100 mM in the colonic lumen depending on the diet, whereas in the (distal) small intestine the concentrations are lower at around 11-13mM [3]. Higher concentrations of 98.2 mM acetate, 3.4 mM propionate and 17.4 mM butyrate have also been reported in the small intestine, but these were measured in ileostomy patients and the increased concentration was likely due to the high microbial activity in the small intestine in these patients [58]. Acetate represents

approximately 60% of the total concentration of SCFAs in the intestine with butyrate and propionate each constituting ~20% [3]. This means that the used concentrations of butyrate and propionate in the present study were relatively close to *in vivo* concentrations in both parts of the gut. For acetate, the highest concentration that was used was within the small intestine concentration range, but was below the concentration range reported for the colon. This may explain the low number of differentially expressed genes following acetate exposure. Alternatively human IECs might be less sensitive to exogenous acetate exposure as they have been described to produce acetate themselves where intracellular concentrations can reach micromolar concentrations, although this mostly happens in nutrient-deprived situations [59]. The timepoint of 24 hours was chosen as SCFAs are chronically exposed in the human intestine, there will likely be different effects at earlier timepoints but these will be less relevant for comparison to the *in vivo* situation.

Exposure to butyrate, propionate and acetate at two concentrations resulted in varying numbers of genes with acetate only inducing a low number of genes compared to butyrate and propionate. This corroborates previously reported observations in IEC layers derived from adult human (and mouse) stem cells, where acetate at 1 and 10 mM also induced differential gene expression to a lesser extent than propionate and butyrate at 1mM and 10mM, albeit only a select number of genes was examined [32]. It is known that SCFAs have an effect on cell differentiation [32, 60, 61]. Therefore, the effects of the SCFAs on the expression of selected marker genes for specific intestinal cell types and on marker genes related to intestinal cell differentiation were evaluated. Again, propionate 10 mM, butyrate 1 mM and butyrate 10 mM exposure had the most pronounced effects on the selected marker genes when compared with the control samples (Table 2). It is widely known that butyrate reduces the expression of LGR5 in adult stem cell derived human intestinal organoids, which is a marker gene for stem cells [32, 62], thereby indicating that differentiation of the cells is induced. In the present study, LGR5 expression is also reduced after exposure to butyrate 10 mM as were most of the other selected cell markers. The acetate 10mM, propionate 1 and 10 mM exposure groups showed less pronounced effects on differentiation markers, but in general the selected markers were mostly downregulated upon exposure. However, exposure to butyrate 1 mM and acetate 1 mM resulted in more upregulated than downregulated marker genes. When comparing the gene expression data of the selected marker genes from the current study with those reported in literature in adult stem cell derived organoids exposed to the same SCFAs under the same conditions [32], marked differences in gene expression were observed, which were most prominent after butyrate 10 mM exposure. In this exposure group 4 out of the 9 studied genes (i.e. ALPi, LYZ, CLDN3 and TJP1) were downregulated in the present study versus upregulated in the study by Pearce et al. (2020) [32]. Furthermore, the IEC layers in the present study appeared to be less sensitive to acetate 10 mM exposure compared with the adult stem cell derived organoids as expression of most genes remained unchanged while they were generally upregulated in the adult stem cell derived organoids [32]. In contrast, acetate 1 mM exposure induced expression of several of the marker genes in the present study, which remained unchanged in the adult stem cell derived organoids [32]. The results show that gene expression, and the potential subsequent effects on cell differentiation, is highly concentration-dependent, but also that the responses are model dependent. Variability in gene expression profiles between different cell models is well-known for cell-line based models, and it appears to be true as well for (adult or induced pluripotent) stem cell derived IEC models. Likely explanations are the differences in

origin of the stem cells (human iPSC versus human adult stem cells), differences between donors and the methodology that is used to differentiate the stem cells, which is often optimized for specific cell marker expression [51–53].

Both the PCA analysis and the hierarchical clustering indicated a distinct effect on gene expression profiles following exposure to 10 mM butyrate compared with all other exposures, while the gene expression profiles following butyrate 1 mM and propionate 10 mM clustered together in both the PCA and the hierarchical clustering. The remaining exposure conditions (i.e. 1 and 10 mM acetate, 1 mM propionate) clustered together with the control exposure group in both the PCA and the hierarchical clustering indicating little effect of the exposure. Pathway analysis (i.e. GSEA) on the data from the exposure groups with a high number of differentially expressed genes (i.e. propionate 10 mM, butyrate 1 mM and butyrate 10 mM) revealed a clear concentration-dependent switch in the differential gene expression in the butyrate exposure groups from mostly upregulated pathways at 1 mM (8 down- and 72 upregulated pathways) to mostly downregulated pathways at 10 mM (89 down- and 18 upregulated pathways). Exposure to the low butyrate concentration appeared to induce metabolism and absorption processes as indicated by the upregulated pathways (7 pathways out of the top 10). Pathways related to genetic information processing were mainly downregulated (5 pathways out of the top 7) and were related to RNA transcription, suggesting that low butyrate concentrations could lead to a downregulation of protein synthesis. Six of the top 10 induced pathways, following exposure to 10 mM butyrate, were related to genetic information processing and could be connected to DNA replication and repair, suggesting that high concentrations can induce DNA damage, but there were no indications of induced apoptosis or cell death. Four of the top 10 downregulated pathways, following exposure to butyrate 10 mM, were related to signal transduction. Propionate 10 mM had overall less affected pathways in comparison with butyrate exposure, 47 pathways in total, and the numbers were less skewed with 16 down- and 31 upregulated pathways. It appears that propionate 10 mM exposure induced absorption and metabolism processes as 7 of the top 10 upregulated pathways were connected to these processes. In the downregulated pathways 5 out of 10 pathways were in the genetic information processing category and related mostly to RNA and protein processing processes. Interestingly, many of the up- and downregulated pathways in the top 10 were similar to those of the butyrate 1 mM exposure, indicating that these treatments seem to have similar effects.

Upregulation of DNA replication and repair pathways, as mainly seen after butyrate 10 mM exposure, indicates DNA damage, which in turn is associated with HDAC inhibition. Indeed butyrate has been described to induce HDAC inhibition [63, 64], corroborating our results after exposure to 10 mM butyrate. This effect appears to be both concentration-dependent and SCFA dependent, as we do not see similarity in upregulated pathways after butyrate 1 mM or propionate 10 mM exposure. Propionate has been described to have a lower HDAC inhibitory capacity than butyrate [65], again corroborating the observations in the current study. Another common finding in literature is that butyrate decreases cell proliferation, which was not observed in the present study. However, this effect is reported from studies that used cancer cells like Caco-2 or HT-29 [9, 19, 60, 66]. As mentioned earlier, these cell-lines are not the most suitable systems to study butyrate effects as cancer cells do not use butyrate as their energy source, which leads to an intracellular build-up of butyrate and eventually leads to cell death. Therefore, human IEC and cell-line model differences in energy homeostasis and thus proliferation may be expected.

A strong downregulation of the p53 pathway was seen in the butyrate 1 mM, 10 mM and propionate 10 mM exposure groups. The p53 pathway is induced in response to stress factors that affect DNA replication and induces apoptosis and senescence [67, 68]. DNA replication pathways were clearly affected after butyrate 10 mM exposure, but there were no signs of induced apoptosis, which could be due to this strong reduction of the p53 pathway. In contrast, in cancer cell lines both p53 dependent and independent apoptosis pathways have been reported to be induced after exposure to butyrate [18, 69–71], but again the large differences between model systems, and the build-up of butyrate in cancer cell lines, could explain these differences in effects.

Some pathways in the category human diseases were strongly regulated after exposure to butyrate 1 mM and 10 mM, and propionate 10 mM, indicating that the SCFAs appear to induce responses that have been linked to certain diseases. Examination of the underlying mechanisms of these disease pathways gives insights in the effects of the SCFAs. The butyrate 10 mM and propionate 10 mM exposure groups downregulated a number of bacterial disease pathways including *E. coli* and *Shigella* infections. Bacterial infections are known to induce inflammation or other immune responses and inspection of the downregulated pathways indeed showed many pathways connected to immune responses that were downregulated, especially after butyrate 10 mM exposure. Commensal bacteria that are known to produce SCFAs are reported to reduce inflammatory intestinal reactions [6, 12, 72]. In the butyrate 1 mM exposure group, the chemical carcinogenesis pathway was the most upregulated pathway. This is a very general pathway including genes of the CYP family, glutathione transferases and sulfotransferases, the observed upregulation is most likely related to butyrate effects on CYP enzymes in relation to metabolism [73–76], which is corroborated by the upregulated metabolism of xenobiotics by cytochrome P450 pathway in the butyrate 1 mM exposure group.

Both butyrate and propionate induced many different types of metabolism related pathways, with amino acid metabolism pathways being regulated the most. Both butyrate and propionate are used as an energy source by intestinal epithelial cells [77, 78], which is confirmed by the upregulated fatty acid metabolism biosynthesis pathway after butyrate 10 mM exposure. This pathway encompasses the metabolism of butyrate and propionate. The alanine, aspartate and glutamate metabolism pathway was also upregulated after butyrate 10 mM exposure. This pathway is very important in energy household and the ability to use dietary amino acids for biosynthesis [79] and it was previously linked to butyrate metabolism via L-glutamate [80]. Lastly, a downregulation of the starch and sucrose metabolism pathway following exposure to butyrate 1 mM and propionate 10 mM was observed. The end product of this pathway, glucose, is one of the main energy sources for cells [81, 82]. This is extremely interesting as a lower dependency of the IEC layers on this pathway suggests that they can switch to SCFAs as an energy source, something that is described not to occur in cancer cell lines like Caco-2 and is considered a major disadvantage of cancer cell lines for SCFA studies.

Reviews on the effects of SCFAs on the human intestine report a wide variety of effects [2, 83] where traditional models were unable to model these due to the butyrate paradox, comparatively the IPSC derived IEC combined with RNA-seq has been able to capture a wide variety of effects pointing toward this model being a more suitable in vitro cell model for SCFA studies when compared with cancer cell lines. This also implies that this IEC model may be better suited for development of more complex *in vitro*

intestinal models combining microbes with intestinal cells in for example gut-on-a-chip devices [84–86]. When building further on this type of model there are other things to consider as well, like how compounds are exposed to the cells. Results from this study and literature have shown a reduction of LGR5 expression upon SCFA exposure indicating a reduction of stem cells. When aiming at developing a cell model for long term studies, a pool of stem cells would be required. *In vivo*, stem cells are protected from exposure by their location in the crypts, which could be modelled *in vitro* for example by recreating the crypts using 3D scaffolds [62, 83, 87].

4.5 Conclusion

The aim of this study was to evaluate the effects of the SCFAs butyrate, propionate and acetate at two concentrations in human iPSC derived IEC layers using RNA-seq analysis. This novel model is a biologically more relevant cell model in comparison to cancer cell lines, but little is known about its performance in relation to SCFA exposure. Transcriptomics analysis revealed unique gene expression profiles for the three SCFAs, with expressions profiles that were also dose-dependent. Exposure to butyrate resulted in the strongest responses, followed by propionate, while acetate only marginally affected the gene expression profiles of the IECs. Several known effects of SCFAs on intestinal cells were confirmed, such as effects on metabolism and immune responses. The changes in metabolic pathways in the intestinal epithelial cell layers in this study demonstrate that there is a switch in energy *homeostasis, this is likely associated with the use of* SCFAs as an energy source by the induced pluripotent stem cell derived intestinal epithelial cells similar to *in vivo* intestinal tissues where butyrate is an important energy source.

Data availability statement

The data that support the findings of this study will be openly available in GEO DataSets (GSE200309, https://www.ncbi.nlm.nih.gov/geo/query/acc.cgi?acc=GSE200309).

Author contributions

Menno Grouls: Conceptualization, Methodology, Writing - Original Draft, Visualization **Aafke Jansen**: Investigation, Writing - Original Draft **Loes P.M. Duivenvoorde**: Investigation, **Guido J.E.J. Hooiveld**: Methodology, Formal analysis, Resources, **Hans Bouwmeester**: Conceptualization, Writing - Review & Editing, Supervision **Meike van der Zande**: Conceptualization, Writing - Review & Editing, Supervision

Acknowledgements

For this work MG was supported by a grant funded by the Dutch Research Council, a Building Blocks of Life project (No. 737.016.003). Work on this project by AJ, LPMD and MvdZ was supported by the Dutch Ministry of Agriculture, Nature and Food Quality (Grant: KB-37-002-020 and Grant: KB37-001-003).

References

1. LeBlanc JG, Milani C, de Giori GS, Sesma F, van Sinderen D, Ventura M. Bacteria as vitamin suppliers to their host: a gut microbiota perspective. Curr Opin Biotechnol. 2013;24:160–8.
2. Koh A, De Vadder F, Kovatcheva-Datchary P, Bäckhed F. From Dietary Fiber to Host Physiology: Short-Chain Fatty Acids as Key Bacterial Metabolites. Cell. 2016;165:1332–45.
3. Cummings JH, Pomare EW, Branch HWJ, Naylor CPE, MacFarlane GT. Short chain fatty acids in human

large intestine, portal, hepatic and venous blood. Gut. 1987;28:1221–7.
4. Martin-Gallausiaux C, Béguet-Crespel F, Marinelli L, Jamet A, Ledue F, Blottière HM, et al. Butyrate produced by gut commensal bacteria activates TGF-beta1 expression through the transcription factor SP1 in human intestinal epithelial cells. Sci Reports 2018 81. 2018;8:1–13.
5. Marinelli L, Martin-Gallausiaux C, Bourhis JM, Béguet-Crespel F, Blottière HM, Lapaque N. Identification of the novel role of butyrate as AhR ligand in human intestinal epithelial cells. Sci Reports 2019 91. 2019;9:1–14.
6. Säemann MD, Böhmig GA, Österreicher CH, Burtscher H, Parolini O, Diakos C, et al. Anti-inflammatory effects of sodium butyrate on human monocytes: potent inhibition of IL-12 and up-regulation of IL-10 production. FASEB J. 2000;14:2380–2.
7. Maa MC, Chang MY, Hsieh MY, Chen YJ, Yang CJ, Chen ZC, et al. Butyrate reduced lipopolysaccharide-mediated macrophage migration by suppression of Src enhancement and focal adhesion kinase activity. J Nutr Biochem. 2010;21:1186–92.
8. Peng L, Li ZR, Green RS, Holzman IR, Lin J. Butyrate Enhances the Intestinal Barrier by Facilitating Tight Junction Assembly via Activation of AMP-Activated Protein Kinase in Caco-2 Cell Monolayers. J Nutr. 2009;139:1619–25.
9. Donohoe DR, Collins LB, Wali A, Bigler R, Sun W, Bultman SJ. The Warburg Effect Dictates the Mechanism of Butyrate-Mediated Histone Acetylation and Cell Proliferation. Mol Cell. 2012;48:612–26.
10. Siavoshian S, Segain JP, Kornprobst M, Bonnet C, Cherbut C, Galmiche JP, et al. Butyrate and trichostatin A effects on the proliferation/differentiation of human intestinal epithelial cells: induction of cyclin D3 and p21 expression. Gut. 2000;46:507–14.
11. Hamer HM, Jonkers D, Venema K, Vanhoutvin S, Troost FJ, Brummer RJ. Review article: the role of butyrate on colonic function. Aliment Pharmacol Ther. 2008;27:104–19.
12. Venegas DP, De La Fuente MK, Landskron G, González MJ, Quera R, Dijkstra G, et al. Short chain fatty acids (SCFAs)mediated gut epithelial and immune regulation and its relevance for inflammatory bowel diseases. Front Immunol. 2019;10 MAR:277.
13. Chen H, Meng L, Shen L. Multiple roles of short-chain fatty acids in Alzheimer disease. Nutrition. 2022;93.
14. Li W, Wu X, Hu X, Wang T, Liang S, Duan Y, et al. Structural changes of gut microbiota in Parkinson's disease and its correlation with clinical features. Sci China Life Sci 2017 6011. 2017;60:1223–33.
15. Sun MF, Zhu YL, Zhou ZL, Jia XB, Xu Y Da, Yang Q, et al. Neuroprotective effects of fecal microbiota transplantation on MPTP-induced Parkinson's disease mice: Gut microbiota, glial reaction and TLR4/TNF-α signaling pathway. Brain Behav Immun. 2018;70:48–60.
16. Wang W, Chen L, Zhou R, Wang X, Song L, Huang S, et al. Increased proportions of Bifidobacterium and the Lactobacillus group and loss of butyrate-producing bacteria in inflammatory bowel disease. J Clin Microbiol. 2014;52:398–406.
17. Kumari R, Ahuja V, Paul J. Fluctuations in butyrate-producing bacteria in ulcerative colitis patients of North India. World J Gastroenterol. 2013;19:3404.
18. Archer SY, Johnson J, Kim HJ, Ma Q, Mou H, Daesety V, et al. The histone deacetylase inhibitor butyrate downregulates cyclin B 1 gene expression via a p21/WAF-1-dependent mechanism in human colon cancer cells. Am J Physiol - Gastrointest Liver Physiol. 2005;289 4 52-4:696–703.
19. Han R, Sun Q, Wu J, Zheng P, Zhao G. Sodium Butyrate Upregulates miR-203 Expression to Exert Anti-Proliferation Effect on Colorectal Cancer Cells. Cell Physiol Biochem. 2016;39:1919–29.
20. Lupton JR. Microbial Degradation Products Influence Colon Cancer Risk: the Butyrate Controversy. J Nutr. 2004;134:479–82.
21. Sengupta S, Muir JG, Gibson PR. Does butyrate protect from colorectal cancer? J Gastroenterol Hepatol. 2006;21:209–18.
22. Ryu SH, Kaiko GE, Stappenbeck TS. Cellular differentiation: Potential insight into butyrate paradox?

Mol Cell Oncol. 2018;5:1212685.
23. Salvi PS, Cowles RA. Butyrate and the Intestinal Epithelium: Modulation of Proliferation and Inflammation in Homeostasis and Disease. Cells 2021, Vol 10, Page 1775. 2021;10:1775.
24. Hill DR, Spence JR. Gastrointestinal Organoids: Understanding the Molecular Basis of the Host–Microbe Interface. Cell Mol Gastroenterol Hepatol. 2017;3:138.
25. Mccracken KW, Howell JC, Wells JM, Spence JR, Org; KM, Org; JH, et al. Generating human intestinal tissue from pluripotent stem cells in vitro. Nat Protoc. 2011;6:1920–8.
26. Finkbeiner SR, Hill DR, Altheim CH, Dedhia PH, Taylor MJ, Tsai YH, et al. Transcriptome-wide Analysis Reveals Hallmarks of Human Intestine Development and Maturation In Vitro and In Vivo. Stem Cell Reports. 2015;4:1140–55.
27. Watson CL, Mahe MM, Múnera J, Howell JC, Sundaram N, Poling HM, et al. An in vivo model of human small intestine using pluripotent stem cells. Nat Med. 2014;20:1310–4.
28. Tamminen K, Balboa D, Toivonen S, Pakarinen MP, Wiener Z, Alitalo K, et al. Intestinal Commitment and Maturation of Human Pluripotent Stem Cells Is Independent of Exogenous FGF4 and R-spondin1. PLoS One. 2015;10:e0134551–e0134551.
29. Onozato D, Yamashita M, Nakanishi A, Akagawa T, Kida Y, Ogawa I, et al. Generation of Intestinal Organoids Suitable for Pharmacokinetic Studies from Human Induced Pluripotent Stem Cells. Drug Metab Dispos. 2018;46:1572–80.
30. Janssen AWF, Duivenvoorde LPM, Rijkers D, Nijssen R, Peijnenburg AACM, van der Zande M, et al. Cytochrome P450 expression, induction and activity in human induced pluripotent stem cell-derived intestinal organoids and comparison with primary human intestinal epithelial cells and Caco-2 cells. Arch Toxicol. 2020;95:907–22.
31. Lukovac S, Belzer C, Pellis L, Keijser BJ, de Vos WM, Montijn RC, et al. Differential modulation by Akkermansia muciniphila and faecalibacterium prausnitzii of host peripheral lipid metabolism and histone acetylation in mouse gut organoids. MBio. 2014;5.
32. Pearce SC, Weber GJ, Van Sambeek DM, Soares JW, Racicot K, Breault DT. Intestinal enteroids recapitulate the effects of short-chain fatty acids on the intestinal epithelium. PLoS One. 2020;15:e0230231.
33. Patro R, Duggal G, Love MI, Irizarry RA, Kingsford C. Salmon provides fast and bias-aware quantification of transcript expression. Nat Methods. 2017;14:417–9.
34. Frankish A, Diekhans M, Ferreira AM, Johnson R, Jungreis I, Loveland J, et al. GENCODE reference annotation for the human and mouse genomes. Nucleic Acids Res. 2019;47:D766–73.
35. Soneson C, Love MI, Robinson MD. Differential analyses for RNA-seq: Transcript-level estimates improve gene-level inferences. F1000Research. 2016;4.
36. Ritchie ME, Phipson B, Wu D, Hu Y, Law CW, Shi W, et al. limma powers differential expression analyses for RNA-sequencing and microarray studies. Nucleic Acids Res. 2015;43:e47–e47.
37. Bourgon R, Gentleman R, Huber W. Independent filtering increases detection power for high-throughput experiments. Proc Natl Acad Sci U S A. 2010;107:9546–51.
38. Robinson MD, Oshlack A. A scaling normalization method for differential expression analysis of RNA-seq data. Genome Biol. 2010;11:R25.
39. Law CW, Chen Y, Shi W, Smyth GK. voom: Precision weights unlock linear model analysis tools for RNA-seq read counts. Genome Biol. 2014;15.
40. Smyth GK. Linear models and empirical bayes methods for assessing differential expression in microarray experiments. Stat Appl Genet Mol Biol. 2004;3.
41. Oliveros JC. An Interactive Tool for Comparing Lists with Venn's Diagrams. Csic. 2015.
42. Blighe K, Lun A. PCAtools: everything Principal Components Analysis. R package version 2.0.0. 2020. https://bioconductor.org/packages/release/bioc/html/PCAtools.html. Accessed 26 Jan 2022.
43. Babicki S, Arndt D, Marcu A, Liang Y, Grant JR, Maciejewski A, et al. Heatmapper: web-enabled heat

mapping for all. Nucleic Acids Res. 2016;44:W147–53.
44. Haber AL, Biton M, Rogel N, Herbst RH, Shekhar K, Smillie C, et al. A single-cell survey of the small intestinal epithelium. Nature. 2017;551:333–9.
45. Busslinger GA, Weusten BLA, Bogte A, Begthel H, Brosens LAA, Clevers H. Human gastrointestinal epithelia of the esophagus, stomach, and duodenum resolved at single-cell resolution. Cell Rep. 2021;34:108819.
46. Allison DB, Cui X, Page GP, Sabripour M. Microarray data analysis: from disarray to consolidation and consensus. Nat Rev Genet 2006 71. 2006;7:55–65.
47. Subramanian A, Tamayo P, Mootha VK, Mukherjee S, Ebert BL, Gillette MA, et al. Gene set enrichment analysis: A knowledge-based approach for interpreting genome-wide expression profiles. Proc Natl Acad Sci. 2005;102:15545–50.
48. Kanehisa M, Furumichi M, Tanabe M, Sato Y, Morishima K. KEGG: new perspectives on genomes, pathways, diseases and drugs. Nucleic Acids Res. 2017;45 Database issue:D353.
49. Heatmapper. http://www.heatmapper.ca/. Accessed 8 Jul 2022.
50. Spence JR, Mayhew CN, Rankin SA, Kuhar MF, Vallance JE, Tolle K, et al. Directed differentiation of human pluripotent stem cells into intestinal tissue in vitro. Nature. 2010;470:105–9.
51. Kabeya T, Qiu S, Hibino M, Nagasaki M, Kodama N, Iwao T, et al. Cyclic AMP signaling promotes the differentiation of human induced pluripotent stem cells into intestinal epithelial cells S. Drug Metab Dispos. 2018;46:1411–9.
52. Kabeya T, Mima S, Imakura Y, Miyashita T, Ogura I, Yamada T, et al. Pharmacokinetic functions of human induced pluripotent stem cell-derived small intestinal epithelial cells. Drug Metab Pharmacokinet. 2020;35:374–82.
53. Iwao T, Kodama N, Kondo Y, Kabeya T, Nakamura K, Horikawa T, et al. Generation of Enterocyte-Like Cells with Pharmacokinetic Functions from Human Induced Pluripotent Stem Cells Using Small-Molecule Compounds. Drug Metab Dispos. 2015;43:603–10.
54. Gribble FM, Reimann F. Enteroendocrine Cells: Chemosensors in the Intestinal Epithelium. http://dx.doi.org.ezproxy.library.wur.nl/101146/annurev-physiol-021115-105439. 2016;78:277–99.
55. Garabedian EM, Roberts LJJ, McNevin MS, Gordon JI. Examining the Role of Paneth Cells in the Small Intestine by Lineage Ablation in Transgenic Mice. J Biol Chem. 1997;272:23729–40.
56. Gerbe F, Legraverend C, Jay P. The intestinal epithelium tuft cells: specification and function. Cell Mol Life Sci. 2012;69:2907.
57. Barker N, Van Es JH, Kuipers J, Kujala P, Van Den Born M, Cozijnsen M, et al. Identification of stem cells in small intestine and colon by marker gene Lgr5. Nat 2007 4497165. 2007;449:1003–7.
58. Zoetendal EG, Raes J, Van Den Bogert B, Arumugam M, Booijink CC, Troost FJ, et al. The human small intestinal microbiota is driven by rapid uptake and conversion of simple carbohydrates. ISME J 2012 67. 2012;6:1415–26.
59. Liu X, Cooper DE, Cluntun AA, Warmoes MO, Zhao S, Reid MA, et al. Acetate Production from Glucose and Coupling to Mitochondrial Metabolism in Mammals. Cell. 2018;175:502-513.e13.
60. Comalada M, Bailón E, De Haro O, Lara-Villoslada F, Xaus J, Zarzuelo A, et al. The effects of short-chain fatty acids on colon epithelial proliferation and survival depend on the cellular phenotype. J Cancer Res Clin Oncol. 2006;132:487–97.
61. Chaturvedi LS, Wang Q, More SK, Vomhof-DeKrey EE, Basson MD. Schlafen 12 mediates the effects of butyrate and repetitive mechanical deformation on intestinal epithelial differentiation in human Caco-2 intestinal epithelial cells. Hum Cell. 2019;32:240–50.
62. Kaiko GE, Ryu SH, Koues OI, Collins PL, Solnica-Krezel L, Pearce EJ, et al. The colonic crypt protects stem cells from microbiota-derived metabolites. Cell. 2016;165:1708.
63. Lee JH, Choy ML, Ngo L, Foster SS, Marks PA. Histone deacetylase inhibitor induces DNA damage, which normal but not transformed cells can repair. Proc Natl Acad Sci U S A. 2010;107:14639–44.

64. Gospodinov A, Popova S, Vassileva I, Anachkova B. The Inhibitor of Histone Deacetylases Sodium Butyrate Enhances the Cytotoxicity of Mitomycin C. Mol Cancer Ther. 2012;11:2116–26.
65. Waldecker M, Kautenburger T, Daumann H, Busch C, Schrenk D. Inhibition of histone-deacetylase activity by short-chain fatty acids and some polyphenol metabolites formed in the colon. J Nutr Biochem. 2008;19:587–93.
66. Park JH, Kotani T, Konno T, Setiawan J, Kitamura Y, Imada S, et al. Promotion of Intestinal Epithelial Cell Turnover by Commensal Bacteria: Role of Short-Chain Fatty Acids. PLoS One. 2016;11.
67. Harris SL, Levine AJ. The p53 pathway: Positive and negative feedback loops. Oncogene. 2005;24:2899–908.
68. Stedman A, Beck-Cormier S, Le Bouteiller M, Raveux A, Vandormael-Pournin S, Coqueran S, et al. Ribosome biogenesis dysfunction leads to p53-mediated apoptosis and goblet cell differentiation of mouse intestinal stem/progenitor cells. Cell Death Differ. 2015;22:1865–76.
69. Matthews GM, Howarth GS, Butler RN. Short-chain fatty acid modulation of apoptosis in the Kato III human gastric carcinoma cell line. Cancer Biol Ther. 2007;6:1051–7.
70. Matthews GM, Howarth GS, Butler RN. Short-Chain Fatty Acids Induce Apoptosis in Colon Cancer Cells Associated with Changes to Intracellular Redox State and Glucose Metabolism. Chemotherapy. 2012;58:102–9.
71. Young GP, Hu Y, Le Leu RK, Nyskohus L. Dietary fibre and colorectal cancer: A model for environment – gene interactions. Mol Nutr Food Res. 2005;49:571–84.
72. Weng M, Walker WA, Sanderson IR. Butyrate regulates the expression of pathogen-triggered IL-8 in intestinal epithelia. Pediatr Res. 2007;62:542–6.
73. Zapletal O, Tylichová Z, Neča J, Kohoutek J, Miroslav Machala ·, Milcová A, et al. Butyrate alters expression of cytochrome P450 1A1 and metabolism of benzo[a]pyrene via its histone deacetylase activity in colon epithelial cell models. Arch Toxicol. 2017;3:2135–50.
74. Mun SJ, Lee J, Chung KS, Son MY, Son MJ. Effect of Microbial Short-Chain Fatty Acids on CYP3A4-Mediated Metabolic Activation of Human Pluripotent Stem Cell-Derived Liver Organoids. Cells 2021, Vol 10, Page 126. 2021;10:126.
75. Rawłuszko AA, Sławek S, Gollogly A, Szkudelska K, Jagodziński PP. Effect of butyrate on aromatase cytochrome P450 levels in HT29, DLD-1 and LoVo colon cancer cells. Biomed Pharmacother. 2012;66:77–82.
76. Walsh J, Gheorghe CE, Lyte JM, van de Wouw M, Boehme M, Dinan TG, et al. Gut microbiome-mediated modulation of hepatic cytochrome P450 and P-glycoprotein: impact of butyrate and fructo-oligosaccharide-inulin. J Pharm Pharmacol. 2020;72:1072–81.
77. Rivière A, Selak M, Lantin D, Leroy F, De Vuyst L. Bifidobacteria and butyrate-producing colon bacteria: Importance and strategies for their stimulation in the human gut. Front Microbiol. 2016;7 JUN:979.
78. Fleming SE, Fitch MD, DeVries S, Liu ML, Kight C. Nutrient Utilization by Cells Isolated from Rat Jejunum, Cecum and Colon. J Nutr. 1991;121:869–78.
79. Wu G. Intestinal mucosal amino acid catabolism. J Nutr. 1998;128:1249.
80. Blachier F, Boutry C, Bos C, Tomé D. Metabolism and functions of L-glutamate in the epithelial cells of the small and large intestines. Am J Clin Nutr. 2009;90.
81. Jang C, Hui S, Lu W, Cowan AJ, Morscher RJ, Lee G, et al. The Small Intestine Converts Dietary Fructose into Glucose and Organic Acids. Cell Metab. 2018;27:351-361.e3.
82. Michal G. An Atlas of Biochemistry and Molecular Biology. 1999.
83. van der Hee B, Wells JM. Microbial Regulation of Host Physiology by Short-chain Fatty Acids. Trends Microbiol. 2021;29:700–12.
84. Kulthong K, Duivenvoorde L, Sun H, Confederat S, Wu J, Spenkelink B, et al. Microfluidic chip for culturing intestinal epithelial cell layers: Characterization and comparison of drug transport between

dynamic and static models. Toxicol Vitr. 2020;65:104815.
85. Kim HJ, Li H, Collins JJ, Ingber DE. Contributions of microbiome and mechanical deformation to intestinal bacterial overgrowth and inflammation in a human gut-on-a-chip. Proc Natl Acad Sci U S A. 2016;113:E7–15.
86. Shah P, Fritz J V., Glaab E, Desai MS, Greenhalgh K, Frachet A, et al. A microfluidics-based in vitro model of the gastrointestinal human-microbe interface. Nat Commun. 2016;7:1–15.
87. Creff J, Courson R, Mangeat T, Foncy J, Souleille S, Thibault C, et al. Fabrication of 3D scaffolds reproducing intestinal epithelium topography by high-resolution 3D stereolithography. Biomaterials. 2019;221:119404.

Supplementary files

Table S1. butyrate 10 mM references indicating their role or relationship to the intestine

KEGG pathway name	Reference
Upregulated pathways	
DNA replication	[1]
Mismatch repair	[2,3]
Fanconi anemia pathway	[4,5]
Homologous recombination	[6,7]
RNA polymerase	[8]
Fatty acid biosynthesis	[9,10]
Nucleotide excision repair	[11]
Endocrine and other factor regulated calcium reabsorption	[12,13]
Alanine, aspartate and glutamate metabolism	[14]
Mineral absorption	[15–18]
Downregulated pathways	
P53 signaling pathway	[19]
Pathogenic Escherichia Coli infection	[20]
Steroid hormone biosynthesis	[21]
Shigellosis	[22,23]
ECM receptor interaction	[24]
NF kappa B signaling pathway	[25,26]
Glutathione metabolism	[27]
Hippo signaling pathway multiple species	[28]
Regulation of actin cytoskeleton	[29]
JAK STAT signaling pathway	[30,31]

Table S2. butyrate 1 mM references indicating their role or relationship to the intestine.

KEGG pathway name	References
Upregulated pathways	
Chemical carcinogenesis	[32]
Mineral absorption	[15–18]

Fat digestion and absorption	[33]
Tryptophan metabolism	[34,35]
Glycine serine and threonine metabolism	[36,37]
Circadian entrainment	[38,39]
Metabolism of xenobiotics by cytochrome P450	[40]
Ubiquinone and other terpenoid quinone biosynthesis	[41]
PPAR signaling pathway	[42,43]
Arachidonic acid metabolism	[44]
Downregulated pathways	
Proteasome	[45,46]
P53 signaling pathway	[19]
Spliceosome	[47]
Ribosome biogenesis in eukaryotes	[48,49]
RNA transport	[50]
Starch and sucrose metabolism	[51,52]
MRNA surveillance pathway	[53,54]

Table S3. propionate 10 mM references indicating their role or relationship to the intestine.

KEGG pathway name	References
Upregulated pathways	
Circadian entrainment	[38,39]
Thiamine metabolism	[55,56]
Mismatch repair	[2,3]
Tryptophan metabolism	[34,35]
Fat digestion and absorption	[33]
Glycine serine and threonine metabolism	[36,37]
Aldosterone regulated sodium reabsorption	[57]
Endocrine and other factor regulated sodium reabsorption	[12,13]
Longevity regulating pathway	[58–60]
Mineral absorption	[15–18]
Downregulated pathways	
P53 signaling pathway	[19]
Proteasome	[45,46]
NF kappa B signaling pathway	[25,26]
Spliceosome	[47]
Pathogenic Escherichia Coli infection	[20]
Ribosome biogenesis in eukaryotes	[48,49]
RNA transport	[50]
Shigellosis	[22,23]

Protein processing in endoplasmic reticulum	[61,62]
Starch and sucrose metabolism	[51,52]

1. Waga S, Stillman B. The DNA replication fork in eukaryotic cells. *Annu Rev Biochem*. 1998;67:721-751. doi:10.1146/annurev.biochem.67.1.721
2. Li GM. Mechanisms and functions of DNA mismatch repair. *Cell Res*. 2008;18(1):85-98. doi:10.1038/cr.2007.115
3. Jiricny J. The multifaceted mismatch-repair system. *Nat Rev Mol Cell Biol*. 2006;7(5):335-346. doi:10.1038/nrm1907
4. Hays L, Frohnmayer D, Frohnmayer L, Larsen K, Owen J. Fanconi Anemia: Guidelines for Diagnosis and Management. *Fanconi Anemia Res Fund, Inc*. Published online June 3, 2014:1-391. Accessed June 22, 2021. http://www.ncbi.nlm.nih.gov/books/NBK1401/
5. Moldovan GL, D'Andrea AD. How the fanconi anemia pathway guards the genome. *Annu Rev Genet*. 2009;43:223-249. doi:10.1146/annurev-genet-102108-134222
6. Michel B, Boubakri H, Baharoglu Z, LeMasson M, Lestini R. Recombination proteins and rescue of arrested replication forks. *DNA Repair (Amst)*. 2007;6(7):967-980. doi:10.1016/j.dnarep.2007.02.016
7. Maloisel L, Fabre F, Gangloff S. DNA Polymerase δ Is Preferentially Recruited during Homologous Recombination To Promote Heteroduplex DNA Extension. *Mol Cell Biol*. 2008;28(4):1373-1382. doi:10.1128/mcb.01651-07
8. Cramer P, Armache KJ, Baumli S, et al. Structure of eukaryotic RNA polymerases. *Annu Rev Biophys*. 2008;37:337-352. doi:10.1146/annurev.biophys.37.032807.130008
9. Hiltunen JK, Chen Z, Haapalainen AM, Wierenga RK, Kastaniotis AJ. Mitochondrial fatty acid synthesis - An adopted set of enzymes making a pathway of major importance for the cellular metabolism. *Prog Lipid Res*. 2010;49(1):27-45. doi:10.1016/j.plipres.2009.08.001
10. Kastaniotis AJ, Autio KJ, Kerätär JM, et al. Mitochondrial fatty acid synthesis, fatty acids and mitochondrial physiology. *Biochim Biophys Acta - Mol Cell Biol Lipids*. 2017;1862(1):39-48. doi:10.1016/j.bbalip.2016.08.011
11. Friedberg EC. How nucleotide excision repair protects against cancer. *Nat Rev Cancer*. 2001;1(1):22-33. doi:10.1038/35094000
12. Van Abel M, Hoenderop JGJ, Van der Kemp AWCM, Van Leeuwen JPTM, Bindels RJM. Regulation of the epithelial Ca2+ channels in small intestine as studied by quantitative mRNA detection. *Am J Physiol - Gastrointest Liver Physiol*. 2003;285(1 48-1). doi:10.1152/ajpgi.00036.2003
13. Van Cromphaut SJ, Dewerchin M, Hoenderop JGJ, et al. Duodenal calcium absorption in vitamin D receptor-knockout mice: Functional and molecular aspects. *Proc Natl Acad Sci U S A*. 2001;98(23):13324-13329. doi:10.1073/pnas.231474698
14. Wu G. Intestinal mucosal amino acid catabolism. *J Nutr*. 1998;128(8):1249. doi:10.1093/jn/128.8.1249
15. Quamme GA. Recent developments in intestinal magnesium absorption. *Curr Opin Gastroenterol*. 2008;24(2):230-235. doi:10.1097/MOG.0b013e3282f37b59
16. Lichten LA, Cousins RJ. Mammalian zinc transporters: Nutritional and physiologic regulation. *Annu Rev Nutr*. 2009;29:153-176. doi:10.1146/annurev-nutr-033009-083312

17. Lönnerdal B. Intestinal regulation of copper homeostasis: A developmental perspective. In: *American Journal of Clinical Nutrition*. Vol 88. American Society for Nutrition; 2008:846S-850S. doi:10.1093/ajcn/88.3.846s
18. Dunn LL, Rahmanto YS, Richardson DR. Iron uptake and metabolism in the new millennium. *Trends Cell Biol*. 2007;17(2):93-100. doi:10.1016/j.tcb.2006.12.003
19. Harris SL, Levine AJ. The p53 pathway: Positive and negative feedback loops. *Oncogene*. 2005;24(17):2899-2908. doi:10.1038/sj.onc.1208615
20. Lai Y, Rosenshine I, Leong JM, Frankel G. Intimate host attachment: Enteropathogenic and enterohaemorrhagic Escherichia coli. *Cell Microbiol*. 2013;15(11):1796-1808. doi:10.1111/cmi.12179
21. Bouguen G, Dubuquoy L, Desreumaux P, Brunner T, Bertin B. Intestinal steroidogenesis. *Steroids*. 2015;103:64-71. doi:10.1016/j.steroids.2014.12.022
22. Schnupf P, Sansonetti PJ. Shigella Pathogenesis: New Insights through Advanced Methodologies . *Microbiol Spectr*. 2019;7(2). doi:10.1128/microbiolspec.bai-0023-2019
23. Sasakawa C. A new paradigm of bacteria-gut interplay brought through the study of Shigella. *Proc Japan Acad Ser B Phys Biol Sci*. 2010;86(3):229-243. doi:10.2183/pjab.86.229
24. Bonnans C, Chou J, Werb Z. Remodelling the extracellular matrix in development and disease. *Nat Rev Mol Cell Biol*. 2014;15(12):786-801. doi:10.1038/nrm3904
25. Neurath MF, Becker C, Barbulescu K. Role of NF-κB in immune and inflammatory responses in the gut. *Gut*. 1998;43(6):856-860. doi:10.1136/gut.43.6.856
26. Pasparakis M. Role of NF-κB in epithelial biology. *Immunol Rev*. 2012;246(1):346-358. doi:10.1111/j.1600-065X.2012.01109.x
27. Wu G, Fang YZ, Yang S, Lupton JR, Turner ND. Glutathione Metabolism and Its Implications for Health. *J Nutr*. 2004;134(3):489-492. doi:10.1093/jn/134.3.489
28. Imajo M, Ebisuya M, Nishida E. Dual role of YAP and TAZ in renewal of the intestinal epithelium. *Nat Cell Biol*. 2015;17(1):7-19. doi:10.1038/ncb3084
29. Pollard TD. The cytoskeleton, cellular motility and the reductionist agenda. *Nature*. 2003;422(6933):741-745. doi:10.1038/nature01598
30. Stempelj M, Kedinger M, Augenlicht L, Klampfer L. Essential Role of the JAK/STAT1 Signaling Pathway in the Expression of Inducible Nitric-oxide Synthase in Intestinal Epithelial Cells and Its Regulation by Butyrate. *J Biol Chem*. 2007;282(13):9797-9804. doi:10.1074/JBC.M609426200
31. Heneghan AF, Pierre JF, Kudsk KA. JAK-STAT and intestinal mucosal immunology. *JAK-STAT*. 2013;2(4). doi:10.4161/JKST.25530
32. Zapletal O, Tylichová Z, Neča J, et al. Butyrate alters expression of cytochrome P450 1A1 and metabolism of benzo[a]pyrene via its histone deacetylase activity in colon epithelial cell models. *Arch Toxicol*. 2017;3:2135-2150. doi:10.1007/s00204-016-1887-4
33. Goodman BE. Insights into digestion and absorption of major nutrients in humans. *Am J Physiol - Adv Physiol Educ*. 2010;34(2):44-53. doi:10.1152/advan.00094.2009
34. Gao J, Xu K, Liu H, et al. Impact of the gut microbiota on intestinal immunity mediated by tryptophan metabolism. *Front Cell Infect Microbiol*. 2018;8(FEB):13. doi:10.3389/fcimb.2018.00013
35. Keszthelyi D, Troost FJ, Masclee AAM. Understanding the role of tryptophan and serotonin metabolism in gastrointestinal function. *Neurogastroenterol Motil*. 2009;21(12):1239-1249. doi:10.1111/j.1365-2982.2009.01370.x

36. Alves A, Bassot A, Bulteau AL, Pirola L, Morio B. Glycine metabolism and its alterations in obesity and metabolic diseases. *Nutrients*. 2019;11(6):1356. doi:10.3390/nu11061356
37. Wang W, Wu Z, Dai Z, Yang Y, Wang J, Wu G. Glycine metabolism in animals and humans: Implications for nutrition and health. *Amino Acids*. 2013;45(3):463-477. doi:10.1007/s00726-013-1493-1
38. Konturek PC, Brzozowski T, Konturek SJ. Gut clock: Implication of circadian rhythms in the gastointestinal tract. *J Physiol Pharmacol*. Published online 2011.
39. Parkar SG, Kalsbeek A, Cheeseman JF. Potential role for the gut microbiota in modulating host circadian rhythms and metabolic health. *Microorganisms*. 2019;7(2):41. doi:10.3390/microorganisms7020041
40. Thelen K, Dressman JB. Cytochrome P450-mediated metabolism in the human gut wall. *J Pharm Pharmacol*. 2010;61(5):541-558. doi:10.1211/jpp.61.05.0002
41. Dallner G, Sindelar PJ. Regulation of ubiquinone metabolism. *Free Radic Biol Med*. 2000;29(3-4):285-294. doi:10.1016/S0891-5849(00)00307-5
42. Duszka K, Oresic M, May C Le, König J, Wahli W. PPARγ modulates long chain fatty acid processing in the intestinal epithelium. *Int J Mol Sci*. 2017;18(12):2559. doi:10.3390/ijms18122559
43. Wang J, Chao T, Wang G, et al. Transcriptome Analysis of Three Sheep Intestinal Regions reveals Key Pathways and Hub Regulatory Genes of Large Intestinal Lipid Metabolism. *Sci Rep*. 2017;7(1):1-12. doi:10.1038/s41598-017-05551-2
44. Kroetz DL, Zeldin DC. Cytochrome P450 pathways of arachidonic acid metabolism. *Curr Opin Lipidol*. Published online 2002. doi:10.1097/00041433-200206000-00007
45. Smith DM, Benaroudj N, Goldberg A. Proteasomes and their associated ATPases: A destructive combination. *J Struct Biol*. 2006;156(1):72-83. doi:10.1016/j.jsb.2006.04.012
46. Petrof EO, Claud EC, Sun J, et al. Bacteria-free solution derived from Lactobacillus plantarum inhibits multiple NF-kappaB pathways and inhibits proteasome function. *Inflamm Bowel Dis*. 2009;15(10):1537-1547. doi:10.1002/ibd.20930
47. Wahl MC, Will CL, Lührmann R. The Spliceosome: Design Principles of a Dynamic RNP Machine. *Cell*. 2009;136(4):701-718. doi:10.1016/j.cell.2009.02.009
48. Raveux A, Stedman A, Coqueran S, et al. Compensation between Wnt-driven tumorigenesis and cellular responses to ribosome biogenesis inhibition in the murine intestinal epithelium. *Cell Death Differ*. 2020;27(10):2872-2887. doi:10.1038/s41418-020-0548-6
49. Stedman A, Beck-Cormier S, Le Bouteiller M, et al. Ribosome biogenesis dysfunction leads to p53-mediated apoptosis and goblet cell differentiation of mouse intestinal stem/progenitor cells. *Cell Death Differ*. 2015;22(11):1865-1876. doi:10.1038/cdd.2015.57
50. Rodriguez MS, Dargemont C, Stutz F. Nuclear export of RNA. *Biol Cell*. 2004;96(8):639-655. doi:10.1016/j.biolcel.2004.04.014
51. Magallanes-Cruz PA, Flores-Silva PC, Bello-Perez LA. Starch Structure Influences Its Digestibility: A Review. *J Food Sci*. 2017;82(9):2016-2023. doi:10.1111/1750-3841.13809
52. Jang C, Hui S, Lu W, et al. The Small Intestine Converts Dietary Fructose into Glucose and Organic Acids. *Cell Metab*. 2018;27(2):351-361.e3. doi:10.1016/j.cmet.2017.12.016
53. Amrani N, Sachs MS, Jacobson A. Early nonsense: mRNA decay solves a translational problem. *Nat Rev Mol Cell Biol*. 2006;7(6):415-425. doi:10.1038/nrm1942
54. Clement SL, Lykke-Andersen J. No mercy for messages that mess with the ribosome. *Nat Struct Mol*

Biol. 2006;13(4):299-301. doi:10.1038/nsmb0406-299
55. Brown G. Defects of thiamine transport and metabolism. *J Inherit Metab Dis*. 2014;37(4):577-585. doi:10.1007/S10545-014-9712-9/FIGURES/5
56. Lonsdale D. A Review of the Biochemistry, Metabolism and Clinical Benefits of Thiamin(e) and Its Derivatives. *Evidence-based Complement Altern Med*. 2006;3(1):49. doi:10.1093/ECAM/NEK009
57. Lee IH, Campbell CR, Cook DI, Dinudom A. Regulation of epithelial Na+ channels by aldosterone: Role of Sgk1. In: *Clinical and Experimental Pharmacology and Physiology*. Vol 35. John Wiley & Sons, Ltd; 2008:235-241. doi:10.1111/j.1440-1681.2007.04844.x
58. Fontana L, Partridge L, Longo VD. Extending healthy life span-from yeast to humans. *Science (80-)*. 2010;328(5976):321-326. doi:10.1126/science.1172539
59. Kenyon CJ. The genetics of ageing. *Nature*. 2010;464(7288):504-512. doi:10.1038/nature08980
60. Longo VD, Fontana L. Calorie restriction and cancer prevention: metabolic and molecular mechanisms. *Trends Pharmacol Sci*. 2010;31(2):89-98. doi:10.1016/j.tips.2009.11.004
61. Naidoo N. ER and aging-Protein folding and the ER stress response. *Ageing Res Rev*. 2009;8(3):150-159. doi:10.1016/j.arr.2009.03.001
62. Määttänen P, Gehring K, Bergeron JJM, Thomas DY. Protein quality control in the ER: The recognition of misfolded proteins. *Semin Cell Dev Biol*. 2010;21(5):500-511. doi:10.1016/j.semcdb.2010.03.006

Chapter 5

Systematic comparison of transcriptomes of Caco-2 cells cultured under different cellular and physiological conditions

Based on: Elzinga, J., Grouls, M., Hooiveld, G.J.E.J. et al. Systematic comparison of transcriptomes of Caco-2 cells cultured under different cellular and physiological conditions. Arch Toxicol (2023). https://doi.org/10.1007/s00204-022-03430-y.

Janneke Elzinga[1], Menno Grouls[2], Guido J.E.J. Hooiveld[3], Meike van der Zande[4], Hauke Smidt[1], Hans Bouwmeester[2]

1 Laboratory of Microbiology, Wageningen University & Research, Wageningen, The Netherlands
2 Division of Toxicology, Wageningen University & Research, Wageningen, The Netherlands
3 Nutrition, Metabolism and Genomics Group, Division of Human Nutrition and Health, Wageningen University & Research, Wageningen, The Netherlands
4 Wageningen Food Safety Research, Wageningen University & Research, Wageningen, The Netherlands

Abstract

There is a need for standardized *in vitro* models emulating the functionalities of the human intestinal tract to study human intestinal health without the use of laboratory animals. The Caco-2 cell line is a well-accepted and highly characterized intestinal barrier model, which has been intensively used to study intestinal (drug) transport, host-microbe interactions and chemical or drug toxicity. This cell line has been cultured in different *in vitro* models, ranging from simple static to complex dynamic microfluidic models. We aimed to investigate the effect of these different *in vitro* experimental variables on gene expression. To this end, we systematically collected and extracted data from studies in which transcriptome analyses were performed on Caco-2 cells grown on permeable membranes. A collection of 13 studies comprising 100 samples revealed a weak association of experimental variables with overall as well as individual gene expression. This can be explained by the large heterogeneity in cell culture practice, or the lack of adequate reporting thereof, as suggested by our systematic analysis of experimental parameters not included in the main analysis. Given the rapidly increasing use of *in vitro* cell culture models, including more advanced (micro)fluidic models, our analysis reinforces the need for improved, standardized reporting protocols. Additionally, our systematic analysis serves as a template for future comparative studies on *in vitro* transcriptome and other experimental data.

Keywords

Transcriptome, Caco-2, in vitro, 3R, gut-on-a-chip, Good In Vitro Method Practices

5.1 Introduction

After (partial) digestion of food and absorption of fluid, nutrients and drugs in the upper part of the human gastrointestinal tract (GIT), the chyme reaches the colon, where fluid and electrolytes are (re)absorbed. Whereas the small intestine is most important for the uptake of food related chemicals and nutrients, the colon has other essential functions related to human health [1]. The colon abundantly contains microorganisms, estimated to reach a total of ~10^{12} microorganisms [2] which aid in the transformation of food components, *e.g.* yet undigested complex carbohydrates, to compounds such as short-chain fatty acids and vitamins, which contribute to host health [3]. Moreover, intestinal microorganisms have demonstrated a significant impact on drug transformation [4]. The role of the chemical exposure and human intestinal microbiota in various diseases, ranging from intestine-related diseases, including Inflammatory Bowel Disease [5–7], neuronal diseases such as Parkinson's and Alzheimer's [8, 9], and cancer [10–12], to metabolic and psychological disorders [13–16], has sparked the interest in human intestinal health. In this context, there is an increasing need for *in vitro* and *in vivo* models reliably mimicking the human GIT, to investigate intestinal barrier integrity, host-microbe interactions and the toxicological effects of food related chemicals, food components, bacteria-derived metabolites, and drugs.

Murine and porcine *in vivo* models have been commonly used [17–19] to answer a wide range of scientific questions related to human intestinal health. Although those models allow for experiments in the context of the whole organism, they lack translational value in terms of human (intestinal) physiology [20, 21], anatomy [22, 23], and microbiology [24–26]. This further strengthens the existing ethical concerns about the use of animals for safety and efficacy testing of compounds of human interest [27]. More than ever, there is a call for increased insight in existing *in vitro* models mimicking the human intestinal tract as well as for improved *in vitro* models. This may not only help to *refine* protocols of dedicated animal studies, but also *reduce* the number of animals sacrificed for science. Eventually and more importantly, the use of *in vitro* models might partially *replace* the use of animal models [28, 29].

The immortalized cell line Caco-2 is a well-accepted and highly characterized model for the human intestinal epithelium. This cell line was originally isolated in the 1970s from a colorectal tumor [30]. As opposed to other isolated colon carcinoma cell lines [31], Caco-2 cells demonstrated spontaneous differentiation upon long-term culture leading to expression of several morphological and biochemical characteristics of small intestinal enterocytes [32, 33]. Growth and differentiation of Caco-2 cells on permeable membranes allows investigation of the transport properties of the cells [34], and this model has been extensively applied and reported in transport studies for toxicological or pharmaceutical research [34–39]. Additionally, from the parental Caco-2 cell line, several clones have been generated over the years and selected based on characteristics of interest (reviewed in Sambuy *et al.* 2005) [40]. Besides Caco-2 cells, other human intestinal cell lines have also been commonly used as a model of the human intestinal epithelium, including T84 [41] and HT29(-MTX) cells [42–46].

Despite the extensive use of the Caco-2 cell line in commonly used simple cell culture inserts (*e.g.* Transwell, ThinCert), its representativity of the human intestinal epithelium has been debated [47, 48]. In this respect, advanced *in vitro* techniques including the use of microfluidic devices [49, 50] and co-culture with other human cell types or (anaerobic) bacteria [51–53] have been applied to this cell line to mimic

the intestinal tract more accurately in terms of physiology, cell differentiation, drug transport and/or host-microbe interactions [49–53]. Simultaneously, primary epithelial cell cultures, including enteroids and adult and induced pluripotent stem cell derived intestinal models have been developed [54–59] and may be used as alternative to more complex *in vitro* intestinal models depending on the research question. Although these more complex models allow the development of personalized models of the human intestinal tract, the power of Caco-2 cells grown on permeable membranes lies in their culture simplicity, reproducibility, and the considerable number of studies available for comparison. Consequently, in theory, its widespread use should allow systematic comparison of the effects of different culturing parameters on the intestinal cellular response. Such a comparison would not only help to assess the reproducibility of *in vitro* models using Caco-2 cells, but also provide suggestions for adjustments of current *in vitro* techniques to improve their functionality and to better conform to the OECD Guidance Document on Good In Vitro Method Practices (GIVIMP) [60].

In this study, we aimed to compare cellular responses of different Caco-2 cell-based *in vitro* models based on gene expression, in which *in vitro* "model" is specified as "the physical and cellular conditions under which the cells are cultured". We focused only on studies in which transcriptome analysis was performed on Caco-2 grown on permeable membranes, since this outcome allows for a comprehensive description of the cell response and serves as a starting point for investigating other outcomes. We collected published studies on Caco-2 cells cultured as cell layers in cell culture inserts or in devices, such as microfluidic chips, as well as studies with more biologically complex models in which Caco-2 cells were cultured as spheres, co-cultured with other cell types in a different compartment or exposed to human intestinal bacteria or their products. Based on the collected studies (2007-2021), we defined eight relevant experimental variables and utilized a bioinformatics approach to analyze and interpret the effect of these variables on transcriptomic responses. We followed an unbiased approach to explore the contribution of the defined variables to the overall transcriptome profiles. Subsequently, we zoomed in on specific genes and corresponding pathways and biological processes, of which regulation of expression could to a significant extent be explained by one of the variables. Additionally, to complement transcriptome data, we carefully extracted other experimental parameters and evaluated several functional experimental outcomes. Of these, only Trans Epithelial Electrical Resistance (TEER) turned out to be commonly reported and thus was compared between respective studies. Overall, our study comprises a systematic and critical data analysis of *in vitro* models using Caco-2 cells grown on permeable membranes.

5.2 Materials & Methods

5.2.1 Study collection

A schematic overview of the study selection and the corresponding number of series can be found in Fig. 1. The NCBI Gene Expression Omnibus (GEO) was searched for the term "Caco-2 OR Caco2" in May 2021, which resulted in 330 series with unique GEO Series identifier (GSEid) (Supplementary File 1). Title, accession display and/or full-text paper of each series were manually screened to select for data series in which transcriptomic analysis was performed on Caco-2 cells which were cultured in cell culture inserts and on more advanced *in vitro* models with an apical and a basolateral compartment, including adapted inserts that introduce alterations such as flow or an anoxic compartment, gut-on-chips, and 3D spheric cell models. If in doubt, the full text of publication(s) linked to the series was screened. Series were

excluded for which (as primary reason) a) no cell culture insert or advanced *in vitro* model was used; b) transcriptomics was performed on or including other cell types than Caco-2 cells (*i.e.* the mRNA would not only be derived from Caco-2 cells) c) no proper control condition was included (*i.e.* not commonly used medium); d) data had been taken from a previously deposited GEO DataSet and/or; e) study details could not be retrieved (*e.g.* studies were not published). For series of which the description in the database pointed towards the use of a cell culture insert or advanced *in vitro* model, but which were not linked to a publication in GEO, potential corresponding publications were actively searched using PubMed, Scopus, and Google. Additional databases (SRA-database from NCBI, as well as Array Express from EMBL-EBI) were searched using the same strategy but did not retrieve additional studies that were not already present in GEO. Lastly, we included data series from our own work, which had been submitted to NCBI but were only released after the date of the database search (GSE158620 and GSE173729). Next, array platforms on which <15,000 unique genes were analyzed, were excluded from further analysis (Suppl. File 1). Series were divided per platform manufacturer, distinguishing between Affymetrix, Illumina, Agilent, and "others". Because of the low representation of models in the latter three categories (thus resulting in a low statistical power), only studies performed on Affymetrix platforms were included for further analysis.

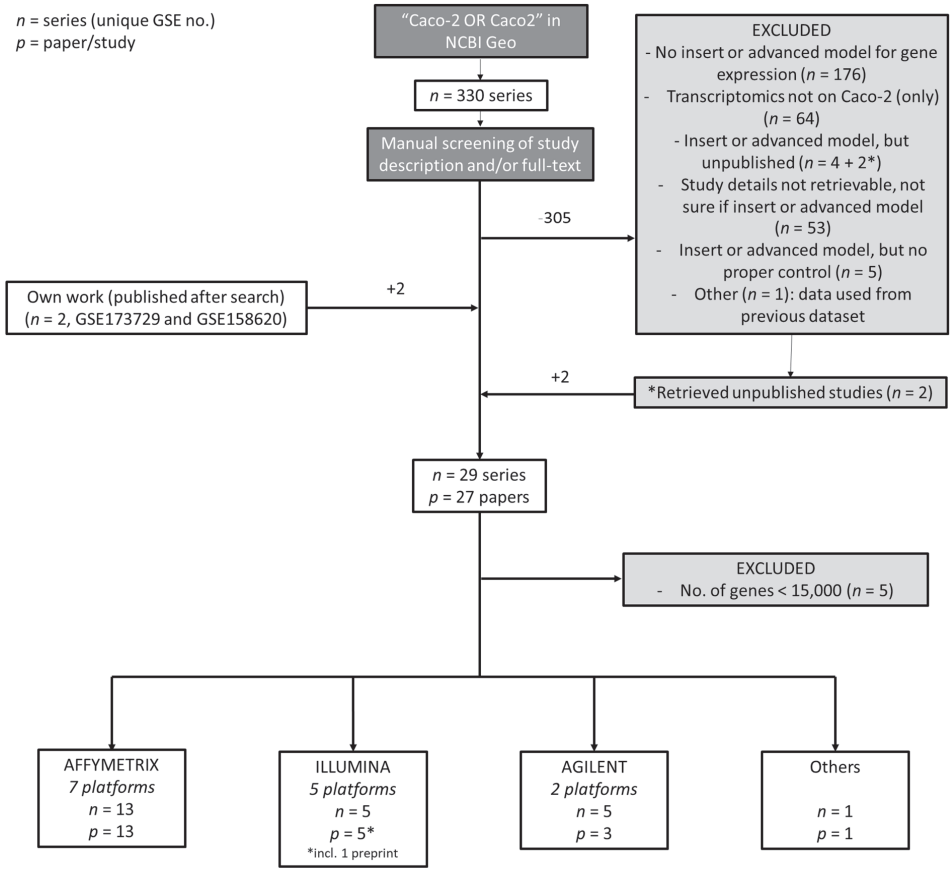

***Figure 1**. Flow chart of study selection process. The NCBI Geo Database was searched for "Caco-2" or "Caco2" in May 2021, which retrieved 330 data series. Exclusion of 306 data series and inclusion of two (own) data series resulted in a final selection of 29 series linked to 27 unique research papers. After exclusion of five data series because of limited numbers of analyzed genes, studies were divided per manufacturer, of which the Affymetrix platform comprised the largest group with thirteen data series corresponding to 13 research papers.*

5.2.2 Data extraction

From all selected data series, only data of samples encompassing Caco-2 cells grown under proper control conditions (*i.e.* regular cell medium) or Caco-2 cells exposed to non-pathogenic intestinal bacteria, or their bacterial products were selected and downloaded. Additional data was manually extracted from full-text papers. Information on experimental set-up was extracted primarily from method-sections or from the Supplementary Information. Some papers referred to previous publications for the used experimental procedures, which then were assessed as well. In case the experimental parameter of interest could not be retrieved, it was considered not reported ("NR"), except for culture temperature and atmosphere (assuming this was 37 °C at 5% CO_2). Additionally, the seeding area of cell culture inserts was based on

standard sizes, in case number of wells or other information was provided. Coating of membranes was considered not applicable ("NA") if not reported, because this was not included in standardized Caco-2 insert protocols [38, 61]. Details for each study can be found in Supplementary File 1. Data on TEER was manually extracted from the text and/or extracted from figures using a digital, on-screen ruler (Measura X, Gekar Tech). Values that had been normalized to a control were excluded.

Each model identified was further categorized based on "GSEid" (GEO Series identifier), "Microbiome" (exposure to non-pathogenic bacteria or their bacterial compounds), "Culture Time" (in which short (< 9 days), medium (≥ 9, but ≤ 17 days) or long (> 17 days) were distinguished), "Oxygen" status in apical compartment (anoxic or oxic), "Flow" (static, dynamic or partially dynamic), "Cell System" (Caco-2 only or co-culture), "Device" (insert or chip) and "Platform" (type of array platform used). Partially dynamic refers to models where flow was applied for the majority of the entire culture time (i.e. > 80%) and/or only either to the apical or basolateral side of the cells. In our dataset, co-cultures consisted of Caco-2 cells cultured in same device with human leukemia monocytic cell line (THP-1), peripheral blood mononuclear or endothelial cells, of which mRNA was extracted from the Caco-2 cells separately.

5.2.3 Transcriptome analysis

All samples were integrated according to an established workflow described before [62]. Briefly, for each experiment raw data files were downloaded from GEO, which were then subjected to background correction and probe-to-probeset (gene) summarization according to the robust multiarray (RMA) algorithm [63]. Since samples were analyzed on multiple Affymetrix array platforms, only those genes were kept that were probed for on all array platforms. This resulted in the inclusion of 11,203 unique shared genes. Per array resulting non-normalized expression estimates of these 11,203 genes were then transformed into rank percentile values, in which the gene with the highest expression estimate was assigned the value of 1 and the lowest expression estimate was set to 0. All expression estimates in between were given a value based on the ranking of expression i.e. 0.01, 0.02 etc. with the steps in between adjusted to the number of genes, and genes with the same expression level were given the same value based on the average rank if they were not tied (i.e. tied for the value of 0.01 would give both a value of 0.015 in case each step was 0.01) [62]. The dataset analyzed in this study consisted of 100 samples, and from each sample expression data of 11,203 genes was extracted. On this shared transcriptome, three different analyses were performed. 1) A multi-level principal component analysis, in which array type was used as blocking variable, performed using the Bioconductor package PCAtools (version 2.6.0) [64]. Based on the Elbow method [65] the relevant number of PCs were determined 2) The top 10% most variable genes were visualized in a heatmap using the package *pheatmap* (v1.0.12) 3) To quantify and interpret sources of variation the package variancePartition (version 1.26.0) was used [66]. This package uses a linear mixed model (LMM) to quantify variation in gene expression attributable to biological or technical variables. To fit the normality assumption of an LMM, the rank percentile values were first transformed using the probit function [62]. The genes of which the variance was explained for at least 40% by one of the variables were related to biologically meaningful changes using gene set overrepresentation analysis (ORA) applying a one-sided Fisher's exact test [67]. Gene sets were retrieved from the expert-curated Kyoto Encyclopedia of Genes and Genomes (KEGG) database [68] or Gene

Ontology: Biological Processes (GOBP) [69, 70]. ORA was performed using the package *clusterProfiler* (v4.3.3) [71]. The whole code will be published online after acceptance of the manuscript.

5.3 Results

5.3.1 Study collection pipeline retrieves 27 unique studies, of which 13 used Affymetrix platforms

Our search strategy to identify studies that performed transcriptome analysis on Caco-2 cells retrieved 330 GEO Series (*i.e.* unique GSEids) (Fig. 1 and Suppl. File 1). Next, 176 series were excluded as in these studies regular wells were used as these Caco-2 models lack the presence of a basolateral compartment, which limits the investigation of transport and (anoxic) host-microbe interactions [40, 72]. Other reasons to exclude series were the following: transcriptomics was performed on or including other cell types, *e.g.* immune cells and microbial cells not separated from Caco-2 (n = 64); no proper control condition was included (n = 5); data had been taken from a previously deposited dataset (n = 1) or data had not been published (yet) and study details could not be retrieved (n = 59). Of the latter category, the description of six series in NCBI pointed at the use of inserts or advanced *in vitro* models, of which two could be retrieved via other search strategies. We included two series of our own (NCBI-submitted) work (GSE158620 and GSE173729), resulting in a total number of unique series corresponding to 27 studies or papers. Across series, different array manufacturers and platforms were used. Five series had to be excluded because of a small number of unique genes analyzed by the platform used (g < 15,000) (Suppl. File 1). Affymetrix platforms comprised the largest group, including 13 series across seven different platforms. Illumina and Agilent platforms were used in five series each (five and two different platforms, resp.) and one series was analyzed on the Stanford SHCU platform ("Others"). For our analysis, we decided to only continue with the series analyzed on Affymetrix platforms, because this group comprised a wider range of *in vitro* models with multiple conditions per model.

Table 4. Overview of Affymetrix studies used for final transcriptome analysis. Studies are presented in chronological order. Each row represents a separate model.

GSEid	Ref.	Platform	No. of samples	Device	Cell-system	Flow	Oxygen	Culture time	Microbiome? If yes, species and number
GSE7259	[12]	Human Genome U133A 2.0 Array	4	Insert	Caco-2	Static	Oxic	Short; Medium	No
GSE15636	[73]	Human Genome U133 Plus 2.0 Array	17	Insert	Caco-2	Static	Oxic	Short	*L. acidophilus NCFM* (Bacterium 1, strain B and SN), *B. lactis* (Bacterium 4 and SN), *L. salivarius* (Bacterium 5 and SN)
GSE17625	[74]	Human Genome U133 Plus 2.0 Array	6	Insert	Co-culture	Static	Oxic	Medium	No
GSE21976	[75]	NuGO array (human) NuGO_Hs1a520180	8	Insert	Caco-2	Static	Anoxic apical compartment	Short	*B. bifidum* PRL2010 (Bacterium 7)
GSE30292	[76]	Human Genome U133 Plus 2.0 Array	3	Insert	Caco-2	Static	Oxic	Long	No
GSE30364	[77]	Human Genome U133 Plus 2.0 Array	3	Insert	Caco-2	Static	Oxic	Medium	No
GSE65790	[53]	Human Gene 1.0 ST Array	2	Insert	Caco-2	Static	Oxic	NR	No
		Human Gene 1.0 ST Array	4	Chip	Co-culture	Dynamic	Oxic	Short	VSL#3 (Bacterial community 1)
GSE79383	[50]	Human Transcriptome Array 2.0	9	Chip	Caco-2	Dynamic	Anoxic apical compartment	Short	*L. rhamnosus* GG (Bacterium 7), LGG + *B. caccae* (Bacterium 7 and 8), separated by PC membrane
GSE81867	[78]	Human Gene 1.0 ST Array	3	Insert	Caco-2	Static	Oxic	Short	No
		Human Gene 1.0 ST Array	3	Insert	Caco-2	Part. Dynamic	Oxic	Short	No
GSE115022	[79]	Human Gene 1.1 ST Array	8	Insert	Caco-2	Static	Oxic	Long	*L. acidophilus* W37 (Bacterium 1, strain A), *L. brevis* W63 (2), *L. casei* W56 (3)
GSE156269	[80]	Human Gene 2.1 ST array	4	Insert	Caco-2	Static	Oxic	Long	No
		Human Gene 2.1 ST array	4	Chip	Caco-2	Dynamic	Oxic	Long	No
GSE158620	[81]	Human Gene 2.1 ST Array	8	Chip	Caco-2	Dynamic	Oxic	Long	No
		Human Gene 2.1 ST Array	8	Insert	Caco-2	Static	Oxic	Long	No
GSE173729	[42]	Human Gene 1.1 ST Array	3	Insert	Caco-2	Static	Oxic	Medium	No
		Human Gene 1.1 ST Array	3	Insert	Caco-2	Dynamic	Oxic	Medium	No

5.3.2 Data extraction results in 100 samples, of which 75% were derived from inserts

From the collected papers, we manually extracted the experimental set-up of each study (Suppl. File 1). After selecting only samples encompassing Caco-2 cells grown under proper control conditions (*i.e.* regular cell medium) or Caco-2 cells exposed to non-pathogenic intestinal bacteria or their bacterial products, we ended up with 100 different samples, including replicates (Suppl. File 1). Of all 100 samples, 75% were derived from Caco-2 cells grown on inserts and 25% from Caco-2 grown on chips (Fig. 2). Note that the model used in GSE8187 (a 96-wells insert with flow) was classified as insert, as opposed to the semantics used by the authors [78]. None of the studies that used an Affymetrix platform cultured Caco-2 as spheres. Across all 100 samples different culture times were applied, ranging from 4-21 days (Suppl. File 2 for full experimental set-up per study), which were further divided into short, medium, or long. One study on inserts did not report the timepoint of analysis. Samples were further categorized based on "GSEid", "Microbiome", "Oxygen", "Flow", "Cell system", "Device" and "Platform" (Table 1).

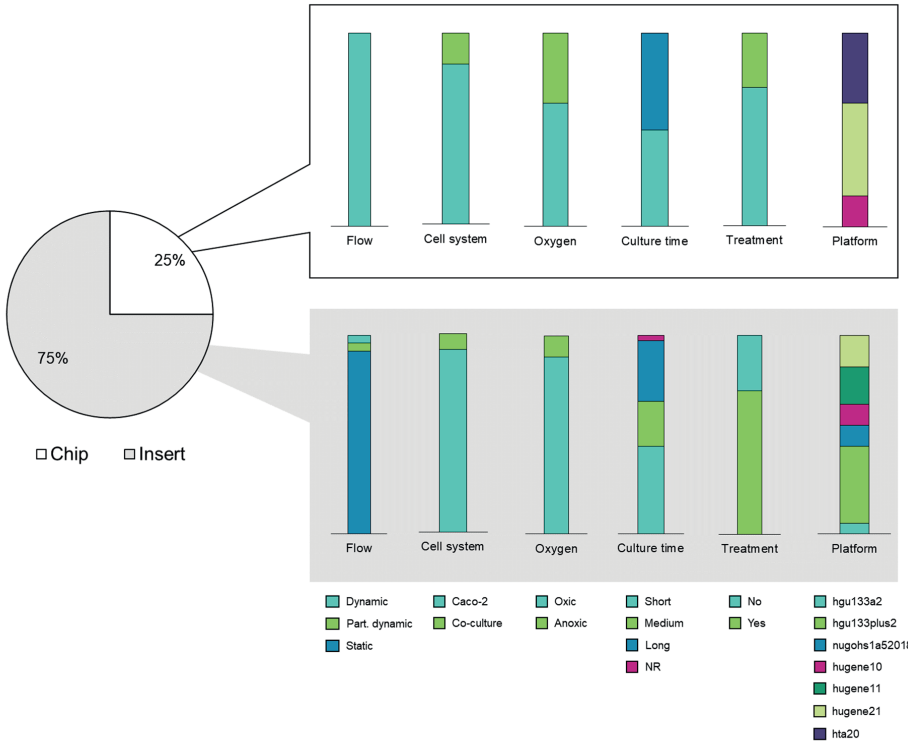

***Figure 2**. Overview of samples per model. Pie chart and bar chart represent no. of samples as percentage of total samples (s = 100) analyzed on an Affymetrix platform. For simplicity, the variable "Microbiome" is only divided into "Yes" and "No". NR = not*

reported; hta20 = Human Transcriptome Array 2.0; hugene21 = Human Gene 2.1 ST Array; hugene11 = Human Gene 1.1 ST Array; hugene10 = Human Gene 1.0 ST Array; nugohs1a520180 = NuGO array (human) NuGO_Hs1a520180; hgu133plus2 = Human Genome U133 Plus 2.0 Array; hgu133a2 = Human Genome U133A 2.0 Array.

5.3.3 Multi-level PCA reveals weak correlation of experimental variables with shared transcriptome

First, we looked at the contribution of the eight pre-defined experimental variables to gene expression profiles, after controlling for the different Affymetrix array platforms. A multi-level PCA was performed (Fig. 3) on the maximum number of genes shared by all array platforms (g = 11,203 genes), referred to as the "shared transcriptome". Based on the Elbow method [65], we only considered the first 13 principal components (PCs) (Fig. 3a-b, Suppl. File 3), of which PC1 accounted for 31% and PC2 explained 15% of the variation in the dataset. Overall, correlation coefficients were low, indicating weak to moderate correlation [82]. We report all variables separately below, starting with the highest correlations on PC1, 2 and 3.

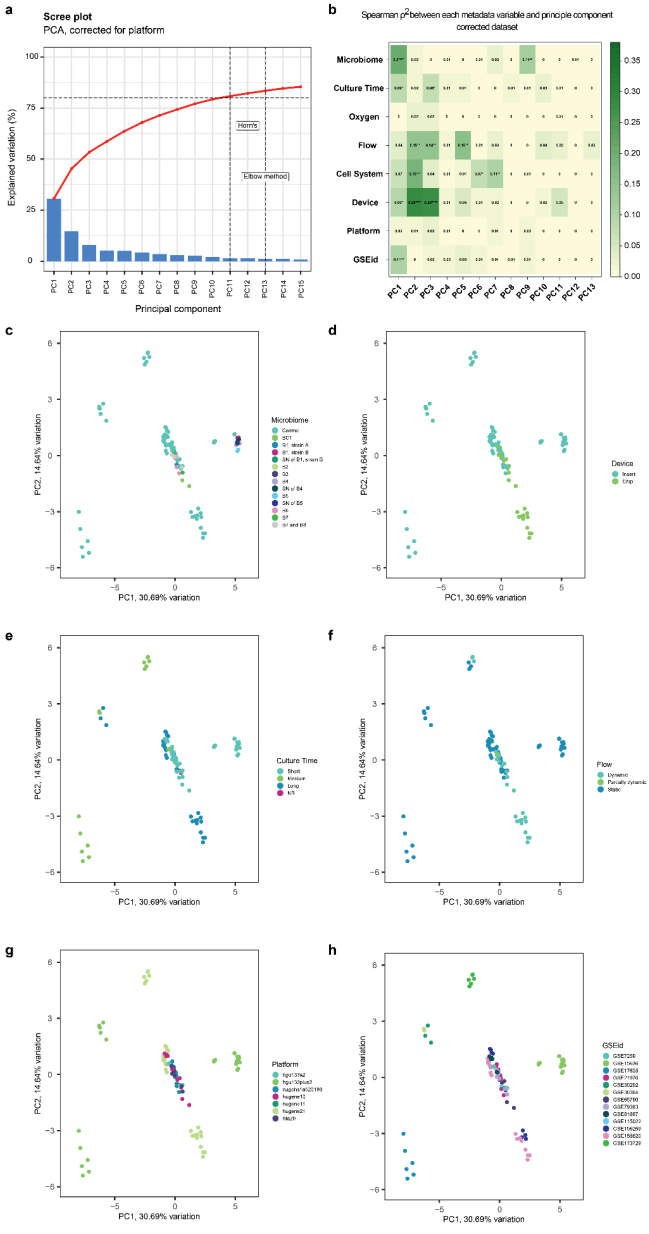

***Figure 3**. Multilevel principal component analysis at model level. After correction for platform, a principal component analysis was performed on a total of 11,203 shared genes, distinguishing eight experimental variables. a) Scree Plot visualizing the variation explained by 18 PCs. b) Spearman correlation ρ2 per model variable for the first 13 PCs. PCA plots of the first two components are*

*provided and labelled by c) microbiome (further defined in Table 1), d) culture time, e) device, f) model, g) array platform and h) GSEid. PCA plots of oxygen and cell system can be found in Online Resource 3. * p <0.05; ** p <0.01; *** p <0.001; **** p <0.0001. B# = Bacterium #; BC# = Bacterial Community #; SN = supernatant; NR = not reported; hta20 = Human Transcriptome Array 2.0; hugene21 = Human Gene 2.1 ST Array; hugene11 = Human Gene 1.1 ST Array; hugene10 = Human Gene 1.0 ST Array; nugohs1a520180 = NuGO array (human) NuGO_Hs1a520180; hgu133plus2 = Human Genome U133 Plus 2.0 Array; hgu133a2 = Human Genome U133A 2.0 Array.*

"Microbiome" was the variable that contributed most significantly to the variation explained by PC1 (ρ = 0.20, $p < 0.0001$, Fig. 3b). Visualization of PC1 against PC2 demonstrated a separate cluster formed by three different bacterial species and their supernatant on PC1. These microbial exposures (See Table 1 for specifications) were all applied within one study [73], but also clustered together with the control condition of that respective study (Fig. 3c, see GSE15636 in Fig. 3h). The variable "Device" contributed significantly to the variation explained by PC2 and PC3 ($\rho^2 = 0.28$ and 0.28, resp., $p < 0.0001$, Fig. 3b). Visualization of PC1 against PC2 demonstrated a grouping of the chips, while the inserts were less congruent (Fig. 3d). Additionally, within the cluster of chips, a separation was observed between the short- and long-term cultured Caco-2 cells on chip (Fig. 3b and e), whereas in general, the variable "Culture Time" contributed significantly, but relatively weakly to the variation explained by PC1 and PC3 ($\rho^2 = 0.09$ and $\rho^2 = 0.08$, $p < 0.05$). Co-culture with other cell types contributed significantly to multiple PCs, mostly to PC2 ($\rho^2 = 0.18$, $p < 0.001$) (Fig. 3b, Suppl. File 3). The (partial) presence or absence of flow contributed significantly to the variation explained by multiple PCs, with a similar contribution to PC2, PC3 and PC5 ($\rho^2 = 0.15$, 0.14 and 0.15 resp., $p < 0.01$). Visualization of the first two principal components, showed that the (partially) dynamic conditions clustered together, except for one study using Semi-Wet interface with Mechanical Stimulation (Fig. 3f**,** see GSE173729 in (Fig. 3h). Interestingly, none of the PCs were significantly associated with the variable "Oxygen" (Fig. 3b, Suppl. File 3). Array platform did not contribute significantly to any principal component (Fig. 3b and g), demonstrating the successful correction of inter-platform differences (Suppl. File 3 for uncorrected data)**.** Finally, GSEid contributed significantly but weakly to the variation explained by PC1 (Fig. 3b and 3h).

Complementary to the multi-level PCA, a clustered heatmap was generated based on the 10% most variable genes of the shared transcriptome (Fig. 4). This analysis did not show clear groupings according to one of the variables. The clustered heatmap shows that the samples from two comparative studies between inserts and chips from Kulthong *et al.* ("GSEid": GSE156269 and GSE158620) [80, 81] clustered based on the device, in line with what was found by PCA. Moreover, the clustered heatmap confirmed separate clustering of the long- from the short-term cultured cells on chip.

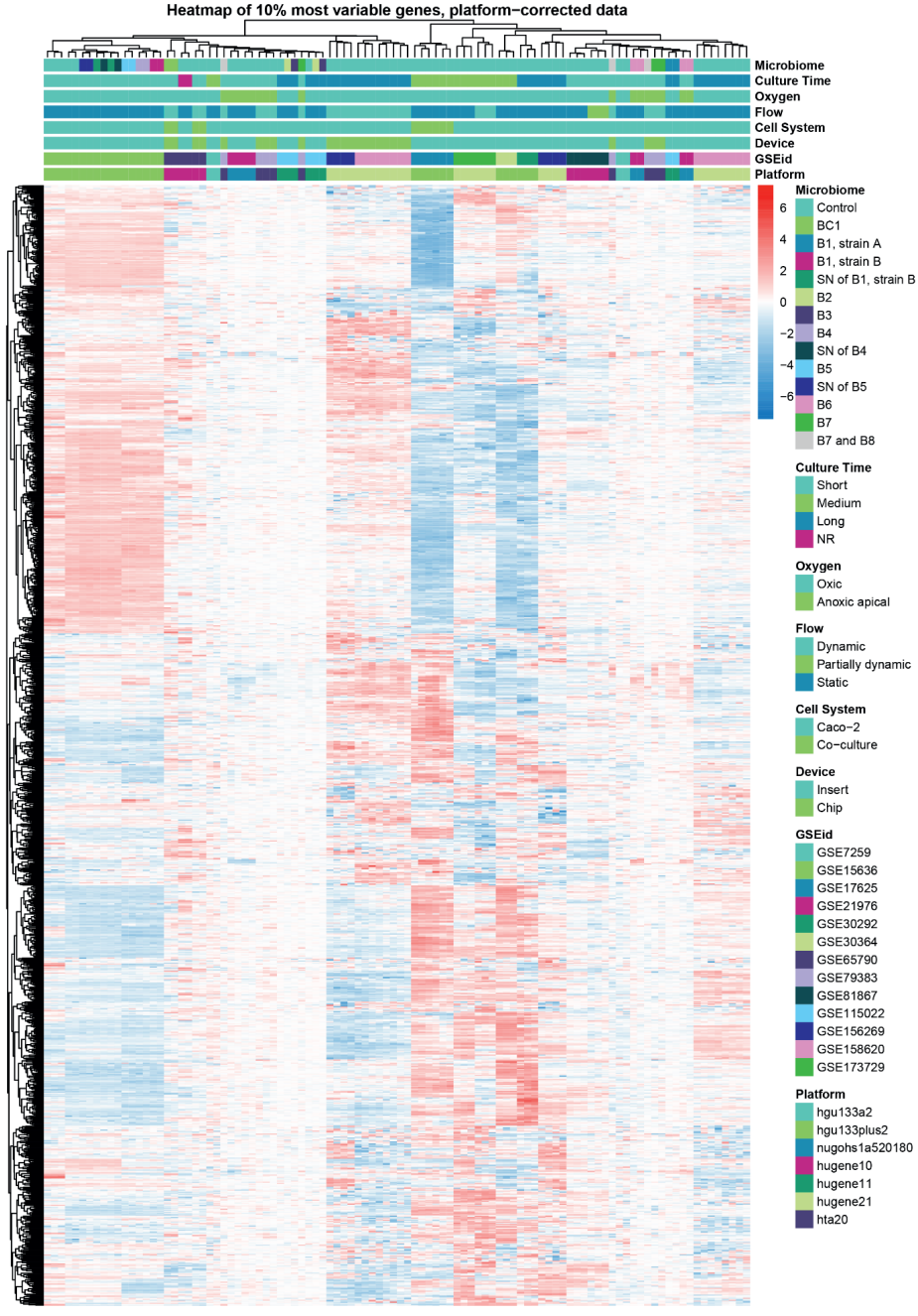
Heatmap of 10% most variable genes, platform−corrected data
Microbiome
Culture Time
Oxygen
Flow
Cell System
Device
GSEid
Platform
6
4
2
0
−2
−4
−6
Microbiome
Control
BC1
B1, strain A
B1, strain B
SN of B1, strain B
B2
B3
B4
SN of B4
B5
SN of B5
B6
B7
B7 and B8
Culture Time
Short
Medium
Long
NR
Oxygen
Oxic
Anoxic apical
Flow
Dynamic
Partially dynamic
Static
Cell System
Caco−2
Co−culture
Device
Insert
Chip
GSEid
GSE7259
GSE15636
GSE17625
GSE21976
GSE30292
GSE30364
GSE65790
GSE79383
GSE81867
GSE115022
GSE156269
GSE158620
GSE173729
Platform
hgu133a2
hgu133plus2
nugohs1a520180
hugene10
hugene11
hugene21
hta20

Figure 4. Clustering of samples (s = 100) based on the expression of the top 10% most variable genes shared between samples (g = 1122). Gene names are left out for readability. Heatmap represents relative gene expression varying from low (blue) to high (red). B# = Bacterium #; BC# = Bacterial Community #; SN = supernatant; hta20 = Human Transcriptome Array 2.0; hugene21 = Human Gene 2.1 ST Array; hugene11 = Human Gene 1.1 ST Array; hugene10 = Human Gene 1.0 ST Array; nugohs1a520180 = NuGO array (human) NuGO_Hs1a520180; hgu133plus2 = Human Genome U133 Plus 2.0 Array; hgu133a2 = Human Genome U133A 2.0 Array.

5.3.4 Variance partition analysis reveals high contribution of "GSEid" to individual gene expression

Next, we focused specifically on the genes of which variance of expression was explained by one of the eight specified experimental variables, by variance partition analysis [66]. Without correction for "Platform", the analysis revealed that the variance per gene was explained to the largest extent by "Platform" with an average of 43% across all genes (g = 11,203) (Suppl. File 4). After correction for "Platform", the variance of genes was explained mostly by "GSEid" (average of 38%), followed by residual, undefined parameters (25%) and "Device" (8%, Fig. 5a). Because of the relatively high contribution of "GSEid", a technical parameter, we decided to focus only on genes of which variance was explained by one of the variables for more than 40%. The number of genes fulfilling this criterium varied from 0 (for "Oxygen") to 5,198 (for "GSEid") (Fig. 5b). The variance in the relatively high number of genes explained by residual parameters, can be explained by other model parameters that we extracted from the respective studies, but could not be included in the variance partition analyses, for instance used cell passages, membrane on which cells were seeded, membrane pore size, seeding area and seeding density. Overall, these model parameters were heterogenous across and within *in vitro* models or were not reported at all by studies (Suppl. File 4).

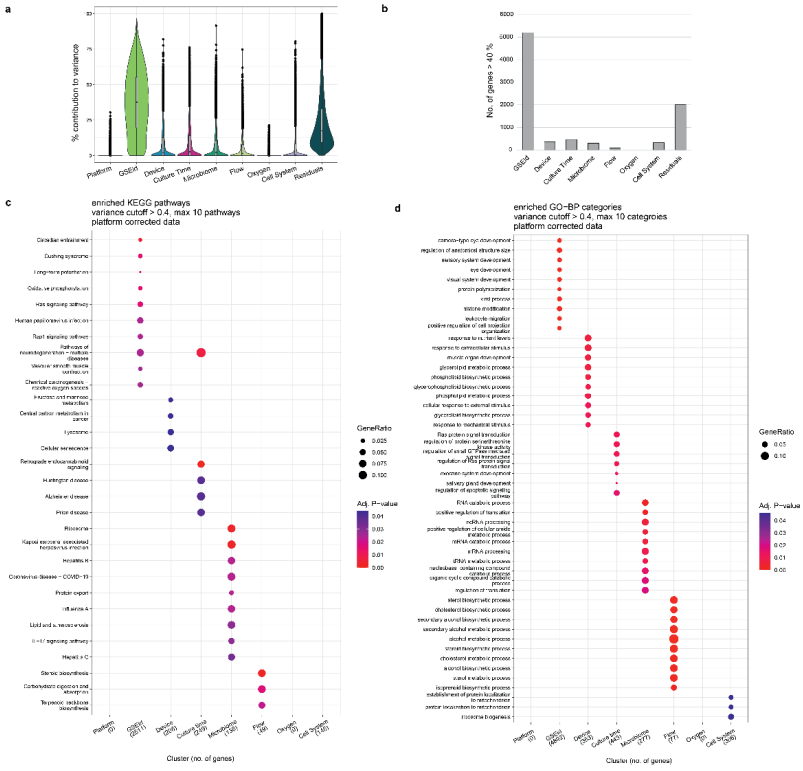

Figure 5*. Variance partition analysis of all genes shared between samples (s = 100, g = 11,203). a) Violin plot shown the percentage contribution of each variable to the expression of all genes. Based on the uncorrected data (Online Resource 4), a cut-off of 40% was chosen. b) Number of genes of which contribution of respective variable was more than 40%. The overrepresentation of pathways within these genes in c) KEGG Pathways and d) GO-BP are displayed per variable.*

Next, we checked per variable which biological processes were enriched among the identified genes, *i.e.* to which pathway(s) these genes were mapped more often than would be expected by chance. We used the KEGG and GOBP databases to retrieve the enriched pathways and biological processes, respectively. Only four variables resulted in significant overrepresentation of KEGG pathways, *i.e.* "GSEid", “Culture Time”, “Microbiome” and “Flow”. Overrepresentation analysis of genes of which variance was explained for more than 40% by “GSEid”, resulted in a heterogenous mix of non-intestine related KEGG pathways, which was the same for “Culture time” (Fig. 5c). Although the microbial exposures included in our dataset concerned non-pathogenic bacteria, overrepresentation analysis of the genes of which the variance was explained to a considerable extent by “Microbiome” revealed pathways related to host-pathogen interactions, such as Kaposi sarcoma-associated herpesvirus infection, COVID-19, hepatitis B and C, Influenza A and IL-17 signaling pathway. Genes of which the variance was explained mainly by “Flow” were enriched in the pathways involved in steroid and terpenoid backbone biosynthesis, but also in the breakdown and absorption of carbohydrates indicating an effect on energy homeostasis.

A similar approach was taken for Gene Ontology Biological Process (GO-BP) categories (Fig. 5d), which resulted in overrepresentation of categories for six variables (“GSEid”, “Device”, “Culture time”, “Microbiome”, “Flow” and “Cell system”). Biological processes overrepresented in "GSEid" included a wide variety of processes, with some clearly unrelated to the intestine as they pertain to the development of other organs. Among the rest there was a focus on stress and adjustments in the cell via for example "histone modification" and “regulation of apoptotic signaling pathway” and two immune-related processes, “viral process” and “leukocyte migration”. Among "Device", "Microbiome", and "Flow" a range of different metabolic and biosynthetic processes showed up, many related to lipid metabolism. Process overrepresentation analysis for "Culture time" and “Cell System” resulted in several processes unrelated to the intestine or expected effects.

5.3.5 Comparison of TEER values reveals heterogeneity in values and reporting quality

Complementary to the transcriptome data, we collected additional functional experimental data from the identified studies to further characterize the used Caco-2 cell models. Among the identified studies, TEER was the only commonly reported outcome, which is a common measure of epithelial barrier integrity in *in vitro* studies using epithelial cell layers. TEER was reported in six Affymetrix studies comprising eight different models, of which one only reported the percentage of change in TEER, disabling comparison with other studies. Another study did not report seeding area, limiting calculations from Ohms/cm^2 to Ohms * cm^2. We extracted TEER values from six different models from four different studies across time points ranging from 2-12 days (Fig. 6), demonstrating a wide range of values.

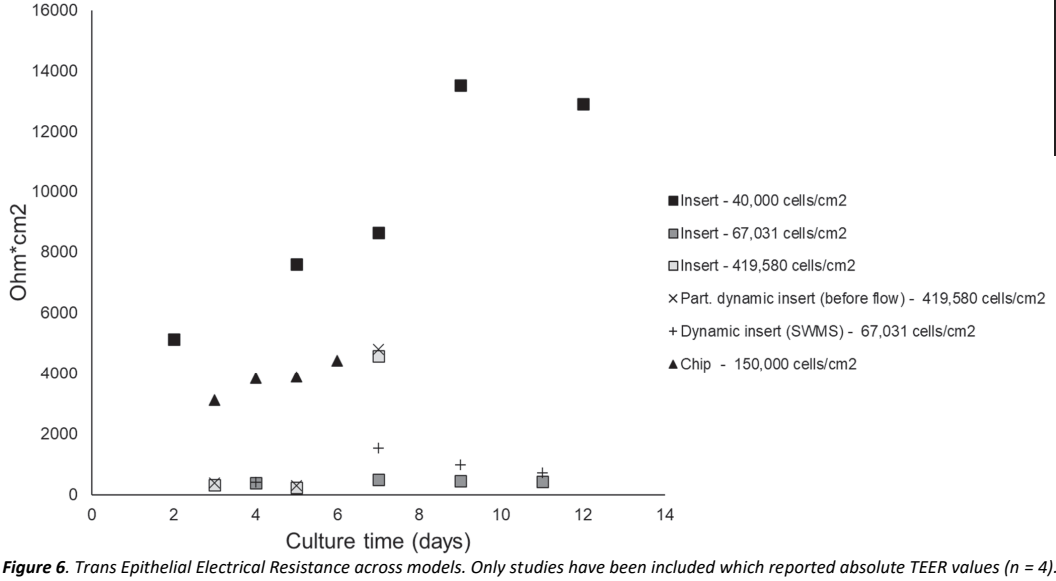

***Figure 6**. Trans Epithelial Electrical Resistance across models. Only studies have been included which reported absolute TEER values (n = 4). Model conditions are presented individually, including initial seeding density. All conditions are oxic. Values were extracted from graphs using a digital ruler. Each data point represents the mean of 2-4 technical or biological replicates.*

5.4 Discussion

In this study, we systematically compared transcriptomes of Caco-2 cells grown on permeable membranes using different *in vitro* systems modelling the human intestinal tract. We used the most frequently applied model, Caco-2 grown on inserts, as baseline for the comparison to other models incorporating an apical and basolateral compartment, allowing transport. Our shared transcriptome analysis indicated that of the studied parameters, the following had a significant, albeit relatively weak, influence on gene expression: the device in which Caco-2 cells were cultured; the presence of flow; and the exposure to non-pathogenic bacteria or their bacterial compounds. When looking at the individual gene level, however, variance in expression was mostly determined by the study (*i.e.* GSEid). This points at a large heterogeneity in cell culture practices in *in vitro* models, which is supported by our analysis of experimental parameters from the respective studies (Online Resource 1), including variables such as passage number, Caco-2 sub-clone and protocol used, all of which can influence the results [40, 83–85]. Because these variables cannot be expressed as a number or concern an ambiguous range without a common starting point (*e.g.* for cell culture passage), these could not be included in the analysis. Additionally, we demonstrated a lack of proper reporting of experimental variables, which has been stressed previously [60]. Our systematic analysis sets the scene for similar future analyses of (-omics) data between *in vitro* models, and therefore is a next step towards transparent reporting of *in vitro* studies to achieve an increased acceptance of non-laboratory animal study-derived data in life sciences.

Our multi-level PCA demonstrated that the variables “Flow” and “Device” had a similar effect. This is probably because dynamic samples were often derived from chips, except for three samples derived from inserts. These three concerned Caco-2 cells grown under Semi-Wet interface with Mechanical Stimulation, in which the cells are cultured under minimal liquid in the apical compartment and put on an orbital shaker [86]. Interestingly, visualization of PC1 against PC2 revealed that these samples clustered separately from the other dynamic samples (chips), but the same was true for the static control (insert) of this study [42], indicating that other factors explain the separate clustering of these samples. Overall, differences in (micro)fluidic design of included dynamic samples complicated inter-model comparison. Although most of the samples still clustered together, it would be informative to quantify shear stress or the resulting shear stress on the cells, as opposed to distinguishing only between static, dynamic and partially dynamic. Shear stress values were, however, not reported for all studies (except three [53, 80, 81] or could, in some cases, not be calculated with the available information.

“Microbiome” was relatively strongly associated with (shared) gene expression, despite the heterogeneity in bacterial treatments tested in the included studies. For microbiome-specific effects of the tested bacteria, we refer to the individual papers corresponding to the studies (Species and corresponding references in Table 1). To facilitate co-culture of Caco-2 with intestinal (anaerobic) bacteria an *in vitro* model that is (at least) partially anoxic is required. Remarkably, our analyses demonstrated that the partial lack of oxygen did not seem to influence Caco-2 gene expression in the included *in vitro* models at all. For the studies that included microbes, the actual concentration of oxygen in the apical compartment was not always quantified. Therefore, the question remains whether the lack of association of oxygen with gene expression is due to failure of the respective studies to create an anoxic atmosphere in the apical compartment or that the absence of oxygen on one side simply does not affect gene expression of Caco-

2 cells (*e.g.* because oxygen supply via the other side is sufficient). It would be advantageous for future studies to monitor and report O_2 concentrations, as has been done already in inserts [87] as well as more advanced *in vitro* models [51].

Because we observed a large heterogeneity in culture time between studies, we decided to define three groups based on cell culture time ranges. The definition of total culture time varied between studies. For instance, Dihal *et al.* accounted for the preconfluent phase of cells once seeded, by starting to count from day 2 after seeding [12], whereas other studies considered the time of seeding as the starting point. In the case of "Culture time" there is a consensus in literature that there is a direct relation with differentiation and thus, gene expression. Although the exact time until a plateau is reached differs for each differentiation marker, the generally accepted culture time for full differentiation is 21 days [38, 40, 61, 88]. In our dataset, total culture times differed between studies using inserts, which could depend on the study aim. For instance, for studying barrier properties, fifteen days of culture was shown to be sufficient [84]. However, we observed no strong influence of the variable "Culture time" on gene expression in our PCA. This could be due to the inclusion of chips and studies with adjusted protocols, both reported to change the relationship between culture time and differentiation [49, 89, 90]. Amongst others, the shear stress that cell experience on chips have been described to enhance differentiation of intestinal cell lines thereby reducing the total culturing time [49, 89]. This became apparent within the group of chips, where the short-cultured cells were separated from the long-term cultured cells in both the PCA (PC1 against PC2) and the heatmap cluster analysis. Within inserts the lack of association between "Culture time" and gene expression is likely due to the inclusion of studies such as GSE30292, in which cells were maintained at low density by subpassaging cells at 50% confluence, instead of the density prescribed by ATCC (between 80-90%) [76, 91] Subsequently, these cells were cultured for a long period on inserts, *e.g.* three weeks showing a profound effect on gene expression over time. Interestingly, both our PCA and heatmap cluster analysis demonstrated that these samples clustered together with medium-term cultured cells, and not with other long-term cultured cells (all maintained at normal density before seeding). It was already shown previously that low-density cells, although expressing the same level of differentiation markers as high-density (90%) grown cells, have a slower exit from cell cycle, including a delay in downregulation of cyclin A and increase of differentiation marker sucrase [90]. Although low-density grown cells should have differentiated to the same extent as high-density grown cells after three weeks [90, 91], our data suggests that low-density maintained cells grown for a long period on inserts demonstrate a transcriptome profile more similar to high-density maintained cells grown for a medium period on inserts. This reinforces the need for clear reporting on cell maintenance practice. Overall, the effects of, a.o., flow and seeding density on the interaction between culture time and gene expression, have potentially obscured the expected effect of culture time on gene expression. For future analyses, these interactions could be included as a separate variable in the PCA. This, however, requires proper quantification of these interactions, which is now hampered by model heterogeneity and incomplete reporting.

Our variance partition analysis provided an overview of which pathways or biological processes were associated with each of the selected variables. In the case of the KEGG pathways only four variables contributed to pathways. The pathways associated with "Microbiome" were immune system-related, though the microorganisms included in our study are non-pathogenic bacteria, while the pathways are

associated with infectious diseases. This is likely because both groups of microbiota act on Toll-like and other pattern recognition receptors [92, 93], but with probably opposing downstream effects. We did not find similar processes associated in the GOBP analysis, where "Microbiome" was mostly associated with RNA and translation processes, which are rather broad. The parameter "Flow" was only associated with two pathways, *i.e.* steroid and terpenoid backbone synthesis, and these were supported by the GOBP analysis, where "Flow" associated with many processes related to these pathways. Similar GOBPs were enriched in the genes mainly determined by "Device", which is likely due to the overlap between these two variables, as discussed previously. Both the variable "Culture time" and "Cell System" were associated with several RNA related processes but did not show a clear direction of effect in the other processes. Better harmonization of *in vitro* models or more accurate categorization of models (including more variables, see below), would probably point at more specific categories of pathways and processes, with a higher overlap between the KEGG and GOBP analysis.

The relatively low correlation coefficients in the PCA, as well as the high number of genes of which variance was explained to a substantial extent by residual variables, indicated that a substantial number of variables is still missing in our analysis. Future analyses would be stronger by including other experimental variables like passage number, seeding density, and seeding membrane. Our systematic extraction of these parameters revealed a large heterogeneity between studies, making it impossible to reach significant outcomes when these parameters are used as input. We extracted other parameters as well, such as cell medium composition in terms of fetal calf serum, antibiotics, and other supplements; specific clones used and medium refreshment frequency, demonstrating similar heterogeneity. All these parameters have been reported to affect Caco-2 cell behavior [40], and therefore should be reported when publishing data, as also suggested by the MIAME- and MINSEQE guidelines (outlining the Minimum Information About a Microarray Experiment or Minimum Information About a Next-generation Sequencing Experiment that should be included when describing a microarray or sequencing study) [94, 95]. In general, the degree to which data was deposited in MIAME- or MINSEQE-compliant public data repositories, like NCBI Geo and ArrayExpress, limited the availability of our transcriptome-centered approach. For instance, we encountered studies that had not deposited their data in these repositories [89, 96] and *vice versa*, data series which had not been linked to the correct study (see number of retrieved studies Fig. 1). We cannot determine how many relevant, unpublished studies we missed, since the description in NCBI on the exact *in vitro* model used was not always complete. In the context of the increasing global interest in Open Science, the importance of depositing open data in public repositories was recently stressed [97]. Specifically for microarray gene expression analyses, researchers demonstrated limited repeatability of published microarray studies, which was due to inadequate reporting on the used methods and other factors like software unavailability, or unclear reporting of the results [98]. The quality and ability to reuse data from other end points has been complicated by reporting issues as well. This is exemplified by TEER measurements, the most reported outcome in our dataset (other than gene expression). We concluded, however, that even the reporting quality of TEER was low, *i.e.* in terms of number of replicates used; culture area; normalization to blank inserts and temperature at which the measurement was performed. Note that in a few studies [94] TEER was solely monitored as a quality measure of the monolayer, although the reported required minimum varied between studies (150-330 Ω cm^2) or was not defined. Similarly, a standardized method to measure TEER on chip devices

has not been established yet [77, 79]. Our data reinforces the need for standardized TEER protocols and reporting guidelines for inserts, chips and other devices that are currently being developed.

All variables taken together, the data used for this study reiterates the need for a universally accepted Caco-2 cell culturing method, which also includes proper reporting of all variables and read-outs. The lack of adequate reporting is a commonly known problem in *in vitro* research [99], which limits the reproducibility and translatability of animal-free methods. Moreover, our study demonstrates that poor reporting quality of (meta)data also limits integration of existing *in vitro* data in systematic analyses across models or studies, re-emphasizing the need for Findable, Accessible, Interoperable, Reusable (FAIR) data guiding principles [100]. Additionally, the need to apply novel-approach methods in, for instance, chemical risk assessment as well as in fundamental and clinical research is increasing. In this context, the development of an *in vitro* critical appraisal (IV-CAT) tool to improve the peer-review as well as the quality of published *in vitro* research, as proposed by De Vries and Whaley [101] is highly appreciated.

In summary, our study aimed to compare transcriptome responses of Caco-2 cells in different *in vitro* models as systematically as possible. Our analysis comprised both a transcriptome-wide and gene-specific approach, has the potential to find associations of predefined experimental variables with gene expression and uncover biological pathways associated with these variables. We complemented this analysis with manual extraction of other data, including model parameters and functional outcomes such as TEER. In this way, this paper can serve as an example for future comparison to *in vitro* models. Currently, controls are designed with only their own experiment in mind, failing to consider variables that are important to allow for comparison to other studies. More importantly, the results show the need for standardization and benchmarking of both current and future *in vitro* models. This should start with proper reporting of model parameters [102], as only in this way research can be reproduced and compared. We acknowledge that benchmarking of an *in vitro* model depends largely on the research question, *e.g.* whether the *in vitro* model is used for risk assessment, drug development or uncovering fundamental biological knowledge. Current approaches might still function in cases where you compare a potent exposure to controls across studies, but it fails to allow for extraction of more subtle effects of (underreported) model and experimental variables, reducing potential value of data. For current *in vitro* methods, the OECD is already working towards improving models via GIVIMP, setting standards on models and reporting [60]. At the same time, there the is also a push to apply (part of) this knowledge in organ-on-chip technology in (to-be-) developed models [103, 104] by standardizing chip design. But application in the development of these models should go further than just technical design. A continued push in this direction is key and responsibility lies with not only the researchers that should execute experiments according to existing guidelines [99], but also the funding agents deciding to invest in the application or development of *in vitro* models as well as journal editors and peer reviewers critically evaluating the work. Only in this way, researchers will be able to unlock the full potential of *in vitro* models, to eventually reduce, refine, and replace the need for animal testing.

Acknowledgement

For this work JE and MG were supported by a grant funded by the Dutch Research Council, a Building Blocks of Life project (No. 737.016.003). Work on this project by MvdZ was supported by the Dutch

Ministry of Agriculture, Nature and Food Quality (Grant: KB-37-002-020). The authors acknowledge the constructive comments on this work provided by Ivonne M. C. M. Rietjens and Clara Belzer.

Conflict of interest

The authors declare that they have no conflict of interest.

Data Availability

The datasets analyzed during the current study have been generated by others and are available in the NCBI Gene Expression Omnibus (GEO), https://www.ncbi.nlm.nih.gov/geo/. The code to

analyze the data is deposited online on Zenodo.org, https://zenodo.org/

record/7525836#.Y77gohWZO3A.

References

1. Silverthorn DU, Johnson BR, Ober WC, Ober CE, Silverthorn AC. Human physiology : an integrated approach. 2016.
2. Sender R, Fuchs S, Milo R. Revised Estimates for the Number of Human and Bacteria Cells in the Body. PLoS Biol. 2016;14.
3. Salvador V, Cherbut C, Barry JL, Bertrand D, Bonnet C, Delort-Laval J. Sugar composition of dietary fibre and short-chain fatty acid production during in vitro fermentation by human bacteria. Br J Nutr. 1993;70:189–97.
4. Sousa T, Paterson R, Moore V, Carlsson A, Abrahamsson B, Basit AW. The gastrointestinal microbiota as a site for the biotransformation of drugs. Int J Pharm. 2008;363:1–25.
5. Derrien M, Belzer C, de Vos WM. Akkermansia muciniphila and its role in regulating host functions. Microbial Pathogenesis. 2017;106.
6. Venegas DP, De La Fuente MK, Landskron G, González MJ, Quera R, Dijkstra G, et al. Short chain fatty acids (SCFAs)mediated gut epithelial and immune regulation and its relevance for inflammatory bowel diseases. Front Immunol. 2019;10 MAR:277.
7. Lomer MCE, Thompson RPH, Powell JJ. Fine and ultrafine particles of the diet: influence on the mucosal immune response and association with Crohn's disease. Proc Nutr Soc. 2002;61:123–30.
8. Chen H, Meng L, Shen L. Multiple roles of short-chain fatty acids in Alzheimer disease. Nutrition. 2022;93.
9. Sun MF, Zhu YL, Zhou ZL, Jia XB, Xu Y Da, Yang Q, et al. Neuroprotective effects of fecal microbiota transplantation on MPTP-induced Parkinson's disease mice: Gut microbiota, glial reaction and TLR4/TNF-α signaling pathway. Brain Behav Immun. 2018;70:48–60.
10. Abreu MT, Peek Jr. RM. Gastrointestinal malignancy and the microbiome. Gastroenterology. 2014;146:1534-1546 e3.
11. Arthur JC, Perez-Chanona E, Muhlbauer M, Tomkovich S, Uronis JM, Fan TJ, et al. Intestinal inflammation targets cancer-inducing activity of the microbiota. Science (80-). 2012;338:120–3.
12. Dihal AA, Tilburgs C, van Erk MJ, Rietjens IM, Woutersen RA, Stierum RH. Pathway and single gene analyses of inhibited Caco-2 differentiation by ascorbate-stabilized quercetin suggest enhancement of

cellular processes associated with development of colon cancer. Mol Nutr Food Res. 2007;51:1031–45.
13. Allen AP, Dinan TG, Clarke G, Cryan JF. A psychology of the human brain-gut-microbiome axis. Soc Pers Psychol Compass. 2017;11:e12309.
14. Hartstra A V, Bouter KEC, Bäckhed F, Nieuwdorp M. Insights Into the Role of the Microbiome in Obesity and Type 2 Diabetes. Diabetes Care. 2014;38:159–65.
15. Sarkar A, Harty S, Lehto SM, Moeller AH, Dinan TG, Dunbar RIM, et al. The Microbiome in Psychology and Cognitive Neuroscience. Trends Cogn Sci. 2018;22:611–36.
16. Singer-Englar T, Barlow G, Mathur R. Obesity, diabetes, and the gut microbiome: an updated review. Expert Rev Gastroenterol Hepatol. 2019;13:3–15.
17. Etienne-Mesmin L, Chassaing B, Desvaux M, De Paepe K, Gresse R, Sauvaitre T, et al. Experimental models to study intestinal microbes-mucus interactions in health and disease. FEMS Microbiol Rev. 2019;43:457–89.
18. Gustafsson JK, Ermund A, Ambort D, Johansson ME, Nilsson HE, Thorell K, et al. Bicarbonate and functional CFTR channel are required for proper mucin secretion and link cystic fibrosis with its mucus phenotype. J Exp Med. 2012;209:1263–72.
19. Yissachar N, Zhou Y, Ung L, Lai NY, Mohan JF, Ehrlicher A, et al. An Intestinal Organ Culture System Uncovers a Role for the Nervous System in Microbe-Immune Crosstalk. Cell. 2017;168:1135-1148 e12.
20. Mak IWY, Evaniew N, Ghert M. Lost in translation: animal models and clinical trials in cancer treatment. Am J Transl Res. 2014;6:114.
21. McGonigle P, Ruggeri B. Animal models of human disease: challenges in enabling translation. Biochem Pharmacol. 2014;87:162–71.
22. Thompson GR, Trexler PC. Gastrointestinal structure and function in germ-free or gnotobiotic animals. Gut. 1971;12:230–5.
23. Kararli TT. Comparison of the gastrointestinal anatomy, physiology, and biochemistry of humans and commonly used laboratory animals. Biopharm Drug Dispos. 1995;16:351–80.
24. Nguyen TLA, Vieira-Silva S, Liston A, Raes J. How informative is the mouse for human gut microbiota research? Dis Model Mech. 2015;8:1–16.
25. Turnbaugh PJ, Ley RE, Hamady M, Fraser-Liggett CM, Knight R, Gordon JI. The human microbiome project. Nature. 2007;449:804–10.
26. Faith JJ, Rey FE, O'Donnell D, Karlsson M, McNulty NP, Kallstrom G, et al. Creating and characterizing communities of human gut microbes in gnotobiotic mice. ISME J. 2010;4:1094–8.
27. Ferdowsian HR, Beck N. Ethical and Scientific Considerations Regarding Animal Testing and Research. PLoS One. 2011;6:e24059.
28. Russell Burch, R. L., WMS. The principles of humane experimental technique. 1959.
29. Rahman S, Ghiboub M, Donkers JM, van de Steeg E, van Tol EAF, Hakvoort TBM, et al. The Progress of Intestinal Epithelial Models from Cell Lines to Gut-On-Chip. Int J Mol Sci. 2021;22.
30. Fogh J, Fogh JM, Orfeo T. One hundred and twenty-seven cultured human tumor cell lines producing tumors in nude mice. J Natl Cancer Inst. 1977;59:221–6.
31. Chantret I, Barbat A, Dussaulx E, Brattain MG, Zweibaum A. Epithelial polarity, villin expression, and enterocytic differentiation of cultured human colon carcinoma cells: a survey of twenty cell lines. Cancer Res. 1988;48:1936–42.
32. Matsumoto H, Erickson RH, Gum JR, Yoshioka M, Gum E, Kim YS. Biosynthesis of alkaline

phosphatase during differentiation of the human colon cancer cell line Caco-2. Gastroenterology. 1990;98 5 Pt 1:1199–207.
33. Pinto M, Robine-Leon S, Appay MD, Kedinger M, Triadou N, Dussaulx E, et al. Enterocyte-like differentiation and polarization of the human colon carcinoma cell line Caco-2 in culture. BiolCell. 1983;47:323–30.
34. Wilson G, Hassan IF, Dix CJ, Williamson I, Shah R, Mackay M, et al. Transport and permeability properties of human Caco-2 cells: An in vitro model of the intestinal epithelial cell barrier. J Control Release. 1990;11:25–40.
35. Bouwmeester H, Poortman J, Peters RJ, Wijma E, Kramer E, Makama S, et al. Characterization of translocation of silver nanoparticles and effects on whole-genome gene expression using an in vitro intestinal epithelium coculture model. ACS Nano. 2011;5:4091–103.
36. Brand W, van der Wel PA, Rein MJ, Barron D, Williamson G, van Bladeren PJ, et al. Metabolism and transport of the citrus flavonoid hesperetin in Caco-2 cell monolayers. Drug Metab Dispos. 2008;36:1794–802.
37. Hidalgo IJ, Raub TJ, Borchardt RT. Characterization of the human colon carcinoma cell line (Caco-2) as a model system for intestinal epithelial permeability. Gastroenterology. 1989;96:736–49.
38. Hubatsch I, Ragnarsson EGE, Artursson P. Determination of drug permeability and prediction of drug absorption in Caco-2 monolayers. Nat Protoc. 2007;2:2111–9.
39. Yamashita S, Furubayashi T, Kataoka M, Sakane T, Sezaki H, Tokuda H. Optimized conditions for prediction of intestinal drug permeability using Caco-2 cells. Eur J Pharm Sci. 2000;10:195–204.
40. Sambuy Y, De Angelis I, Ranaldi G, Scarino ML, Stammati A, Zucco F. The Caco-2 cell line as a model of the intestinal barrier: influence of cell and culture-related factors on Caco-2 cell functional characteristics. Cell Biol Toxicol. 2005;21:1–26.
41. Donato RP, El-Merhibi A, Gundsambuu B, Mak KY, Formosa ER, Wang X, et al. Studying Permeability in a Commonly Used Epithelial Cell Line: T84 Intestinal Epithelial Cells. In: Turksen K, editor. Permeability Barrier: Methods and Protocols. Totowa, NJ: Humana Press; 2011. p. 115–37.
42. Elzinga JI, van der Lugt B, Belzer C, Steegenga WT. Characterization of increased mucus production of HT29-MTX-E12 cells grown under Semi-Wet interface with Mechanical Stimulation. PLoS One. 2021;16:e0261191.
43. Hilgendorf C, Spahn-Langguth H, Regårdh CG, Lipka E, Amidon GL, Langguth P. Caco-2 versus Caco-2/HT29-MTX Co-cultured Cell Lines: Permeabilities Via Diffusion, Inside- and Outside-Directed Carrier-Mediated Transport. J Pharm Sci. 2000;89:63–75.
44. Lesuffleur T, Barbat A, Dussaulx E, Zweibaum A. Growth adaptation to methotrexate of HT-29 human colon carcinoma cells is associated with their ability to differentiate into columnar absorptive and mucus-secreting cells. Cancer Res. 1990;50:6334–43.
45. Lefebvre DE, Venema K, Gombau L, Valerio LG, Raju J, Bondy GS, et al. Utility of models of the gastrointestinal tract for assessment of the digestion and absorption of engineered nanomaterials released from food matrices. Nanotoxicology. 2015;9:523–42.
46. Zweibaum A, Laburthe M, Grasset E, Louvard D. Use of Cultured Cell Lines in Studies of Intestinal Cell Differentiation and Function. In: Comprehensive Physiology. 2011. p. 223–55.
47. Delie F, Rubas W. A human colonic cell line sharing similarities with enterocytes as a model to examine oral absorption: advantages and limitations of the Caco-2 model. Crit Rev Ther Drug Carr Syst.

1997;14:221–86.
48. Press B, Di Grandi D. Permeability for intestinal absorption: Caco-2 assay and related issues. Curr Drug Metab. 2008;9:893–900.
49. Kim HJ, Ingber DE. Gut-on-a-Chip microenvironment induces human intestinal cells to undergo villus differentiation. Integr Biol. 2013;5:1130.
50. Shah P, Fritz J V., Glaab E, Desai MS, Greenhalgh K, Frachet A, et al. A microfluidics-based in vitro model of the gastrointestinal human-microbe interface. Nat Commun. 2016;7:1–15.
51. Jalili-Firoozinezhad S, Gazzaniga FS, Calamari EL, Camacho DM, Fadel CW, Bein A, et al. A complex human gut microbiome cultured in an anaerobic intestine-on-a-chip. Nat Biomed Eng 2019 37. 2019;3:520–31.
52. Kämpfer AAM, Urbán P, Gioria S, Kanase N, Stone V, Kinsner-Ovaskainen A. Development of an in vitro co-culture model to mimic the human intestine in healthy and diseased state. Toxicol Vitr. 2017;45:31–43.
53. Kim HJ, Li H, Collins JJ, Ingber DE. Contributions of microbiome and mechanical deformation to intestinal bacterial overgrowth and inflammation in a human gut-on-a-chip. Proc Natl Acad Sci U S A. 2016;113:E7–15.
54. Huch M, Knoblich JA, Lutolf MP, Martinez-Arias A. The hope and the hype of organoid research. Dev. 2017;144:938–41.
55. Janssen AWF, Duivenvoorde LPM, Rijkers D, Nijssen R, Peijnenburg AACM, van der Zande M, et al. Cytochrome P450 expression, induction and activity in human induced pluripotent stem cell-derived intestinal organoids and comparison with primary human intestinal epithelial cells and Caco-2 cells. Arch Toxicol. 2020;95:907–22.
56. Mccracken KW, Howell JC, Wells JM, Spence JR, Org; KM, Org; JH, et al. Generating human intestinal tissue from pluripotent stem cells in vitro. Nat Protoc. 2011;6:1920–8.
57. Sato T, Stange DE, Ferrante M, Vries RGJ, van Es JH, van den Brink S, et al. Long-term Expansion of Epithelial Organoids From Human Colon, Adenoma, Adenocarcinoma, and Barrett's Epithelium. Gastroenterology. 2011;141:1762–72.
58. Sato T, Vries RG, Snippert HJ, Van De Wetering M, Barker N, Stange DE, et al. Single Lgr5 stem cells build crypt-villus structures in vitro without a mesenchymal niche. Nat 2009 4597244. 2009;459:262–5.
59. Spence JR, Mayhew CN, Rankin SA, Kuhar MF, Vallance JE, Tolle K, et al. Directed differentiation of human pluripotent stem cells into intestinal tissue in vitro. Nature. 2010;470:105–9.
60. OECD. Guidance Document on Good In Vitro Method Practices (GIVIMP). 2018.
61. Natoli M, Leoni BD, D'Agnano I, Zucco F, Felsani A. Good Caco-2 cell culture practices. Toxicol In Vitro. 2012;26:1243–6.
62. Angel PW, Rajab N, Deng Y, Pacheco CM, Chen T, Le Cao KA, et al. A simple, scalable approach to building a cross-platform transcriptome atlas. PLoS Comput Biol. 2020;16:e1008219.
63. Irizarry RA, Hobbs B, Collin F, Beazer-Barclay YD, Antonellis KJ, Scherf U, et al. Exploration, normalization, and summaries of high density oligonucleotide array probe level data. Biostatistics. 2003;4:249–64.
64. Blighe K, Lun A. PCAtools: everything Principal Components Analysis. R package version 2.0.0. 2020. https://bioconductor.org/packages/release/bioc/html/PCAtools.html. Accessed 26 Jan 2022.
65. Thorndike RL. Who belongs in the family? Psychometrika. 1953;18:267–76.

66. Hoffman GE, Schadt EE. variancePartition: interpreting drivers of variation in complex gene expression studies. BMC Bioinformatics. 2016;17:483.
67. Draghici S, Khatri P, Martins RP, Ostermeier GC, Krawetz SA. Global functional profiling of gene expression. Genomics. 2003;81:98–104.
68. Kanehisa M, Furumichi M, Tanabe M, Sato Y, Morishima K. KEGG: new perspectives on genomes, pathways, diseases and drugs. Nucleic Acids Res. 2017;45 Database issue:D353.
69. Gene Ontology C. The Gene Ontology resource: enriching a GOld mine. Nucleic Acids Res. 2021;49:D325–34.
70. Ashburner M, Ball CA, Blake JA, Botstein D, Butler H, Cherry JM, et al. Gene ontology: tool for the unification of biology. The Gene Ontology Consortium. Nat Genet. 2000;25:25–9.
71. Wu T, Hu E, Xu S, Chen M, Guo P, Dai Z, et al. clusterProfiler 4.0: A universal enrichment tool for interpreting omics data. Innov. 2021;2:100141.
72. Balimane P V, Chong S. Cell culture-based models for intestinal permeability: a critique. Drug Discov Today. 2005;10:335–43.
73. Putaala H, Barrangou R, Leyer GJ, Ouwehand AC, Bech Hansen E, Romero DA, et al. Analysis of the human intestinal epithelial cell transcriptional response to Lactobacillus acidophilus, Lactobacillus salivarius, Bifidobacterium lactis and Escherichia coli. Benef Microbes. 2010;1:283–95.
74. Ishimoto Y, Nakai Y, Satsu H, Totsuka M, Shimizu M. Transient up-regulation of immunity- and apoptosis-related genes in Caco-2 cells cocultured with THP-1 cells evaluated by DNA microarray analysis. Biosci Biotechnol Biochem. 2010;74:437–9.
75. Turroni F, Bottacini F, Foroni E, Mulder I, Kim JH, Zomer A, et al. Genome analysis of Bifidobacterium bifidum PRL2010 reveals metabolic pathways for host-derived glycan foraging. Proc Natl Acad Sci U S A. 2010;107:19514–9.
76. Christensen J, El-Gebali S, Natoli M, Sengstag T, Delorenzi M, Bentz S, et al. Defining new criteria for selection of cell-based intestinal models using publicly available databases. BMC Genomics. 2012;13:274.
77. Rossi O, Karczewski J, Stolte EH, Brummer RJM, Van Nieuwenhoven MA, Meijerink M, et al. Vectorial secretion of interleukin-8 mediates autocrine signalling in intestinal epithelial cells via apically located CXCR1. BMC Res Notes. 2013;6:1–10.
78. Sakharov D, Maltseva D, Knyazev E, Nikulin S, Poloznikov A, Shilin S, et al. Towards embedding Caco-2 model of gut interface in a microfluidic device to enable multi-organ models for systems biology. BMC Syst Biol. 2019;13 Suppl 1:19.
79. Lépine AFP, de Wit N, Oosterink E, Wichers H, Mes J, de Vos P. Lactobacillus acidophilus Attenuates Salmonella-Induced Stress of Epithelial Cells by Modulating Tight-Junction Genes and Cytokine Responses. Front Microbiol. 2018;9.
80. Kulthong K, Hooiveld G, Duivenvoorde L, Miro Estruch I, Marin V, van der Zande M, et al. Transcriptome comparisons of in vitro intestinal epithelia grown under static and microfluidic gut-on-chip conditions with in vivo human epithelia. Sci Rep. 2021;11:3234.
81. Kulthong K, Hooiveld G, Duivenvoorde LPM, Miro Estruch I, Bouwmeester H, van der Zande M. Comparative study of the transcriptomes of Caco-2 cells cultured under dynamic vs. static conditions following exposure to titanium dioxide and zinc oxide nanomaterials. Nanotoxicology. 2021;15:1233–52.
82. Akoglu H. User's guide to correlation coefficients. Turk J Emerg Med. 2018;18:91–3.

83. Larregieu CA, Benet LZ. Drug Discovery and Regulatory Considerations for Improving In Silico and In Vitro Predictions that Use Caco-2 as a Surrogate for Human Intestinal Permeability Measurements. AAPS J. 2013;15:483–97.
84. Zucco F, Batto AF, Bises G, Chambaz J, Chiusolo A, Consalvo R, et al. An inter-laboratory study to evaluate the effects of medium composition on the differentiation and barrier function of Caco-2 cell lines. Altern Lab Anim. 2005;33:603–18.
85. Briske-Anderson MJ, Finley JW, Newman SM. The Influence of Culture Time and Passage Number on the Morphological and Physiological Development of Caco-2 Cells. Proc Soc Exp Biol Med. 1997;214:248–57.
86. Navabi N, McGuckin MA, Lindén SK. Gastrointestinal cell lines form polarized epithelia with an adherent mucus layer when cultured in semi-wet interfaces with mechanical stimulation. PLoS One. 2013;8:e68761.
87. Ulluwishewa D, Anderson RC, Young W, Mcnabb WC, van Baarlen P, Moughan PJ, et al. Live Faecalibacterium prausnitzii in an apical anaerobic model of the intestinal epithelial barrier. Cell Microbiol. 2015;17:226–40.
88. Vachon PH, Beaulieu JF. Transient mosaic patterns of morphological and functional differentiation in the Caco-2 cell line. Gastroenterology. 1992;103:414–23.
89. Kim SH, Chi M, Yi B, Kim SH, Oh S, Kim Y, et al. Three-dimensional intestinal villi epithelium enhances protection of human intestinal cells from bacterial infection by inducing mucin expression. Integr Biol. 2014;6:1122–31.
90. Natoli M, Leoni BD, D'Agnano I, D'Onofrio M, Brandi R, Arisi I, et al. Cell growing density affects the structural and functional properties of Caco-2 differentiated monolayer. J Cell Physiol. 2011;226:1531–43.
91. ATCC. Caco-2 [Caco2] | ATCC. 2021. https://www.atcc.org/products/htb-37. Accessed 22 May 2022.
92. Perdigon G, Alvarez S, Rachid M, Aguero G, Gobbato N. Immune system stimulation by probiotics. J Dairy Sci. 1995;78:1597–606.
93. Isolauri E. Probiotics in human disease. Am J Clin Nutr. 2001;73:1142S-1146S.
94. Brazma A, Hingamp P, Quackenbush J, Sherlock G, Spellman P, Stoeckert C, et al. Minimum information about a microarray experiment (MIAME)-toward standards for microarray data. Nat Genet. 2001;29:365–71.
95. Brazma A, Ball C, Bumgarner R, Furlanello C, Miller M, Quackenbush J, et al. MINSEQE: Minimum Information about a high-throughput Nucleotide SeQuencing Experiment - a proposal for standards in functional genomic data reporting. 2012. https://doi.org/10.5281/ZENODO.5706412.
96. Greenhalgh K, Ramiro-Garcia J, Heinken A, Ullmann P, Bintener T, Pacheco MP, et al. Integrated In Vitro and In Silico Modeling Delineates the Molecular Effects of a Synbiotic Regimen on Colorectal-Cancer-Derived Cells. Cell Rep. 2019;27:1621-1632.e9.
97. Forero DA, Curioso WH, Patrinos GP. The importance of adherence to international standards for depositing open data in public repositories. BMC Res Notes. 2021;14:405.
98. Ioannidis JPA, Allison DB, Ball CA, Coulibaly I, Cui X, Culhane AC, et al. Repeatability of published microarray gene expression analyses. Nat Genet. 2009;41:149–55.
99. Hartung T, de Vries R, Hoffmann S, Hogberg HT, Smirnova L, Tsaioun K, et al. Toward Good In Vitro Reporting Standards. ALTEX - Altern to Anim Exp. 2019;36:3–17.

100. Wilkinson MD, Dumontier M, Aalbersberg IjJ, Appleton G, Axton M, Baak A, et al. The FAIR Guiding Principles for scientific data management and stewardship. Sci Data. 2016;3:160018.
101. de Vries R, Whaley P. In Vitro Critical Appraisal Tool (IV-CAT): Tool Development Protocol. 2018. https://doi.org/10.5281/ZENODO.1493498.
102. Emmerich CH, Harris CM. Minimum Information and Quality Standards for Conducting, Reporting, and Organizing In Vitro Research. In: Handbook of Experimental Pharmacology. Springer; 2020. p. 177–96.
103. hDMT. Translational Organ-on-Chip Platform - TOP: Translational Organ-on-Chip Platform. 2021. https://top.hdmt.technology/. Accessed 26 Apr 2022.
104. Vollertsen AR, Vivas A, van Meer B, van den Berg A, Odijk M, van der Meer AD. Facilitating implementation of organs-on-chips by open platform technology. Biomicrofluidics. 2021;15:51301.

Supplementary files

This excel file can be found as part of the Online Resources of the publication at: 10.1007/s00204-022-03430-y direct link to the file: https://static-content.springer.com/esm/art%3A10.1007%2Fs00204-022-03430-y/MediaObjects/204_2022_3430_MOESM1_ESM.xlsx

Supplementary file 1. Summary of data regarding study collection and data extraction, including a) Retrieved 330 GEO Series (n = 330) in the GEO Database, including excluding criteria b) number of genes analyzed per array platform, including excluded platforms c) data extraction from all studies using Affymetrix platforms, including model specifications and experimental set-up d) sample overview of all samples (n = 100) analyzed on Affymetrix platforms

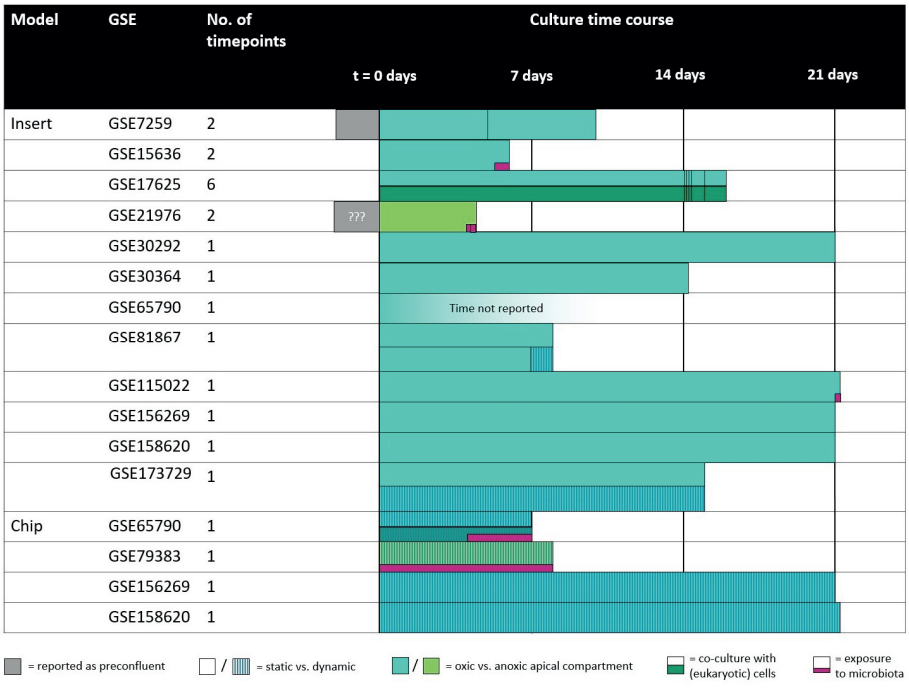

Supplementary file 2. Overview of experimental set-up per model analyzed on Affymetrix platforms.

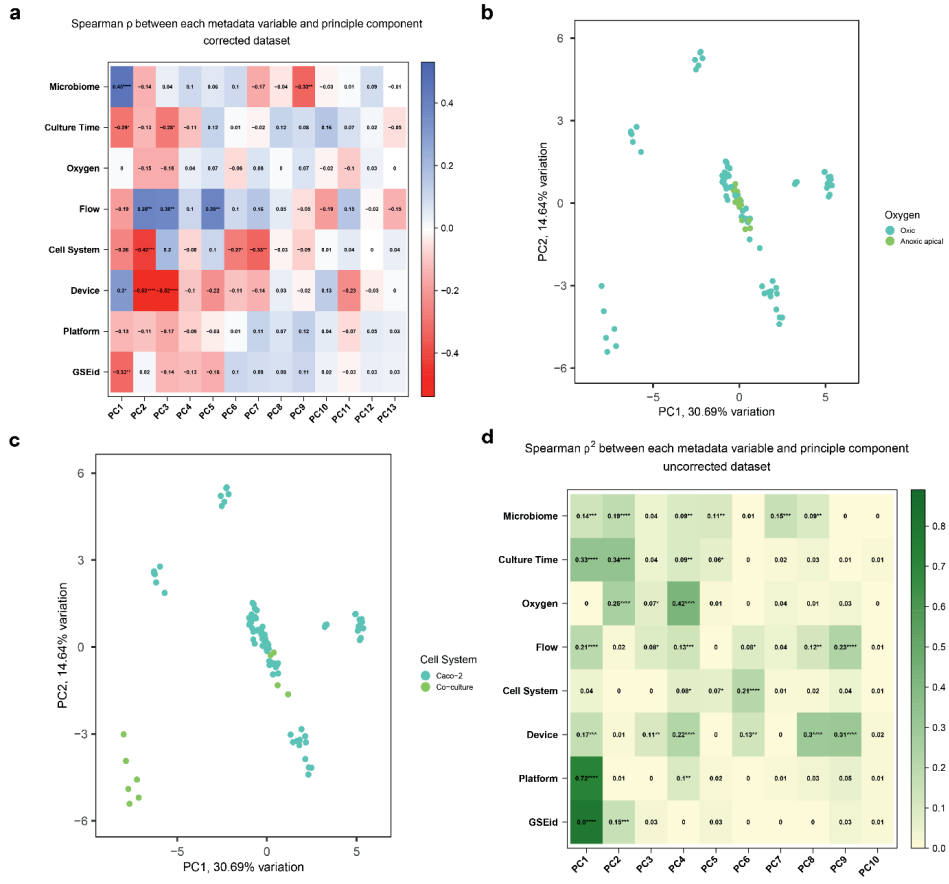

Supplementary file 3. Multilevel principal component analysis at model level. After correction for platform, a principal component analysis was performed on a total of 11,203 shared genes, distinguishing eight experimental variables. a) Spearman correlation PC per model variable for the first 13 PCs. PCA plots of the first two components are provided and labelled by b) oxygen c) cells system. d) Spearman correlation ρ^2 per model variable for the first 13 PCs without correction for platform. * p <0.05; ** p <0.01; *** p <0.001; **** p <0.0001.

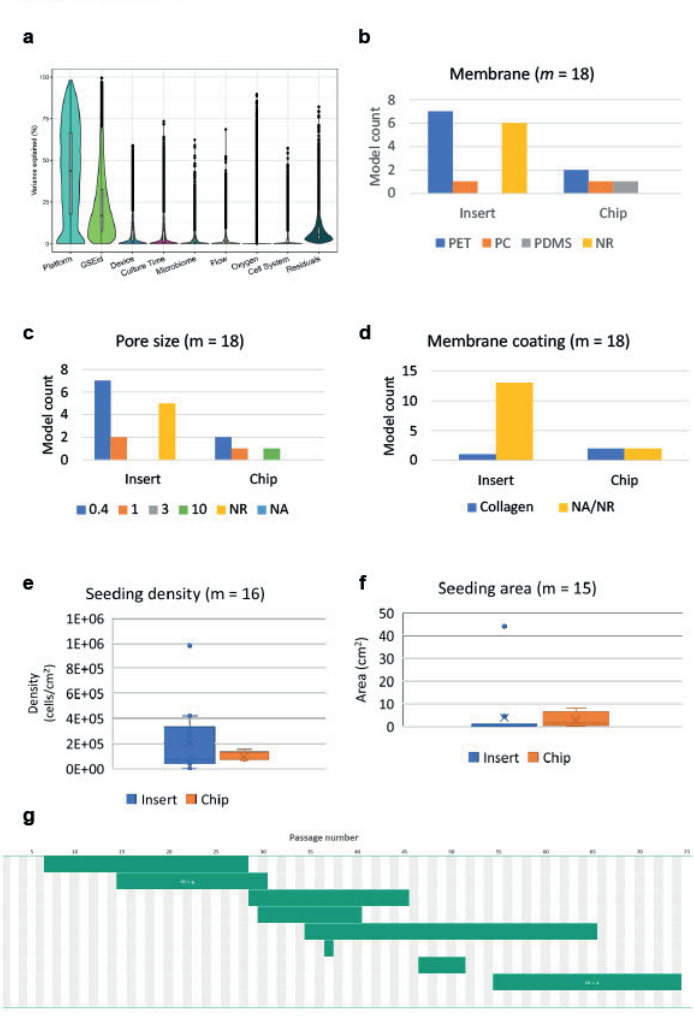

Supplementary file 4. Variance partition analysis of all genes shared between samples (s = 100, g = 11,203). **a)** Violin plot shown the percentage contribution of each variable to the expression of all genes without correction for platform. Additional data was extracted per model, including **b)** membrane on which the cells were seeded, **c)** pore size of the membrane, **d)** membrane coating, **e)** seeding density, **f)** seeding area and **g)** passage number used.

Chapter 6

General Discussion

6.1 Research in this thesis

An overview of the current state of human intestinal *in vitro* models was provided in **Chapter 1**. These *in vitro* models are constantly improved by the incorporation of new scientific insights and the use of novel methodologies. In addition, also in **Chapter 1**, the compounds tested and measured to evaluate responses throughout the research described in this thesis were introduced to give insight in their origin and role in the human intestine. In the following part a short overview is given of the results obtained. The aim of the research in this thesis was to explore the use, advantages and disadvantages of available intestinal models to study interactions of intestinal cells with TLR agonists and metabolites from the intestinal microbiota and to fill in some of the gaps in available knowledge needed for future studies in this direction.

In **Chapter 2** cell lines were assessed for their ability to respond to five toll-like receptor (TLR) agonists encompassing a wide range of TLRs and TLR agonists that originate from representative intestinal bacterial and viral species. A comparison is made between four different cell models, each with varying complexity, that aim to *in vitro* mimic the *in vivo* intestinal epithelium. The first and most basic model consisted of a cell layer of differentiated Caco-2 cells grown on the apical side of a membrane in a Transwell format. Caco-2 cells emulate enterocytes, and this basic model is most commonly used for *in vitro* studies on the transport of compounds in the small intestine [1, 2]. The second model combined Caco-2 cells with mucus secreting HT29-MTX cells grown in a 3:1 ratio as cell layers, and as such this model emulated both enterocytes and goblet cells. For future studies this model is promising due to the inclusion of mucus produced normally by the goblet cells. The mucus layer is both a barrier for compounds and intestinal microbiota before reaching the cellular intestinal epithelium, while mucus also is a food source for part of the intestinal microbiota. The third model combined the previous two cell lines grown on the apical side of a membrane in a Transwell format with HMVEC-d cells grown on the basolateral side of the membrane, thus also including a cell model for the blood vessel endothelial cells that need to be passed by compounds absorbed by the intestine. This increased model complexity helps to account for the potential role of all these cells in the response to bacterial TLR agonists, either after transport of these TLR agonists to the TLRs that are present on the basolateral side of the *in vitro* model on the intestinal or endothelial cells, or for instance by propagation of immune signals from the epithelial cells from the apical to the basolateral side of the Transwell. The last model used in **Chapter 2** consisted of HT29-p cells, the parental line of HT29-MTX, that can differentiate into enterocytes or potentially other cell types depending on the used culturing method. In the study the HT29-p cell line remained mostly undifferentiated but did show epithelial morphology such as microvilli.

Following exposure of all the above mentioned cell models to the TLR agonists the IL-8 release was analyzed in both the apical and basolateral compartment. Il-8 excretion was selected as the readout because this cytokine is widely used as a marker for pro-inflammatory signaling. The levels of excreted IL-8 were higher on the basolateral side in all models except for the HT29-p cell model. This corresponds to the biological function of IL-8 *in vivo*, as it serves as a chemoattractant for neutrophils from the lamina propria and blood or lymphatic vessels. Of the five agonists, only flagellin, which binds to TLR5, induced a response in all four models. The HT29-p model was the only cell model that additionally responded to Poly(I:C) that binds to TLR3. This has important implications when using cell lines to test interactions with microbiota. Likely only flagellated bacteria can properly induce an immune response *in vitro* using the

tested cell models upon exposure. Inversely, bacteria that do not produce flagellin might be labeled as not causing inflammation in the human intestine when tested using these models though that might not be representative of the *in vivo* situation. Thus, the results obtained show the importance of knowing the limitations of the used *in vitro* models. Though HT29-p showed slightly broader immunomodulatory capacity this was only observed for the viral agonist, which could be important when using these cell systems in a disease model but may be of less influence when studying interactions with the microbiota.

In **Chapter 3** advanced intestinal cell models were exposed to the same TLR agonists as used in **Chapter 2**, to see if these models display a more pronounced immunomodulatory capacity. Both induced pluripotent stem cell (iPSC) derived organoids and cells from the primary human small intestinal epithelial (PHSIE) cell model are known to display a wide variety of cell types in a single intestinal epithelial model. Both cell models are reported to contain enterocytes, Paneth cells and stem cells. The PHSIE model has also been described to contain M cells and tuft cells, while the iPSC derived organoids were described to contain enteroendocrine and mesenchymal cells. Both models are derived from healthy donors and lack the mutations and other cellular modification that have been associated with cell lines because of their cancerous cell origin.

In these experiments the TLR expression and secretion of multiple cytokines was measured. The (basal) TLR expression showed a large difference between both models, with the iPSC derived organoids having a higher gene expression for six out of the eight analyzed TLRs. Under non-stimulated conditions the iPSC derived organoids secreted measurable levels of four different cytokines (CCL20, CXCL10, IL-6 and IL-8) while the PHSIE cell model under non-stimulated conditions, only secreted IL-8. Flagellin exposure induced a response in both models, the exposure resulted in a secretion of CXCL10 by both models, while additionally increased levels of IL-8 were secreted by the iPSC derived organoids. The induction of pro-inflammatory IL-8 responses by flagellin in the iPSC derived organoids matched with what was observed for the cell models in **Chapter 2**, while the lack of IL-8 induction upon flagellin exposure in the PHSIE deviates from what is observed in the other models. The iPSC derived organoids actually showed an inverse response to Poly(I:C) with a decrease in IL-8 secretion compared with the control. The iPSC derived organoids did show a response to ssRNA while the PHSIE cell model showed a response to LPS via IL-6 and IL-8 secretion. The TLR expression in iPSC derived organoids was modified upon exposures to most of the agonists, only ssRNA exposure did not significantly affect the TLR gene expression. In the PHSIE model TLR gene expression was only changed for TLR9 after Pam3CSK4 exposure.

Compared to results presented in **Chapter 2** the expanded cytokine readouts applied in **Chapter 3** allowed for a better overview of effects, resulting in detection of induced expression of two additional cytokines; CXCL10 and IL-6. Looking at the immunomodulatory capacity of both models the iPSC derived organoids show a wider variety of responses to the range of TLR agonists. Though when looking at the goal of combining the cell models with microbiota the cytokine response to LPS of the PHSIE cell model does offer a potential advantage as that constitutes an extra response to a bacterial TLR agonist.

In **Chapter 4** the focus switched from the interaction of microbiota derived TLR agonists with the intestinal epithelium to the interaction with and via short chain fatty acids (SCFAs), which are important signaling molecules produced by intestinal microbiota. SCFAs have been attributed with many different (intestinal) effects; SCFAs are being used as an energy source by intestinal cells and are even claimed to play a role in

neuronal diseases [3–5]. Butyrate, propionate and acetate account for the majority of SCFAs in the human intestine and were used in **Chapter 4**. In cell lines (i.e. Caco-2 cells) butyrate has been shown to be cytotoxic due to the inability of the cells to metabolize butyrate leading to intracellular butyrate accumulation. Advanced cell models, like iPSC derived cell layers, do not suffer from this drawback and can be applied as a model to study the interaction between SCFAs and the human intestinal epithelium as done in the experiments performed in **Chapter 4**. To get a complete overview of the effects on gene expression of the exposure to the three SCFAs a transcriptome analysis was performed using RNA-sequencing. Each SCFA induced its own unique gene expression profile, showing that they each have a different effect on the intestinal epithelium. Butyrate exposure resulted in the most pronounced effect matching with previous findings in adult stem cell derived organoids, followed by propionate showing less effects and acetate showing comparatively little effects. Importantly, multiple known effects of the SCFAs were confirmed in the iPSC derived cell model when checking the changes in pathways using Gene Set Enrichment Analysis. The effects encompassed the immune system, metabolic pathways, DNA replication and multiple other processes showing the power of RNA-sequencing as a readout. The absence of apoptosis related pathways showed that using iPSC derived cell layers solves some of the problems observed when using cell lines to study effects of SCFAs. Thus, the iPSC model provides a better *in vitro* model to further elucidate the interaction between SCFAs and the human intestine.

In **Chapter 5**, the potential consequences of different cell culturing methods used for growing intestinal epithelial cells was explored. This was done because recent technological advances on microfluidic systems as advanced cell culturing devices have come with a lot of promise on the effects that these culturing devices have on the cells grown in them. **Chapter 5** aimed to elucidate how the culturing conditions in such devices influence the cell biological effects. In this chapter the effect of different culturing conditions on the basal gene expression in the transcriptome was studied. To this end, existing data sets were collected from the literature encompassing data sets from cells cultured in both traditional Transwell and advanced cell culturing devices. Data sets were extracted from publications and eight variables were defined for analysis, "Culture Time", “GSEid”, “Microbiome”, “Oxygen”, “Flow”, “Cell system”, “Device” and “Platform”. The variables that have been reported previously to affect genes associated with cell differentiation, i.e. flow and device, appeared not to substantially affect the gene expression based on the analysis. Overall, most of the variables did not show strong effects on the transcriptome, with only “Microbiome” showing effects that matched with expected effects related to influencing immune related pathways.

The extraction of information from the selected studies showed the importance of proper reporting and design of studies. Some factors that are known to have a large effect on cell lines such as passage number could not be properly analyzed because they were often not reported. Absence of such details does not necessarily impair the study on its own but weakens its value for the scientific field as it becomes more difficult to compare the outcome of a study with other studies. As for this analysis gene expression in control (i.e. non-exposed cells) was studied the observed effects appeared not very strong albeit highly sensitive to minor changes in culturing conditions. In toxicological experiments, where cells are exposed to compounds, much stronger effects on the transcriptome are to be expected, likely overwhelming the minor influences of changes in culture conditions.

6.2 General discussion and future perspectives

There is a need for robust *in vitro* models with good predictivity towards expected *in vivo* responses for both safety and efficacy testing of chemicals and drugs. Only in this way will these models become the new golden standard in the field of chemical risk assessment and drug development. The use of animal models is under increasing pressure due to a scientific need for models that better predict human toxicological safety, and societal opposition. This development is in line with the so-called 3R principles, replacement, reduction and refinement of animal experiments, aiming to step by step improve welfare conditions of animals still used in toxicological risk assessment and work towards complete replacement of data derived from animal studies by data derived from *in vitro* and *in silico* models. Below several aspects needed to make this transition, with a focus on intestinal cell models, will be discussed and a future outlook will be provided.

First of all, it will be discussed how the ability to use human cells or tissues allows for models that better reflect human biology, reducing the uncertainty that comes from the difference between experimental animals and humans. Secondly, it will be discussed how advances in culturing devices can better recapitulate the human physiology and thus support the transition towards *in vitro* models, and how these devices are combined with advanced cell models. Lastly, the applicability of these novel *in vitro* models in toxicological sciences, especially regulatory toxicology in a societal context will be discussed.

6.3 Improving the human relevance of intestinal models

Existing intestinal epithelial models based on Caco-2 and other cell-lines are constantly improved by modifying culturing methods, such as exploring different cell culture medium compositions [6–8]. This can be illustrated by the example related to the use of fetal calf serum (FCS). FCS is a commonly used medium component and it contains a lot of components needed for cell growth. However, it comes with a number of drawbacks. First of all, it is sourced from animals, with batch to batch variability in the composition which adds to differences between experiments using different batches of FCS. At the same time there are ethical concerns since these calves are specifically raised for extraction of FCS, which goes against the goal of animal-free testing with *in vitro* experiments [9–11]. Therefore, more studies are needed to explore novel and animal-free FCS alternatives better. In experiments with intestinal cell models where a synthetic medium was used instead of animal derived FCS more variation in barrier integrity and differentiation was reported between laboratories compared to using a traditional medium containing FCS [8]. In contrast, other articles where traditional FCS containing medium was compared with synthetic MITO+^{TM} FCS free medium reported improved transport activity of Caco-2 cells grown in the synthetic medium[12]. More studies are thus needed to define a proper and reliable replacement for FCS in cell culture medium for intestinal cell models.

Adequate and harmonized parameters to define the differentiation status of the intestinal cells used in experiments is a next critical factor to improve the quality of the outcome of *in vitro* studies. There is a general consensus that there is a direct relationship between culture time and differentiation of cells. Depending on what endpoint is being measured in an experiment, the exact point at which Caco-2 cells reach optimal activity differs but the general consensus is that a culturing time of 21 days is sufficient for full differentiation [1, 13–15]. As such this is the most widely used time point when culturing and using

Caco-2 cells. This has translated to other intestinal cells being grown for the same period of time since the initial comparison is often to Caco-2 cells. There have been reports of protocols using short term culturing that result in Caco-2 cells that perform similarly to Caco-2 cells upon 21 day in cultures in terms of TEER and transporter activity [16]. But such protocols are not widely embraced due to uncertainty on the complete cell differentiation status, while the 21 days protocol has been tried and tested elaborately. Besides culture time the way Caco-2 cells are maintained prior to seeding has also been shown to affect their functioning after 21 days. When cells are passaged at either high or low density during maintenance they proliferate differently and respond to exposure of toxic compounds differently [14]. Thus, there is a need for a number of well-defined end-points to validate the differentiation state of Caco-2 cells, since use of only TEER measurements as often done may turn out to be too limited. Variations in culture protocols used by different scientific groups reduce the ease of translation of results between laboratories, sticking to a single standardized protocol provides the best option to achieve that the differentiation state will be similar in experiments using Caco-2 cells. Thus, reaching consensus on a standardized protocol is important, and would help increase the value of the Caco-2 cell model.

There are also other cell lines than the Caco-2 cell line that can be used as intestinal models such as T84 cells that have been shown to better mimic colonocytes [7] or HT29-MTX cells that mimic goblet cells [17]. Having a wider array of cells available allows for the selection of the “optimal” cell type for the specific research question. However, the main application for HT29-MTX cells has been their use in a co-culture model with Caco-2 cells. The combination of Caco-2 and HT29-MTX cells results in a model that contains the two most abundant cell types present within the human intestine, enterocytes and goblet cells. *In vivo* goblet cells introduce a mucus layer that can act as a barrier for diffusion of compounds [18, 19]. Interestingly, a study using the Caco-2/HT29-MTX co-cultures indicated increased permeability for a large number of model compounds that undergo passive absorption across these cell-layers, with paracellularly translocated compounds showing the comparatively highest crossing of the co-culture cell layers compared to Caco-2 monoculture models. For carrier-mediated compounds this was inverted with HT29-MTX co-cultures showing lower translocation [6]. Older research similarly showed that passively (transcellularly) transported compounds transported faster in co-cultures [20]. This indicates that the mucus does not seem to function as a barrier for these compounds, and that the lower number of transporters due to the lower number of Caco-2 cells does have an influence. Similarly, to the results in **Chapter 2**, these co-cultures appear to have lower TEER values, indicating lower integrity of the tight-junctions. This could explain the observed difference in translocation and showing that the tight junctions may be more important for limiting transport across the cell layer than the mucus layer.

For other applications this co-culture model also offers advantages, for example for co-culturing with bacteria. The mucus is an important food source, and place to grow in, while it also has a role as a barrier against microbial agents and it is involved in the clearance of microbial TLR agonists, thereby protecting the intestinal cells [21, 22]. However, proper production of this mucus layer *in vitro* might require alternative protocols such as Semi-Wet interface culturing on a shaking plate to increase mucus production to acceptable levels [23]. Organs-on-a-chip culturing devices that impose shear forces on the cells by their dynamic cell culture flows may also offer such a stimulation of mucus production [24–26].

Besides co-culture models with other intestinal epithelial cell types there are also opportunities to include cells with a different biological origin and function. The first type of cells that are often used for such co-cultures are endothelial cells, the cells that line the blood or lymphatic vessels. These could act as another barrier for transport of bacteria or compounds, but more importantly are responsible for the propagation of (immune) signals from the epithelial cells and as such are involved in generating local intestinal tissue immune responses [27, 28]. There are multiple sources of endothelial cells that have been applied in combination with intestinal epithelial cells, for instance HUVEC (human umbilical vein epithelial cells), HMVEC-d (human dermal microvascular endothelial cells) and HIMEC (human intestinal microvascular endothelial cells). While the first two cell types have been used more extensively in research, less is known about the latter. The intestinal origin of the HIMEC could be an important reason to include it in future intestinal models [24, 28]. The results in **Chapter 2** did not show much additional value of the addition of HMVEC-d for the immunomodulatory capacity of the models, however exposure to the TLR agonists tested might have been too limited due to the limited concentration that reaches the basolateral side to capture all potential interactions.

The second type of cells that are often added to the co cultures are immune cells such as peripheral blood mononuclear cells (PBMCs) [27–30]. This addition can allow for the modelling of the recruitment of immune cells following exposure to a challenge and thus of a cellular immune response of the intestinal tissue. A model combining intestinal epithelial cells derived from human intestinal organoids with macrophages isolated from the PBMCs showed a clear interaction between the two with the macrophages stimulating the immune response of the epithelial cells [29]. Similar to the endothelial cells the immune cells also play an important role in modelling the interaction with the microbiota. A complete system therefore likely requires inclusion of cell types from different functional backgrounds; epithelial, endothelial and immune cells, and maybe even more.

6.4 Moving from cell lines to stem cells

Another development is to replace cell lines in the intestinal *in vitro* models with cells derived from stem cells. The first steps were taken by propagating adult stem cells isolated from human intestinal tissues into 3D intestinal organoids by applying certain growth factors during differentiation [31, 32]. These 3D structures contain many of the cell types found in the *in vivo* human intestine and form a polarized structure where the apical side (i.e. lumen side) is on the inside of the organoid. A comparable organoid was created using iPSCs that form a structure that also contains multiple cell types as found in the human intestine [33–36]. These miniature intestines also show the typical crypt and villi structures as found in the human intestine. Still, one of the major drawbacks is that the apical side is on the interior of the organoids which makes exposure via the luminal side difficult. In addition, organoids are grown in an extracellular matrix that can form a barrier for compounds to reach the organoids. One solution that has been applied are microinjections into the lumen of the 3D organoids, mostly of bacteria [37–39]. While this does allow for exposure on the correct side of the cells it does not allow for large scale experiments and suffers from similar problems as bacterial exposure in Transwells where bacterial overgrowth occurs over time. Another solution that has been applied is inversion of the organoids to create the apical surface on the outside [40, 41]. This solution means that all organoids can be exposed on the lumen side by adding the compound to the medium. However, the extracellular matrix remains as a barrier and transported

compounds can accumulate inside the organoid. Furthermore, determining the amount of transported compound then becomes challenging, as the compound would need to be extracted from the inside of the organoids. The last solution is to grow these stem cell derived models as a monolayer in a Transwell similar to how Caco-2 cells are grown [40, 42, 43]. In this case they are not called organoids anymore since they lack the 3D structure and are often referred to as intestinal epithelial cell layers. This method allows for both an easier exposure and end-point measurement. It also only needs a thin layer of extracellular matrix below the cells instead of being completely embedded in the extracellular matrix like the organoids. Under normal culture conditions the typical intestinal crypt and villi structures seem to be reduced or absent but what is retained is the advantage of multiple cell types as observed *in vivo*. If grown under dynamic flow conditions some of crypt/villi structure can be retained [24, 27]. Overall, these stem cell derived models offer complex models that encompass most cell types found in the human intestine and the fast developments in culturing method design are slowly overcoming some of the drawbacks. In the end, at the current state of the art the Caco-2 cell line is still applied in all kinds of experiments due to its advantages such as ease of use and low costs, especially in toxicology where the repeatability and a large body of existing knowledge on these cells is valued.

6.5 Advancements in culturing devices

Besides improving the biology by using different cells and cell models another avenue to improve intestinal models is provided by better mimicking the physical and biochemical environment of the human intestine. Due to the peristalsis in the human intestine there is constant movement inside the lumen and of the intestinal tissue itself, creating forces that act on the intestinal cells such as shear stress and mechanical stress. Creating these stressors in *in vitro* models has been attempted by using novel technology to improve the devices used to culture the cells in resulting in microfluidic devices.

The first microfluid devices used were composed of polydimethylsiloxane (PDMS) polymers. They consisted of two compartments separated by a membrane also made from PDMS or sometimes made from the same polymer as used in Transwell membranes [26]. Cells grown in such a device, also called a gut-on-a-chip, showed improvements of the morphology of Caco-2 cells, higher expression of the important biomodification enzyme Cyp3A4 and the presence of cells with markers indicative of goblet, Paneth and enteroendocrine cells besides the abundant presence of enterocytes [26]. The proper functioning of these other cell types has to be validated to further support these findings. Other designs of microfluidic devices included more compartments. An example is a device that was made from polycarbonate and used nanoporous membranes to separate the epithelial cells from a chamber containing microbes and a bottom chamber for the perfusion of oxygenated cell culture medium [44]. This model was used to study the interaction between the microbes and the epithelial cells showing many effects on gene expression. It also enabled creation of an environment low in oxygen for the microbial compartment. The separation of the microbes from the epithelial cells does block some of the direct interactions and limits the exposure to transported signaling molecules and TLR agonists. Since then the PDMS based microfluidic device designs have been expanded by including microbiota compartments [27] and an anaerobic compartment with oxygen sensors [25]. Comparable models have already been applied for the measurement of transport of compounds [45], and experiments have been performed to evaluate the influence of different flow rates on the development and differentiation of the intestinal cells grown

in such devices [46]. These microfluidic models do offer a technical challenge for end-users and close collaborations between microfluidic engineers and biologists or toxicologists is needed.

As an alternative to the microfluidic flow devices other approaches have been introduced. One example is the so called OrganoPlate which is a plate where an extracellular matrix forms the barrier between two channels [47]. Cells can be cultured in one channel where they will form a tube-like structure by growing onto the extracellular matrix, flow is created by putting the plate on a rocking platform that moves the medium back and forth through the channel. This technological solution requires less expensive and complex instruments and offers more scalability but it has the disadvantage of the (large) barrier of extracellular matrix that separates the channels which could potentially interfere with for instance transport studies. As these plates are not connected to an external pump, there is no renewal of medium, which might be another disadvantage. Especially if co-culture with microbiota is needed, as a risk of microbial overgrowth is eminent. The OrganoPlate model has already been used to create several intestinal disease models for drug discovery and to model inflammatory processes by including macrophages [29, 48]. Overall, these microfluidic technological advances overcome some of the shortcomings of static systems such as Transwells and offer opportunities for future research.

6.6 Microbiome incorporations into immunocompetent intestinal (epithelial) *in vitro* models

As mentioned before, the microbiome is an integral part of the human intestine. Some researchers go as far as calling it a specific organ [49]. Though the notion that it is an independent organ has been refuted the microbiome is an integral part of the human intestine and should be taken into account when designing an *in vitro* intestinal model that closely mimics the *in vivo* intestine. Multiple studies have started integrating the microbiota into intestinal systems and are reporting on the interaction between the microbiota and the intestinal cells [27, 50]. An important part of this interaction is dependent on the innate immune system of the human intestinal epithelium. Existing knowledge on the presence of TLRs as the main sensing receptors, and responses to agonists via these TLRs is inconsistent and incomplete [51, 52]. This holds true for both cell line and stem cell based models. However, it is important to first define an aim for these models, which is to properly mimic the *in vivo* situation. To set a benchmark there are two factors to assess, the presence of the TLRs and the presence of a response to selected TLR agonists. Studies on human intestinal biopsies suggest the presence of all nine TLRs [53–57], meaning that an *in vitro* intestinal model should preferably also express all nine. The presence of a response to TLR agonist exposure is more difficult to define as there is at present no way to obtain human *in vivo* data to set a benchmark.

The large number of bacteria in the human intestine means that there is a constant presence of TLR agonists although in healthy individuals this does not result in an active(ated) immune system [58, 59]. As such an active immune response might not be considered an important part of an intestinal model to be developed. However, this lack of response is dependent on a balanced microbiome with a proper epithelial barrier including mucus and immune related cells producing antimicrobial products. As such it is important to explore if cell models are able to create an immune response upon a direct exposure and which cell types normally present in the intestinal tissue are involved in these responses. As a first step to test the interaction between the microbiota and the intestinal cells, microbiota derived TLR agonists offer

a good starting point, since they are known to be involved in the innate immune response [60, 61]. The agonists used in this thesis originate from infectious bacteria or mimic those, replicating an exposure that should induce a response *in vivo*. The responses to exposure to the selected TLR agonists can be considered a first step in assessing the immunocompetence of an intestinal model. Follow up research should also consider other types of exposure than the TLR agonists studies in the present thesis, with the next logical step being heat or otherwise inactivated bacteria, to which the intestinal cells can be exposed in simple Transwell models for a long period of time. Inactivated bacteria offer the advantage of the presence of a large number of signaling molecules that both potentially activate and attenuate the immune response to give a better idea of the balance achieved upon exposure.

The next step would be to expose the intestinal cells to living bacteria, which comes with technical challenges. Using a simple Transwell system would limit exposure time due to overgrowth of the system by the bacteria [43]. As the interaction of bacteria and the intestinal tissue in the human body is long term, mimicking real life scenarios would require a proper mucus barrier to protect the intestinal cells from the bacteria, a flow to clear the excess of bacteria [27], and also an anaerobic compartment for the microbiome, which would allow for culturing of the obligate anaerobes as found in the human intestine.

To take the first step in developing such immunocompetent cell systems, well studied cell lines offer the best starting point. However, Caco-2 cells are known to show little to no response to LPS exposure which has been associated with a lack of TLR4 expression [62]. Similarly, the results in **Chapter 2** showed a lack of response to LPS in Caco-2 cells, while the other tested cell lines did not offer a response either, indicating the need for a different model if a response to LPS is important. T84, a model for colonocytes, has been reported to show higher expression of TLR4 but has far lower expression of TLR5 which is responsible for recognizing flagellin. As a model for interaction with the microbiota colonocytes could be more interesting as they mimic the colon where most of the microbiota is present, while the cell lines used in the present thesis mimic the small intestine that contains far fewer bacteria [63]. This indicates that there are clear differences between cell lines, and though the co-cultures that were used did not show additional value there might be other combinations that are worth further exploration.

In the cell line models one should also take into account the polarity of the response; are the cells mostly excreting the cytokines to the apical or basolateral side. And where are the TLRs located? Most of the excretion of IL-8 in **Chapter 2** appeared to occur at the basolateral side of the cells, likely related to the role of IL-8 as a chemoattractant helping to propagate the signal [64, 65]. Similarly, as mentioned, the location of the TLRs can be important. The TLRs are not spread out evenly over the cell and intestine, some are more abundant on the apical or basolateral sides or internally and their presence differs from one to another part of the intestine [51, 66]. The location of the TLRs is of interest given that in the studies performed in the present thesis the intestinal layer was considered to provide a barrier blocking the translocation of the agonists, so exposed TLR agonists remained at the apical side of the intestinal cells. ssRNA40 is an exception since this TLR agonist has to reach TLR8 which is located intracellularly. The intercellular delivery of ssRNA40 was achieved by adding a transfection reagent when exposing cells to ssRNA *in vitro*. So there are a number of aspects to consider here. First of all the HT29-p model produced low TEER values and did not form a proper cell layer. Secondly, as discussed before, the addition of HT29-MTX has been shown to increase paracellular transport of many compounds, which might also allow for

more transport of certain TLR agonists. Thirdly, in rat experiments active transport of FITC-labelled LPS across the intestinal enterocytes was suggested [67]. However, dermal endothelial cells were reported to be responsive to amongst others LPS so the lack of response in the co-culture with HMVEC-d seems to indicate a lack of exposure [68, 69]. These considerations do make it interesting to determine the polarity or TLRs in intestinal models, and in future microfluidic models to improve the polarity of the models [26].

In the advanced models, iPSC derived organoids and PHSIE, expression of all nine TLRs was observed though at varying levels. For adult stem cell derived organoids, expression has only been reported for TLR2, 4 and 5, while the others TLRs have not been measured [70]. When looking at the TLR expression most of the advanced models seem to better mimic the *in vivo* situation than the cell lines. Considering responses to agonist exposure the PHSIE showed a clear advantage due to their response to LPS, even though they showed a relatively low expression of TLR4, which could be important when considering co-culturing with bacteria. However, PHSIE are sold as a commercial model supplied pre-grown on Transwells so applying a similar model on gut-on-a-chip would require development of publicly available methods. On the other hand stem cell derived models have already been successfully grown on chips. Overall, it is important to take the strengths and limitations of each model into account when interpreting interactions with the microbiota and related TLR agonists.

In the studies presented in this thesis, the presence of an immune response after exposure to TLR agonists was set as a benchmark, a lack of response indicating absence of important interactions in the model. However, the findings in **Chapter 3** do indicate the presence of all nine TLRs, at least for the advanced models. At the same time it is known that all TLRs share common pathways after activation, mostly via the MyD88-dependent pathway [51, 61, 71]. The presence of a response to at least one compound in every model indicates the functioning of these shared pathways. Based on the results obtained it remains to be elucidated whether the in some cases limited responses result from inactive TLR proteins, since only their mRNA levels were measured, or that other regulating factors are limited thereby hampering the activation of the immune response. The complexity of the innate immune system, especially in the intestine where there is a large constant presence of bacteria, means that there are many questions left to be answered before a final evaluation can be made on which model best mimics the *in vivo* situation. But, amongst the models we evaluated the iPSC derived ones performed the best.

6.7 Short chain fatty acids in the human intestine

Besides the interaction of the microbes with the intestinal immune system via TLR agonists there is much more communication between the microbiota and the human intestine. One important group of signaling molecules for such interactions are the SCFAs, which have also been used in this thesis. Early studies mostly focused on butyrate exposure to Caco-2 or other cell lines. Part of the interactions of SCFAs and cells is mediated via G protein-coupled receptors [72, 73] which are present in intestinal enterocytes and immune cells [74]. Another way of interaction is via the inhibition of histone deacetylases (HDACs) which has effects on the epigenetics of the cells [75–77].

In cancer cell lines the exposure to SCFAs leads to apoptosis of the cells and butyrate was at some point proposed as a potential treatment for cancer [78, 79]. This apoptosis effect was called the butyrate paradox and multiple explanations have been given for that effect such as internal accumulation of

butyrate in cancer cells in which, due to the Warburg effect, butyrate is not consumed as an energy source [80, 81]. Therefore, cancer derived cell lines are not an adequate model to study the interaction of SCFA and the human intestine if the focus is on a healthy system that is exposed over a longer period of time. Other models such as stem cell based models are a better alternative and adult stem cell derived models have been applied to study this interaction [82, 83]. In the current thesis iPSC derived models were used. Overall, SCFAs have been associated with many effects in the human intestine including effects on the immune response, on homeostasis, the barrier function and SCFAs are used as energy source by the intestinal epithelium [80, 84–90]. This wide variety of effects means that using predefined selective read-outs may fail to capture the whole picture of the interaction. As such an approach using RNA sequencing to capture the whole transcriptome is an appropriate approach to screen for the effect of potential cellular effects. The results of **Chapter 4** clearly show that iPSC derived intestinal layers capture a wide range of responses upon exposure to SCFAs. One drawback of the sequencing approach is that there are likely effects that do now show up when looking at level of gene expression, but only become apparent for instance by studying the proteome. This means that there is still a lot of opportunity for further research when using a similar experimental design but with other endpoints.

Another potential critical point is the choice of concentrations of SCFAs used to expose the intestinal cells *in vitro*. While there are differences in the reported *in vivo* intestinal concentrations, the concentrations used in the experiments in **Chapter 4** are relatively low for acetate [91, 92]. Similar concentrations have been used in studies exposing enteroids derived from adult stem cells to SCFAs [83]. This means that the conclusion in both articles that acetate shows the lowest induction of effects might be due to the low concentration used. At the same time acetate has a different physiological role compared to both butyrate and propionate because it plays a role in acetyl-coenzyme A metabolism and as such there is endogenous production of acetate in mammalian cells [93]. Even though the production is only in the µM range, this presence of endogenously produced acetate could also explain the low response of the intestinal epithelial cell layers to the exogenously added 10 mM of acetate. Lastly, and as discussed above Caco-2 cells have been clearly reported to be an inadequate model for studies with SCFAs due to the butyrate paradox with butyrate inducing apoptosis in the cells [81, 94]. Using the stem cell derived model the induction of apoptosis related pathways was not observed, but a clear decrease in proliferation and LGR5 expression, a marker for cycling stem cells [95], was observed after exposure to butyrate and propionate in adult stem cell derived intestinal organoids [83]. This could have an influence on long term culture in for example a gut-on-a-chip. However, given that *in vivo* stem cells are at the bottom of the crypt where exposure is lower the presence of a crypt villi structure in other *in vitro* models could help avoid this influence [96]. Overall, the research has contributed to the knowledge on the interaction between SCFAs and the human intestine via the immune system, metabolism, energy homeostasis and other pathways combining many of the known effects.

6.8 Standards in using microfluidic based devices to work towards creating reliable gut-on-a-chip models

Microfluidic based models have taken the field of *in vitro* models for several organs including the intestine by storm as potential major contributors to the increased physiological relevance of the models by improving the morphology and differentiation of cells [26]. There are numerous claims that growing cells

in microfluidic devices improves their characteristics compared to their characteristics in existing static models, as reflected by induced villi formation and altered differentiation of the cells [26, 27, 97]. Part of this differentiation has been attributed to the presence of peristalsis like motion induced in some devices, in addition to the shear stress associated with the used fluid flow [27]. After the first few articles reported on these findings many different chips have been designed that were stated to have the same effects. The analysis reported in **Chapter 5**, based on publicly available datasets revealed that the effects on differentiation are potentially not consistent between different devices and/or that the effects are not strong enough to be detected in a comparative transcriptomics analysis. However, single studies that performed a direct comparison of gene expression between cells grown on Transwells and on chips do show that there are distinct differences between the two [24, 97].

The analysis in **Chapter 5** only focused on data sets using Caco-2 cells, which are limited in their differentiation and as such a similar analysis with stem cell based models might give additional insights. This analysis remains to be done in the future as the current transcriptomic dataset from stem cell based models on microfluidic devices was too small to be able to perform a similar comparative analysis. Many of the earlier reported differences and implications of device dependent culturing have been based on differences in histology or the formation of villi [26]. The extent of this effect is directly related to the strength of the shear stress so variations herein between models might be overshadowing the effect of the variable "Flow" since it is categorical not numeric [46]. Earlier reports state that Caco-2 cells grown on the chip system differentiate into different cell types, namely enterocytes, goblet cells and even Paneth cells remain intriguing [26, 27]. These changes would be expected to be accompanied by major shifts in gene expression. Again, this might be an example of an effect that is observed in a single study, which is not detectable in a global comparative analysis as performed in **Chapter 5**. In addition in several literature reported studies, the switch in cell type was proven by the expression of markers associated with these cell types, and different culturing conditions have also been associated with an increase of for example mucin production by Caco-2 cells which is a marker used for goblet cells [98–100]. However, defining Caco-2 cells as a different cell type based on the expression of only these markers is questionable, since the expression of the marker, albeit of interest, does not prove the full functionality associated with goblet cells. Further experiments that include for example single cell sequencing could give insight in cell specific features that express these markers, so that such data can be compared to existing single cell sequencing studies of cells isolated from the *in vivo* intestine [101–103].

6.9 Towards an intestinal model that includes the microbiota

Older experiments trying to study the interaction between the microbiota and intestinal cells ran into multiple issues. When using living bacteria there is a rapid overgrowth of the cells and medium limiting the amount of time the cells can be exposed. This makes chronic studies challenging, and makes it difficult to study long term host-microbe interactions [104, 105]. Such studies have mostly been limited to inactivated bacteria, bacterial supernatant or specific compounds/structures of the bacteria [106]. However, the gut-on-a-chip offers a unique environment where the villi and increased mucus production offer the niche for bacteria to grow while the constant flow removes excess bacteria and ensures constant delivery of nutrients [27, 44]. However, to fully recapitulate the interactions with the microbiota an anoxic environment is needed for the bacteria. Although there are some facultative anaerobes that are present

in the human intestine these do behave differently in the presence of oxygen [107]. Such anaerobic systems have been created in Transwell systems or tubes that can include the culturing of bacteria over longer periods of time, but lack the constant refreshing of media of microfluidic systems [43, 108, 109]. The next step is the application of microfluidic systems where the presence of the separated channels can allow the apical side containing the cells and bacteria to be anoxic while the basolateral side supplies the oxygen for the cells. This allows for the growth of bacteria that are sensitive to oxygen and allows those species that can survive with oxygen to function more similarly to how they grow in the intestine, with the flow allowing for longer term culturing than is possible in static Transwell systems [25, 44]. The lack of influence of the variable "Oxygen" observed in **Chapter 5** indicates that the cells are likely to grow normally with oxygen on only one side. Chip systems are mostly made from PDMS which is a gas permeable plastic [110], so it is important to properly validate that the whole apical side remains anoxic. For the further development of such devices the inclusion of oxygen sensors and sensors for other parameters into the gut-on-chip devices appears to be an essential element.

The large effects observed after exposure to SCFAs in **Chapter 4**, show how significant the effect of interaction with the microbiota can be on the functioning of the intestinal epithelium. So properly studying these interactions is important, and studies with singular or simple co-cultures of bacteria are the next step but only the starting point for follow-up studies. There are multiple ways to go towards more complex microbial communities that better represent the wide variety present *in vivo*. The first aspect that needs to be considered in case of the application *in vitro* of defined microbial communities, is to what extent these communities can recapitulate all the functions of the *in vivo* microbiota [111]. Such representative communities consisting of selected well defined bacterial strains have been applied in both *in vitro* and *in vivo* experiments and are constantly being improved. The advantage is that only known strains of bacteria are applied, so effects can more easily be attributed to a specific strain. However, how these communities are designed is dependent on the definition of a normal community which is once again dependent on current knowledge.

Within the field of toxicology there has been research into using faecal samples in incubations to assess gut microbiota mediated metabolism [112, 113], and faecal transplants are being applied in medicine [114, 115]. Such an approach of directly using the microbiota from the human intestine could also be used in intestinal *in vitro* models to avoid biased selection of bacteria. However, it is also known that microbiota in different parts of the intestine are different [116–118] so it is debatable to what extent faecal samples are representative for the microbial communities present in other intestinal parts as for example bacteria that remain in the mucus may be underrepresented. Furthermore, faecal samples from different donors may also show interindividual variability thereby hampering reproducibility.

The promise of this field has led to the increase in studies using fluidic intestinal *in vitro* models, and many groups are designing their own chip system or otherwise fluidic environment. This creates a situation where results are not easily reproducible because of the large variation in designs. There are a number of commercially available systems attempting to fill this gap, however these do come with substantial costs to purchase both the system and the equipment to run the system. Each design also represents its own closed proprietary system where users will be locked into a single vendor. There are initiatives to promote standardized designs consisting of specific building blocks with well defined characteristics so that people

can use multiple vendors or could attempt to create them themselves [119]. However, any standard needs to be widely accepted to avoid creating just another model that competes with the existing ones. Only recently a publication emerged that properly models and calculates the shear stress in chips [46], with older publications lacking clarity on their calculations. All such variables should be well defined in the different systems to aid translation of observed effects between chip designs, and, eventually, to the *in vivo* situation.

6.10 Making the step to application in toxicology and replacement of animal studies

A major goal of the work described in this thesis is to contribute to the replacement of animal testing with *in-vitro* alternatives by improving the *in vivo* physiological relevance of intestinal models. The previous discussion mostly focused on scientific/academic applications of the intestinal models. However, it is also important to reflect on how to apply *in vitro* models in toxicological risk assessment of compounds to actually make a step towards a future risk assessment without reliance on animal testing derived data. This indicates a need for *in vitro* to *in vivo* extrapolation of the observed effects.

Human cell based intestinal models can be of use to 1) test effects of compounds on the intestine, which is especially relevant for compounds for which the intestine is the target organ, or 2) to study the transport and intestinal metabolism of compounds by the intestinal cells and thus the expected *in vivo* bioavailability. Traditional Caco-2 models have been useful in the prediction of transport of many compounds but more advanced models could help fill in the gap for specific compounds, for instance for those that are transported by transporters that are poorly expressed. Studies have already shown improved expression of Cyp450 genes in iPSC derived intestinal organoids [120] but there is still a need for a study looking at expression and presence of transporters in stem cell derived models. The inclusion of the microbiome in the *in vitro* model, as discussed above, should only be considered when it gives additional value, while for most transport studies a simpler model with only intestinal cells will likely suffice.

Chapter 5 has already shown the limited availability of existing data on system parameters for the chip models, and there are similarly little data available on system parameters generally applied for stem cell based models. A study using these data sets and validating the presence of the transporters would offer a wealth of future knowledge for the field of toxicology. Selecting the right intestinal model to test absorption prior to clinical trials could avoid an expensive clinical trial on a drug that will fail due to limited oral bioavailability and needs a different route of administration.

Especially adult or induced pluripotent stem cell based intestinal models offer a lot of promise as disease models. They have been proposed as a tool in personalized medicine, where medication can be tested on a patient's own cells prior to treatment. Any medication will have off target effects, and the worse the disease the more side effects of a drug treatment are acceptable. Using such a personalized approach to test efficacy and/or optimize dosage can minimize harm to the patient. Disease models from patients could similarly be used to test efficacy of novel medication prior to clinical trials. Biobanks of patient material are already being constructed for use in research [121] and can help avoid clinical trials on drugs doomed to fail due to lack of bioavailability. Though such an approach will only work for a limited number of diseases, mainly those affecting cell functioning, it still has a lot of potential to reduce the number of

animal trials. Examples of diseases where stem cell based models have already been established are multiple intestinal atresia [122], IBD [48], cystic fibrosis [123, 124], cancer [125], and many non-intestinal diseases [126].

While it is questionable if personalized toxicology is the future, stem cell based intestinal models could find their place focusing on sub-populations with specific expression patterns of enzymes and/or specific transporters. Working towards actual replacement of animal studies will need well-defined and robust models that can be replicated in well-equipped labs by well-trained personnel. A model will only be accepted as a replacement once regulators can be convinced that it functions as well or better than the gold standard, which currently consists of animal models. This requires knowledge on all possible variables that can influence the functioning of the model. For Caco-2 cells there is already a wealth of knowledge on the influence of factors like passage number, medium composition, strain differences and inter-laboratory differences. For advanced models there is currently a lot of cutting edge development that is constantly pushing the field forward, however regulatory acceptance would require a consistent protocol and design that can be properly benchmarked. A nice example of such development is the collaboration of the USA Wyss Institute and FDA to test the potential applications of chip models in toxicology [127, 128].

Stem cell based models are derived directly from human material and will show a lot of inter-donor variation. It is yet not solved how this can be used and implemented in a regulatory setting. Biobanks of material are considered as part of a solution by offering a consistent availability of material from the same source, but material will still be limited. In this case iPSC derived models might be more favorable compared to adult stem cell models, as iPSC cells can be maintained and proliferated similar to cell lines, though this is far more laborious. Having consistent availability of a single batch of cells, similar to well defined strains of laboratory animals, allows for more reproducibility between labs.

Using advanced models especially with advanced microfluidic devices can be expensive. While this might be less of an issue for pharmaceutical industries, large investments in academic settings might be more challenging. If costs are too exceptional it might limit research towards using these novel *in vitro* model systems in New Approach Methodology strategies for replacing animal testing.

One major disadvantage of *in vitro* models will always be that they represent a single organ that only encompasses part of the body. Animal models offer a complete body and give an overview of both where the medication ends up and what it does. To translate the data from *in vitro* experiments to the whole body there is a need for physiologically based pharmacokinetic (PBPK) models, that take data from the different organs and combine that to model the kinetics and if combined with a quantitative *in vitro* to *in vivo* extrapolation (QIVIVE) to effects on a whole body. Traditional Transwell systems allow one to easily calculate the apparent transport rates or permeability coefficients, which can be used in PBPK modelling to define kinetic constants to describe the rate of absorption. However, novel approaches need to be developed to calculate such coefficients based on data obtained in dynamic flow systems. So far publications have either applied the traditional calculation designed for static systems or reported transport only as a percentage of the total exposed amount [45, 129]. Working out how to translate the values obtained from chip systems to the *in vivo* situation provides an important future challenge.

Existing academic practices and studies help expanding the knowledge base, which helps to, in the future, minimize the number of animals needed in future studies to predict human hazards and risks. A major part of clinical trials using novel drug candidates fail due to unwanted toxicity/side effects or due to species related differences in pharmacokinetic properties of the novel candidates, likely due to unexpected absorption, compared to what was observed in non-clinical studies.

Realistically the transition towards the use of *in vitro* alternatives in (regulatory) toxicology will be dependent on many steps. It is important to consider the many stakeholders involved in this transition. First of all, there are the (academic and corporate) researchers that are the first to develop, apply and test, novel methodologies. Secondly there are the companies that need validated models that can quickly and as cheaply as possible be applied for safety testing of compounds. Thirdly there are the governmental agencies as they have to approve alternative methods and the data derived from these models. Important aspects within this framework are the reliability and reproducibility of the novel *in vitro* methods and the data obtained. Lastly there is also a role for NGOs such as stichting Proefdiervrij, and Animal rights that influence and communicate societal pressure and provide funding for research on alternatives. For a first step all these stakeholders would need to come together to agree on which models to prioritize, which endpoints to be of importance and to identify approaches that have the highest potential. By making sure that there is consensus on where to focus, funding should be made available to work on those targets.

If a consensus can be reached the next step would be benchmarking and validation of the selected model(s), and only if needed improving on these existing models to increase the reliability and reproducibility. This will be dependent on funding from the government and industry, and requires that funding becomes available for benchmarking studies, which are not necessarily ground-breaking scientific studies with high breakthrough potential. So funding should not solely be focused on (scientific) novelty. In current projects where industry is involved focus is often still too much on novel industry applications or on novel methods and not necessarily on validation of existing methods. Execution of benchmarking studies should be performed by a combination of researchers in an academic setting and those that work in industry. On the side of the academic researchers there is also a need for more appreciation of benchmarking studies, often considered repetitive science. In addition to funding there will also be a need to be able to publish the results obtained.

The last step in the whole process will mostly be dependent on the governmental and regulatory agencies, as they will have to approve and accept the New Approach Methodologies. Within these steps there should be no direct need for comparison with the golden standard, in this case the *in vivo* animal tests. The focus should be on creating show cases that reveal that *in vitro* alternatives can adequately predict effects on humans.

6.11 Concluding remarks

The second and third chapter of this thesis showed some of the constraints of intestinal models with regards to their immunomodulatory capacity. None of the cell models tested could fully mimic the *in vivo* known responses and thus be defined as optimal, but recommendations can be made for the most competent model, being the iPSC derived organoids, and the data can be used to interpret future study results. The fourth chapter clearly showed that iPSC derived intestinal cell layers work well as a model for

studies on interaction with the microbiota via SCFAs. Many pathways that are known to be associated with SCFAs *in vivo*, were shown to be modulated in the *in vitro* model system. The fifth chapter showed that there is a need for more accurate reporting of the experimental characteristics of advanced intestinal *in vitro* systems in order to facilitate future reproducibility. Existing claims about fluidic systems do not simply hold for all different *in vitro* intestinal models. The presented approach for a meta-analysis does pave the way for comparable studies on transcriptomics data from experiments that use stem cells, and advanced microfluidic devices. Overall, the results of the thesis show that there are important differences between different *in vitro* intestinal models resulting in the importance of properly considering the strengths and weaknesses of each model when designing a study. Matching the research question with the most appropriate model makes sure that the outcomes can be properly interpreted, and that time is not wasted on potentially unnecessary complexity that comes with advanced models.

References

1. Sambuy Y, De Angelis I, Ranaldi G, Scarino ML, Stammati A, Zucco F. The Caco-2 cell line as a model of the intestinal barrier: influence of cell and culture-related factors on Caco-2 cell functional characteristics. Cell Biol Toxicol. 2005;21:1–26.
2. Wilson G, Hassan IF, Dix CJ, Williamson I, Shah R, Mackay M, et al. Transport and permeability properties of human Caco-2 cells: An in vitro model of the intestinal epithelial cell barrier. J Control Release. 1990;11:25–40.
3. Venegas DP, De La Fuente MK, Landskron G, González MJ, Quera R, Dijkstra G, et al. Short chain fatty acids (SCFAs)mediated gut epithelial and immune regulation and its relevance for inflammatory bowel diseases. Front Immunol. 2019;10 MAR:277.
4. Chen H, Meng L, Shen L. Multiple roles of short-chain fatty acids in Alzheimer disease. Nutrition. 2022;93.
5. Li W, Wu X, Hu X, Wang T, Liang S, Duan Y, et al. Structural changes of gut microbiota in Parkinson's disease and its correlation with clinical features. Sci China Life Sci 2017 6011. 2017;60:1223–33.
6. Hilgendorf C, Spahn-Langguth H, Regårdh CG, Lipka E, Amidon GL, Langguth P. Caco-2 versus Caco-2/HT29-MTX Co-cultured Cell Lines: Permeabilities Via Diffusion, Inside- and Outside-Directed Carrier-Mediated Transport. J Pharm Sci. 2000;89:63–75.
7. Devriese S, Van den Bossche L, Van Welden S, Holvoet T, Pinheiro I, Hindryckx P, et al. T84 monolayers are superior to Caco-2 as a model system of colonocytes. Histochem Cell Biol 2017 1481. 2017;148:85–93.
8. Zucco F, Batto AF, Bises G, Chambaz J, Chiusolo A, Consalvo R, et al. An inter-laboratory study to evaluate the effects of medium composition on the differentiation and barrier function of Caco-2 cell lines. Altern Lab Anim. 2005;33:603–18.
9. Gstraunthaler G, Lindl T, Van Der Valk J. A plea to reduce or replace fetal bovine serum in cell culture media. Cytotechnology. 2013;65:791–3.
10. Gstraunthaler G, Lindl T, Van Der Valk J. A severe case of fraudulent blending of fetal bovine serum strengthens the case for serum-free cell and tissue culture applications. Altern Lab Anim. 2014;42:207–9.
11. Jochems CEA, Van der Valk JBF, Stafleu FR, Baumans V. The use of fetal bovine serum: ethical or scientific problem? Altern Lab Anim. 2002;30:219–27.

12. Ferruzza S, Rossi C, Sambuy Y, Scarino ML. Serum-reduced and serum-free media for differentiation of Caco-2 cells. ALTEX - Altern to Anim Exp. 2013;30:159–68.
13. Hubatsch I, Ragnarsson EGE, Artursson P. Determination of drug permeability and prediction of drug absorption in Caco-2 monolayers. Nat Protoc. 2007;2:2111–9.
14. Natoli M, Leoni BD, D'Agnano I, Zucco F, Felsani A. Good Caco-2 cell culture practices. Toxicol In Vitro. 2012;26:1243–6.
15. Vachon PH, Beaulieu JF. Transient mosaic patterns of morphological and functional differentiation in the Caco-2 cell line. Gastroenterology. 1992;103:414–23.
16. Yamashita S, Konishi K, Yamazaki Y, Taki Y, Sakane T, Sezaki H, et al. New and better protocols for a short-term Caco-2 cell culture system. J Pharm Sci. 2002;91:669–79.
17. Martínez-Maqueda D, Miralles B, Recio I. HT29 cell line. In: The Impact of Food Bioactives on Health: In Vitro and Ex Vivo Models. Springer International Publishing; 2015. p. 113–24.
18. Bajka BH, Rigby NM, Cross KL, Macierzanka A, Mackie AR. The influence of small intestinal mucus structure on particle transport ex vivo. Colloids Surfaces B Biointerfaces. 2015;135:73–80.
19. Ensign LM, Henning A, Schneider CS, Maisel K, Wang Y-Y, Porosoff MD, et al. Ex vivo characterization of particle transport in mucus secretions coating freshly excised mucosal tissues. Mol Pharm. 2013;10:2176.
20. Walter E, Janich S, Roessler BJ, Hilfinger JM, Amidon GL. HT29-MTX/Caco-2 cocultures as an in vitro model for the intestinal epithelium: in vitro-in vivo correlation with permeability data from rats and humans. J Pharm Sci. 1996;85:1070–6.
21. Hansson GC. Role of mucus layers in gut infection and inflammation. Curr Opin Microbiol. 2012;15:57–62.
22. Ouwerkerk JP, De Vos WM, Belzer C. Glycobiome: Bacteria and mucus at the epithelial interface. Best Pract Res Clin Gastroenterol. 2013;27:25–38.
23. Elzinga JI, van der Lugt B, Belzer C, Steegenga WT. Characterization of increased mucus production of HT29-MTX-E12 cells grown under Semi-Wet interface with Mechanical Stimulation. PLoS One. 2021;16:e0261191.
24. Kasendra M, Tovaglieri A, Sontheimer-Phelps A, Jalili-Firoozinezhad S, Bein A, Chalkiadaki A, et al. Development of a primary human Small Intestine-on-a-Chip using biopsy-derived organoids. Sci Reports 2018 81. 2018;8:1–14.
25. Jalili-Firoozinezhad S, Gazzaniga FS, Calamari EL, Camacho DM, Fadel CW, Bein A, et al. A complex human gut microbiome cultured in an anaerobic intestine-on-a-chip. Nat Biomed Eng 2019 37. 2019;3:520–31.
26. Kim HJ, Ingber DE. Gut-on-a-Chip microenvironment induces human intestinal cells to undergo villus differentiation. Integr Biol. 2013;5:1130.
27. Kim HJ, Li H, Collins JJ, Ingber DE. Contributions of microbiome and mechanical deformation to intestinal bacterial overgrowth and inflammation in a human gut-on-a-chip. Proc Natl Acad Sci U S A. 2016;113:E7–15.
28. Maurer M, Gresnigt MS, Last A, Wollny T, Berlinghof F, Pospich R, et al. A three-dimensional immunocompetent intestine-on-chip model as in vitro platform for functional and microbial interaction studies. Biomaterials. 2019;220:119396.
29. Beaurivage C, Kanapeckaite A, Loomans C, Erdmann KS, Stallen J, Janssen RAJ. Development of a

human primary gut-on-a-chip to model inflammatory processes. Sci Reports 2020 101. 2020;10:1–16.
30. Kämpfer AAM, Urbán P, Gioria S, Kanase N, Stone V, Kinsner-Ovaskainen A. Development of an in vitro co-culture model to mimic the human intestine in healthy and diseased state. Toxicol Vitr. 2017;45:31–43.
31. Sato T, Vries RG, Snippert HJ, Van De Wetering M, Barker N, Stange DE, et al. Single Lgr5 stem cells build crypt-villus structures in vitro without a mesenchymal niche. Nat 2009 4597244. 2009;459:262–5.
32. Sato T, Stange DE, Ferrante M, Vries RGJ, van Es JH, van den Brink S, et al. Long-term Expansion of Epithelial Organoids From Human Colon, Adenoma, Adenocarcinoma, and Barrett's Epithelium. Gastroenterology. 2011;141:1762–72.
33. Tamminen K, Balboa D, Toivonen S, Pakarinen MP, Wiener Z, Alitalo K, et al. Intestinal Commitment and Maturation of Human Pluripotent Stem Cells Is Independent of Exogenous FGF4 and R-spondin1. PLoS One. 2015;10:e0134551–e0134551.
34. Mccracken KW, Howell JC, Wells JM, Spence JR, Org; KM, Org; JH, et al. Generating human intestinal tissue from pluripotent stem cells in vitro. Nat Protoc. 2011;6:1920–8.
35. Kabeya T, Mima S, Imakura Y, Miyashita T, Ogura I, Yamada T, et al. Pharmacokinetic functions of human induced pluripotent stem cell-derived small intestinal epithelial cells. Drug Metab Pharmacokinet. 2020;35:374–82.
36. Iwao T, Kodama N, Kondo Y, Kabeya T, Nakamura K, Horikawa T, et al. Generation of Enterocyte-Like Cells with Pharmacokinetic Functions from Human Induced Pluripotent Stem Cells Using Small-Molecule Compounds. Drug Metab Dispos. 2015;43:603–10.
37. Bertaux-Skeirik N, Feng R, Schumacher MA, Li J, Mahe MM, Engevik AC, et al. CD44 plays a functional role in Helicobacter pylori-induced epithelial cell proliferation. PLoS Pathog. 2015;11.
38. Engevik MA, Yacyshyn MB, Engevik KA, Wang J, Darien B, Hassett DJ, et al. Human Clostridium difficile infection: altered mucus production and composition. Am J Physiol Gastrointest Liver Physiol. 2015;308:G510–24.
39. Leslie JL, Huang S, Opp JS, Nagy MS, Kobayashi M, Young VB, et al. Persistence and toxin production by Clostridium difficile within human intestinal organoids result in disruption of epithelial paracellular barrier function. Infect Immun. 2015;83:138–45.
40. Stroulios G, Stahl M, Elstone F, Chang W, Louis S, Eaves A, et al. Culture methods to study apical-specific interactions using intestinal organoid models. J Vis Exp. 2021;2021.
41. Co JY, Margalef-Català M, Monack DM, Amieva MR. Controlling the polarity of human gastrointestinal organoids to investigate epithelial biology and infectious diseases. Nat Protoc 2021 1611. 2021;16:5171–92.
42. Wang Y, DiSalvo M, Gunasekara DB, Dutton J, Proctor A, Lebhar MS, et al. Self-renewing Monolayer of Primary Colonic or Rectal Epithelial Cells. Cell Mol Gastroenterol Hepatol. 2017;4:165-182.e7.
43. Sasaki N, Miyamoto K, Maslowski KM, Ohno H, Kanai T, Sato T. Development of a Scalable Coculture System for Gut Anaerobes and Human Colon Epithelium. Gastroenterology. 2020;159:388-390.e5.
44. Shah P, Fritz J V., Glaab E, Desai MS, Greenhalgh K, Frachet A, et al. A microfluidics-based in vitro model of the gastrointestinal human-microbe interface. Nat Commun. 2016;7:1–15.
45. Kulthong K, Duivenvoorde L, Mizera BZ, Rijkers D, Dam G Ten, Oegema G, et al. Implementation of a dynamic intestinal gut-on-a-chip barrier model for transport studies of lipophilic dioxin congeners. RSC Adv. 2018;8:32440–53.

46. Fois CAM, Schindeler A, Valtchev P, Dehghani F. Dynamic flow and shear stress as key parameters for intestinal cells morphology and polarization in an organ-on-a-chip model. Biomed Microdevices. 2021;23:1–12.
47. Trietsch SJ, Naumovska E, Kurek D, Setyawati MC, Vormann MK, Wilschut KJ, et al. Membrane-free culture and real-time barrier integrity assessment of perfused intestinal epithelium tubes. Nat Commun 2017 81. 2017;8:1–8.
48. Beaurivage C, Naumovska E, Chang YX, Elstak ED, Nicolas A, Wouters H, et al. Development of a Gut-on-a-Chip Model for High Throughput Disease Modeling and Drug Discovery. Int J Mol Sci. 2019;20.
49. Baquero F, Nombela C. The microbiome as a human organ. Clin Microbiol Infect. 2012;18 Suppl 4 SUPPL. 4:2–4.
50. Tian Z, Yang L, Li P, Xiao Y, Peng J, Wang X, et al. The inflammation regulation effects of Enterococcus faecium HDRsEf1 on human enterocyte-like HT-29 cells. http://dx.doi.org.ezproxy.library.wur.nl/101080/1976835420161160955. 2016;20:70–6.
51. Abreu MT. Toll-like receptor signalling in the intestinal epithelium: how bacterial recognition shapes intestinal function. Nat Rev Immunol 2010 102. 2010;10:131–44.
52. Grouls M, van der Zande M, de Haan L, Bouwmeester H. Responses of increasingly complex intestinal epithelium in vitro models to bacterial toll-like receptor agonists. Toxicol Vitr. 2022;79:105280.
53. Otte JM, Cario E, Podolsky DK. Mechanisms of Cross Hyporesponsiveness to Toll-Like Receptor Bacterial Ligands in Intestinal Epithelial Cells. Gastroenterology. 2004;126:1054–70.
54. Cario E, Podolsky DK. Differential alteration in intestinal epithelial cell expression of Toll-like receptor 3 (TLR3) and TLR4 in inflammatory bowel disease. Infect Immun. 2000;68:7010–7.
55. Fusunyan RD, Nanthakumar NN, Baldeon ME, Walker WA. Evidence for an innate immune response in the immature human intestine: Toll-like receptors on fetal enterocytes. Pediatr Res. 2001;49 4 I:589–93.
56. Furrie E, Macfarlane S, Thomson G, Macfarlane GT. Toll-like receptors-2, -3 and -4 expression patterns on human colon and their regulation by mucosal-associated bacteria. Immunology. 2005;115:565–74.
57. Naik S, Kelly EJ, Meijer L, Pettersson S, Sanderson IR. Absence of Toll-like receptor 4 explains endotoxin hyporesponsiveness in human intestinal epithelium. J Pediatr Gastroenterol Nutr. 2001;32:449–53.
58. Kamada N, Chen GY, Inohara N, Núñez G. Control of pathogens and pathobionts by the gut microbiota. Nat Immunol 2013 147. 2013;14:685–90.
59. Kamada N, Seo SU, Chen GY, Núñez G. Role of the gut microbiota in immunity and inflammatory disease. Nat Rev Immunol. 2013;13:321–35.
60. Ozinsky A, Underhill DM, Fontenot JD, Hajjar AM, Smith KD, Wilson CB, et al. The repertoire for pattern recognition of pathogens by the innate immune system is defined by cooperation between Toll-like receptors. Proc Natl Acad Sci U S A. 2000;97:13766–71.
61. Kawasaki T, Kawai T. Toll-like receptor signaling pathways. Front Immunol. 2014;5 SEP:461.
62. Böcker U, Yezerskyy O, Feick P, Manigold T, Panja A, Kalina U, et al. Responsiveness of intestinal epithelial cell lines to lipopolysaccharide is correlated with Toll-like receptor 4 but not Toll-like receptor 2 or CD14 expression. Int J Colorectal Dis. 2003;18:25–32.
63. Sender R, Fuchs S, Milo R. Revised Estimates for the Number of Human and Bacteria Cells in the

Body. PLoS Biol. 2016;14.
64. Miller MD, Krangel MS. Biology and biochemistry of the chemokines - a family of chemotactic and inflammatory cytokines. Crit Rev Immunol. 1992;12:17–46.
65. Mitsuyama K, Toyonaga A, Sasaki E, Watanabe K, Tateishi H, Nishiyama T, et al. IL-8 as an important chemoattractant for neutrophils in ulcerative colitis and Crohn's disease. Clin Exp Immunol. 1994;96:432–6.
66. Price AE, Shamardani K, Lugo KA, Deguine J, Roberts AW, Lee BL, et al. A Map of Toll-like Receptor Expression in the Intestinal Epithelium Reveals Distinct Spatial, Cell Type-Specific, and Temporal Patterns. Immunity. 2018;49:560-575.e6.
67. Tomita M, Ohkubo R, Hayashi M. Lipopolysaccharide Transport System across Colonic Epithelial Cells in Normal and Infective Rat. Drug Metab Pharmacokinet. 2004;19:33–40.
68. Fitzner N, Clauberg S, Essmann F, Liebmann J, Kolb-Bachofen V. Human skin endothelial cells can express all 10 TLR genes and respond to respective ligands. Clin Vaccine Immunol. 2008;15:138–46.
69. Faure E, Equils O, Sieling PA, Thomas L, Zhang FX, Kirschning CJ, et al. Bacterial lipopolysaccharide activates NF-κB through toll-like receptor 4 (TLR-4) in cultured human dermal endothelial cells. Differential expression of TLR-4 and TLR-2 in endothelial cells. J Biol Chem. 2000;275:11058–63.
70. Kayisoglu O, Weiss F, Niklas C, Pierotti I, Pompaiah M, Wallaschek N, et al. Original research: Location-specific cell identity rather than exposure to GI microbiota defines many innate immune signalling cascades in the gut epithelium. Gut. 2021;70:687.
71. Takeda K, Akira S. TLR signaling pathways. Semin Immunol. 2004;16:3–9.
72. Priyadarshini M, Wicksteed B, Schiltz GE, Gilchrist A, Layden BT. SCFA Receptors in Pancreatic β Cells: Novel Diabetes Targets? Trends Endocrinol Metab. 2016;27:653–64.
73. Ge H, Li X, Weiszmann J, Wang P, Baribault H, Chen JL, et al. Activation of G protein-coupled receptor 43 in adipocytes leads to inhibition of lipolysis and suppression of plasma free fatty acids. Endocrinology. 2008;149:4519–26.
74. van der Hee B, Wells JM. Microbial Regulation of Host Physiology by Short-chain Fatty Acids. Trends Microbiol. 2021;29:700–12.
75. Riggs MG, Whittaker RG, Neumann JR, Ingram VM. n-Butyrate causes histone modification in HeLa and Friend erythroleukaemia cells. Nature. 1977;268:462–4.
76. Davie JR. Inhibition of histone deacetylase activity by butyrate. J Nutr. 2003;133 7 Suppl.
77. Waldecker M, Kautenburger T, Daumann H, Busch C, Schrenk D. Inhibition of histone-deacetylase activity by short-chain fatty acids and some polyphenol metabolites formed in the colon. J Nutr Biochem. 2008;19:587–93.
78. Sengupta S, Muir JG, Gibson PR. Does butyrate protect from colorectal cancer? J Gastroenterol Hepatol. 2006;21:209–18.
79. Hague A, Manning AM, Hanlon KA, Hart D, Paraskeva C, Huschtscha LI. Sodium butyrate induces apoptosis in human colonic tumour cell lines in a p53-independent pathway: Implications for the possible role of dietary fibre in the prevention of large-bowel cancer. Int J Cancer. 1993;55:498–505.
80. Donohoe DR, Collins LB, Wali A, Bigler R, Sun W, Bultman SJ. The Warburg Effect Dictates the Mechanism of Butyrate-Mediated Histone Acetylation and Cell Proliferation. Mol Cell. 2012;48:612–26.
81. Ryu SH, Kaiko GE, Stappenbeck TS. Cellular differentiation: Potential insight into butyrate paradox? Mol Cell Oncol. 2018;5:1212685.

82. Lukovac S, Belzer C, Pellis L, Keijser BJ, de Vos WM, Montijn RC, et al. Differential modulation by Akkermansia muciniphila and faecalibacterium prausnitzii of host peripheral lipid metabolism and histone acetylation in mouse gut organoids. MBio. 2014;5.
83. Pearce SC, Weber GJ, Van Sambeek DM, Soares JW, Racicot K, Breault DT. Intestinal enteroids recapitulate the effects of short-chain fatty acids on the intestinal epithelium. PLoS One. 2020;15:e0230231.
84. Martin-Gallausiaux C, Béguet-Crespel F, Marinelli L, Jamet A, Ledue F, Blottière HM, et al. Butyrate produced by gut commensal bacteria activates TGF-beta1 expression through the transcription factor SP1 in human intestinal epithelial cells. Sci Reports 2018 81. 2018;8:1–13.
85. Marinelli L, Martin-Gallausiaux C, Bourhis JM, Béguet-Crespel F, Blottière HM, Lapaque N. Identification of the novel role of butyrate as AhR ligand in human intestinal epithelial cells. Sci Reports 2019 91. 2019;9:1–14.
86. Säemann MD, Böhmig GA, Österreicher CH, Burtscher H, Parolini O, Diakos C, et al. Anti-inflammatory effects of sodium butyrate on human monocytes: potent inhibition of IL-12 and up-regulation of IL-10 production. FASEB J. 2000;14:2380–2.
87. Maa MC, Chang MY, Hsieh MY, Chen YJ, Yang CJ, Chen ZC, et al. Butyrate reduced lipopolysaccharide-mediated macrophage migration by suppression of Src enhancement and focal adhesion kinase activity. J Nutr Biochem. 2010;21:1186–92.
88. Peng L, Li ZR, Green RS, Holzman IR, Lin J. Butyrate Enhances the Intestinal Barrier by Facilitating Tight Junction Assembly via Activation of AMP-Activated Protein Kinase in Caco-2 Cell Monolayers. J Nutr. 2009;139:1619–25.
89. Siavoshian S, Segain JP, Kornprobst M, Bonnet C, Cherbut C, Galmiche JP, et al. Butyrate and trichostatin A effects on the proliferation/differentiation of human intestinal epithelial cells: induction of cyclin D3 and p21 expression. Gut. 2000;46:507–14.
90. Hamer HM, Jonkers D, Venema K, Vanhoutvin S, Troost FJ, Brummer RJ. Review article: the role of butyrate on colonic function. Aliment Pharmacol Ther. 2008;27:104–19.
91. Cummings JH, Pomare EW, Branch HWJ, Naylor CPE, MacFarlane GT. Short chain fatty acids in human large intestine, portal, hepatic and venous blood. Gut. 1987;28:1221–7.
92. Zoetendal EG, Raes J, Van Den Bogert B, Arumugam M, Booijink CC, Troost FJ, et al. The human small intestinal microbiota is driven by rapid uptake and conversion of simple carbohydrates. ISME J 2012 67. 2012;6:1415–26.
93. Liu X, Cooper DE, Cluntun AA, Warmoes MO, Zhao S, Reid MA, et al. Acetate Production from Glucose and Coupling to Mitochondrial Metabolism in Mammals. Cell. 2018;175:502-513.e13.
94. Salvi PS, Cowles RA. Butyrate and the Intestinal Epithelium: Modulation of Proliferation and Inflammation in Homeostasis and Disease. Cells 2021, Vol 10, Page 1775. 2021;10:1775.
95. Barker N, Van Es JH, Kuipers J, Kujala P, Van Den Born M, Cozijnsen M, et al. Identification of stem cells in small intestine and colon by marker gene Lgr5. Nat 2007 4497165. 2007;449:1003–7.
96. Kaiko GE, Ryu SH, Koues OI, Collins PL, Solnica-Krezel L, Pearce EJ, et al. The colonic crypt protects stem cells from microbiota-derived metabolites. Cell. 2016;165:1708.
97. Kulthong K, Duivenvoorde L, Sun H, Confederat S, Wu J, Spenkelink B, et al. Microfluidic chip for culturing intestinal epithelial cell layers: Characterization and comparison of drug transport between dynamic and static models. Toxicol Vitr. 2020;65:104815.

98. Van Klinken BJW, Oussoren E, Weenink JJ, Strous GJ, Büller HA, Dekker J, et al. The human intestinal cell lines Caco-2 and LS174T as models to study cel-type specific mucin expression. Glycoconj J. 1996;13:757–68.
99. Shekels LL, Lyftogt CT, Ho SB. Bile acid-induced alterations of mucin production in differentiated human colon cancer cell lines. Int J Biochem Cell Biol. 1996;28:193–201.
100. Mattar AF, Teitelbaum DH, Drongowski RA, Yongyi F, Harmon CM, Coran AG. Probiotics up-regulate MUC-2 mucin gene expression in a Caco-2 cell-culture model. Pediatr Surg Int. 2002;18:586–90.
101. Gao S, Yan L, Wang R, Li J, Yong J, Zhou X, et al. Tracing the temporal-spatial transcriptome landscapes of the human fetal digestive tract using single-cell RNA-sequencing. Nat Cell Biol. 2018;20:721–34.
102. Haber AL, Biton M, Rogel N, Herbst RH, Shekhar K, Smillie C, et al. A single-cell survey of the small intestinal epithelium. Nature. 2017;551:333–9.
103. Busslinger GA, Weusten BLA, Bogte A, Begthel H, Brosens LAA, Clevers H. Human gastrointestinal epithelia of the esophagus, stomach, and duodenum resolved at single-cell resolution. Cell Rep. 2021;34:108819.
104. Zoumpopoulou G, Tsakalidou E, Dewulf J, Pot B, Grangette C. Differential crosstalk between epithelial cells, dendritic cells and bacteria in a co-culture model. Int J Food Microbiol. 2009;131:40–51.
105. Ty F, Cj S, 2# A, Jm, Rl W, Ra B, et al. A novel human enteroid-anaerobe co-culture system to study microbial-host interaction under physiological hypoxia. bioRxiv. 2019;:555755.
106. Putaala H, Barrangou R, Leyer GJ, Ouwehand AC, Bech Hansen E, Romero DA, et al. Analysis of the human intestinal epithelial cell transcriptional response to Lactobacillus acidophilus, Lactobacillus salivarius, Bifidobacterium lactis and Escherichia coli. Benef Microbes. 2010;1:283–95.
107. Clements LD, Miller BS, Streips UN. Comparative Growth Analysis of the Facultative Anaerobes Bacillus subtilis, Bacillus licheniformis, and Escherichia coli. Syst Appl Microbiol. 2002;25:284–6.
108. Ulluwishewa D, Anderson RC, Young W, Mcnabb WC, van Baarlen P, Moughan PJ, et al. Live Faecalibacterium prausnitzii in an apical anaerobic model of the intestinal epithelial barrier. Cell Microbiol. 2015;17:226–40.
109. Sadabad MS, Von Martels JZH, Khan MT, Blokzijl T, Paglia G, Dijkstra G, et al. A simple coculture system shows mutualism between anaerobic faecalibacteria and epithelial Caco-2 cells. Sci Rep. 2015;5:1–9.
110. Markov DA, Lillie EM, Garbett SP, McCawley LJ. Variation in diffusion of gases through PDMS due to plasma surface treatment and storage conditions. Biomed Microdevices. 2014;16:91.
111. Elzinga J, van der Oost J, de Vos WM, Smidt H. The Use of Defined Microbial Communities To Model Host-Microbe Interactions in the Human Gut. Microbiol Mol Biol Rev. 2019;83.
112. van Dongen KCW, van der Zande M, Bruyneel B, Vervoort JJM, Rietjens IMCM, Belzer C, et al. An in vitro model for microbial fructoselysine degradation shows substantial interindividual differences in metabolic capacities of human fecal slurries. Toxicol Vitr. 2021;72:105078.
113. Van Dongen KCW, Belzer C, Bakker W, Rietjens IMCM, Beekmann K. Inter- and Intraindividual Differences in the Capacity of the Human Intestinal Microbiome in Fecal Slurries to Metabolize Fructoselysine and Carboxymethyllysine. J Agric Food Chem. 2022;70:11759–68.
114. Kassam Z, Hundal R, Marshall JK, Lee CH. Fecal Transplant via Retention Enema for Refractory or Recurrent Clostridium difficile Infection. Arch Intern Med. 2012;172:191–3.

115. MacConnachie AA, Fox R, Kennedy DR, Seaton RA. Faecal transplant for recurrent Clostridium difficile-associated diarrhoea: a UK case series. QJM An Int J Med. 2009;102:781–4.
116. Jin J, Fall M, Liu Q, Rietjens IMCM, Xing F. Comparative Microbial Conversion of Deoxynivalenol and Acetylated Deoxynivalenol in Different Parts of the Chicken Intestine as Detected in Vitro and Translated to the in Vivo Situation. J Agric Food Chem. 2021;69:15384–92.
117. Donaldson GP, Lee SM, Mazmanian SK. Gut biogeography of the bacterial microbiota. Nat Rev Microbiol. 2016;14:20.
118. Zoetendal EG, De Vos WM. Effect of diet on the intestinal microbiota and its activity. Curr Opin Gastroenterol. 2014;30:189–95.
119. hDMT. Translational Organ-on-Chip Platform - TOP: Translational Organ-on-Chip Platform. 2021. https://top.hdmt.technology/. Accessed 26 Apr 2022.
120. Janssen AWF, Duivenvoorde LPM, Rijkers D, Nijssen R, Peijnenburg AACM, van der Zande M, et al. Cytochrome P450 expression, induction and activity in human induced pluripotent stem cell-derived intestinal organoids and comparison with primary human intestinal epithelial cells and Caco-2 cells. Arch Toxicol. 2020;95:907–22.
121. Diaferia GR, Cardano M, Cattaneo M, Spinelli CC, Dessì SS, Deblasio P, et al. The science of stem cell biobanking: Investing in the future. J Cell Physiol. 2012;227:14–9.
122. Bigorgne AE, Farin HF, Lemoine R, Mahlaoui N, Lambert N, Gil M, et al. TTC7A mutations disrupt intestinal epithelial apicobasal polarity. J Clin Invest. 2014;124:328–37.
123. Dekkers JF, Wiegerinck CL, De Jonge HR, Bronsveld I, Janssens HM, De Winter-De Groot KM, et al. A functional CFTR assay using primary cystic fibrosis intestinal organoids. Nat Med 2013 197. 2013;19:939–45.
124. Schwank G, Koo BK, Sasselli V, Dekkers JF, Heo I, Demircan T, et al. Functional Repair of CFTR by CRISPR/Cas9 in Intestinal Stem Cell Organoids of Cystic Fibrosis Patients. Cell Stem Cell. 2013;13:653–8.
125. Neal JT, Li X, Zhu J, Giangarra V, Grzeskowiak CL, Ju J, et al. Organoid Modeling of the Tumor Immune Microenvironment. Cell. 2018;175:1972-1988.e16.
126. Grskovic M, Javaherian A, Strulovici B, Daley GQ. Induced pluripotent stem cells--opportunities for disease modelling and drug discovery. Nat Rev Drug Discov. 2011;10:915–29.
127. Buchanan V. Text - H.R.2565 - 117th Congress (2021-2022): FDA Modernization Act of 2021. 2021.
128. FDA Researchers to Evaluate 'Organs-on-Chips' Technology | FDA. https://www.fda.gov/food/cfsan-constituent-updates/fda-researchers-evaluate-organs-chips-technology. Accessed 17 Jan 2023.
129. Shim KY, Lee D, Han J, Nguyen NT, Park S, Sung JH. Microfluidic gut-on-a-chip with three-dimensional villi structure. Biomed Microdevices. 2017;19:1–10.

Chapter 7

English Summary

Summary

To implement the 3Rs principle within toxicological sciences, meaning to refine, reduce and replace animal studies is a challenging task for toxicologists. There are both strong scientific and societal reasons to reduce the number of animal experiments for the safety assessment of compounds. For this reason cell based models are continuously being developed and improved. On one hand steps are being taken to improve the biology by improving existing human cell lines based models or by switching to more advanced alternatives such as human stem cell based models. On the other hand the rapid development of microfluidic organ-on-a-chip technology has changed up the physical environment that the cells are grown in, attempting to better emulate the tissue environment that the human cells grow in, *in vitro*. Both approaches have been applied for many organs amongst which the intestines. The intestines are the most important location for uptake of all kinds of compounds that humans are orally exposed to. However, the intestines have one major difference compared to most other organs, the presence of the microbiota in the intestinal lumen. To work towards an improved intestinal model, bacteria should be included in the considerations when selecting the best cell and/or technological model to use. The main aim of this thesis to explore both well-established existing models such as cell lines as well as more advanced models such as stem cell based model for their ability to be used in future models that include both the intestinal epithelium and the microbiome.

An important interaction between the intestinal epithelium and the intestinal microbiota happens via the local immune system. Bacteria (or parts thereof) and (fragments of) other infectious agents called agonists are recognized by intestinal epithelial cells via Toll-like receptors that initiate the innate immune response. C**hapter 2** cell line based intestinal models were checked for their capacity to respond to a number of agonists by initiating a pro-inflammatory response. To this end four different models were grown *in vitro*, Caco-2 mono-culture, Caco-2/HT29-MTX co-culture, Caco-2/HT29-MTX/HMVEC-d tri-culture and HT29-p monoculture. Caco-2 cells are enterocytes that are responsible for transport of compounds, HT29-MTX are goblet cells that produce the mucus layer as found in the intestine, HMVEC-d are primary blood and lymph endothelial cells and HT29-p are mostly undifferentiated intestinal cells but do form epithelial structures that contain microvilli. All cells were grown on Transwell inserts, with the intestinal epithelial cells on the apical side and, if applicable, the endothelial cells on the basolateral side. Cells were exposed to five agonists, Pam3CSK4, LPS, ssRNA, poly(I:C) and Flagellin, and inflammation was assessed by measuring excretion of IL-8, a pro-inflammatory cytokine. Only flagellin induced excretion of IL-8 in all four models, mostly on the apical side. Only HT29-p responded to a second agonist namely poly(I:C), it was also the only model that excreted more towards the basolateral side. Overall, all of the models only showed a limited response to agonists and expanding with other cell lines than the traditional Caco-2 cell line did not alleviate this problem.

Next the responses of a comparable panel of TLR agonists exposed to primary and stem cell based models was explored. For this, in **Chapter 3** the cell lines were replaced with two more advanced models. Firstly, induced pluripotent stem cell based (iPSC) derived organoids and secondly the primary human small intestinal epithelial (PHSIE) model. Both models incorporate more of the cell types found in the human gut. With iPSC derived organoids containing enterocytes, stem cells, Paneth cells, goblet

cells, enteroendocrine cells and mesenchymal cells and PHSIE containing enterocytes, stem cells, Paneth cells, M cells and tuft cells. So both models have a different composition but show vast improvements compared to cell line based models in this aspect. Since iPSC derived organoids are 3D structures grown in Matrigel sampling was limited to only the medium which represents the basolateral side, while PHSIE cells only had limited volume apically so sampled were only taken from the basolateral side. The measurements were expanded with both more cytokines, CCL20, CXCL10, IL-6 and IL-8, and by measuring TLR1, 2, 3, 4, 5, 7, 8 and 9 gene expression. Overall, the iPSC derived organoids produced more cytokines than the PHSIE model without stimulation. After exposure to agonists the iPSC derived organoids secreted all four cytokines while for the PHSIE this was limited to the secretion of IL-8. The iPSC derived organoids responded to three out of five tested agonists while the PHSIE model only responded to one out of three tested agonists. TLR expression was also shown to be responsive to agonist exposure, offering additional value when measured. When looking to use the models to study interaction with the microbiota the iPSC derived organoids offer the best model out of those tested, while the PHSIE model performed similarly to the cell lines.

Direct stimulation of the immune system is far from the only way that the microbiota interact with the human intestine. They also produce a wide array of compounds that can act as signaling molecules, shaping the communication between the two. One group of such compounds are short-chain fatty acids (SCFAs) that are produced by the breakdown of dietary fibers by the intestinal microbiota. SCFAs behave markedly different in some cell lines, compared to *in vivo*, since they cause apoptosis. This implies that cell line based models cannot be used to study the SCFA cell interaction. Primary and or stem cell based models do not suffer from this problem and in **Chapter 4** iPSC derived intestinal epithelial cell layers were exposed to the three most abundantly present SCFAs namely, butyrate, propionate and acetate. To capture the wide variety of responses of intestinal epithelial cells, the effects were measured using RNA-sequencing, giving a wholistic overview of the effects. Each SCFA showed a unique gene expression profile, with butyrate showing most effects followed by propionate. For these two the changes in gene expression were also translated to an effect on pathways, giving more insight into the biological consequences of differences in gene expression as inducted. The pathway analysis clearly showed that there were changes in the energy household indicating that the SCFA were used as an energy source by the cells. The lack thereof is given as one of the possible explanations for the apoptosis observed in cell lines. Similarly, many other effects attributed to SCFAs were observed, such as those on the immune system. The iPSC derived intestinal epithelial cell layers were shown to be an appropriate model to study this interaction, so would properly mimic this part of the interaction with the microbiome.

The rapid development of novel culturing methods has resulted in a considerable amount of new intestinal *in vitro* models. Examples are culturing cells in microfluidic devices or on continuous shaking plates. Early work reported effects on Caco-2 differentiation due to the shear and other stresses experienced. The ever increasing body of publicly available microarray data of both traditional and advanced models using Caco-2 means that an overarching analysis can be done to see if these effects show up consistently. In **Chapter 5** data sets obtained from the literature of both traditional Caco-2 grown on Transwells and in advanced models were systematically collected and the effects of eight variables, "Culture Time", “GSEid”, “Microbiome”, “Oxygen”, “Flow”, “Cell system”, “Device” and “Platform” on gene expression was evaluated. The associations between the variables and observed

differences was weak, with no clear effect of parameters like “Flow” which is associated with the before mentioned shear stress. When using a pathway analysis it did become clear that the variable “Microbiome” interacted with immune system related pathways. This shows that some effects, if strong enough, can be found using this method of analysis. Overall this analysis showed that the large heterogeneity in study design and inconsistent reporting on variables influences the value of publicly available data for further analysis. The study did set a proper template for future analysis once more data is available.

This thesis has added to the critical assessment of existing and novel intestinal models that can potentially be used in conjunction with the microbiome. In this field advanced models such as iPSC derived models have shown promise and offer clear advantages over traditional cell lines and advanced primary cell based models.

Appendix

Acknowledgements
List of publications
Overview of completed training

Acknowledgements

My PhD was a long journey that is finally coming to an end, and as with any journey it could not have been completed without the support of many people. And now that I'm finishing this chapter of my life it is important to acknowledge everyone that has contributed in one way or another.

I would like to start by thanking my supervisors, Hans, Meike and Ivonne. I remember leaving Wageningen right after my interview where I was told I'd hear from Hans in a few days, it ended up being the same day. Over the years we've had discussions on many different subjects, some related to my work and some about yours. I appreciate the tireless work you put into my PhD over the years, I've never had to wait long for input on anything I sent. And with any setback, in work or my personal life, I could always count on your support.

Similarly, a lot of the work was dependent on the input and feedback from Meike, just having that extra expert at the table in many of the meetings helped a lot with all the work. Thank you for all the time you put into my papers and the support in getting part of the work done at WFSR.

While I was finishing my MSc internship report Ivonne asked me the question; are you interested in a PhD? After my affirmation she referred me to Hans and sent me on this journey. I would like to thank you for offering me that opportunity at that time. I would also like to thank you for the moments we came to you with our progress where you helped us set our priorities straight and the quick responses when sending any work that had to be approved.

There were three official supervisors during my PhD but there was one more person that was present during pretty much every meeting and played a pivotal role in getting all the work done. Laura always made sure that our plans would actually translate to the lab. You would also always look out for me when things got stressful and always offered any support that was needed.

This project was designed around the combined work of three different groups, toxicology, microbiology from Wageningen and MESA+ from Twente. I would first like to thanks Janneke, my fellow PhD and project partner at microbiology. Without your collaboration a lot of the work we did would not have happened. Even though a lot of it didn't go the way we had hoped you always soldiered on. The different views you had on things we took for granted at toxicology always gave a lot of inspiration and were important reminders to always reconsider facts I took for granted. Secondly, I would like to thank Elsbeth the PhD at MESA+ in Twente. You were always willing to provide time and input into getting the gut-on-a-chip up and running in Wageningen, no matter the number of setbacks we had. Even though we didn't manage in the end I still learned a lot from the exchanges we had. Besides the PhDs I would also like to thank all the supervisors from the other groups, Hauke, Clara, Mathieu and Loes, for their input.

During my PhD I used many techniques and went into many different subjects. Finding the right equipment we didn't have or the expert to give support and input was very important. This started with trying to get into the field of adult stem cell based organoids. First of all I have to thank Bart Spee and Loes Oosterhoff that worked at the faculty of veterinary medicine in Utrecht at the time. They took the time to give us our first introduction into culturing organoids and helped us contact the right people to advance. Getting the material to grow the organoids is a massive challenge on its own and went through many avenues to achieve this. I would like to thanks those I directly interacted with which are Daisy

Dalloyaux from Nijmegen, Anouk Boudewijn from WUR and prof. dr. H.J.T. Rutten from the Catharina hospital in Eindhoven. Even though corona threw a spanner in the works your willingness to help supply material is very much appreciated. Also thanks to Aafke Janssen from WFSR for all the support on the work with iPSC derived intestinal models, your work was also instrumental to finishing my PhD.

While trying to translate the production of the gut-on-a-chip from Twente to Wageningen we needed access to both a plasma oven and a spin coater. For the plasma oven I first have to thank Annemieke and Barend from Organic Chemistry and later on Ketan from Physical Chemistry and Soft Matter. For access the spincoater I would like to thank Remco from colloid chemistry. Without everyone allowing us to use their equipment we would not have been able to progress in our research.

We used many omics approaches, from microarray to RNAseq and comparing existing data sets. For both the design of the work and analysis of the data we were dependent on Guido Hooiveld from food sciences. No matter how many questions or requests we threw at him he always took the time to respond. As such I would like to sincerely thank you for the guidance and input without which I would not have been able to finish my work.

Doing research is not a cheap endeavor and as such is dependent on funding from outside sources. First of all I would like to thank NWO, and especially the people involved in the Building Block of Life call. Within the project we also received secondments from multiple companies that also provided input during our yearly meetings. I would first like to thank WFSR, for the time of Meike to supervise my project, the workspace and the experimental time and support for my work. Secondly, I would like to thank Galapagos, both for their input in knowledge and for running some of my samples for analysis. Lastly, I would like to thank all the other companies for their input, Micronit, DSM and metal membranes. Getting feedback from industry experts always helps look at things from a different perspective and helps find novel ideas.

A PhD is a long endeavor and requires an interest in research, and though a part of that interest is intrinsic there are also a number of people that contributed to it that I would like to thank. First of all my BSc thesis supervisors, Melvin Siliakus and Serve Kengen. I was the first biology student they accepted for a BSc thesis after I approached the department of microbiology. This allowed me to take my first steps on a lab and gave me my first taste of research. Next for my MSc thesis I would like to thank Jochem Louisse and again Laura for supporting my first step into the field of toxicology. And lastly Stephen Hecht for hosting my internship in Minnesota. Without these people I would not have continued in academia and their support gave me the belief that a PhD was the way to go for me.

An enjoyable work environment is very much dependent on the colleagues you work with. My work started not at TOX but at WFSR, close by but completely different in environment. First of all I would like to thank Loes, you gave me my first instructions on how to work with Caco-2 and helped me get started on the lab at WFSR. A short chat with Milou could end up taking the whole afternoon, no matter whether the talk was work related or just any random subject. Phim would also often join in, and entrust me with any Dutch translation work whenever she got another confusing letter from the government. I would also like to shortly thank all the other colleagues at WFSR for the coffee/lunch breaks and other events.

After a year at WFSR I moved to TOX at helix, from the well organized environment with mostly long-time employees to the environment full of PhD and thesis students. My home here was in office 4032,

though my first impression was apparently not too good. I remember Biyao telling me she was scared of me the first time she saw me. Luckily she opened up later on and I enjoyed our outings and dinners over the years. I enjoyed the mostly serious and calm but sometimes lively work environment in our office with Biyao, Shengsheng, Diego, Aziza, Jiaqi, Liang and intermittently Jing. Thank you for all the support over the years.

Within such a large number of PhDs there are always going to be wildly different people. Artem is a great example of this, never just accepting the troubles that come with a PhD and always choosing his own direction. The talks and drinks with you were always a breath of fresh air. Chen thanks for the talks and dinners, it was always fun to talk and compare how completely different our goals outside of work were.

While I thought Biyao was the exception in finding me scary, Akanksha showed up and shared her experience. Luckily, she quickly found out through Biyao that that was not the case. I enjoyed our little interactions every morning when you were sneaking into the office and the meetups we had outside of work. Thank you for making me real curry and taking time to be my paranymph. If anyone reminded how lacking my sports activities were it would be Aafke. Your motivation for both your extracurricular and work activities was always inspiring. Thank you for taking the time to be my paranymph even while recuperating.

I would also like to thank all the other people at the TOX department. Firstly all the staff for all the entertaining coffee/lunch breaks and Christmas events. Especially the secretaries, Lidy, Gerda, Carla and Letty for the all the quick responses to my questions. And lastly to all the other PhDs, I enjoyed the time we all spent together during activities like the PhD trip and the Sinterklaas parties. I don't think I've seen people compete so fiercely over simple presents.

There is also life outside of the university, and without the people there I would never have gotten through my PhD. I lived in dijkgraaf during my student days where I made many friends. First I would like to thank Evert for the dinners and talks, having someone else that was also doing a PhD somewhere else to talk to was always reassuring. Once I started my PhD I wanted to leave the student housing to look for a calmer environment, and luckily Jeroen was also looking for a place to stay around that time. I enjoyed the years we spent living at morfelden-walldorfplein, with the many things we did together including our holiday to Greece. Having someone that grew up in a completely different environment that worked in a completely different field always allowed me to put certain things in perspective.

I would also like to thank my friend group, Wiebe, Milo, Wouter, Paul, Steven, Jurian, Björn, Niels, Louis and Rik. The years I spent with you guys both before and during my PhD helped me become who I am today. You guys have and always will support me through thick and thin. I enjoyed all the things we've done together and look forward to all the ones we'll do in the future.

I grew up practicing Judo up until I moved to Wageningen but never lost contact with the people I got to know there. One of my teachers, Gerrit, would always say the same thing when you fell and got hurt. Just acknowledge the pain and then move on and continue training. I applied that many times during my setbacks in my experiments. I would also like to thank the rest of the group, Lia, Henny, Johan, Ben and Anny for all the support and enjoyable city trips over the years.

Besides all the friend and co-workers thanking the most important support is left for last, my family. My father caused my interest in toxicology and was the reason I ended up at TOX. My mother supported any and all choices I made and would always support me in any which way possible. Rene and Cockie thanks you for the love and encouragement over the years. There are many things you can share with your parents but sometimes you need someone that's more similar in age. My sister was always there for me to talk, though we argued a lot when we were young we found common ground later in life and I enjoyed all the things we did together. Thank you for all the invites and support over the years Floor. I would also like to thank her partner, Stephan, for the support.

Only when writing something like this do you realize how many people have contributed to my work in one way or another. It is pretty much impossible that I didn't forget some people and my apologies for that.

List of Publications

This thesis

- Grouls M, van der Zande M, de Haan L, Bouwmeester H. **Responses of increasingly complex intestinal epithelium in vitro models to bacterial toll-like receptor agonists.** Toxicol In Vitro. 2022 Mar;79:105280. doi: 10.1016/j.tiv.2021.105280. Epub 2021 Nov 27. PMID: 34843883.
- Grouls M, Janssen AWF, Duivenvoorde LPM, Hooiveld GJEJ, Bouwmeester H, van der Zande M. **Differential gene expression in iPSC-derived human intestinal epithelial cell layers following exposure to two concentrations of butyrate, propionate and acetate.** Sci Rep. 2022 Aug 17;12(1):13988. doi: 10.1038/s41598-022-17296-8. PMID: 35977967; PMCID: PMC9385623.
- Elzinga J, Grouls M, Hooiveld GJEJ, van der Zande M, Smidt H, Bouwmeester H. **Systematic comparison of transcriptomes of Caco-2 cells cultured under different cellular and physiological conditions.** Arch Toxicol. 2023 Mar;97(3):737-753. doi: 10.1007/s00204-022-03430-y. Epub 2023 Jan 21. PMID: 36680592; PMCID: PMC9862247.

Other Publications

- Yuan JM, Grouls M, Carmella SG, Wang R, Heskin A, Jiang Y, Tan YT, Adams-Haduch J, Gao YT, Hecht SS. **Prediagnostic levels of urinary 8-epi-prostaglandin F2α and prostaglandin E2 metabolite, biomarkers of oxidative damage and inflammation, and risk of hepatocellular carcinoma. Carcinogenesis.** 2019 Aug 22;40(8):989-997. doi: 10.1093/carcin/bgy180. PMID: 30615102; PMCID: PMC7967701.

Overview of completed training activities

Discipline specific activities

Molecular Toxicology, PET, 2019
Cell Toxicology, PET, 2020
Pathobiology, PET, 2019
Organ Toxicology, PET, 2020
Epidemiology, PET, 2018
Immunotoxicology, PET, 2018
Toxicogenomics, PET, 2019
The VLAG online lecture series, VLAG, 2020
General Toxicology, TOX/WUR, 2023
Conference NVT, NVT, 2019

General courses

VLAG PhD week, VLAG, 2021
Laboratory Animal Science, PET, 2019
Risk Assessment, PET, 2018
Philosophy and Ethics of FS & T, VLAG, 2021

Assisting in teaching and supervision activities

TOX-30306, 2018-2020
Supervising MSc students, 2017-2021

Other activities

Preparation of research proposal, TOX/WUR, 2017
PhD study tour, TOX/WUR, 2018
Project meetings, WFSR/WUR, 2017-2021
Organizing committee Conference NVT, NVT, 2019

The research presented in this thesis was financially supported by The Dutch Research Council (NWO) in the framework of the Building Blocks of Life (project nr. 737.016.003).

Financial support from Wageningen University for printing this thesis is gratefully acknowledged.

Cover design by René J.E. Grouls

Printed by ProefschriftMaken